FRØYDIS SOLAAS

ANALYTICAL AND NUMERICAL STUDIES OF SLOSHING IN TANKS

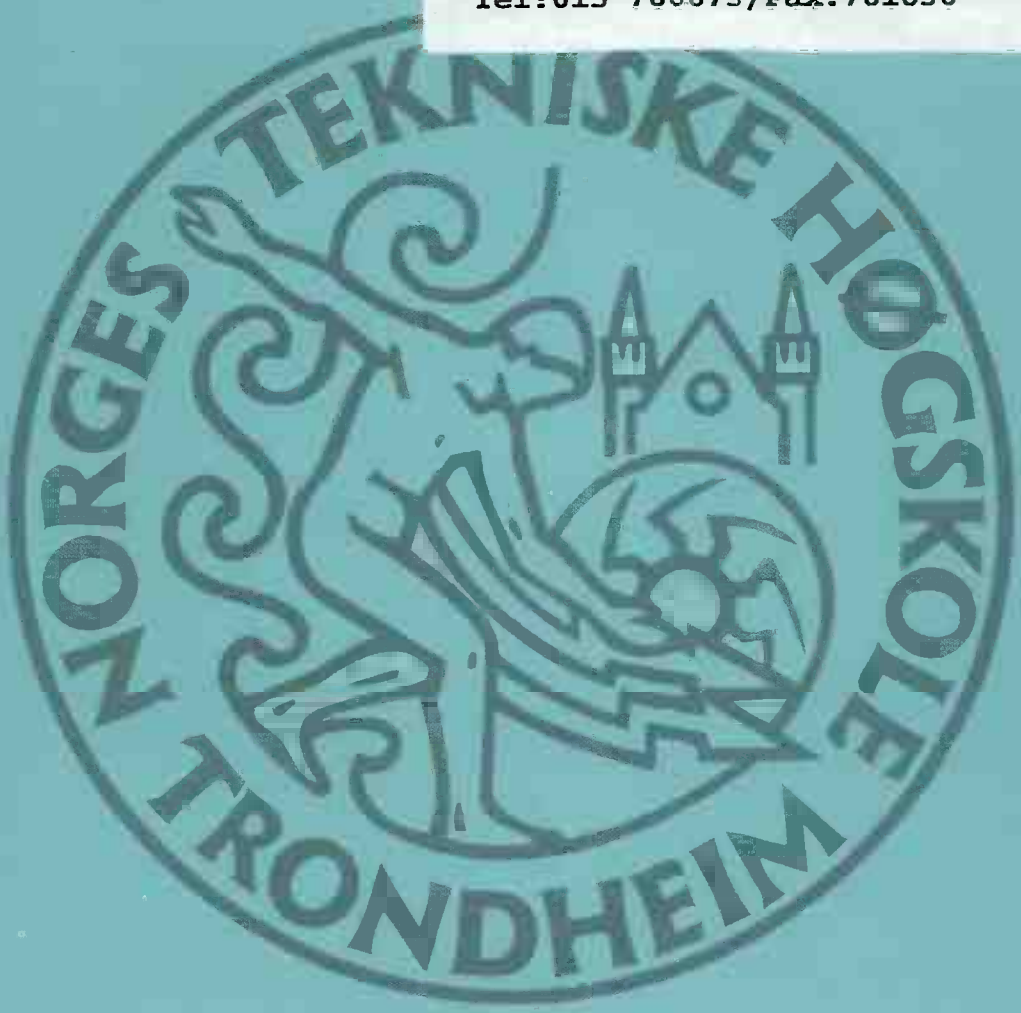

NTH
UNIVERSITETET I TRONDHEIM
NORGES TEKNISKE HØGSKOLE

DOKTOR INGENIØRAVHANDLING 1995:103
INSTITUTT FOR MARIN HYDRODYNAMIKK
TRONDHEIM

MTA-rapport 1995:107

Analytical and Numerical Studies of Sloshing in Tanks

Dr.ing. Thesis

by

Frøydis Solaas
Department of Marine Hydrodynamics
The Norwegian Institute of Technology

NTH-Trykk 1995

Abstract

Linear and nonlinear analytical potential theory solutions of the sloshing problem are studied for a two-dimensional rectangular tank and a vertical circular cylindrical tank. The nonlinear analytical solution is based on a perturbation scheme. The tank is forced to oscillate harmonically with small amplitudes of sway with frequency in the vicinity of the lowest natural frequency of the fluid inside the tank. The tank breadth and water depth is assumed to be O(1). The excitation and the response are assumed to be $O(\varepsilon)$ and $O(\varepsilon^{1/3})$ respectively. Laplace equation is solved with nonlinear boundary conditions and the steady-state velocity potential and free surface elevation are found as power-series in $\varepsilon^{1/3}$ correct to third order for the two-dimensional tank and to second order for the circular cylindrical tank. The nonlinear analytical method is not restricted to rectangular or circular cylindrical tanks. To extend the method to other tank shapes, where it is not possible to solve the equations analytically, a combined analytical and numerical method is developed. A boundary element numerical method is used to determine the eigenfunctions and eigenvalues of the problem. These are used in the nonlinear analytical free surface conditions, and the velocity potential and free surface elevation for each boundary value problem in the perturbation scheme are determined by the boundary element method. Both the analytical and combined analytical and numerical method are restricted to tanks with vertical walls in the free surface.

The suitability of a commercial program, FLOW-3D, to estimate sloshing is studied. This program solves the Navier-Stokes equations by use of the finite difference method. The fractional volume of fluid method (VOF) is used to trace the free surface as function of time. Most of the work is concentrated on calculating the fluid motions inside tanks for cases where the analytical solution is known or there exist model tests results to compare with. In addition, the effect of changing numerical parameters is studied. For some of the cases there was good agreement between the numerical results and the model tests, but for other there was not. To some extent, the numerical results were dependent on the choice of numerical parameters like element size, the convergence criterium in the pressure iteration routine and the method for numerical differencing used in the momentum equation.

Acknowledgement

This study has been carried out with guidance from professor Odd M. Faltinsen whose guidance and encouragement during this work are appreciated.

I am grateful for the encouragement from and the many valuable discussions with my colleagues and friends at the Department of Marine Hydrodynamics and at MARINTEK. I would also like to express my gratitude to Ernst W. M. Hansen at SINTEF, who gave me access to the FLOW-3D program and supported me during the work with this code.

This work has been supported by a scholarship provided by The Research Council of Norway (NFR). In addition financial support is received from The Faculty of Marine Engineering, The Department of Marine Hydrodynamics and MARINTEK A.S.

CONTENTS

Nomenclature

a	- half of the tank breadth, b = 2a [m]
a	- radius of circular cylindrical tank [m]
a_0	- amplitude of any oscillation
a_n	- the amplitude of oscillation n oscillations later than a_0
A	- constant
$A_0^{(2)}$ and $A_1^{(2)}$	- constants in second order velocity potential for rectangular tank
$A_0^{(3)}$, $A_1^{(3)}$, $A_2^{(3)}$	- constants in third order velocity potential for rectangular tank
A_1	- right hand side in second order dynamic free surface condition
A_2	- right hand side in third order dynamic free surface condition
A(I,J)	- influence matrix
$A_{mn}(t)$	- generalized coordinates of the mn'th natural mode of motion for circular cylindrical tank
A_n	- coefficients, n = 0,1,2,.....
A_k	- coefficients, k = 0,1,2,.....
A(x,y)	- time independent part of the right hand side in the second order combined free surface elevation, in two dimensions; A(x)
A31(x)	- $N^3\cos(\omega t)$-terms in third order combined free surface condition
A33(x)	- $N^3\cos(3\omega t)$-terms in third order combined free surface condition
ALPHA	- parameter which controls the weightening of upstream and central differencing in the FLOW-3D approximation of the advective flux terms in Navier-Stokes equation.
b	- tank breadth, b = 2a [m]
B	- constant
B_1	- right hand side in second order kinematic free surface condition
B_2	- right hand side in third order kinematic free surface condition
B_1 , B_2 , B_3	- for circular cylindrical tank; parts of the combined nonlinear free surface condition
B(I,J)	- influence matrix
B_n	- coefficients, n = 0,1,2,.....
$B_{mn}(t)$	- generalized coordinates of the mn'th natural mode of motion for circular cylindrical tank
$B_n^{(3)}$	- coefficients in third order velocity potential for rectangular tank
c_i	- small disturbance used in the stability analysis
C	- constant
C_n	- coefficients, n = 0,1,2,.....
D	- constant
D_n	- coefficients, n = 0,1,2,.....
E	- constant
EPSI	- convergence criterion in the pressure iteration in FLOW-3D
EPSADJ	- controls the automatic adjustment of EPSI
f_i	- generalized coordinates
$f_i^{(0)}$	- generalized coordinates for steady state motion
f(x,y)	- tank motion function, in two dimensions; f(x)
f_{nm}	- functions in nonlinear theory, m=1,2,3

F	- constant
F(x,y,z,t)	- volume of fluid function
F_x	- total force in x-direction [N]
F_1	- constant depending upon circular cylindrical tank geometry
$F_{i,k,k}$	- volume of fluid in element number i,j,k
g	- gravitational acceleration [m/s^2]
h	- liquid depth inside the tank [m]
i	- imaginary unit
J_m	- Bessel functions of first kind, m=0,1,2,...
k	- wave number
k	- element number used to find the derivatives near the walls in the combined numerical and analytical method
K	- coefficient
K_1 ,K_2 ,K_3 ,K_4 ,K_5	- constants in third order equations for rectangular tank
K_1 and K_2	- constants depending upon circular cylindrical tank geometry
K_n	- coefficients, n = 0,1,2,.....
l	- length of tank in y-direction
L_3 ,L_4 ,L_5	- constants in third order equations for rectangular tank
M	- constant
M_n	- coefficients, n=1,2,3,4,5,6
N	- constant
N_{EL}	- total number of elements
N_{FREE}	- number of elements on the free surface
p	- pressure [N/m^2]
$p_{i,j,k}$	- pressure in element number i,j,k [N/m^2]
r,θ,z	- cylindrical coordinate system
S	- boundary
S_B	- body surface
S_F	- free surface
t	- time [s]
T	- period of oscillation
T_n	- natural periods, n = 1,2,..... [s]
T_1	- first natural period [s]
T_2	- second natural period [s]
T_3	- third natural period [s]
u	- velocity component in x-direction [m/s]
u_r	- velocity component in r-direction [m/s]
u_θ	- velocity component in θ-direction [m/s]
$u_{i,j,k}$	- velocity component in x-direction in element number i,j,k [m/s]
V	- velocity vector
V	- volume of fluid in the tank [m^3]
v	- velocity component in y-direction [m/s]
v_n	- velocity of a boundary surface in direction normal to the surface
v_r	- container velocity in r-direction
w	- velocity component in z-direction [m/s]
x,y,z	- cartesian coordinate system
x_b	- container motion in sway $x_b = \varepsilon_0 \sin(\omega t)$ [m]

x_1 , z_1	- arbitrary point in the fluid domain
Y_m	- Bessel functions of second kind, m=0,1,2,...
α	- small value defining the difference between frequency of oscillation and the first eigenfrequency for nonlinear theory
α_0	- constant in second order velocity potential
α_{11}	= tanh (ξ_{11}/a h)
γ	- generalized amplitude of motion for circular cylindrical tank, $\gamma = f_1^{(0)}$
δ	- logarithmic decrement
δ_{sj}	- element length
ε	- magnitude of container motion
ε_0	- amplitude of container motion in sway [m]
ζ	- free surface elevation [m]
ζ	- generalized amplitude of nonplanar motion in circular cylindrical tank, $\zeta^2 = \gamma^2 + F_1/K_2 1/\gamma$
ζ_1	- first order free surface elevation
ζ_2	- second order free surface elevation
ζ_3	- third order free surface elevation
ζ_n	- free surface elevation of n'th order
Θ	- container motion in roll $\Theta = \Theta_0 \sin(\omega t)$
Θ_0	- amplitude of container roll motion [rad.]
λ	- roots from stability analysis for circular cylindrical tank
λ_m	- eigen numbers or values, m = 0,1,2,..., $\lambda_m = \sigma_m^2 / g$
λ_{mn}	= ξ_{mn}/a for circular cylindrical tank
μ	- damping coefficient
μ_{crit}	- critical damping, $\mu_{crit} = 2\sigma_1$
ν	- transformed frequency; value defining difference between frequency of oscillation and the first eigenfrequency for circular cylindrical tank
ξ_{mn}	- roots of $J_m'(\xi_{mn}) = 0$, m,n=0,1,2....
σ_1 or σ_{11}	- first natural frequency
σ_n	- natural frequency number n
τ	- time scale used in the stability analysis $\tau = 1/2\varepsilon^{2/3}\omega t$
Φ	- velocity potential of liquid moving relative to the container
Φ_T	- total velocity potential
Φ_1	- first order velocity potential for circular cylindrical tank
Φ_2	- second order velocity potential for circular cylindrical tank
Φ_3	- third order velocity potential for circular cylindrical tank
ϕ_c	- velocity potential of container motion
ϕ_1	- velocity potential of container motion in roll part 1, linear theory
ϕ_2	- velocity potential of container motion in roll part 2, linear theory
ϕ_n	- velocity potential of n'th order
ϕ_1	- first order velocity potential
ϕ_2	- second order velocity potential
ϕ_3	- third order velocity potential
ϕ_1	- first order velocity potential at z = 0 for circular cylindrical tank

ϕ_2 - second order velocity potential at z = 0 for circular cylindrical tank
ϕ_3 - third order velocity potential at z = 0 for circular cylindrical tank
χ_1 - sin(ωt)-terms in first order velocity potential for circular cylindrical tank
Ψ_1 - cos(ωt)-terms in first order velocity potential for circular cylindrical tank
χ_2 - sin(2ωt)-terms in second order velocity potential circular cylindrical tank
Ψ_2 - cos(2ωt)-terms in second order velocity potential circular cylindrical tank
χ_3 - sin(3ωt)-terms in third order velocity potential for circular cylindrical tank
Ψ_3 - cos(3ωt)-terms in third order velocity potential for circular cylindrical tank
Ψ - Green's function
ψ_n - eigen functions, n = 0,1,2,...
ψ_{nm} - eigen functions, n, m = 0,1,2,...
ω - frequency of oscillations [rad/s]
ω - vorticity vector
ρ - fluid density
φ_1 - Ncos(ωt)-terms in first order velocity potential
φ_2 - $N^2/2\cos(2\omega t)$-terms in second order velocity potential
$\varphi_3^{(3)}$ - $N^3\cos(3\omega t)$-terms in third order velocity potential
$\varphi_3^{(1)}$ - $N^3\cos(\omega t)$-terms in third order velocity potential
$\varphi_3^{(0)}$ - cos(ωt)-terms in third order velocity potential

$\partial/\partial n$ - differentiation in normal direction
$\partial/\partial x$ - differentiation in x-direction
$\partial/\partial y$ - differentiation in y-direction
$\partial/\partial z$ - differentiation in z-direction

Δx, Δy, Δz - cell size in x-, y- and z-directions
δx, δy, δz - cell size in x-, y- and z-directions

1 INTRODUCTION

Sloshing is a phenomenon known from many everyday situations. When you are carrying a cup of coffee, a bucket of water or any other container filled with liquid having a free surface, you will experience that even very small movements of the container may result in violent motions of the liquid inside the container. Such fluid displacements are in general called sloshing.

1.1 The nature of sloshing

Sloshing may be a transient motion, where the fluid is oscillating with its resonance frequencies and set in motion by a momentary movement of the container. The effect of the lower frequencies will dominate the fluid motion. It may also be due to steady state resonance oscillation, if the tank motion has sufficient energy content in the vicinity of one of the resonance periods of the liquid inside the container.

The magnitude and nature of sloshing will depend on the liquid depth and tank shape, together with the modes, frequencies and amplitudes of the tank motion. Lateral sloshing primarily occur due to lateral or angular tank movements. For shallow liquid depth, a hydraulic jump or bore will occur for frequencies of oscillation around resonance. The bore will run from one side of the tank to the other, as shown in Figure 1.1

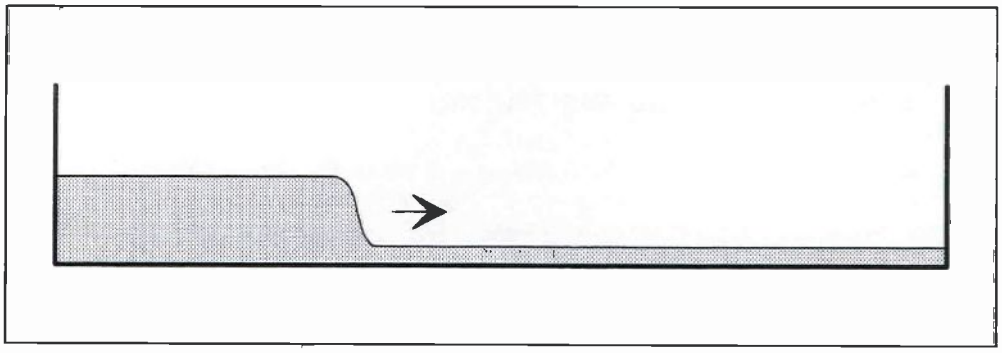

Figure 1.1 Shallow water condition close to the lowest resonance period where a bore will move back and forth between the tank walls.

The first natural mode of motion of the liquid inside a tank is an antisymmetric standing wave with small amplitude. The shape of the mode is shown in Figure 4.2.

A typical large amplitude wave motion for non-shallow liquid depth, is shown in Figure 1.2. This non-symmetric wave motion is not entirely a standing wave, but is often referred to as a standing wave.

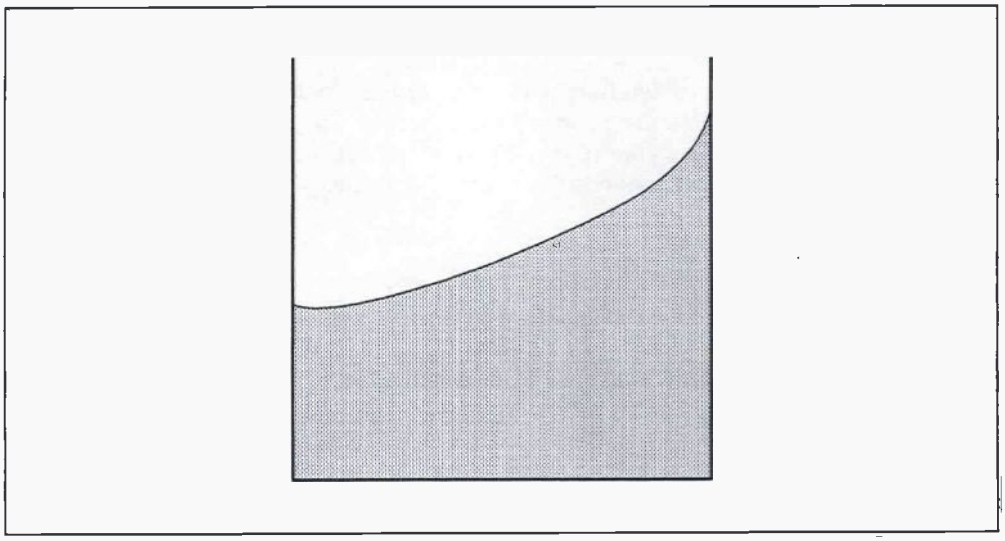

Figure 1.2 Large amplitude wave in non-shallow liquid depth.

Rotational sloshing or swirl motion may arise for instance in vertical circular cylindrical or spherical tanks. This is an instability of the antisymmetric lateral sloshing mode. Vertical sloshing, which is usually symmetric, may arise due to motions of the tank normal to the equilibrium free surface.

1.2 Background and motivation

There is a lot of cases where sloshing may be a problem. For almost any moving vehicle which contains fluid with free surface, sloshing has to be considered, and it will influence both the tank and the support structure design.

Due to wave induced motions, sloshing is likely to be excited in tanks on oceangoing vessels and floating offshore structures.

For oil cargo ship tanks and liquid natural gas (LNG) carriers the dimensions of the tanks are often such that the highest resonant sloshing periods and the ship motions are in the same period range, and then the possibility of violent resonant sloshing motions is large. For slack ship tanks, sloshing may give large impact loads on the tanks, and it has been the cause of tank damage.

According to Bass et. al. (1985), typical operational fill levels for LNG ships are 95 to 97 percent of the tank height because of boil-off. LNG tanks contain no internal structures, so the dynamic loads due to the sloshing can be significant even in these fully loaded conditions. Fill levels less than this may occur when the ship is returning in ballast and chill-down liquids are needed to maintain cold tanks. Partial unloading of the tanks and loading or unloading at

sea may also give long time periods with partially filled tanks.

According to Faltinsen et.al. (1974), a tank failure in a LNG ship merits special consideration because of the risk of brittle fracture of the primary structure (low temperature shock), the expensive repair costs of the complicated tank designs, the high out-of-service costs and a potentially explosive cargo.

Sloshing may also occur in separators and storage tanks on floating oil and gas production platforms. Internal sloshing of oil and water will highly effect the separation efficiency of gravity separators.

Sloshing may also be a problem in containers for transportation of living fish. In such containers not only the forces on the structure are important, but also the pressures and accelerations in the water. Such containers or transportation tanks have to be designed in a way that prevents the fish from being damaged or die during the transportation.

In floating enclosed fish-rearing tanks, the wave motions, pressure and accelerations in the tank during the sloshing will affect the fish and disturb the necessary circulation of the water inside the tank. This circulation is necessary to provide the fish with oxygen. When such tanks are to be designed one should try to avoid large sloshing motions in the tanks.

For aircraft and space missiles fuel tanks, sloshing will highly influence the dynamic stability of the vehicle.

On shore, sloshing may occur in storage tanks exited by earthquakes. In Japan, several cases of earthquake induced sloshing have caused the damage of petroleum storage tanks, (see for example Hara and Shibata (1987)).

Also for offshore storage tanks placed on the seabed as gravity structures sloshing due to earthquakes may be a problem. For such tanks both displacements of the foundation of the structure and wall deflections due to the dynamic pressure distributions around its outside have to be considered, (see Chakrabarti (1993)).

Other on shore cases where sloshing may occur are in tank lorries and railway tanks and in bottles on an assembly line in a brewery.

So, there are a lot of cases where it is important to be able to predict if sloshing will occur or not and to calculate which fluid motions, pressure, forces and moments it will create. But sloshing is difficult to predict theoretically because it is a highly nonlinear phenomenon with large fluid motions, breaking waves and spray.

1.3 Overview of the present work

This work starts with a literature survey of theoretical and experimental sloshing studies. An overview of the present work is given in Figure 1.3. Both analytical solutions, combined

analytical and numerical methods as well as direct numerical solvers are used in this study.

The analytical solutions are based on potential flow, that is, solution of Laplace equation with boundary conditions on the container walls and free surface. Both linear and nonlinear analytical steady-state solutions are studied for forced harmonic motions of the tanks. It is implicitly assumed that the slopes of the water surface are small.

Sloshing is affected by liquid fill depth, tank geometry, and tank motion (amplitude and frequency). If the intention is to get a prediction of if sloshing may occur or not, the eigenperiods may be calculated from linear theory and compared with possible tank motion spectra. For a LNG cargo tank, for example, the lowest natural frequency is in the same frequency range as the motion of a ship, and then sloshing may be a problem.

Linear solutions are valid for small oscillations with excitation frequencies not close to the resonance frequencies. Linear theory based on potential flow predicts infinite response for an excitation frequency equal to one of the resonance frequencies.

The nonlinear analytical solutions are based on a perturbation scheme where the lowest order term is of a similar mathematical form as the linear solution. However the amplitude is different. Even if the linear theories are developed and presented earlier by other authors (see for example Abramson (1966)), they are presented here to make the presentation of the nonlinear analytical solutions easier to follow. Potential theory predicts no damping, so, in addition to the already mentioned linear solutions, a linear steady-state solution with a damping term is incorporated.

The nonlinear analytical solutions follow ideas suggested by Moiseev (1958). He proposes a general method without much details, and his solution method for small oscillations of a general shaped tank in the vicinity of the first natural frequency, is studied here and outlined in more detail. Then the method is used on a two-dimensional rectangular tank and a circular cylindrical tank, and a similar solution as the one derived by Faltinsen (1974) is obtained for the two-dimensional rectangular tank, and as the one obtained by Hutton (1963) for a vertical circular cylindrical tank. Two misprints were detected in the expressions given in Faltinsens paper, but they have little influence on the obtained values of the free surface elevation in the example. Hutton's paper contains several misprints, and the solution for the second order potential contains a constant term which is not determined in his paper, neither is the method for determining it given. This constant term is determined in the present work.

The nonlinear analytical solution follows a perturbation scheme where the forced motion amplitude of the tank is assumed to be of order ε relative to the tank dimensions and the fluid response is of order $\varepsilon^{1/3}$. The tank breadth and water depth are of the same order of magnitude, O(1). Forced harmonic oscillations of the tank is assumed. Laplace equation is solved with nonlinear boundary conditions and the steady-state velocity potential and free surface elevation are found as a power-series in $\varepsilon^{1/3}$ correct to ε for the two-dimensional tank and to $\varepsilon^{2/3}$ for the circular cylindrical tank.

In the two-dimensional tank only planar sloshing may occur due to the harmonic oscillations of the tank. In addition, rotational sloshing may be activated for a vertical circular cylindrical

tank. Both the planar and the rotational solutions are studied, and a stability analysis, like the one given in Hutton (1963), is performed. Regions for stable and unstable sloshing motions in a tank with given dimensions are established. It is important to be aware of these three-dimensional effects when dealing with three-dimensional numerical tools or model tests.

A nonlinear theoretical solution based on Moiseev's idea is not restricted to rectangular or circular cylindrical tanks. However, for a more general tank shape we have to rely on a combined analytical and numerical method. This is shown in details for a two-dimensional tank. The method is limited to tanks with vertical walls in the free surface.

A boundary element method is used to determine the eigenfunctions and eigenvalues of the problem. These are used in the nonlinear analytical free surface conditions following from Moiseev's idea. The velocity potential and free surface elevation for each boundary value problem in the perturbation scheme are determined by the boundary element method. We are not aware of any similar studies.

The method to determine the eigenfunctions and eigenfrequencies is verified by comparing with linear analytical solutions for a rectangular tank, a two-dimensional tank with circular cross section and V-shaped tanks with 30 and 45 degrees inclination of the walls. The combined analytical and numerical method is verified by comparing with the nonlinear analytical solution for forced sway motion of a two-dimensional rectangular tank. Extensive convergence tests are performed by increasing the number of elements used in the boundary element method.

The combined analytical and numerical method can be generalized to forced roll motion and to three dimensional tanks. This is not examined in detail.

Advantages by using this combined analytical and numerical method are that one is able to examine sloshing in many different tanks and have good control of numerical errors. But, the method cannot predict impact pressure, overturning waves, and viscous losses due to for instance flow separation around baffles. Neither can it predict hydraulic jumps that occur in shallow water. The method is based on forced harmonic motion of the tank, and it is not obvious how to generalize it to irregular forced motion. Reports about different direct solvers of Navier-Stokes equation with complete nonlinear boundary conditions claim they are able to analyze all these cases. We therefore wanted to study the feasibility of a method like that, and chose the computer program FLOW-3D for further studies. This is a well established commercial code with a broad class of engineering applications. It would be impossible to test all the direct numerical methods reported in the literature survey. Our conclusions about the validity of FLOW-3D can of course not be generalized to other direct numerical methods, but the conclusions are indicative of numerical problems in solving the sloshing problem.

FLOW-3D solves the Navier-Stokes equations by use of a finite difference code. The numerical methods used in the code have been tested out by for example Hirt (1981) and Hirt and Sicilian (1985), and are documented in the users manual. Our intention has not been to verify the numerical code, but to study the suitability of the program to estimate sloshing. The effect of changing numerical parameters is examined, but most of the work is concentrated on calculating the fluid motions inside tanks for cases where the analytical solution is known

or there exist model test results to compare with. The comparisons gave variable results. For some of the cases there were good agreement between the numerical results and model tests, for other cases not. To some extent, the numerical results were dependent on the choice of numerical parameters like the element size, the convergence criterium in the pressure iteration routine and the method for numerical differencing used in the momentum equation. These are topics which are hardly discussed in the papers presenting the different numerical methods reported in the literature survey.

Only two-dimensional flow is studied here, but if the program is used for three-dimensional sloshing it is important to be aware of the possibility of rotational sloshing and instable solutions, as demonstrated in the nonlinear analytical solution for the vertical circular cylindrical tank. The occurrence of instabilities and rotational sloshing may be used to verify if the code gives good estimation of three-dimensional effects in the sloshing problem.

1.4 Organisation of this thesis

This thesis is divided into 8 chapters. Chapter 2 contains a review of literature treating the sloshing problem. Both analytical, numerical and model tests are mentioned. Chapter 3 states the general assumptions, boundary conditions and definitions used in the potential theory solutions of the sloshing problem in chapter 4,5 and 6.

Chapter 4 contains linear analytical steady-state solutions for harmonical sway and roll motions of a two-dimensional rectangular tank and a vertical circular cylindrical tank. The solutions can in practice be used for oscillation frequencies far away from resonance and small amplitudes of forced oscillations of the tank. A damping term is introduced into the linear steady-state solution in chapter 4.3.

In Chapter 5 the nonlinear solution method of Moiseev (1958) is studied and used on sway motion of a two-dimensional rectangular tank and a vertical circular cylindrical tank. This method is also the foundation for the two-dimensional combined analytical and numerical method developed in chapter 6, which uses a combination of the analytical solution and a boundary element method. The combined analytical and numerical method is verified by comparisons with the nonlinear solution for the two-dimensional rectangular tank. Then the use of the method on other tank forms is studied. It is shown analytically in chapter 5 that the nonlinear solution based on Moiseev's idea is only valid for tanks with vertical walls at the still water level.

In chapter 7 a finite difference code for the solution of the Navier-Stokes equations is studied. The FLOW-3D program and the theory behind it are presented and the program run on some cases where the theoretical solution is known or there exist published results from model tests.

Chapter 8 contains comparisons and discussions of the different methods, conclusions and recommendations for further work.

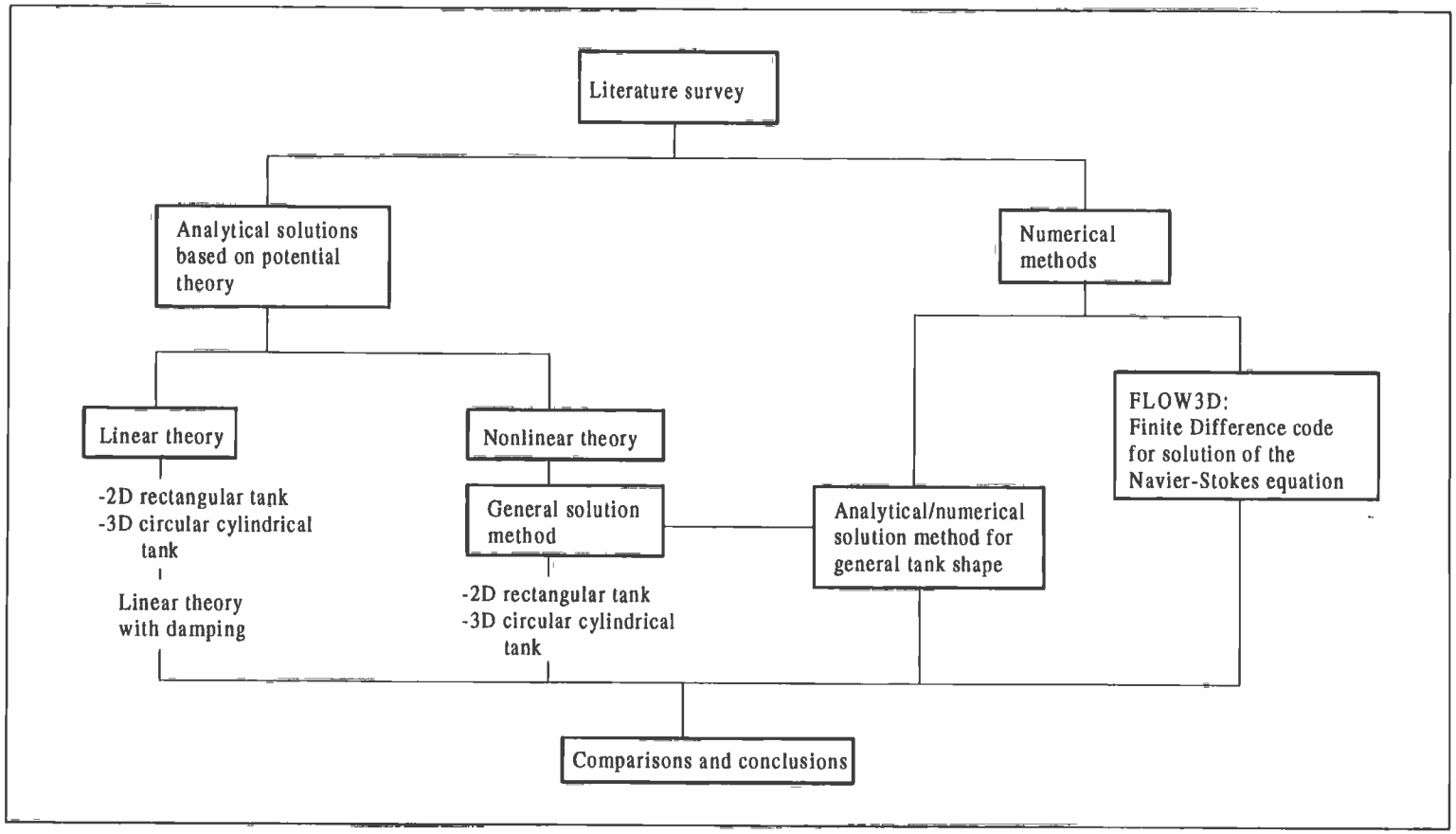

Figure 1.3 Overview of present work.

2 LITERATURE SURVEY

Several studies on the problem of liquid motions with free surface inside moving containers have been carried out for the last 40 years. There has been particular large interest in problems related to aircraft and rocket fuel tanks, and cargo, ballast or fuel tanks for ships.

In the NASA report "The dynamic behavior of liquids in moving containers" edited by Abramson (1966), there is given a comprehensive review of the studies on sloshing up to 1966, specially related to aircraft and rocket fuel tanks. On the subject of liquid sloshing in slack ship tanks, Det norske Veritas held a seminar in May 1976, where the nature of sloshing phenomena and loads, methods and tools to predict them, along with some results from model and full scale measurements were presented. Bass, Bowles and Cox (1980) present an evaluation of dynamic loads in LNG cargo tanks. This paper gives a comprehensive review of worldwide scale-model sloshing data up to 1980.

This chapter presents a review of literature treating the sloshing problem. Both analytical and numerical solutions together with literature containing results from model tests are presented.

2.1 Analytical solutions

Analytical solutions are mostly based on potential theory. The wave elevation, velocities of the water, pressure in the tank, and total forces and moments are expressed in terms of the velocity potential.

Solutions of linearized problems are valid for small oscillations far away from the resonance frequencies. The natural frequencies of the fluid inside the tank are defined as the ones calculated from the linear analytical solutions. At oscillation frequencies equal to the resonance frequencies the linear potential theory predicts an infinite response amplitude of the fluid.

In reality, the nature of sloshing is nonlinear and at times, the nonlinearities will govern the character of the liquid motion. Abramson (1966) has divided the nonlinear effects into three classes: (a) those which arise primarily as a consequence of the geometry of the container (like nonvertical walls and tank compartmenting), and are apparent even for rather small amplitudes of excitation, (b) those which arise primarily as a consequence of large amplitude excitation and response, and (c) those which involve essentially different forms of liquid behavior produced by coupling or instabilities of various lateral sloshing modes.

In the presented analytical solutions of the sloshing problem, the tank is forced harmonically with horizontal motion (sway or surge) or rotational motion about an axis in the centreplane of the tank (roll or pitch). The different tank motions are defined in Figure 3.1. In a real problem the tank motion will not be harmonically, and there will often be a coupling between the motion of the fluid inside the tank and the motion of the vehicle containing the tank. This coupling is not taken care of in the presented analytical solutions, but for a linear problem it should be straightforward to do. For a linear problem it is also possible to find the fluid

response of irregular motions of the tank. But, if the fluid motion is nonlinearly dependent on the forced oscillation amplitude, it is not obvious how to solve the problem for irregular motions of the tanks.

Another limitation of the analytical solutions is the tank configurations for which the system of equations may be solved. Impulse pressure and impact loads, breaking waves, vortex shedding from baffles or other damping devices, effect of draining or water inlet to the tank are not taken into account in the analytical solutions.

2.1.1 Linear solutions

For some tank configurations, where it has been possible to solve the governing equations analytically, the eigenfrequencies and functions are given in Lamb (1945). In art.190 the solution is given for a rectangular tank, and in art.191 for a circular cylindrical tank. In art.258 the eigenfrequencies and functions are given for the two-dimensional flow across a channel whose section consists of two straight lines inclined at 45 degrees to the horizontal. For the flow across a channel where the walls are inclined 30 degrees to the horizontal, the second eigenfunction and frequency are given. For a channel with circular cross section, only the first antisymmetrical eigenfrequency is given.

Abramson (1966) presented the potential theory solutions for sloshing in tanks undergoing harmonical oscillations for various tank shapes. The tanks are rigid with no sinks or sources. A linear solution for a three-dimensional rectangular tank is given. This solution is similar to the two-dimensional solution developed in chapter 4.1, when the y-dependence in the equations is removed. For vertical circular cylindrical tanks solutions for various compartmenting of the tanks are given. The solution for the ring sector compartmented tank may be simplified to an uncompartmented tank and then the solution is equivalent to the solution developed in chapter 4.2. Linear solutions for sloshing in horizontal circular cylindrical tanks, spherical, toroidal and conical tanks are also given.

In the linear solutions presented in Abramson (1966) various modes of excitation of the containers are considered, but coupling arising from more than one excitation mode has been neglected. Solutions are given for sway, roll and bending motions of the tanks.

2.1.2 Nonlinear solutions

Nonlinear theory has to be used to predict the response of the fluid inside the tank near the lowest resonance frequency.

The general nonlinear theory of Moiseev (1958) is the foundation for some studies of nonlinear liquid sloshing. He suggested a method for determination of the free oscillations (that is, oscillations free from the disturbing force that caused it) and forced oscillations (that is, the disturbing force is applied continuously) of the liquid in generally shaped tanks.

Hutton (1963) used the theory of Moiseev (1958) to study small forced sway oscillation near the first resonance frequency of a vertical circular cylindrical tank, and Faltinsen (1974) to develop a nonlinear theory for sloshing in a two-dimensional rigid tank. In Faltinsen (1974), the tank is forced to oscillate harmonically with small amplitudes of sway or roll oscillation in the vicinity of the lowest natural frequency for the fluid inside the tank. Comparison between theory and experiments showed reasonable results for a rectangular tank with water depth / tank breadth ratio, h/b, equal to 0.5. When the fluid impacted the tank top, the agreement between theory and experiment became less good due to violation of the basic assumptions in the theory.

In these nonlinear solutions, the breadth of the tank is chosen to be of O(1), and the depth of O(1) or infinite. The response is assumed to be $O(\varepsilon^{1/3})$, where ε is the order of magnitude of the amplitude of a characteristic forced motion of the tank. A nonlinear, nonviscid boundary-value problem of potential flow is formulated and the steady-state solution is found as a power series in $\varepsilon^{1/3}$, in Faltinsen (1974) correctly to $O(\varepsilon)$, and in Hutton (1963) correctly to $O(\varepsilon^{2/3})$.

The stability of the steady-state solutions was also studied. This was done by introducing small perturbations in the steady-state solutions.

In chapter 5.1, the general nonlinear theory of Moiseev for oscillations near the resonance frequency is studied in more detail. In chapter 5.2 the method is used on a rectangular tank and a solution similar to Faltinsen's solution is obtained. Hutton's solution is studied in chapter 5.3.

The theories of Moiseev (1958) and of Hutton (1963) are presented in Abramson (1966), together with the theory of Penny and Price (1952) for free oscillations in a two dimensional tank with infinite depth.

2.1.3 Shallow water theory

The shallow water depth case is characterized by the formation a bore (often mentioned as a hydraulic jump) and travelling waves for excitation periods around the natural period.

Verhagen and Wijngaarden (1965) are dealing with the oscillations of the fluid inside a rectangular container. The container is undergoing forced roll oscillations. The water depth in the container is shallow. That is, the ratio between water depth and tank breadth $h/b << 1$.

The hydraulic jump is a nonlinear phenomenon and Verhagen and Wijngaarden (1965) have applied a theory developed for one-dimensional gas flow to the fluid oscillations in order to calculate the strength and phase of the jump. The period range, dependent on the tank width, water depth and oscillation amplitude, for which a hydraulic jump exists, is also obtained. Calculated free surface elevations and moments, for a tank with $h/b = 0.075$, oscillations near resonance with amplitudes between 1 and 4 degrees, are compared with results from model tests and show good agreement.

According to Olsen and Johnsen (1975), the shallow water theory gives reasonable predictions of the free surface elevations and forces on the tank for h / b smaller than approximately 0.1 and roll amplitudes smaller than 4 degrees, and that it also predicts reasonably well the conditions (with respect to excitation frequency and amplitude) under which a hydraulic jump will occur.

The shallow water theory of Verhagen and Wijngaarden (1965) does not contain viscous effects. In Faltinsen et.al. (1974) it is shown that for a tank with h/b equal to 0.12, viscosity has influence on the impact pressure for small amplitudes of sway oscillation ($\varepsilon_0/b=0.01$), and that it has little influence for larger amplitudes of oscillation ($\varepsilon_0/b=0.1$).

2.1.4 Solutions with damping

The above presented solutions are based on potential theory and hence there are no energy dissipation or damping in the systems. For an initial-value problem this implies that a steady-state solution cannot be achieved. Transient effects do not die out. Model tests presented by Faltinsen (1974) show that the fluid motion will finally oscillate with a period much the same as the forced oscillation, but with some beating effect or more frequencies present. This suggests that there is damping present in reality.

Faltinsen (1978) has introduced an artificial damping term to simulate the effect of viscous damping in the potential-theory model. The main purpose of this damping term is to take care of transient effects. The motion amplitude in steady-state oscillations should normally not be influenced by the damping. The damping effect is introduced as a fictitious small term in the Euler equation. It expresses a force opposing the fluid velocity. This causes an additional term in the dynamic free-surface condition that is proportional to the velocity potential.

Faltinsen (1978) included the fictitious damping term into a linear initial-value solution for the sloshing inside a two-dimensional rectangular tank excited by transverse harmonic oscillations.

Case and Parkinson (1957) have used a linear theory to predict the damping of free oscillating surface waves of small amplitude in a vertical circular cylinder. Viscous dissipation in the boundary layers at the tank walls is the primary cause of damping. The viscous flow in the boundary layers is assumed to be laminar. Expressions for the damping in the body of the liquid are also developed. This term corresponds to the damping term developed by Lamb (1945), art.348, for the effect of viscosity on free oscillatory waves in deep water.

Keulegan (1958) has studied the energy dissipation of free oscillating waves in rectangular basins. He assumed that the loss of energy of the waves is localized in the boundary layers adjacent to the solid walls. The fluid motion in the boundary layers is assumed to be laminar. The velocity at the outer edge of the boundary layers is approximated by the velocity from second order potential theory. This is the velocity which would be present at the walls in the absence of the boundary layers. Dissipation in the boundary layers is assumed to be due to viscous effects associated with ordinary viscosity and velocity gradients. The losses in the main body of the fluid due to viscosity are computed by the method of Lamb (1945), art.348.

Stephens, Leonard and Perry (1962) obtained an analytical expression for the damping of the first antisymmetrical mode of motion of the fluid in a vertical circular cylindrical tank. This equation is originally developed by Miles (1956) and is similar to the expressions developed by Case and Parkinson (1957) for the damping due to viscous effects on the tank walls and bottom. Abramson (1966) has presented empirical expressions for damping coefficients for tanks of various geometries.

Demirbilek (1983 part I) has studied the motion of a viscous fluid in a rolling rectangular tank. A linear theory for incompressible, viscous liquid sloshing is used and a boundary value problem formulated, where the stream function formulation is used to express the combined continuity and momentum equation. Laminar flow is assumed. Demirbilek (1983 part II) adopted a truncated infinite Fourier series-type solution for the linearized boundary value problem. Demirbilek (1983 part III) investigated the effect of Reynolds number, Froude number (which is not defined in the paper) and the depth/breadth ratio on the sloshing in a rectangular tank. For the range of parameters studied, the results exhibit an increase in the value of the dissipated energy for the case of shallow liquid depth. The decrease in dissipated viscous energy with increasing water depth is associated with that the fluid motion near the bottom of the tank decreases with increasing water depth.

2.2 Numerical solutions

Both finite difference, finite element and boundary element methods have been used to study liquid sloshing in moving containers.

Two terms which are used in the presentation of the methods have to be explained. That is the Eulerian and the Lagrangian description of the fluid domain. In the Eulerian description the coordinate net or grid is fixed with respect to the reference frame, so that the fluid moves through the grid from element to element. The Lagrangian description is characterized by a coordinate system or net which moves with the fluid, so each computational element always contains the same fluid elements.

2.2.1 Finite difference methods

The philosophy of the finite difference methods is to replace the partial derivatives appearing in the governing equations of fluid dynamics with algebraic difference quotients. Then a system of algebraic equations which can be solved for the flow-field variables at specific, discrete grid points in the flow are obtained. The finite difference method needs a structured grid. An Eulerian approach is used.

When finite difference methods are used in three dimensions they are also referred to as finite volume methods.

All the referred methods are based on the Marker and Cell (MAC) method and the SOLA codes. The MAC method divides the computational domain into cells. A system of marker

particles are initially placed in the cells containing fluid and they are subsequently moved with the local velocity. A cell with no marker particles is considered to contain no fluid. A cell with marker particles lying adjacent to an empty cell is called a surface cell. Harlow and Welch (1965) describe the MAC method for two-dimensional incompressible flow. The fluid may be bounded in part by the walls of an irregular box or by symmetry lines. A prescribed time and space dependent pressure may be applied to the surface. The unsteady Navier-Stokes equations for laminar flow are solved by a finite difference scheme in both time and space. Harlow and Welch found that it had advantages in free surface flow to use velocity and pressure instead of stream function and vorticity as the primary physical variables. The free surface boundary conditions of vanishing stress, or of prescribed normal stress is easier to apply.

The Marker and Cell method is described in detail by Welch et. al. (1965).

A simplified version of the MAC method, the SOLA and SOLA-SURF code, was developed by Hirt, Nichols and Romero in 1975. These programs are highly simplified, do not use marker particles and do not have built-in setups for internal obstacles or other complicating refinements.

SOLA is a solution technique for incompressible flow without free surfaces in a two-dimensional plane or axis-symmetric coordinates. SOLA-SURF is an extension of the SOLA code that permits a free surface or curved rigid boundary (free-slip) to be located across the top or bottom of the fluid region. These surfaces are defined in terms of their height with respect to the bottom of the computational mesh. One important limitation of this code is that the surfaces must be single valued functions of the horizontal coordinate.

During the period from 1975 to 1981 a series of simplified codes with the generic name SOLA were developed. Flow Science, Inc. made in 1981 a three-dimensional extension of the most successful of these codes, the SOLA-VOF (Volume of Fluid). SOLA-VOF is a combination of the SOLA finite difference scheme for solving Navier-Stokes equation and the volume of fluid, VOF, technique for tracing free boundaries of fluids. This code was the basis for the development of the FLOW-3D code, which is described and used in chapter 7.

Hirt (1986) describes different versions and applications of the SOLA codes. Hirt and Nichols (1981) describe the fractional volume of fluid (VOF) method for calculation of the dynamics of free boundaries. In each cell of the mesh it is customary to use one value for each dependent variable. To be able to follow the free surface and only use one storage word for this in each mesh cell, a function F is defined. The average value of F in a cell represents the fractional volume of the cell occupied by fluid. A unit value of F would correspond to a cell full of fluid, while a zero value would indicate that the cell contains no fluid. Cells with F-values between zero and one must then contain a free surface. The derivatives of F are used to find where the fluid is located in the cell. Thus, the VOF method provides the same information as the Marker and Cell method, but with use of only one storage word for each cell.

There are several references where the presented methods are based on the Marker and Cell (MAC) method, Volume of Fluid (VOF) method or one of the SOLA codes.

The NASA-VOF3D code is described by Torrey, Mjolsness and Stein (1987). This is a three-dimensional version of the volume of fluid method specifically designed to calculate confined flows in a low gravity environment. The presented version of the code is restricted to cylindrical geometry. The code allows multiple free surfaces with surface tension and wall adhesion. It has also a partial cell treatment that allows curved boundaries and internal obstacles.

The two-dimensional MSLOSH (Mitsubishi SLOSHing simulation program), presented by Tozawa and Sueoka (1989) has introduced a method to determine impact pressures and a moving coordinate system in addition to the SOLA-VOF scheme. In Tozawa and Sueoka (1989) several results from model tests are shown, but there are not shown any comparisons between the computed pressure and the measured pressure.

Su and Wang (1990) have extended the VOF method to allow simulations of three-dimensional liquid sloshing in a container of arbitrary geometry. They demonstrate the occurrence of swirling modes of the free surface in an vertical cylindrical cylinder subjected to lateral excitation. Their results were compared with model tests results for the free surface elevation given in Abramson (1966). For frequencies of oscillation less than the first natural frequency of the fluid in the tank, the numerical results agreed well with the experimental data. When the excitation frequency is higher than the natural frequency, the numerical obtained free surface elevation was up to approximately 25 percent higher than the experimental results. The numerical code predicted swirl motion for the same frequencies and amplitudes of oscillation as given in Abramson (1966). No comments were made on numerical convergence, like the effect of element and time step size.

Navickas et.al. (1981) applied the SOLA-SURF code to the sloshing problem in a two-dimensional closed container with high filling level, undergoing arbitrary time-dependent accelerations in horizontal and vertical directions. They extended the SOLA-SURF code by including a model for liquid compressibility during impacts on the ceiling of the tank assuming small changes of density. It was reported that the results compared well to test data at points of greatest interest, such as initial corner impact. From this it seems that the effect of compressibility is important in describing impact phenomena. However this is not in agreement with the experience in other ship slamming problems. For instance Kvålsvold (1994) studied the wetdeck slamming problem. Even if the maximum pressure can be as high as the acoustic pressure, it does not matter for the structural response. An initial force impulse and dynamic hydroelastic effects are what is important. Navickas et.al. (1981) do only show pictures of the fluid motion in the tank from the experiments and numerical computations. Results from pressure or force measurements are not shown. Neither do they discuss numerical convergence of the code.

Arai, Cheng and Inoue (1992) present a method for calculating sloshing in three-dimensional tanks with internal structures. The method is based on the MAC and SOLA codes. To be able to simulate liquid impact on the tank ceiling a linear combination of the boundary conditions of free surface and rigid wall is used in the region of transition of the boundary condition from free surface to rigid wall. This region is just beneath the tank ceiling. This combined boundary condition is not effective for very violent sloshing with nearly flat impact.

The impact pressure when the wave is hitting the tank walls or top is difficult to determine correctly. According to Tozawa and Sueoka (1989) the impact pressure in the SOLA-VOF code will depend on the time step and mesh spacing, and the reason for this is that the normal velocities of the fluid and the tank wall are not the same prior to impact. Arai, Cheng and Inoue (1992) have investigated the effect of mesh size and concluded that if a element size equal to 10 times the time step size and the vertical velocity of the fluid was chosen, reasonable values of the impact pressure were obtained.

Lloyd's Register of Shipping has developed a two-dimensional finite difference program, LR.FLUIDS, which predicts the sloshing behavior of fluids in arbitrary shaped tanks when excited by ship motions in a seaway. This method is described by Mikelis, Miller and Taylor (1984) and by Mikelis and Robinson (1985).

The LR.FLUID program is based on the SOLA-SURF code. The code has been modified to cope with a variety of tank shapes and steep free surfaces and free surfaces in vicinity of vertical internal structures. Sloping boundaries are modelled by rectangular steps of the grid. Internal structures of thin sections such as baffles, stiffeners and girders can be included. The program allows several forms of excitation; (1) a "sloshing excitation spectrum" which employs a continuously and smoothly varying period and amplitude of motion, (2) harmonic forced excitation in one, two or three degrees of freedom, (3) irregular forced excitation, and (4) coupled sloshing and ship motions. In the coupled mode of excitation the simulation proceeds in time by a parallel and coupled set of computations of the ship motion equations and of the sloshing analysis. As the liquid cargo moves, it transmits a force and moment on the tank and consequently onto the ship. These liquid induced loads are computed for every time step by an integration of the pressures around the tank boundary, and are introduced in the equations of ship motions. In turn these equations are solved, thus providing values of displacements, velocities and accelerations which are used to excite the sloshing simulation in the subsequent time step.

The program, described by Mikelis, Miller and Taylor (1984), gives good results for the free surface elevations compared with model test for filling depths from 0.15 times the tank depth to 0.90 times the tank depth. Comparisons of the pressure shows that the difference between the model tests results and the numerical results is larger for the pressure transducers which move in and out of water, than the ones which are always submerged. For example, there is practically no difference in the numerical and experimental pressure for a transducer at the lower part of the tank wall for the water depth/tank depth ratio 0.75, angular amplitude of oscillation 0.1 rad. and period of oscillation 1.057 sec. (See Figure 6 in Mikelis, Miller and Taylor (1984)). But for a pressure transducer on the tank ceiling, the measured pressure is up to 1.5 times the pressure obtained in the numerical code. We should note that the differences in the measured and the computed pressures vary from case to case.

On the topic of convergence, Mikelis, Miller and Taylor (1984) reported that the predicted pressures were practically unaffected by a halving of the element size used in the computations, and that they have used the stability conditions given in Welch et. al. (1965) to ensure stability of the computations. In the present computations, the iteration for satisfying the continuity equation and the boundary conditions at each time step in each of the computational cells is carried out by scanning the cells from left to right and from bottom to

top of the grid. This results in an accumulation of numerical error at the top right corner of the mesh, which gives some asymmetry in the time history of the forces on the tank. Mikelis, Miller and Taylor report that when they modified the code in such a way that the scanning of cells was alternating with the tank motion, this asymmetry disappears.

2.2.2 Finite element methods

The finite element method is a technique for solving partial differential equations. The domain is divided into elements which form a grid. The elements are usually triangular or quadrilateral. The grid does not need to be structured. This means that very complex geometries can be handled.

The solution of the problem is assumed a priori to have a prescribed form given as functions which, for instance, vary linearly between neighboring nodal points on the elements. The nodes are typical points of the elements such as vertices, mid-side points and mid-element points. The assumed solution is inserted into the differential equations which are to be solved. The assumed solutions will not completely satisfy the differential equations, and a *residual* or error is obtained. This residual is minimalized in a weighted manner by multiplying with a weighting function and by integrating this product over the defined domain.

The boundary conditions are incorporated as known values on the nodal points on the elements.

Historically, the finite element method originates from structural mechanics, where the partial differential formulation of a problem can be replaced by an equivalent variational formulation, i.e. the minimalization of some energy integral over the domain. This formulation constitutes a natural integral formulation for the finite element method. In structural analysis Lagrangian description of the mesh is used, where the mesh follows the structural deformations.

Lately, the element method is used more and more in fluid dynamics. Here, both Lagrangian formulation, where the mesh is moving with the fluid and Eulerian formulation, where the fluid flows through the mesh, are used.

The element method is described in more detail in for example Dick (1993).

All finite element methods presented in this chapter are treating two-dimensional flow. Both potential flow and viscous flow are studied by use of element methods.

Ikegawa (1974) and Washizu and Ikegawa (1974) used the finite element method to analyze nonlinear sloshing of liquid in a two-dimensional rectangular container. The container is forced to oscillate in horizontal direction. The fluid is assumed to be non-viscous and irrotational, and the boundary conditions on the free surface are nonlinear. The fluid domain is divided into triangular elements, and the finite element and the finite difference method are used spacewise and timewise, respectively. The free surface elevation and the velocity potential in each element are calculated for each time step in the procedure. Free oscillations with small amplitude of the liquid motion in the container gave a value of the first natural

frequency of the fluid motion close to (1 percent difference) the one obtained from linear theory. Except for this, the validation of the method is poorly documented in the two papers. Numerical convergence of the method is not discussed, and the results in the shown example can not be compared with results from other methods or tests, since the amplitude of oscillation of the tank motion is not given.

Washizu, Nakayama and Ikegawa (1978) and Nakayama and Washizu (1980) extended Ikegawa's method and studied forced vertical and forced roll oscillations respectively. Nakayama and Washizu (1980) are comparing the numerical obtained pressure distribution at the right tank wall with results from model tests for one case with frequency of oscillation equal to 1.19 times the first natural frequency. Except for one point just above the still water line, there is good agreement between the results. Beyond this only comparisons with linear theory are shown. Both the chosen shape of the elements, the form of the prescribed functions and weighing functions and the time step size, will influence the solution. This is not discussed.

Ramaswamy, Kawahara and Nakayama (1986) present a Lagrangian finite element method for calculation of two-dimensional sloshing of incompressible, viscous fluids. Forced roll oscillations of a rectangular tank are analyzed. Due to the definition of the Lagrangian description, the volume of each element must remain constant. To satisfy this constraint a velocity correction procedure is employed. The fluid flow is mathematically described by the incompressible Navier-Stokes equations for laminar flow, the equation of continuity and boundary conditions at the walls and the actual free surface. The boundary condition on the free surface is that the normal stress should be equal to the atmospheric pressure and the tangential stress should vanish. The pressure and velocity in each element are calculated for each time step. Some computational results for nonviscous and viscid flow are shown, but no comparisons with results from other methods or tests are shown, neither is the influence of numerical parameters on the results discussed.

To solve viscous free surface flow problem involving large free surface motions Ramaswamy and Kawahara (1987) have developed an arbitrary Lagrangian-Eulerian kinematical description of the fluid domain. The nodal points can be displaced independently of the fluid motion. This allows greater distortions in the fluid motions than a purely Lagrangian method. The technique is referred to as an arbitrary Lagrangian-Eulerian method because there are three options for moving vertices: (1) they can flow with the fluid for Lagrangian description, (2) they can remain fixed for Eulerian description or (3) they can move in an arbitrarily prescribed way. In practical applications, the hydrodynamics problem would be run for a while with the pure Lagrangian code and then stopped when the mesh begins to get somewhat disordered. Then a code which reorganizes the mesh takes over and smoothes out the mesh. During this reorganization of the mesh, there is no time change. Then the mesh would be passed back to the hydrodynamics code for more time-dependent calculations. Stability criteria are discussed, and some results from numerical calculations shown.

Also Huerta and Liu (1988) have developed an arbitrary Lagrangian-Eulerian finite element technique to study nonlinear viscous flow with large free surface motions. They have demonstrated the method for a large-amplitude sloshing problem. On the free surface, a Lagrangian description is used in the vertical direction, and the vertical mesh velocities for

the interior elements vary linearly with depth. An Eulerian description is chosen in the horizontal direction everywhere. The streamlines and free surface elevation for the first and third sloshing mode are shown. The obtained eigenfrequencies compare well with model test and theoretical results.

2.2.3 Boundary element methods

Boundary element methods or source and/or dipole panel methods are based on potential flow where viscous effects are neglected and the fluid is assumed incompressible and the flow irrotational. The flow is then governed by Laplace equation.

The velocity potential is expressed as singularities, like sources and/or dipoles, which are distributed over the boundary of the fluid region. The singularity densities are determined by satisfying the boundary conditions. This results in integral equations which have to be numerically solved.

From the boundary element method we get the velocity potential in the fluid, and from this we may find the velocities, pressures and forces.

Faltinsen (1978) has developed a two-dimensional numerical method for calculating sloshing in a rectangular tank based on boundary integral technique. A low order panel method is used. The surface surrounding the fluid (wetted tank surface and instantaneous free surface) is divided into plane elements, and the singularities are sources, with constant densities over each element. The exact nonlinear free-surface conditions and the linearized body boundary conditions are satisfied at the midpoints of the elements. The problem is solved as an initial-value problem. Certain marked points on the free surface, which always have the same x-coordinate, are followed in time. The calculation proceeds by time-stepping and at each time-step an integral equation must be solved. To simulate the effect of viscous damping in the potential-theory model, an artificial damping term is introduced. This damping term is described in chapter 2.1.4 and 4.3. The results are compared with linear analytical solutions. In the beginning of the calculations there is good agreement. However, the numerical solution shows the typical nonlinear behavior that the distance from the mean surface level to the trough is smaller than the distance from the mean surface level to the crest. The obtained free surface elevations are dependent on the chosen value of the damping term. For periods of oscillation close to the first natural period when the wave motions are large, the numerical solution breaks down before the steady state solution is reached. The reason for this may be that the liquid motion becomes too violent. The method is not limited to a rectangular tank, but it is necessary that the tank is vertical at the free surface. By following fluid particles on the free surface instead of points with the same x-coordinate, it would be possible to simulate overturning waves.

Nakayama and Washizu (1981) have applied the boundary element method to the analysis of nonlinear liquid sloshing in a two-dimensional rigid rectangular container subjected to forced horizontal, vertical or roll oscillations. The boundary is divided into line elements. On the free surface the element ends always have the same x-coordinate. The results compared well with linear theory and the results from the finite element method of Ikegawa (1974).

Shiojiri and Hagiwara (1990) have used a boundary element method and developed a computational method for two-dimensional nonlinear sloshing in containers of arbitrary shape. The tank walls may be inclined and the nodal points on the free surface can move arbitrarily. The boundary integral equation is discretized by boundary element with linear interpolation function. Shiojiri and Hagiwara (1990) are showing comparisons between the free surface elevations from the numerical calculations and from model tests for a rectangular tank and a triangular (V-shaped) tank. The results agreed well for the rectangular tank. The differences between the free surface displacement along the wall were up to 30 percent for the V-shaped tank.

Shiojiri and Hagiwara (1990) and Nakayama and Washizu (1981) have introduced an artificial damping term in the solution, but they have not studied the effect of different values of the damping terms.

Schilling and Siekman (1982) have used a boundary element method to calculate sloshing in tanks with rotational symmetry. The tank is upright and excited harmonically normal to its symmetry axis. A cylindrical coordinate system fixed to the tank center of the undisturbed free surface is used. The impenetrable wall surface is supposed to be piecewise smooth. The time-independent velocity potential is represented by a distribution of sources on the bounding surface, together with an analytical solution of the Laplace equation. The amplitudes of the fluid motion normal to the equilibrium shape of the free surface are assumed to be small enough to linearize the free surface boundary conditions. The numerical results show good agreement with analytical linear theory. The accuracy of the numerical results is lowered as higher excitation frequencies are applied.

2.3 Model tests

In most of the above presented literature the authors have used results from model tests to compare with the results from their analytical or numerical methods.

Abramson (1966) gives results from model tests with tanks of various shapes. Rectangular tanks, spherical tanks and circular cylindrical tanks; uncompartmented or with different compartmenting. The effect of viscosity and tank shape, and of different damping devices are outlined. These studies are mainly related to liquid fuel tanks on space vehicles.

In Abramson, Chu and Kana (1966) forces and liquid free surface elevations for a vertical circular and a half-cylindrical tank, undergoing translational (sway) oscillations with small oscillation amplitudes, are given. For vertical circular cylindrical tanks there are also given some results in Hutton (1963), Sudo et.al. (1989) and in Barron and Roy Chng (1989) where stability of the fluid motions are studied.

To study sloshing in partially filled large offshore storage tanks Chakrabarti (1993) has done model tests with a cylindrical tank placed in a wave tank and supported to the floor of the tank on springs. External waves introduce movements of the tank due to elasticity in the wall and foundation and sloshing motions inside the tank are excited.

Results from model tests with rectangular and prismatic tanks with nonshallow liquid depth are given in Faltinsen (1974) and Olsen and Johnsen (1975). Free surface elevation, pressure and forces on the tank are measured for sway and roll motions of the tanks.

Results are given in Verhagen and Wijngaarden (1965) and in Olsen and Johnsen (1975) for shallow liquid depth in rectangular tanks.

Bosch and Vugts (1966) have studied roll damping of ships by free surface tanks. The wave motions inside a tank with shallow water depth and its effect on the ship motion are studied. Different water depths in the tank and positions of the tank with respect to the axis of rotation are studied.

In Det norske Veritas (1976) and Faltinsen et. al. (1974) there are given results from full scale measurements and model tests for sloshing in LNG carriers with prismatic and spherical tanks. In Faltinsen et. al.(1974) scaling criteria of modelling of LNG slosh behavior are considered, and in Det norske Veritas (1976) equipment for experimental work are described.

A comprehensive worldwide review of scale-model sloshing data for sloshing loads in both prismatic and spherical LNG cargo tanks with a wide range of fill depths, excitation frequencies and amplitudes is presented in Bass, Bowles and Cox (1980). The data are reduced to a common format for the purpose of defining design load coefficients. Additional laboratory experiments are conducted to establish the sloshing dynamic pressure-time histories which are necessary for structural response analysis. In Bass et.al. (1985) the state-of-the-art of modeling criteria for model tests with sloshing in LNG are outlined.

In Navickas et.al. (1981) the free surface configuration for model tests with a two-dimensional rectangular tank with chambered upper corners and height filling level is shown.

Mikelis, Miller and Taylor (1984) present results from model tests with a prismatic and a rectangular tank. The tanks are forced into roll motions and pressures on the tank walls and ceiling are measured. Results from experiments on a ship model with incorporated partially filled tanks are also presented and show the effect of coupling between sloshing and ship motions. Some of the same results are shown in Mikelis and Robson (1985).

Hamlin et. al. (1986) describe two sets of experiments. In the first one the objective was to measure sloshing forces on representative structural members within partially filled shiplike tank models and pressures on the boundaries. In the second one the effects of fill depth, excitation amplitude, superposition of different tank motions with different phase relations, different roll axis locations, and the effectiveness of various baffle configurations were studied.

Lepelletier and Raichlen (1988) have done model tests with translational motion of rectangular tanks with small water depths. The wave amplitude was measured at different locations in the tank for long time series of oscillations. Time histories of the free surface oscillations are shown for different periods of oscillations.

Tozawa and Sueoka (1989) have done experiments with roll oscillation of a model of the

center tank of an oil tanker. Tests are run for different filling ratios and in some cases vertical webs are installed in the tank.

Arai (1986) has done model tests with a two-dimensional rectangular tank undergoing harmonical roll motions. Pressures are measured on the tank wall for different water depths and with and without internal structures in the tank.

In Arai, Cheng and Inoue (1992) results from model tests with two-dimensional tanks with different tank ceiling inclinations and three-dimensional box shaped tanks with and without an internal bottom plate are given. The tanks are moved in roll and pressures are measured on the tank wall and ceiling. Photos of the free surface configuration in some of the test cases are shown. Results for two-dimensional tanks are also given in Arai (1984) and for three-dimensional box shaped tanks in Arai et.al. (1992).

2.4 Conclusions

Both analytical, numerical and experimental methods are used to study the free surface motion of fluid inside rigid containers. In table 2.1 there is given a summary of the analytical and numerical methods and the properties of the methods. The properties of the methods mentioned in table 2.1 are the ones which are described in the given literature. In the table it is not made any attempt to evaluate the goodness of the methods. Possibilities for extension of the methods to other tank configurations, more degrees of freedom of motion, coupling with ship motion etc. are not considered in the table.

Generally, the problem of liquid sloshing is a nonlinear phenomenon. The nonlinear analytical methods are limited to some simple tank geometries where it is possible to find the analytical solutions of the governing equations. The mathematical expressions are getting quite voluminous and difficult to handle, specially for the three-dimensional cases. But if the intention is for example to study the relationship between response amplitude and frequency, analytical solutions give a good description of the problem. The stability of the sloshing motions, and for three-dimensional cases, the occurrence of rotational sloshing, may also be studied by use of the nonlinear theory. In addition, the analytical solutions are valuable in verification of numerical codes.

Forces and moments on the tank may be obtained from the analytical solutions by integrating the pressure. The pressure is determined from the velocity potential. Local impact pressures which occur when the water hits the wall or the tank top cannot be predicted. The analytical solutions cannot handle breaking waves and spray. The analytical solutions may give good results for the special tank shapes, water depths, excitation amplitudes and frequencies where they apply. Linear theory can be used for small oscillations far away from resonance. The nonlinear analytical solutions for finite water depth can only handle forced harmonic oscillation with small excitation amplitudes. The shallow water theory predicts the conditions under which a hydraulic jump occur and gives reasonably good results for small oscillation amplitudes. The theory is valid for a frequency band around the first natural slosh frequency.

Both finite difference, boundary element and finite element methods are used to study the sloshing problem.

All finite difference methods in the presented literature are based on the Marker and Cell and the SOLA codes. The methods may be divided into two groups dependent on the way the methods treat the free surface; (1) The codes based on the SOLA-SURF technique, where the free surface elevation is given as a single valued function, and (2) the codes which uses the volume of fluid method (VOF).

For the SOLA-SURF codes, the slope of the free surface have to remain less than the cell aspect ratio. Because of the way that the VOF method keeps track of which cells contain fluid or not, the method can in principle be used for steep irregular surface contours and breaking waves in both shallow and nonshallow water. Methods based on the SOLA-SURF code may handle two-dimensional tanks. The VOF method is used both in two and three dimensions.

In principle, all the finite difference methods may handle different tank shapes, tanks with internal structures and different tank motions. In addition the codes based on the VOF method may handle large fluid motions, breaking waves and waves hitting the tank top. How good they are able to do this seems to vary from case to case, even when criteria for time step size and stability is taken care of, like in the FLOW-3D code presented in chapter 7.

Except for Ramaswamy and Kawahara (1987), which are studying a tank with inclined walls, all of the presented papers where the finite element method is used are dealing with two-dimensional rectangular tanks. But in principle, since the grid does not have to be structured, the finite element method should be able to handle complex tank geometries. The finite element method has been used for both potential flow and viscous flow. It is not clear from the papers how well the finite element methods are able to handle breaking waves, and how they eventually take care of the elements when an overturning wave is hitting the free surface again. The finite element method described by Nakayama and Washizu (1980) is said to be applicable to the analysis of the travelling wave in shallow water. This is not shown in the paper.

Generally, the papers treating the use of the finite element methods in the sloshing problem contain very few comparisons with model tests or theory. So, the given information is not enough as a basis for an evaluation of the methods. Both the chosen shape of the elements and the form of the prescribed functions and weighing functions will influence the solution, and should be investigated.

While in the finite difference and finite element methods one have to discretizise the whole fluid domain into meshes or elements, only the boundary of the fluid region has to be discretizised in the boundary element methods. Boundary element methods are used for two and three dimensional tanks, and may handle different tank shapes.

The boundary element methods are based on potential flow. This means that viscous effects are neglected. Since potential flow predicts no damping, steady state can never be reached in an initial value solution and an artificial damping term must be introduced into the solution to filter unphysical transient effects from the initial conditions.

None of the papers are studying the effect on the solution of different element lengths and time step size on the solution.

If certain marked points on the free surface are followed in time the boundary element method should be able to calculate breaking waves. It is not clear how to take care of the elements when an overturning wave is hitting the free surface again.

Method	Fluid properties	Tank shape	Motion	Degree of freedom	Water level	Breaking waves
Linear analytical solutions	Potential flow	Various 2D and 3D	Small, forced harmonically, far away from resonance	All	General	No
	Viscous flow	2D rectangular	Forced harmonically	Roll	General	
Nonlinear analytical solutions	Potential flow	2D rectangular	Small, forced harmonically motions near resonance	Horizontal or roll	Non-shallow and infinite	No
			Forced harmonically motions near resonance	Roll	Shallow	
		3D circular cylindrical	Small, forced harmonically motions near resonance	Horizontal	Non-shallow	
Boundary element methods (BEM)	Potential flow	Rotational symmetry	Forced harmonically	Horizontal	Non-shallow	No
	Potential flow with artificial damping	2D rectangular and inclined walls	Forced harmonically	Horizontal, vertical or roll		
Finite element methods (FEM)	Potential flow	2D rectangular	Forced harmonically	Horizontal, vertical or roll	Non-shallow and Shallow	(?)
	Viscous flow	2D rectangular and inclined walls	Forced harmonically	Roll	Non-shallow	
Finite difference methods (FDM) based on SOLA-SURF code	Viscous and nonviscous flow	2D arbitrary	Forced harmonically, irregular or coupled with ship motions	Horizontal, vertical, roll and coupled	Non-shallow	No
Finite difference methods based on VOF or with marker particles	Viscous and nonviscous flow	3D arbitrary	Forced harmonically or irregular	All, also coupled	Non-shallow and shallow	Yes

Table 2.1 Summary of methods and properties of methods used in the sloshing problem

3 POTENTIAL THEORY AND THE BOUNDARY VALUE PROBLEM

This chapter states the general assumptions and definitions in the potential theory solutions of the sloshing problem in chapter 4,5 and 6.

3.1 General formulation

The fluid is assumed to be homogeneous, nonviscous and incompressible. The flow field is irrotational, and there are no sinks or sources. The fluid is irrotational when the vorticity vector

$$\omega = \nabla \times V \tag{3.1}$$

is zero everywhere in the fluid. The fluid velocity vector V can then be expressed as

$$V = \nabla \Phi_T \tag{3.2}$$

i.e. as the gradient of a time-dependent velocity potential $\Phi_T(x,y,z,t)$ or $\Phi_T(r,\theta,z,t)$ in cartesian and cylindrical coordinates respectively. The cartesian coordinate system x,y,z is defined in Figure 3.1 and the cylindrical coordinate system in Figure 4.4.

The subscript T denotes that this is the total velocity potential. In cartesian coordinates we can write the velocity components along the x, y and z axis as

$$u = \frac{\partial \Phi_T}{\partial x} \qquad v = \frac{\partial \Phi_T}{\partial y} \qquad w = \frac{\partial \Phi_T}{\partial z} \tag{3.3}$$

In cylindrical coordinates the velocity components along the r,θ and z are

$$u_r = \frac{\partial \Phi_T}{\partial r} \qquad u_\theta = \frac{1}{r}\frac{\partial \Phi_T}{\partial \theta} \qquad w = \frac{\partial \Phi_T}{\partial z} \tag{3.4}$$

From equation (3.2) and the assumption of incompressibility

$$\nabla \cdot V = 0 \tag{3.5}$$

it follows that the velocity potential must satisfy the Laplace equation

$$\nabla^2 \Phi_T = 0 \tag{3.6}$$

The velocity potential Φ_T is then determined from the solution of the Laplace equation with appropriate boundary conditions. The pressure distribution follows from Bernoulli's equation

$$p + \rho g z + \rho \frac{\partial \Phi_T}{\partial t} + \frac{\rho}{2} V \cdot V = C \tag{3.7}$$

where p is the pressure, ρ is the fluid density, g is the gravitational acceleration, z=0 is the mean free-surface level and the constant C can, for the sloshing cases in chapter 4, 5 and 6, be related to the atmospheric pressure.

3.2 The boundary conditions

The solution has to satisfy the following boundary conditions on the free surface and the container walls and bottom.

3.2.1 Free surface conditions

The pressure on the free surface is set equal to a constant atmospheric pressure. Neglecting surface tension, the dynamic free surface condition can be written as

$$g\zeta + \frac{\partial \Phi_T}{\partial t} + \frac{1}{2}\left[\left(\frac{\partial \Phi_T}{\partial x}\right)^2 + \left(\frac{\partial \Phi_T}{\partial y}\right)^2 + \left(\frac{\partial \Phi_T}{\partial z}\right)^2\right] = 0 \tag{3.8}$$

on the free surface $z=\zeta(x,y,t)$. In cylindrical coordinates the dynamic free surface condition is

$$g\zeta + \frac{\partial \Phi_T}{\partial t} + \frac{1}{2}\left[\left(\frac{\partial \Phi_T}{\partial r}\right)^2 + \frac{1}{r^2}\left(\frac{\partial \Phi_T}{\partial \theta}\right)^2 + \left(\frac{\partial \Phi_T}{\partial z}\right)^2\right] = 0 \tag{3.9}$$

on the free surface $z=\zeta(r,\theta,t)$.

A fluid particle on the free-surface is assumed to stay on the free-surface. This leads to the kinematic free-surface condition. In cartesian coordinates

$$\frac{\partial \zeta}{\partial t} + \frac{\partial \Phi_T}{\partial x}\frac{\partial \zeta}{\partial x} + \frac{\partial \Phi_T}{\partial y}\frac{\partial \zeta}{\partial y} - \frac{\partial \Phi_T}{\partial z} = 0 \tag{3.10}$$

on the free surface $z=\zeta(x,y,t)$, and in cylindrical coordinates

$$\frac{\partial \zeta}{\partial t} + \frac{\partial \Phi_T}{\partial r}\frac{\partial \zeta}{\partial r} + \frac{1}{r^2}\frac{\partial \Phi_T}{\partial \theta}\frac{\partial \zeta}{\partial \theta} - \frac{\partial \Phi_T}{\partial z} = 0 \tag{3.11}$$

on the free surface $z=\zeta(r,\theta,t)$.

If the displacements, velocities and slopes of the liquid-free surface are small, the free-surface conditions may be linearized. This leads to the following linearized dynamic free-surface condition

$$g\zeta + \frac{\partial \Phi_T}{\partial t} = 0 \quad \text{on the mean free surface, } z = 0 \tag{3.12}$$

and the linearized kinematic free-surface condition

$$\frac{\partial \zeta}{\partial t} - \frac{\partial \Phi_T}{\partial z} = 0 \quad \text{on the mean free surface, } z = 0 \tag{3.13}$$

By eliminating ζ between these two relations, a single equation is obtained as

$$\frac{\partial^2 \Phi_T}{\partial t^2} + g\frac{\partial \Phi_T}{\partial z} = 0 \quad \text{on the mean free surface, } z = 0 \tag{3.14}$$

The free surface displacement, ζ, is obtained from the linearized dynamic free-surface condition when the velocity potential is known.

3.2.2 Body boundary conditions

The kinematic boundary condition is

$$\frac{\partial \Phi_T}{\partial n} = v_n \quad \text{at the container walls and bottom} \tag{3.15}$$

where $\partial/\partial n$ denotes differentiation in the direction normal to the surface of the rigid body in contact with the fluid, and v_n is the velocity of the boundary surface in the direction normal to the surface. Equation (3.15) expresses impermeability, i.e. that no fluid enters or leaves the body surface.

3.3 Definitions of motions

In the figure below, the definitions of the rigid-body motion modes are given. The sway motion is also referred to as translational motion or oscillation of the tank, and it is a oscillation along the x-axis. The roll motion is a rotational motion around the y-axis, and the heave motion is a vertical motion along the z-axis.

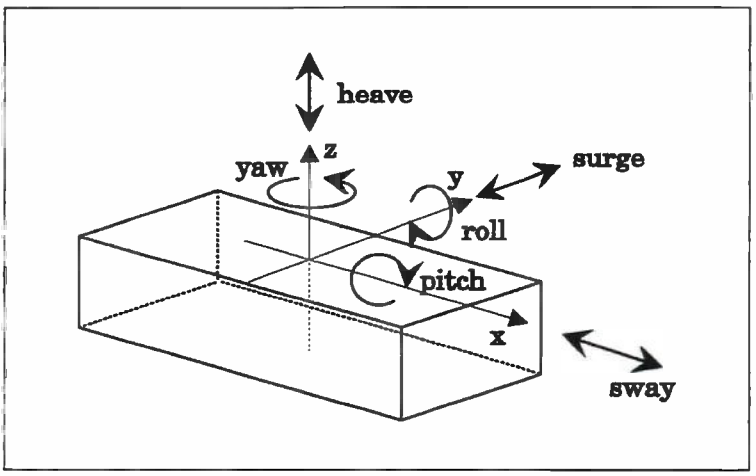

One should note that this is not a standard coordinate system for ship motion calculations. There it is common to define surge as translatory motion along the x-axis, sway as translatory motion along the y-axis and roll and pitch as angular motions around the x- and y-axis respectively.

Figure 3.1 Definition of rigid-body motion modes.

4 LINEAR POTENTIAL THEORY SOLUTIONS

Linear theory is used in this chapter to determine the eigenfrequencies and the velocity potential for the water inside a rigid rectangular two-dimensional tank and a vertical circular cylindrical tank. The velocity potential is determined for sway and roll motion of the tank.

The main reasons for presenting the linear theory are to make a basis for the nonlinear solutions presented in chapter 5 and 6, to make the presentation of the nonlinear solution in chapter 5 easier to follow and to determine the eigenfrequencies, which are used in the verification of the method in chapter 6. Linear solutions are also used for comparisons in chapter 7.

The general formulation of the problem is given in chapter 3. Laplace equation is solved with linearized boundary conditions on the tank bottom, walls and free surface. It is not possible to find the solution of this system of equations for all tank forms. In Abramson (1966) the potential theory solutions are presented for several tank shapes of rigid tanks. The velocity potential for sloshing due to sway and roll motion of a three-dimensional rectangular tank is given and is equivalent to the two-dimensional solution developed in chapter 4.1, when the y-dependence in the equations is removed and the coordinate system moved from having z=0 in the free surface to having z=0 in half of the water depth. The solution for a ring sector compartmented circular cylindrical tank, given in Abramson (1966), may be simplified to be equivalent to the solution developed in chapter 4.2 for sway and roll motion of a vertical circular cylindrical tank.

Since potential theory predicts no energy dissipation inside the tank, a damping term is introduced into the governing equations in chapter 4.3, and the effect of different values of the damping term is studied.

To be able to use linear theory, the displacements, velocities, and slopes of the liquid-free surface have to be small. This means that the frequencies of the tank motions have to be far away from resonance and the oscillation amplitudes of the tank motions small. If linear theory is used on frequencies near or at the resonance frequencies, the solution will blow up to infinity.

The velocity potential may be written as the sum of the container motion, ϕ_c, and the potential of the liquid moving relative to the container, Φ. That is

$$\Phi_T = \phi_c + \Phi \tag{4.1}$$

If the container is stationary, $\phi_c = 0$. If the container is in motion ϕ_c can be found by integrating the equation

$$\nabla \phi_c = V(container) \tag{4.2}$$

where V is the velocity of the container and the constant of integration may be taken as zero, since it can be absorbed in Φ.

4.1 Linear theory of lateral sloshing in a moving two-dimensional rectangular tank

The determination of the velocity potential for sway and roll motion of the two-dimensional rectangular tank follows notes from Faltinsen (1972). The tank geometry and coordinate system are shown in Figure 4.1. The tank breadth is 2a and the water depth h.

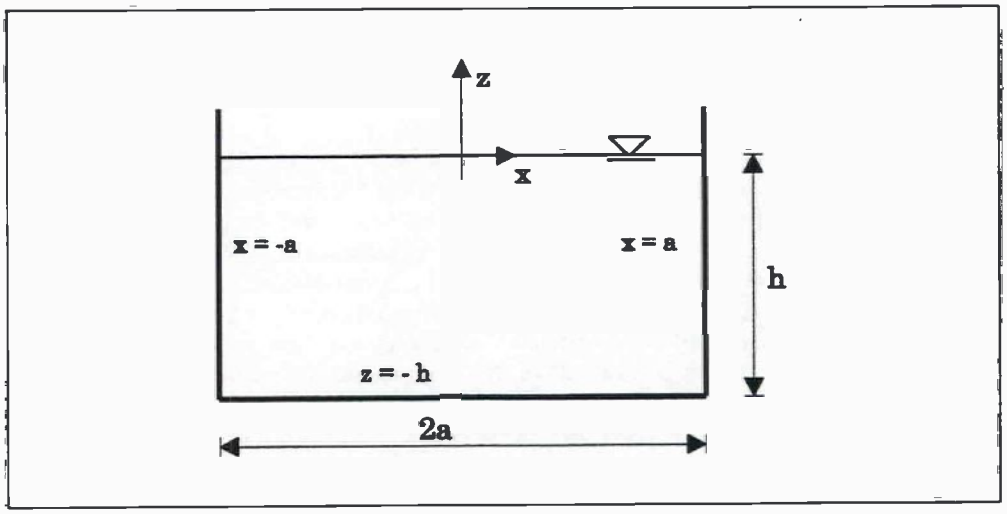

Figure 4.1 Container geometry and coordinate system for a two-dimensional rectangular tank.

4.1.1 The natural frequencies

The natural frequencies are obtained by studying linear free oscillations in the tank. That is, the fluid motion is free from the disturbing force that caused it, so there are no excitations of the tank.

The flow field of a liquid with free surface in a rectangular tank is obtained from the solution of the Laplace equation

$$\nabla^2\Phi = 0 \tag{4.3}$$

with the boundary conditions

$$\frac{\partial\Phi}{\partial z} = 0 \quad \text{at the tank bottom } z = -h \tag{4.4}$$

$$\frac{\partial\Phi}{\partial x} = 0 \quad \text{at the tank walls } x = \pm a \tag{4.5}$$

$$\frac{\partial^2\Phi}{\partial t^2}+g\frac{\partial\Phi}{\partial z}=0 \quad \text{at the mean free surface } z=0 \tag{4.6}$$

This linear boundary value problem may be solved by employing the method of separation of variables. From the Laplace equation and the body boundary conditions, a solution on the form

$$\Phi(x,z,t)=\sum_{n=0}^{n=\infty} C_n\cos[k(x+a)]\cosh[k(z+h)]\ \cos(\omega t) \tag{4.7}$$

is obtained. Here k = nπ/2a, and the unknown constants C_n can be obtained from the initial conditions.

The equation for the eigenvalues of the liquid, the natural frequencies, is obtained by putting equation (4.7) into the free surface condition. This gives

$$\sigma_n^2 = gk\tanh(kh) \quad \text{where} \quad k=\frac{n\pi}{2a} \quad \text{and} \quad n=1,2,... \tag{4.8}$$

The natural periods are then

$$T_n = \frac{2\pi}{\sqrt{\frac{n\pi}{2a}g\tanh\left[\frac{n\pi}{2a}h\right]}} \qquad \text{where } n=1,2,\ldots \tag{4.9}$$

It is seen from (4.9), that the natural periods of the liquid increases with decreasing liquid depth and with increasing tank breadth. This is also shown in Figure 6.5. For large values of nh/2a (i.e., nh/2a > 1), the approximation

$$\sigma_n^2 = kg \tag{4.10}$$

may be used. For small values of kh, the following approximation may be used

$$\sigma_n^2 = gk^2h \tag{4.11}$$

The velocity potential contains both symmetrical and antisymmetrical modes of motion. The first antisymmetrical mode is given by n=1 and is a wave with length equal to twice the tank breadth. The first symmetrical mode is given by n=2 and the wave length is equal to the tank breadth, as shown in Figure 4.2.

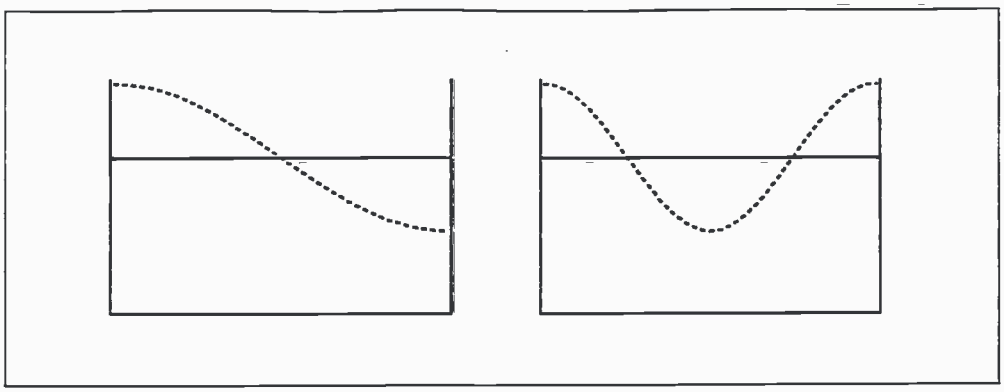

Figure 4.2 Modes of liquid motion: n=1 gives the first antisymmetrical sloshing mode (left) and n=2 the first symmetrical sloshing mode.

4.1.2 Forced sway oscillations

The linear, steady-state velocity potential is to be determined for forced sway oscillation of the tank $x_b = \varepsilon_0 \sin(\omega t)$ normal to the container wall. ε_0 is the amplitude of the container motion. The boundary conditions in this problem are:

$$\frac{\partial \Phi_T}{\partial x} = \varepsilon_0 \omega \cos(\omega t) \quad \text{at the tank wall } x = \pm a \tag{4.12}$$

$$\frac{\partial \Phi_T}{\partial z} = 0 \quad \text{at the bottom of the container } z = -h \tag{4.13}$$

$$\frac{\partial^2 \Phi_T}{\partial t^2} + g\frac{\partial \Phi_T}{\partial z} = 0 \quad \text{at the free surface } z = 0 \tag{4.14}$$

By extracting the container motion

$$\Phi_T = \Phi + \varepsilon_0 \omega x \cos(\omega t) \tag{4.15}$$

the boundary conditions for the disturbance potential, which are homogeneous at the container walls, are obtained as (4.4) at the tank bottom, (4.5) at the tank walls and

$$\frac{\partial^2 \Phi}{\partial t^2} + g\frac{\partial \Phi}{\partial z} = \varepsilon_0 x \omega^3 \cos(\omega t) \quad \text{at the free surface } z = 0 \tag{4.16}$$

By using separation of variables, the Laplace equation, by satisfying (4.4) and (4.5), and by observing from the right hand side in (4.16) that the x-dependence has to be antisymmetric, it follows that the velocity potential is given by

$$\Phi(x,z,t)=\sum_{n=0}^{\infty} C_n \cos(\omega t)\sin\left[\frac{2n+1}{2a}\pi x\right]\cosh\left[\frac{2n+1}{2a}\pi (z+h)\right] \tag{4.17}$$

To determine the unknown coefficients C_n from the free surface condition the right hand side of the boundary condition has to be expanded into a Fourier-series. If the velocity potential is put into the free surface condition, the following expression is obtained

$$\sum_{n=0}^{\infty} C_n \sin\left(\frac{2n+1}{2a}\pi x\right)\left\{-\omega^2\cosh\left(\frac{2n+1}{2a}\pi h\right)+g\frac{2n+1}{2a}\pi\sinh\left(\frac{2n+1}{2a}\pi h\right)\right\}=\omega^3\varepsilon_0 x \tag{4.18}$$

for $-a\le x\le a$ and $z=0$. The left hand side of this formula is an odd Fourier-series for $-2a\le x\le 2a$ where each second term is missing. To find C_n the right hand side may be written as Fourier-series in $-2a\le x\le 2a$. It is then necessary to define a function f(x) for $-2a\le x\le 2a$ so that $f(x)=x$ for $-a\le x\le a$ and so defined outside $-a\le x\le a$ that each second term in the Fourier-series of f(x) are missing. This means that f(x) in $0\le x\le 2a$ must have $x=a$ as a symmetric line. A corresponding evaluation is valid for $-2a\le x0$. So

$$f(x)=\begin{cases} x \text{ for } -a\le x\le a \\ 2a-x \text{ for } a\le x\le 2a \\ -2a-x \text{ for } -2a\le x\le -a \end{cases} \tag{4.19}$$

f(x) is now written as a Fourier-series

$$f(x)=\sum_{k=1}^{\infty} A_k \sin\left(\frac{k\pi}{2a}x\right) \tag{4.20}$$

where

$$A_k=\frac{2}{2a}\int_0^{2a} f(x)\sin\left(\frac{k\pi}{2a}x\right)dx=\begin{cases} \frac{2}{a}\left[\frac{2a}{(2n+1)\pi}\right]^2(-1)^n & \text{for } k=2n+1 \\ 0 & \text{for } k=2n \end{cases} \tag{4.21}$$

This gives

$$C_n=\frac{\varepsilon_0\omega\frac{2}{a}\left[\frac{2a}{(2n+1)\pi}\right]^2(-1)^n}{\cosh\left[\frac{2n+1}{2a}h\pi\right]}\frac{\omega^2}{\sigma_n^2-\omega^2} \tag{4.22}$$

where

$$\sigma_n^2=g\left(\frac{2n+1}{2a}\right)\pi\tanh\left[\frac{2n+1}{2a}h\pi\right] \tag{4.23}$$

These are the eigenfrequencies for the antisymmetrical modes.

The total velocity potential for sway motion of a rectangular tank contains only antisymmetrical modes and is obtained as

$$\Phi_T = \varepsilon_0 \omega \cos(\omega t)\left\{ x + \sum_{n=0}^{\infty} \frac{\omega^2}{\sigma_n^2-\omega^2} \frac{2}{a}\left[\frac{2a}{(2n+1)\pi}\right]^2 (-1)^n \frac{\sin\left[\frac{2n+1}{2a}\pi x\right]\cosh\left[\frac{2n+1}{2a}\pi (z+h)\right]}{\cosh\left[\frac{2n+1}{2a} h\pi\right]}\right\} \tag{4.24}$$

The first term in equation (4.24) is the velocity potential of the rigid body motion and satisfies the boundary conditions at the tank walls. The second term is the disturbance potential. Its normal velocities vanish at the tank walls. The free surface condition is satisfied by both parts of the velocity potential. It is seen from the term $\omega^2 / (\sigma_n^2-\omega^2)$, that the solution will blow up at resonance, that is when the frequency of oscillation ω, is equal to one of the resonance frequencies σ_n.

Free surface displacement

The surface displacement of the liquid, which is measured from the undisturbed position of the liquid, may be obtained from the linearized dynamic free surface condition, when the velocity potential is known. The free surface condition gives

$$\zeta = -\frac{1}{g}\frac{\partial \Phi_T}{\partial t} \quad \text{on } z=0 \tag{4.25}$$

and the free surface displacement is then

$$\zeta = \frac{\omega^2 \varepsilon_0}{g} \sin(\omega t)\left\{ x + \sum_{n=0}^{\infty} \frac{\omega^2}{\sigma_n^2-\omega^2} \frac{2}{a}\left[\frac{2a}{(2n+1)\pi}\right]^2 (-1)^n \sin\left[\frac{(2n+1)}{2a}\pi x\right]\right\} \tag{4.26}$$

Pressure and horizontal force on the tank

The excess pressure relative to the atmospheric pressure is obtained from Bernoulli's equation. By integration of the pressure distribution, the liquid forces and moments can be obtained. By linearizing, the Bernoulli's equation is obtained as

$$p + \rho \frac{\partial \Phi_T}{\partial t} + \rho g z = 0 \tag{4.27}$$

The pressure at a point (x,z) is then

$$p=\rho\,\varepsilon_0\omega^2\sin(\omega t)\left\{x+\sum_{n=0}^{\infty}\frac{\omega^2}{\sigma_n^2-\omega^2}\,\frac{2}{a}\left[\frac{2a}{(2n+1)\pi}\right]^2(-1)^n\frac{\sin\left[\frac{2n+1}{2a}\pi x\right]\cosh\left[\frac{2n+1}{2a}\pi(z+h)\right]}{\cosh\left[\frac{2n+1}{2a}h\pi\right]}\right\}-\rho g z \tag{4.28}$$

The linear hydrodynamic force on the tank in x-direction follows by integrating the pressure from the tank bottom to the still water level. It can be written as

$$F_x=\rho\,\varepsilon_0\omega^2 2ahl\sin(\omega t)\left\{1+\sum_{n=0}^{\infty}\frac{\omega^2}{\sigma_n^2-\omega^2}\,\frac{16a}{h}\,\frac{\tanh\left[\frac{2n+1}{2a}\pi h\right]}{(2n+1)^3\pi^3}\right\} \tag{4.29}$$

where l is the length unit of the tank in the y-direction. The fluid velocity relative to the tank may be determined by derivation of the velocity potential.

4.1.3 Forced roll oscillations

The steady state velocity potential is to be determined for a rotational excitation $\Theta=\Theta_0\sin(\omega t)$ of the container about an axis located at x=0 and in the middle between the tank bottom and the undisturbed fluid surface, z=-h/2. Θ_0 is the amplitude of the roll motion of the tank. The tank and its coordinate system are shown in Figure 4.3.

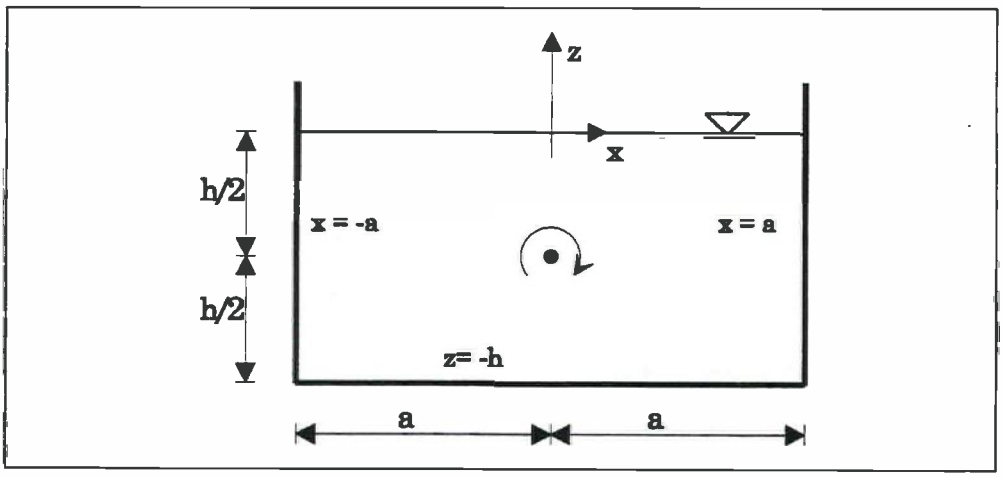

Figure 4.3 Coordinate system for roll motion of rectangular tank.

The body boundary conditions are

$$\frac{\partial \Phi_T}{\partial x} = \omega \Theta_0 \cos(\omega t)\left(z+\frac{h}{2}\right) \quad \text{at the tank wall } x=\pm a \tag{4.30}$$

$$\frac{\partial \Phi_T}{\partial z} = -\omega \Theta_0 \cos(\omega t) x \quad \text{at the tank bottom } z=-h \tag{4.31}$$

and the linear free surface condition, equation (4.14).

The velocity potential of the tank motion

To find the velocity potential of the tank motion a velocity potential, $\phi_c = \phi_1 + \phi_2$, which satisfies the boundary condition on the tank walls and the tank bottom, is constructed. The two potentials ϕ_1 and ϕ_2 satisfy Laplace equation.

The potential ϕ_1 is defined to satisfy

$$\frac{\partial \phi_1}{\partial x} = \omega \Theta_0 \cos(\omega t)\left(z+\frac{h}{2}\right) \quad \text{at the tank wall } x=\pm a \tag{4.32}$$

and

$$\frac{\partial \phi_1}{\partial z} = 0 \quad \text{at the tank bottom } z=-h \tag{4.33}$$

The potential ϕ_2 is defined to satisfy

$$\frac{\partial \phi_2}{\partial x} = 0 \quad \text{at the tank wall } x=\pm a \tag{4.34}$$

and

$$\frac{\partial \phi_2}{\partial z} = -\omega \Theta_0 \cos(\omega t) x \quad \text{at the tank bottom } z=-h \tag{4.35}$$

The solution for ϕ_2 is determined by separation of variables. The x-dependence is antisymmetric and together with Laplace equation and the boundary condition on x=±a, the solution for ϕ_2 is

$$\phi_2 = \sum_{n=0}^{\infty} A_n \cosh\left(\frac{2n+1}{2a}\pi z\right) \sin\left(\frac{2n+1}{2a}\pi x\right) \tag{4.36}$$

The boundary condition on z=-h gives

$$\left.\frac{\partial \phi_2}{\partial z}\right|_{z=-h} = \sum_{n=0}^{\infty} A_n \frac{2n+1}{2a}\pi \sinh\left(-\frac{2n+1}{2a}\pi h\right) \sin\left(\frac{2n+1}{2a}\pi x\right) = -\omega \Theta_0 \cos(\omega t) x \tag{4.37}$$

To find A_n, the right hand side of the equation may be written as a Fourier-series in $-2a \le x \le 2a$ in the same manner as for the transverse motion. This gives

$$A_n = \frac{\omega \Theta_0 \cos(\omega t) \frac{2}{a} \left[\frac{2a}{(2n+1)\pi} \right]^3 (-1)^n}{\sinh\left(\frac{2n+1}{2a} \pi h \right)} \tag{4.38}$$

The solution for ϕ_1 is also determined by separation of variables. The z-dependence is antisymmetric about z = - h/2 and together with Laplace equation and the boundary condition on z = - h, the solution for ϕ_1 may be written

$$\phi_1 = \sum_{n=0}^{\infty} B_n \sin\left[\frac{2n+1}{h} \pi \left(z + \frac{h}{2} \right) \right] \sinh\left(\frac{2n+1}{h} \pi x \right) \tag{4.39}$$

The boundary condition on x=a gives

$$\left. \frac{\partial \phi_1}{\partial x} \right|_{x=a} = \sum_{n=0}^{\infty} B_n \frac{2n+1}{h} \pi \sin\left[\frac{2n+1}{h} \pi \left(z + \frac{h}{2} \right) \right] \cosh\left(\frac{2n+1}{h} \pi a \right) = \omega \Theta_0 \cos(\omega t) \left(z + \frac{h}{2} \right) \tag{4.40}$$

The left hand side is an odd Fourier-series for $-h \le z+h/2 \le h$ where each second term are missing. To find B_n the right hand side of the equation is written as a Fourier-series in $-h \le z' \le h$, where $z' = z+h/2$, in the same manner as for the transverse motion. This gives

$$B_n = \frac{\omega \Theta_0 \cos(\omega t) \frac{4}{h} \left[\frac{h}{(2n+1)\pi} \right]^3 (-1)^n}{\cosh\left(\frac{2n+1}{h} \pi a \right)} \tag{4.41}$$

and then, the velocity potential for the tank motion is obtained as

$$\phi_c = \omega \Theta_0 \cos(\omega t) \sum_{n=0}^{\infty} \frac{1}{(2n+1)^3 \pi^3} (-1)^n \left\{ \frac{16a^2}{\sinh\left(\frac{2n+1}{2a} \pi h \right)} \cosh\left(\frac{2n+1}{2a} \pi z \right) \sin\left(\frac{2n+1}{2a} \pi x \right) + \right. \tag{4.42}$$

$$\left. \frac{4h^2}{\cosh\left(\frac{2n+1}{h} \pi a \right)} \sin\left[\frac{2n+1}{h} \pi \left(z + \frac{h}{2} \right) \right] \sinh\left(\frac{2n+1}{h} \pi x \right) \right\}$$

The total velocity potential

The total velocity potential is $\Phi_T = \Phi + \phi_c$, where ϕ_c is the velocity potential for the container motion, given above, and Φ is the velocity potential for the liquid moving relative to the container. Φ_T must satisfy the free surface condition (4.14) at the mean free surface z=0. Assuming that the time dependence of the velocity potential is $\Phi(x,z,t) = \phi(x,z)\cos(\omega t)$, the free surface boundary condition will be

$$-\omega^2\Phi + g\frac{\partial\Phi}{\partial z} =$$

$$\omega^3\Theta_0\cos(\omega t)\sum_{n=0}^{\infty}\frac{(-1)^n}{(2n+1)^3\pi^3}\left\{\frac{16a^2\sin\left(\frac{2n+1}{2a}\pi x\right)}{\sinh\left(\frac{2n+1}{2a}\pi h\right)}+\frac{4h^2(-1)^n\sinh\left(\frac{2n+1}{h}\pi x\right)}{\cosh\left(\frac{2n+1}{h}\pi a\right)}\right\} \tag{4.43}$$

A Fourier-series expansion of $\sinh[\pi x(2n+1)/h]$ is now needed. This expansion is carried out in appendix A. The boundary condition on z=0 may now be written as:

$$-\omega^2\Phi + g\frac{\partial\Phi}{\partial z} =$$

$$\omega^3\Theta_0\cos(\omega t)\sum_{\nu=0}^{\infty}(-1)^{\nu}\sin\left(\frac{2\nu+1}{2a}\pi x\right)\frac{8a}{\pi^2(2\nu+1)^2}\left\{\frac{h}{2}-\frac{4a\tanh\left(\pi\frac{2\nu+1}{4a}h\right)}{(2\nu+1)\pi}+\frac{g}{\sigma_\nu^2}\right\} \tag{4.44}$$

If the velocity potential for the liquid is written as

$$\Phi = \sum_{n=0}^{\infty}K_n\sin\left(\frac{2n+1}{2a}\pi\ x\right)\cosh\left(\frac{2n+1}{2a}\pi\,(z+h)\right)\cos(\omega t) \tag{4.45}$$

and is put into the boundary condition on z=0, K_n is obtained as

$$K_n = \frac{\omega^3\Theta_0(-1)^n\frac{8a}{\pi^2(2n+1)^2}\left[\frac{h}{2}-\frac{4a\tanh\left(\frac{2n+1}{4a}\pi h\right)}{(2n+1)\pi}+\frac{g}{\sigma_n^2}\right]}{-\omega^2\cosh\left(\frac{2n+1}{2a}\pi h\right)+g\pi\frac{2n+1}{2a}\sinh\left(\frac{2n+1}{2a}\pi h\right)} \tag{4.46}$$

and the velocity potential for the liquid motion is then

$$\Phi = \omega\Theta_0\cos(\omega t)\sum_{n=0}^{\infty}\frac{8a(-1)^n}{\pi^2(2n+1)^2}\left[\frac{h}{2}-\frac{4a\tanh\left(\frac{2n+1}{4a}\pi h\right)}{(2n+1)\pi}+\frac{g}{\sigma_n}\right]$$
$$\left(\frac{\omega^2}{\sigma_n^2-\omega^2}\right)\sin\left(\frac{2n+1}{2a}\pi x\right)\frac{\cosh\left(\frac{2n+1}{2a}\pi (z+h)\right)}{\cosh\left(\frac{2n+1}{2a}\pi h\right)} \qquad (4.47)$$

where the eigenfrequencies σ_n are given by equation (4.23).

4.1.4 Combination of sway and roll

If sway and roll motions of the tank are to be combined, the contribution from the two modes of motion to the velocity potential may be added, since linear theory is used. Note that there may be a phase difference between the two motions, which may be included by introducing a phase angle, β, in one of the solutions, for example in the sway motion as $x_b=\varepsilon_0\sin(\omega t+\beta)$.

4.2 Linear theory of lateral sloshing in a moving vertical circular cylindrical tank

Lateral sloshing occurs primarily in response to translational or roll/pitch motions of the tank. The velocity potential is determined for sway, roll and rotation about z-axis (yaw) motion of the circular cylindrical tank. The obtained results for translational motion are in accordance with the results given in Abramson (1966). The tank geometry and coordinate system are shown in Figure 4.4.

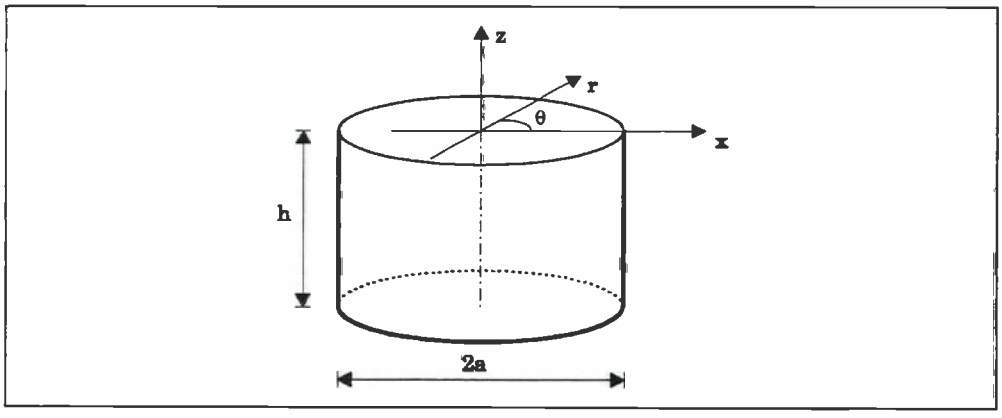

Figure 4.4 Coordinate system for a vertical circular cylindrical tank.

4.2.1 The natural frequencies

The flow field of a liquid with free surface in a cylindrical container is obtained from the solution of the Laplace equation with the boundary condition (4.4) at the tank bottom z = -h,

$$\frac{\partial \Phi}{\partial r}=0 \quad \text{at the cylinder wall } r=a \tag{4.48}$$

and the linearized free surface condition (4.6) are the mean free surface z=0.

In the same manner as for the two-dimensional case, this linear boundary value problem may be solved by employing the method of separation of variables. Laplace equation, together with the body boundary conditions give a solution in the form

$$\Phi(r,\theta,z,t)=\sum_{m=0}^{\infty}\sum_{n=0}^{\infty} C_{mn}\, e^{i\omega t}\cos(m\theta)\frac{\cosh\left[\xi_{mn}\left(\frac{z}{a}+\frac{h}{a}\right)\right]}{\cosh\left(\xi_{mn}\frac{h}{a}\right)} J_m\left(\xi_{mn}\frac{r}{a}\right) \tag{4.49}$$

Here i means the complex unit. When complex quantities are used, it is understood that it is the real value of the quantity that has physical meaning. J_m, m=0,1,..., are Bessel functions of the first kind. The r-dependence cannot include Bessel functions of the second kind, Y_m, since $Y_m(\xi_{mn}r/a)$ becomes infinite as $r\to 0$. The unknown constants C_{mn} can be obtained from the initial conditions and the values ξ_{mn} are the positive roots of the equation

$$J_m'(\xi)=0 \tag{4.50}$$

The equation for the eigenvalues of the liquid, the natural frequencies, is obtained from the free surface condition to be

$$\sigma_{mn}^2=\frac{g}{a}\xi_{mn}\tanh\left(\xi_{mn}\frac{h}{a}\right) \qquad m,n=0,1,... \tag{4.51}$$

In the case m = 0, the motion is symmetrical about r = 0, and the lowest roots of $J_0'(\xi_{0n})=J_1(\xi_{0n})=0$ are given in Table 4.1. The most interesting modes of the antisymmetrical class are those corresponding to m=1. The lowest roots of $J_1'(\xi_{1n}) = 0$ are given in Table 4.2

n	ξ
1	0.0000
2	3.8317
3	7.0160

Table 4.1 **Lowest roots of $J_0'(\xi_{0n})=0$.**

n	ξ
1	1.841
2	5.332
3	8.536

Table 4.2 **Lowest roots of $J_1'(\xi_{1n})=0$.**

The eigenfrequencies of the liquid decrease with decreasing liquid depth and with increasing tank radius. For large values of h/a (i.e., h/a > 2), the following approximation is accurate.

$$\sigma_{mn}^2 = \frac{g}{a}\xi_{mn} \tag{4.52}$$

For small values of h/a, the approximation

$$\sigma_{mn}^2 = g\left(\frac{\xi_{mn}}{a}\right)^2 h \tag{4.53}$$

may be used.

4.2.2 Forced sway oscillations

The linear steady-state velocity potential is to be determined for forced excitation $x_b=\varepsilon_0 e^{i\omega t}$ normal to the container wall. The boundary conditions are:

$$\frac{\partial \Phi_T}{\partial r} = i\omega\varepsilon_0 e^{i\omega t}\cos\theta \quad \text{at the circular cylindrical tank wall } r=a \tag{4.54}$$

(4.13) at the tank bottom, and the linearized free surface condition (4.14). By extracting the container motion

$$\Phi_T = [\Phi + i\omega\varepsilon_0 r\cos\theta]e^{i\omega t} \tag{4.55}$$

boundary conditions for the disturbance potential, which are homogeneous at the container walls, are obtained as (4.48) at the cylinder walls, (4.4) at the tank bottom, and

$$g\frac{\partial \Phi}{\partial z} - \omega^2\Phi = i\omega^3\varepsilon_0 r\cos\theta \quad \text{at the free surface } z=0 \tag{4.56}$$

Therefore the disturbance potential $\Phi(r,\theta,z)$ which satisfies the Laplace equation has the same form as in equation (4.49).

$$\Phi(r,\theta,z) = \sum_{m=0}^{\infty}\sum_{n=0}^{\infty} C_{mn}\cos(m\theta)\frac{\cosh\left[\xi_{mn}\left(\frac{z}{a}+\frac{h}{a}\right)\right]}{\cosh\left(\xi_{mn}\frac{h}{a}\right)} J_m\left(\xi_{mn}\frac{r}{a}\right) \tag{4.57}$$

To determine the unknown coefficients C_{mn} from the free surface condition the right hand side of the boundary condition has to be expanded into a series. When the velocity potential from equation (4.57) is put into the free surface condition (4.56), the following expression is obtained

$$C_{mn} J_m\left(\xi_{mn}\frac{r}{a}\right)\cos(m\theta)\left[\omega_{mn}^2 - \omega^2\right] = i\omega^3\varepsilon_0 r\cos\theta \tag{4.58}$$

$f(\theta) = \cos\theta$ is expanded into a Fourier series

$$f(\theta) = a_0 + \sum_{m=1}^{\infty} a_m \cos(m\theta) \tag{4.59}$$

where the coefficients are given as

$$a_0 = \frac{1}{\pi}\int_0^{\pi} f(\theta)\, d\theta \quad \text{and} \quad a_m = \frac{2}{\pi}\int_0^{\pi} f(\theta)\cos(m\theta)\, d\theta \tag{4.60}$$

This gives $a_0 = 0$, $a_1 = 1$ and $a_{m\neq 1} = 0$. That is, m = 1 and then

$$C_n J_1\left(\xi_n \frac{r}{a}\right)\left(\sigma_n^2 - \omega^2\right) = i\omega^3 \varepsilon_0 r \tag{4.61}$$

f(r) = r is expanded into a Bessel series

$$r = f(r) = \sum_{n=0}^{\infty} A_{1n} J_1\left(\xi_{1n}\frac{r}{a}\right) \qquad 0 < \frac{r}{a} < 1 \tag{4.62}$$

where ξ_{1n} are the positive roots of $J_1'(\xi)=0$ and the coefficient

$$A_n = \frac{2\xi_n^2}{(\xi_n^2 - 1)J_1^2(\xi_n)}\int_0^1 \frac{r}{a} J_1\left(\xi_n \frac{r}{a}\right) r \frac{dr}{a} = \frac{2a}{(\xi_n^2 - 1)J_1(\xi_n)} \tag{4.63}$$

This gives

$$C_n = \frac{i\omega^3 \varepsilon_0 2a}{(\sigma_n^2 - \omega^2)(\xi_n^2 - 1)J_1(\xi_n)} \tag{4.64}$$

and the total velocity potential for translational oscillation of the container in x-direction of the form $\varepsilon_0 e^{i\omega t}$ is then

$$\Phi(r,\theta,z,t) = i\omega\varepsilon_0 e^{i\omega t} a\cos\theta \left\{ \frac{r}{a} + 2\sum_{n=0}^{\infty} \frac{J_1(\xi_n \frac{r}{a})\left(\frac{\omega}{\sigma_n}\right)^2 \cosh\left[\xi_n\left(\frac{z}{a}+\frac{h}{a}\right)\right]}{(\xi_n^2 - 1)J_1(\xi_n)\cosh(\xi_n \frac{h}{a})\left(1 - \frac{\omega^2}{\sigma_n^2}\right)} \right\} \tag{4.65}$$

The first term is the potential of the rigid body and satisfies the boundary condition at the tank walls. The second part, the disturbance potential, vanishes at the tank walls. The free surface condition is satisfied by both parts of the formula. ξ_n are the roots of the equation $J_1'(\xi_n) = 0$, which are the antisymmetrical modes corresponding to m=1. So, the velocity potential for sway motion of the tank, contains only antisymmetrical modes of motion.

Free surface displacement

The free surface displacement of the liquid are obtained from the linearized dynamic free

surface condition to be

$$\zeta = \omega^2 \varepsilon_0 e^{i\omega t} \frac{a}{g} \cos\theta \left\{ \frac{r}{a} + 2 \sum_{n=0}^{\infty} \frac{J_1\left(\xi_n \frac{r}{a}\right)}{(\xi_n^2 - 1) J_1(\xi_n) \left(\frac{\sigma_n^2}{\omega^2} - 1\right)} \right\} \tag{4.66}$$

In the free surface displacement, the first term represents the displacement with respect to small excitation frequency. For these the surface displacement of the liquid (neglecting terms of ω^4) forms a plane of the form $r\cos\theta$. With increasing excitation amplitude ε_0, the free surface amplitude becomes larger.

Pressure and liquid forces

The excess pressure relative to the atmospheric pressure is obtained from the Bernoulli's equation. By integration of the pressure distribution, the liquid forces and moments can be obtained. From the linearized Bernoulli's equation the total excess pressure at a point (r,θ,z) is obtained as

$$p = \rho g \omega^2 \varepsilon_0 e^{i\omega t} a \cos\theta \left\{ \frac{r}{a} + 2 \sum_{n=0}^{\infty} \frac{J_1\left(\xi_n \frac{r}{a}\right) \cosh\left[\xi_n \left(\frac{h}{a} + \frac{z}{a}\right)\right]}{(\xi_n^2 - 1) J_1(\xi_n) \cosh\left(\xi_n \frac{h}{a}\right) \left(\frac{\sigma_n^2}{\omega^2} - 1\right)} \right\} - \rho g z \tag{4.67}$$

The resulting force on the tank in x-direction is given by

$$F_x = \left[\int_{-h}^{0} \int_{0}^{2\pi} p a \cos\theta \, d\theta \, dz \right]_{r=a} = \rho \pi a^2 h \omega^2 \varepsilon_0 e^{i\omega t} \left\{ 1 + 2 \sum_{n=0}^{\infty} \frac{\tanh\left(\xi_n \frac{h}{a}\right)}{\frac{\xi_n h}{a} (\xi_n^2 - 1) \left(\frac{\sigma_n^2}{\omega^2} - 1\right)} \right\} \tag{4.68}$$

4.2.3 Forced roll oscillations

A rotational (roll-type motion) excitation of the container about the y-axis is considered. The origo of the coordinate system is placed in the middle between the tank bottom and the undisturbed fluid surface, as shown in Figure 4.5.

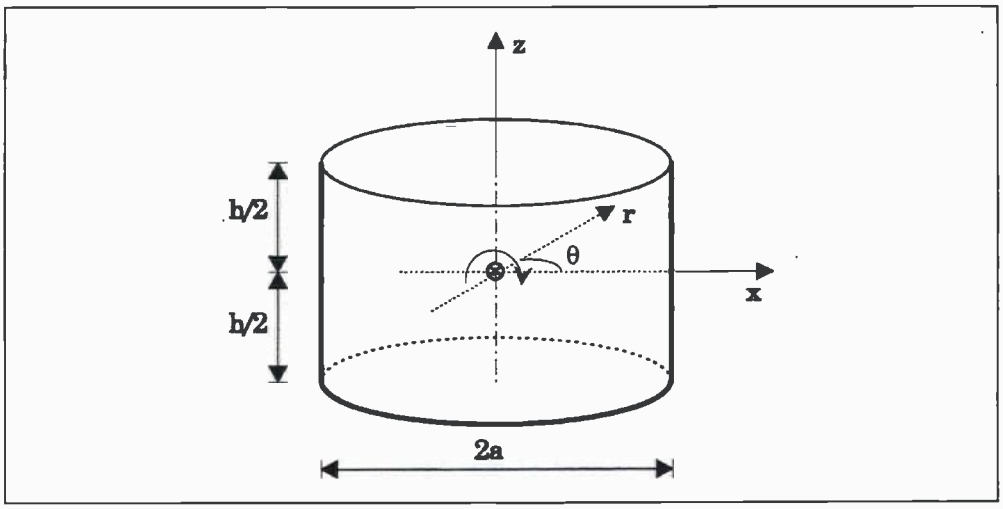

Figure 4.5 Coordinate system, roll motion of vertical circular cylindrical tank.

For a forced excitation $\Theta=\Theta_0 e^{i\omega t}$ about the y-axis, the boundary conditions are:

$$\frac{\partial \Phi_T}{\partial r} = i\omega\Theta_0 e^{i\omega t} z\cos\theta \quad \text{at the tank wall } r=a \tag{4.69}$$

$$\frac{\partial \Phi_T}{\partial z} = -i\omega\Theta_0 e^{i\omega t} r\cos\theta \quad \text{at the tank bottom } z=-\frac{h}{2} \tag{4.70}$$

$$\frac{\partial^2 \Phi_T}{\partial t^2} + g\frac{\partial \Phi_T}{\partial z} = 0 \quad \text{at the free surface } z=\frac{h}{2} \tag{4.71}$$

The total potential may be written as

$$\Phi_T = i\omega r z \Theta_0 \cos\theta\, e^{i\omega t} + \Phi\, e^{i\omega t} \tag{4.72}$$

where the first part is the rigid body potential and the second part is the velocity potential for the water inside the tank. The boundary condition at the tank wall can be made homogeneous by extracting the container motion. This gives

$$\frac{\partial \Phi}{\partial r} = 0 \quad \text{at the tank wall } r=a \tag{4.73}$$

$$\frac{\partial \Phi}{\partial z} = -2i\omega\Theta_0 r\cos\theta \quad \text{at the tank bottom } z=-\frac{h}{2} \tag{4.74}$$

and

$$g\frac{\partial\Phi}{\partial z}-\omega^2\Phi = i\omega\left(\frac{r}{a}\right)a^2\Theta_0\cos\theta\left(\frac{\omega^2}{2}\frac{h}{a}-\frac{g}{a}\right) \quad \text{at the free surface } z=\frac{h}{2} \tag{4.75}$$

Both boundary conditions can not be made homogeneous, and Laplace equation is solved with the obtained inhomogeneous boundary conditions. The solution of the Laplace equation which satisfies the boundary condition at the tank wall r=a, is obtained by separation of variables to be

$$\Phi=\left[A\cosh\left(\xi_{mn}\frac{z}{a}\right)+B\sinh\left(\xi_{mn}\frac{z}{a}\right)\right]J_m\left(\xi_{mn}\frac{r}{a}\right)\cos(m\theta) \tag{4.76}$$

where ξ_{mn} are the positive roots of $J_m'(\xi)$, m,n=0,1,2,3,....

The boundary condition at the tank bottom z=-h/2 gives, when $F(\theta)=\cos\theta$ are expanded into a Fourier series and f(r)=r are expanded into a Bessel series, m=1 and

$$A_n\sinh\left(\frac{\xi_n}{a}\frac{h}{2}\right)-B_n\cosh\left(\frac{\xi_n}{a}\frac{h}{2}\right)=\frac{4i\omega\Theta_0a^2}{\xi_n(\xi_n^2-1)J_1(\xi_n)} \tag{4.77}$$

In the same manner, the free surface condition at z=h/2 gives

$$kg\left[A_n\sinh\left(k\frac{h}{2}\right)+B_n\cosh\left(k\frac{h}{2}\right)\right]-\omega^2\left[A_n\cosh\left(k\frac{h}{2}\right)+B_n\sinh\left(k\frac{h}{2}\right)\right]=K\left(\omega^2\frac{h}{2}-g\right) \tag{4.78}$$

where

$$k=\frac{\xi_n}{a} \quad \textit{and} \quad K=\frac{2ai\omega\Theta_0}{(\xi_n^2-1)J_1(\xi_n)} \tag{4.79}$$

Equation (4.77) and (4.78) gives

$$B_n=\frac{K}{\cosh(kh)\left(\frac{\sigma_n^2}{\omega^2}-1\right)}\left[\sinh\left(k\frac{h}{2}\right)\left(\frac{h}{2}-\frac{3g}{\omega^2}\right)+\frac{2}{k}\cosh\left(k\frac{h}{2}\right)\right] \tag{4.80}$$

and

$$A_n=\frac{K}{\cosh(kh)\left(\frac{\sigma_n^2}{\omega^2}-1\right)}\left[\cosh\left(k\frac{h}{2}\right)\left(\frac{h}{2}-\frac{3g}{\omega^2}\right)+\frac{2}{k}\frac{\cosh^2\left(k\frac{h}{2}\right)}{\sinh\left(k\frac{h}{2}\right)}\right]-\frac{2K}{k\sinh\left(k\frac{h}{2}\right)} \tag{4.81}$$

The total velocity potential for rotational excitation $\Theta = \Theta_0 e^{i\omega t}$ is then

$$\Phi_T = \left\{ i\omega r z \Theta_0 + \left[A_n \cosh\left(\xi_n \frac{z}{a}\right) + B_n \sinh\left(\xi_n \frac{z}{a}\right) \right] J_1\left(\xi_n \frac{r}{a}\right) \right\} \cos(\theta) e^{i\omega t} \qquad (4.82)$$

where A_n and B_n are given above.

4.2.4 Forced yaw oscillations

For a forced rotation of the tank about the z-axis (yaw motion) The boundary condition will be

$$\frac{\partial \Phi_T}{\partial z} = 0 \quad \text{at the tank bottom } z = -h \qquad (4.83)$$

$$\frac{\partial \Phi_T}{\partial r} = 0 \quad \text{at the tank wall } r = a \qquad (4.84)$$

$$\frac{\partial^2 \Phi_T}{\partial t^2} + g \frac{\partial \Phi_T}{\partial z} = 0 \quad \text{at the free surface } z = 0 \qquad (4.85)$$

There will not be any motion of the water inside the circular cylindrical tank due to yaw motion of the tank, when linear potential theory is used .

4.3 Introduction of a damping term in the potential theory model

Potential theory predicts no energy dissipation inside the tank, but experimental results with free oscillations in a tank, Case and Parkinson (1957), showed clearly damped behaviour of the liquid response. There will always be some energy dissipation during sloshing motions. The amount of energy dissipation will depend on the tank shape, interior structures, wall roughness and boundary layer friction, fluid viscosity, free surface boundary layer and turbulence. This energy dissipation is related to damping of the fluid motion.

To simulate the effect of viscous damping in a linear potential-theory model for sloshing in a rectangular tank, Faltinsen (1978) introduced a fictitious small term in the Euler equation, which is the assumption of the existence of a force which opposes the particle velocity. The Euler equation is then given by

$$\frac{D\vec{v}}{Dt} = -\frac{1}{\rho} g \nabla z - \mu \nabla \Phi_T \qquad (4.86)$$

where the μ may be seen as a kind of viscosity coefficient. By integration, he obtained a modified Bernoulli equation

$$\frac{p}{\rho}+gz+\frac{\partial\Phi_T}{\partial t}+\frac{1}{2}\left\{\left(\frac{\partial\Phi_T}{\partial x}\right)^2+\left(\frac{\partial\Phi_T}{\partial z}\right)^2\right\}+\mu\Phi_T=C \tag{4.87}$$

where C is a constant. This means that the dynamic free-surface condition get an additional term $\mu\Phi_T$. The kinematic free-surface condition reminds unchanged, and the combined linear free-surface condition becomes

$$\frac{\partial^2\Phi_T}{\partial t^2}+\mu\frac{\partial\Phi_T}{\partial t}+g\frac{\partial\Phi_T}{\partial z}=0 \quad \text{at the free surface } z=0 \tag{4.88}$$

The damping coefficient, μ, is assumed to be small,much smaller than the critical damping

$$\mu_{crit}=2\sigma_1 \tag{4.89}$$

where σ_1 is the first natural frequency. The damping coefficient may be written as

$$\mu=\frac{2\delta}{T_1} \tag{4.90}$$

for small μ, where δ is the logarithmic decrement, defined in Abramson (1966) as

$$\delta = \ln\frac{\textit{Maximum amplitude of any oscillation}}{\textit{Maximum amplitude 1 cycle later}} \tag{4.91}$$

From equation (4.91) and (4.90) the amplitude after n oscillation periods may be determined by

$$a_n = \left(\frac{1}{e^{\delta}}\right)^n a_0 \tag{4.92}$$

where a_0 is the amplitude of any oscillation and a_n is the amplitude n oscillations later. If, for example, μ is 5 percent of critical damping, the logarithmic decrement $\delta = 0.314$, and after 10 oscillation periods an initial amplitude of 1 is reduced to 0.04.

4.3.1 Steady-state solution with effect of damping included for sloshing in a two-dimensional rectangular tank

Faltinsen (1978) has developed a linear initial-value solution for lateral sloshing in a two-dimensional rectangular tank excited by transverse harmonic oscillations $x_b=\varepsilon_0\sin(\omega t)$. A linear steady state solution where the effect of damping is included may be obtained by setting the time t to be very large in Faltinsens solution.

This gives the following velocity potential

$$\Phi_T = \sum_{n=0}^{\infty} \sin\left(\frac{2n+1}{2a}\pi x\right)\left\{A\cos(\omega t)\frac{2}{a}\left(\frac{2a}{(2n+1)\pi}\right)^2(-1)^n \right. \tag{4.93}$$

$$\left. +\cosh\left(\frac{2n+1}{2a}\pi (z+h)\right)\left[C_n\cos(\omega t)+D_n\sin(\omega t)\right]\right\}$$

where $A = \varepsilon_0 \omega$. C_n and D_n are given by

$$C_n = \frac{\omega K_n(\sigma_n^2-\omega^2) - \mu^2\omega K_n}{(\sigma_n^2-\omega^2)^2+\mu^2\omega^2} \tag{4.94}$$

and

$$D_n = \frac{\mu K_n(\sigma_n^2-\omega^2) + \mu\omega^2 K_n}{(\sigma_n^2-\omega^2)^2+\mu^2\omega^2} \tag{4.95}$$

where

$$K_n = \frac{\omega A}{\cosh\left[\frac{2n+1}{2a}\pi h\right]}\frac{2}{a}\left[\frac{2a}{(2n+1)\pi}\right]^2(-1)^n \tag{4.96}$$

The free surface displacement of the liquid, which is measured from the undisturbed position of the liquid, is obtained from the linearized dynamic free surface condition

$$\zeta = -\frac{1}{g}\left(\frac{\partial\Phi_T}{\partial t}+\mu\Phi_T\right) \quad on\ z=0 \tag{4.97}$$

to be

$$\zeta = -\frac{1}{g}\sum_{n=0}^{\infty}\sin\left(\frac{(2n+1)}{2a}\pi x\right)\left\{A\frac{2}{a}\left(\frac{2a}{(2n+1)\pi}\right)^2(-1)^n(-\omega\sin(\omega t)+\mu\cos(\omega t)) \right. \tag{4.98}$$

$$\left. +\cosh\left(\frac{2n+1}{2a}\pi h\right)\left[(-\omega C_n+\mu D_n)\sin(\omega t)+(\mu C_n+\omega D_n)\cos(\omega t)\right]\right\}$$

The magnitude of the liquid damping is difficult to predict and the problem is essentially nonlinear. Keulegan (1958) has studied the energy dissipation of sloshing in rectangular tanks. He assumes that the loss of energy of the waves is localized in the boundary layers adjacent to the solid walls. For a tank with 2a=1.0 m, filled with water with kinematic viscosity 10^{-6} m^2/s, h=0.5 m and l=0.1 m, his formulas give the total logarithmic decrement δ=0.0212. This corresponds to a damping coefficient μ=0.0359, which is 0.34 percent of the critical damping. Then it takes 150 oscillations to reduce the amplitude from 1 to 0.04.

In Figure 4.6, the maximum free surface displacement is shown as a function of frequency for different damping values, for a rectangular tank with water depth 0.5 meter and length 1.0 meter undergoing sway oscillations with amplitude 0.025 meter. The resonance frequency for the water inside the tank is equal to 5.32 rad/sec. That is, 1.18 sec. As seen from the figure, the damping has only influence on the free surface displacement for frequencies near resonance. The value μ equal to 0.036 has very little influence on the solution, except for the resonance frequency, where it prevents the solution from blowing up to infinity.

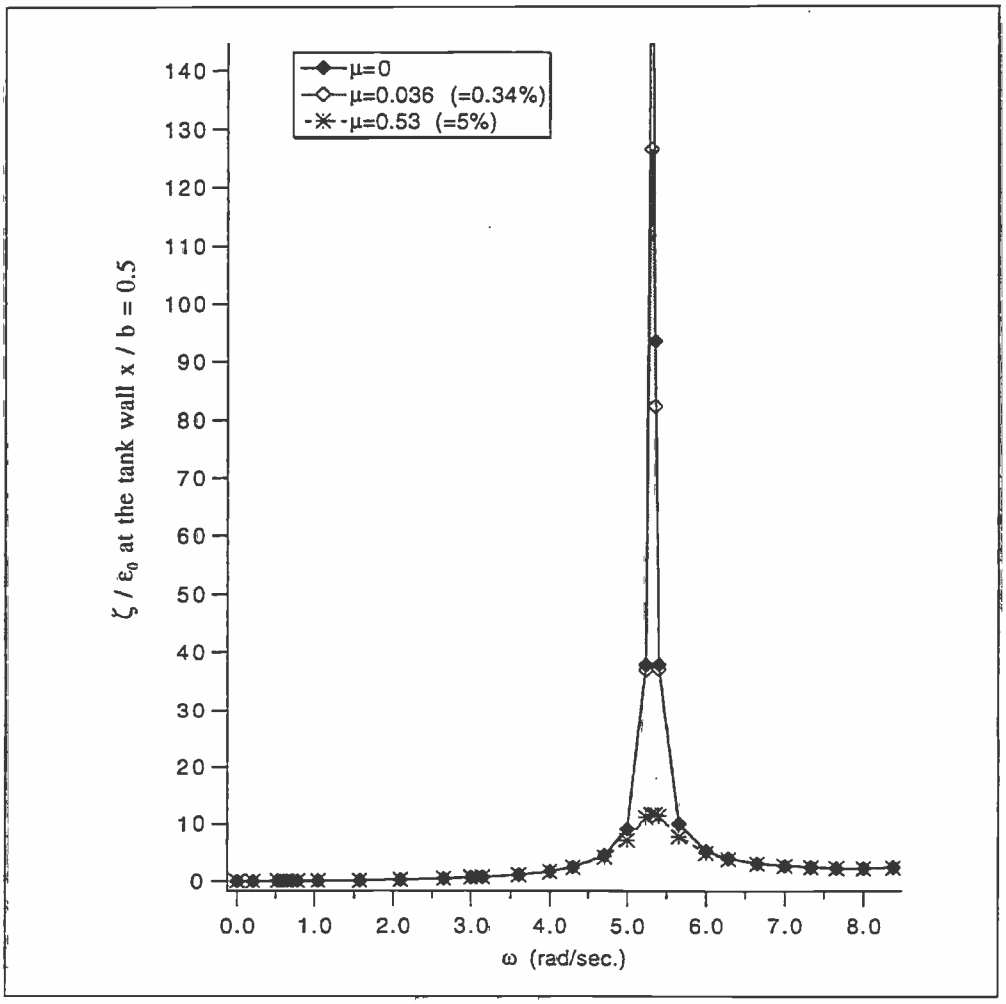

Figure 4.6 **Free surface displacement ζ as a function of frequency for different damping values μ, for a rectangular tank with h/b=0.5 and ε_0=0.025 m.**

4.4 Summary and conclusions

Potential theory is used, and a linear boundary value problem is solved to determine the eigenfrequencies, velocity potential and free surface elevation inside a two-dimensional rectangular tank and inside a vertical circular cylindrical tank. The velocity potential is determined for harmonic sway and roll motion of both a rectangular tank and a vertical circular cylindrical tank.

From the eigenvalue problem both symmetric and antisymmetric eigenfrequencies are determined. Due to sway and roll motion, antisymmetric waves arise inside the tank.

Linear theory is valid for small displacements, velocities and slopes of the liquid-free surface. This means that the frequencies of the tank motions have to be far away from resonance. If linear theory is used for frequencies at the resonance frequencies, the solution will blow up to infinity. When a damping term is introduced into the free-surface condition of the linear boundary value problem, the infinite peak around resonance will be reduced to a finite value dependent on the magnitude of the damping term. Using realistic viscous damping terms will give very high response values at resonance. Away from resonance the influence of the damping term is small.

5 NONLINEAR ANALYTICAL POTENTIAL THEORY SOLUTIONS

Nonlinear response of water inside rigid tanks, undergoing translational (sway) oscillations with frequency near the lowest resonance frequency, is studied analytically in this chapter.

The work follows the method suggested by Moiseev (1958) for the determination of sloshing in an arbitrarily shaped tank. He proposes a general method without much details. His solution method for oscillations near the first resonance frequency is studied and outlined more detailed here. Then the method is used to solve the problem for a two-dimensional rectangular tank and a vertical circular cylindrical tank. His method is used to generalize the solution to other tank shapes in chapter 6. It is shown in chapter 5.1.6 that conservation of mass requires vertical tank walls at the free-surface. This limits the number of tank shapes that the method may be used for.

The results for the rectangular tank are in accordance with the results given in Faltinsen (1974), except for two of the third order terms in the velocity potential. For the circular cylindrical tank, the analysis gives results slightly different from the results obtained in the work by Hutton (1963). But, according to Abramson (1966), Hutton's report contains some misprints, which may be the reason for the differences between the two results. In addition, the constant term in the second order potential is not derived in Huttons report, neither is the method for how to determine it given.

For three-dimensional sloshing, it is important to be aware of the possibility of rotational sloshing in addition to the lateral sloshing modes considered in chapter 4.2. Hutton (1963) considered both lateral and rotational sloshing, as shown in chapter 5.3. In addition he studied the stability of the different solutions.

5.1 General nonlinear solution method for forced oscillations near resonance

The fluid is assumed to satisfy Laplace equation and the nonlinear boundary conditions given in chapter 3.

Moiseev (1958) assumes that the body motion is of order ε relative to the cross-dimensions of the tank. The body boundary conditions are expanded in Taylor series about the mean oscillatory position. Since the solution is found correct to $O(\varepsilon)$, it implies that the body boundary conditions are the same as in linear theory. The only nonlinear character in the boundary value problem enters through the free surface boundary conditions on the actual free surface $z=\zeta$. The response is assumed to be of $O(\varepsilon^{1/3})$, and then, the free surface conditions results in nonlinear terms to $O(\varepsilon)$. In a linear analysis, the response is assumed to be of $O(\varepsilon)$. However, when the tank is driven at or near the lowest resonant frequency, the wave height and fluid velocities are not small. It is therefore not appropriate to assume that they are of $O(\varepsilon)$, and it is essential that the nonlinear terms in

the free surface are taken into account.

5.1.1 General formulations

The tank is forced to oscillate harmonically with small amplitudes in transverse direction with frequency, ω, near the lowest resonance frequency, σ_1.

$$\omega^2 = \sigma_1^2 + \varepsilon^{2/3}\alpha \tag{5.1}$$

The natural frequencies σ_m are related to the eigen numbers λ_m by

$$\sigma_m^2 = g\lambda_m \tag{5.2}$$

and then the following relation is obtained:

$$g = \frac{\omega^2}{\lambda_m} - \varepsilon^{2/3}\frac{\alpha}{\lambda_m} \tag{5.3}$$

The velocity potential is written as

$$\Phi_T = \Phi + \phi_c \tag{5.4}$$

where Φ is the potential of the liquid moving relative to the container, ϕ_c takes care of the body boundary conditions due to the tank motion. It is formally written as

$$\phi_c = \frac{\varepsilon}{\omega} f(x,y)\cos(\omega t) \tag{5.5}$$

The nonlinear dynamic free surface condition may then be written

$$g\zeta + \frac{\partial\Phi}{\partial t} + \frac{1}{2}(\nabla\Phi)^2 = \frac{\varepsilon}{\omega} f(x,y)\sin(\omega t) \quad on\ z=\zeta \tag{5.6}$$

and the kinematic free surface condition

$$\frac{\partial\zeta}{\partial t} + \frac{\partial\Phi}{\partial x}\frac{\partial\zeta}{\partial x} + \frac{\partial\Phi}{\partial y}\frac{\partial\zeta}{\partial y} - \frac{\partial\Phi}{\partial z} = 0 \quad on\ \ z=\zeta \tag{5.7}$$

The velocity potential for the water inside the tank and the free surface elevation are written as

$$\Phi = \sum_{n=1}^{\infty} \phi_n \varepsilon^{n/3}, \qquad \zeta = \sum_{n=1}^{\infty} \zeta_n \varepsilon^{n/3} \tag{5.8}$$

According to Moiseev (1958), $\varepsilon^{n/3}$ is the only choice of $\varepsilon^{(a/b)\,n}$ that gives meaningfully results.

The dynamic and the kinematic free surface conditions are expanded into Taylor series about z=0, and the terms of the same order are collected.

5.1.2 First order equations

The dynamic and kinematic surface conditions of the 1. order, that is terms of order $\varepsilon^{1/3}$, will be:

$$\frac{\partial \phi_1}{\partial t} + \frac{\omega^2}{\lambda_1}\zeta_1 = 0 \quad on\ z=0$$
$$\frac{\partial \zeta_1}{\partial t} = \frac{\partial \phi_1}{\partial z} \quad on\ z=0 \tag{5.9}$$

A combination of the free surface conditions gives

$$\frac{\partial^2 \phi_1}{\partial t^2} + \frac{\omega^2}{\lambda_1}\frac{\partial \phi_1}{\partial z} = 0 \quad on\ z=0 \tag{5.10}$$

where $\lambda_1 = \sigma_1^2/g$ is the first eigenvalue. If the first order velocity potential is written on the form

$$\phi_1 = \sum_{n=0}^{\infty} f_{n1}\psi_n \tag{5.11}$$

where ψ_n are the eigenfunctions, the following system of equations is obtained for the functions f_{n1}:

$$f_{n1}'' + \frac{\lambda_n}{\lambda_1}\omega^2 f_{n1} = 0, \qquad n=0,1,2,3,.... \tag{5.12}$$

where the following relation for the eigenfunctions on the free surface

$$\left(\frac{\partial \psi_n}{\partial z}\right)_{z=0} = \lambda_n \psi_n \tag{5.13}$$

is used. A periodic solution having a period of $2\pi/\omega$ implies that

$$f_{n1} = 0 \quad for\ n\neq 1$$
$$f_{11} = M\sin(\omega t) + N\cos(\omega t) \quad for\ n=1 \tag{5.14}$$

where N and M are constants to be determined by the third order equations. The velocity potential of order $\varepsilon^{1/3}$ is then

$$\phi_1 = \psi_1(x,y,z)(M\sin(\omega t) + N\cos(\omega t)) \tag{5.15}$$

The free surface elevation is given from the dynamic free surface condition to be

$$\zeta_1 = -\frac{\lambda_1}{\omega}\psi_1(x,y,z=0)(M\cos(\omega t) - N\sin(\omega t)) \tag{5.16}$$

5.1.3 Second order equations

The second order terms in the free surface conditions, terms of order $\varepsilon^{2/3}$, are

$$\frac{\partial \phi_2}{\partial t} + \frac{\omega^2}{\lambda_1}\zeta_2 = A_1 \quad on\ z=0$$
$$\frac{\partial \zeta_2}{\partial t} = \frac{\partial \phi_2}{\partial z} + B_1 \quad on\ z=0 \tag{5.17}$$

where the constants A_1 and B_1 are

$$A_1 = -\frac{1}{2}(\nabla\phi_1)^2 - \zeta_1\frac{\partial^2\phi_1}{\partial z\partial t} \qquad on\ z=0$$
$$= \left(\frac{N^2-M^2}{2}\right)\cos(2\omega t)\left(-\frac{1}{2}(\nabla\psi_1)^2 - \lambda_1\psi_1\frac{\partial\psi_1}{\partial z}\right) + MN\sin(2\omega t)\left(-\frac{1}{2}(\nabla\psi_1)^2 - \lambda_1\psi_1\frac{\partial\psi_1}{\partial z}\right)$$
$$+\left(\frac{N^2+M^2}{2}\right)\left(-\frac{1}{2}(\nabla\psi_1)^2 + \lambda_1\psi_1\frac{\partial\psi_1}{\partial z}\right) \tag{5.18}$$

and

$$B_1 = -\frac{\partial\phi_1}{\partial x}\frac{\partial\zeta_1}{\partial x} - \frac{\partial\phi_1}{\partial y}\frac{\partial\zeta_1}{\partial y} + \zeta_1\frac{\partial^2\phi_1}{\partial^2 z} \qquad on\ z=0$$
$$= \left[\left(\frac{N^2-M^2}{2}\right)\sin(2\omega t) + MN\cos(2\omega t)\right]\left[\frac{\lambda_1}{\omega}\left(\frac{\partial\psi_1}{\partial x}\right)^2 + \frac{\lambda_1}{\omega}\left(\frac{\partial\psi_1}{\partial y}\right)^2\right] \tag{5.19}$$

We should note that ψ_1 are given on the mean free surface z = 0. Combination of the free surface conditions gives

$$\frac{\partial^2\phi_2}{\partial t^2} + \frac{\omega^2}{\lambda_1}\frac{\partial\phi_2}{\partial z} = \frac{\partial A_1}{\partial t} - \frac{\omega^2}{\lambda_1}B_1 \quad on\ z=0 \tag{5.20}$$

or

$$\frac{\partial^2\phi_2}{\partial t^2} + \frac{\omega^2}{\lambda_1}\frac{\partial\phi_2}{\partial z} = \left(MN\cos(2\omega t) + \frac{M^2-N^2}{2}\sin(2\omega t)\right)A(x,y)\omega \quad on\ z=0 \tag{5.21}$$

where

$$A(x,y) = -(\nabla\psi_1)^2 - 2\lambda_1\psi_1\frac{\partial\psi_1}{\partial z} - \left(\frac{\partial\psi_1}{\partial x}\right)^2 - \left(\frac{\partial\psi_1}{\partial y}\right)^2 + \psi_1\frac{\partial^2\psi_1}{\partial z^2} \quad on\ z=0 \tag{5.22}$$

In order to determine the potential, the second order potential ϕ_2 and the A(x,y) are written as

$$\phi_2 = \sum_{n=0}^{\infty} f_{n2}\varphi_n(x,y,z)\ , \qquad A(x,y) = \sum_{n=0}^{\infty} \alpha^{(n)}\varphi_n(x,y,z=0) \tag{5.23}$$

Then the following system of equations is obtained for the functions f_{n2}:

$$f_{n2}'' + \frac{\lambda_n}{\lambda_1}\omega^2 f_{n2} = \left(MN\cos(2\omega t) + \frac{M^2-N^2}{2}\sin(2\omega t)\right)\alpha^{(n)}\omega, \qquad n=0,1,2,3,..... \tag{5.24}$$

with the solution

$$f_{n2} = MNd^{(n)}\cos(2\omega t) + \frac{M^2-N^2}{2}d^{(n)}\sin(2\omega t) \tag{5.25}$$

where

$$d^{(n)} = \frac{\alpha^{(n)}}{\omega\left(\frac{\lambda_n}{\lambda_1} - 4\right)} \tag{5.26}$$

if $\lambda_n \neq 4\lambda_1$. In order to satisfy conservation of mass, the velocity potential must contain a homogeneous solution, $\phi_2^h = \alpha_0 t$, (see Faltinsen (1974)). Here α_0 is a constant, which is determined from conservation of mass. This can be expressed as

$$\iint_{x\ y} \zeta_2\, dxdy = 0 \tag{5.27}$$

The second order velocity potential is then

$$\phi_2 = \alpha_0 t + \sum_{n=0}^{\infty}\psi_n d^{(n)}\left(MN\cos(2\omega t) + \frac{M^2-N^2}{2}\sin(2\omega t)\right) \tag{5.28}$$

We should note that Moiseev's solution contains a homogeneous solution of the second order equations on the form

$M_1\cos(\omega t) + N_1\sin(\omega t)$.

This solution is not taken into account here, since the constants M_1 and N_1 have to be determined from the fourth order equations.

The second order free surface elevation is obtained from the dynamic free surface condition. It follows that

$$\zeta_2 = \frac{\lambda_1}{\omega^2}\left(A_1 - \frac{\partial \phi_2}{\partial t}\right) \quad on\ z=0 \tag{5.29}$$

or

$$\zeta_2 = \frac{\lambda_1}{\omega^2}\left[\left(MN\sin(2\omega t) + \frac{N^2-M^2}{2}\cos(2\omega t)\right)\left(-\frac{1}{2}(\nabla\psi_1)^2 - \lambda_1\psi_1\frac{\partial\psi_1}{\partial z}\right)\right.$$

$$+\frac{N^2+M^2}{2}\left(-\frac{1}{2}(\nabla\psi_1)^2 + \lambda_1\psi_1\frac{\partial\psi_1}{\partial z}\right) \tag{5.30}$$

$$\left.-\alpha_0 - \sum_{n=0}^{\infty}\psi_n d^{(n)} 2\omega\left(-MN\sin(2\omega t) + \frac{M^2-N^2}{2}\cos(2\omega t)\right)\right] \quad on\ z=0$$

5.1.4 Third order equations

The third order free surface conditions with terms of order ε are:

$$\frac{\partial \phi_3}{\partial t} + \frac{\omega^2}{\lambda_1}\zeta_3 = \frac{\alpha}{\lambda_1}\zeta_1 + A_2 + \frac{1}{\omega}f(x,y)\sin(\omega t) \quad on\ z=0$$

$$\frac{\partial \zeta_3}{\partial t} = \frac{\partial \phi_3}{\partial z} + B_2 \quad on\ z=0 \tag{5.31}$$

Here

$$A_2 = -\nabla\phi_1\cdot\nabla\phi_2 - \zeta_1\frac{\partial^2\phi_2}{\partial z\partial t} - \zeta_2\frac{\partial^2\phi_1}{\partial z\partial t} - \zeta_1\nabla\phi_1\cdot\frac{\partial}{\partial z}\{\nabla\phi_1\} - \frac{1}{2}\zeta_1^2\frac{\partial^3\phi_1}{\partial z^2\partial t} \quad on\ z=0 \tag{5.32}$$

and

$$B_2 = -\frac{\partial\phi_1}{\partial x}\frac{\partial\zeta_2}{\partial x} - \frac{\partial\phi_2}{\partial x}\frac{\partial\zeta_1}{\partial x} - \frac{\partial\phi_1}{\partial y}\frac{\partial\zeta_2}{\partial y} - \frac{\partial\phi_2}{\partial y}\frac{\partial\zeta_1}{\partial y}$$

$$-\zeta_1\frac{\partial}{\partial z}\left\{\frac{\partial\phi_1}{\partial x}\frac{\partial\zeta_1}{\partial x} + \frac{\partial\phi_1}{\partial y}\frac{\partial\zeta_1}{\partial y}\right\} + \zeta_1\frac{\partial^2\phi_2}{\partial z^2} + \zeta_2\frac{\partial^2\phi_1}{\partial z^2} + \frac{1}{2}\zeta_1^2\frac{\partial^3\phi_1}{\partial z^3} \quad on\ z=0 \tag{5.33}$$

The combined free surface condition for the third order equations is then

$$\frac{\partial^2\phi_3}{\partial t^2} + \frac{\omega^2}{\lambda_1}\frac{\partial\phi_3}{\partial z} = \frac{\partial A_2}{\partial t} - \frac{\omega^2}{\lambda_1}B_2 + \frac{\alpha}{\lambda_1}\frac{\partial\zeta_1}{\partial t} + f(x,y)\cos(\omega t) \quad on\ z=0 \tag{5.34}$$

The total expressions for the combined free surface equation are given in appendix B.

5.1.5 Two-dimensional tank

For the two-dimensional case the constant M may be set equal to zero to study stable planar sloshing, and the expressions will not be so voluminous as in the three-dimensional case.

First order potential

When M=0, the velocity potential of order $\varepsilon^{1/3}$ is given from equation (5.15) to be

$$\phi_1 = \psi_1(x,z)N\cos(\omega t) \tag{5.35}$$

and the free surface elevation from the dynamic free surface condition is

$$\zeta_1 = \frac{\lambda_1}{\omega}\psi_1(x,z=0)N\sin(\omega t) \tag{5.36}$$

Second order potential

For the two-dimensional case, the equations have no y-dependence, and the right hand sides A_1 and B_1 in the free surface conditions will be

$$\begin{aligned} A_1 &= -\frac{1}{2}(\nabla\phi_1)^2 - \zeta_1\frac{\partial^2\phi_1}{\partial z\partial t} \qquad on\ z = 0 \\ &= \frac{N^2}{2}\cos(2\omega t)\left(-\frac{1}{2}(\nabla\psi_1)^2 - \lambda_1\psi_1\frac{\partial\psi_1}{\partial z}\right) + \frac{N^2}{2}\left(-\frac{1}{2}(\nabla\psi_1)^2 + \lambda_1\psi_1\frac{\partial\psi_1}{\partial z}\right) \end{aligned} \tag{5.37}$$

and

$$B_1 = -\frac{\partial\phi_1}{\partial x}\frac{\partial\zeta_1}{\partial x} + \zeta_1\frac{\partial^2\phi_1}{\partial^2 z} = \frac{N^2}{2}\sin(2\omega t)\frac{\lambda_1}{\omega}\left(\frac{\partial\psi_1}{\partial x}\right)^2 \quad on\ z = 0 \tag{5.38}$$

We should note that ψ_1 is given on z=0. Combination of the free surface conditions gives

$$\frac{\partial^2\phi_2}{\partial t^2} + \frac{\omega^2}{\lambda_1}\frac{\partial\phi_2}{\partial z} = -\frac{N^2}{2}\sin(2\omega t)A(x)\omega \quad on\ z=0 \tag{5.39}$$

where

$$A(x) = -(\nabla\psi_1)^2 - 2\lambda_1\psi_1\frac{\partial\psi_1}{\partial z} - \left(\frac{\partial\psi_1}{\partial x}\right)^2 + \psi_1\frac{\partial^2\psi_1}{\partial z^2} \quad on\ z=0 \tag{5.40}$$

The second order potential ϕ_2 and the A(x) are written in the terms of series of the eigenfunctions

$$\phi_2 = \sum_{n=0}^{\infty} f_{n2}\psi_n(x,z)\ , \qquad A(x,) = \sum_{n=0}^{\infty} \alpha^{(n)}\psi_n(x,z=0) \tag{5.41}$$

The system of equations for the functions f_{n2} is

$$f_{n2}'' + \frac{\lambda_n}{\lambda_1}\omega^2 f_{n2} = -\frac{N^2}{2}\sin(2\omega t)\,\alpha^{(n)}\omega, \qquad n=0,1,2,3,..... \tag{5.42}$$

with the solution

$$f_{n2} = -\frac{N^2}{2}d^{(n)}\sin(2\omega t) \tag{5.43}$$

where

$$d^{(n)} = \frac{\alpha^{(n)}}{\omega\left(\frac{\lambda_n}{\lambda_1} - 4\right)} \tag{5.44}$$

if $\lambda_n \neq 4\lambda_1$. To obtain conservation of mass, the integral over the free surface

$$\int_x \zeta_2\, dx = 0 \tag{5.45}$$

The second order velocity potential is then

$$\phi_2 = \alpha_0 t - \sum_{n=0}^{\infty}\psi_n d^{(n)}\frac{N^2}{2}\sin(2\omega t) \tag{5.46}$$

where the constant α_0 is obtained from equation (5.45) to be

$$\int_x \alpha_0 dx = \frac{N^2}{2}\cos(2\omega t)\int_x\left(-\frac{1}{2}(\nabla\psi_1)^2 - \lambda_1\psi_1\frac{\partial\psi_1}{\partial z}\right)dx$$

$$+\frac{N^2}{2}\cos(2\omega t)\,2\omega\sum_{n=0}^{\infty} d^{(n)}\int_x\psi_n dx \tag{5.47}$$

$$+\frac{N^2}{2}\int_x\left(-\frac{1}{2}(\nabla\psi_1)^2 + \lambda_1\psi_1\frac{\partial\psi_1}{\partial z}\right)dx$$

For α_0 to become a constant, the time dependent parts on the right hand side of this

expression have to be equal to zero. This leads to restrictions on the tank shape. This is shown in chapter 5.1.6.

The second order free surface elevation is

$$\zeta_2 = \frac{\lambda_1}{\omega^2}\left[\frac{N^2}{2}\cos(2\omega t)\left(-\frac{1}{2}(\nabla\psi_1)^2 - \lambda_1\psi_1\frac{\partial\psi_1}{\partial z}\right) + \frac{N^2}{2}\left(-\frac{1}{2}(\nabla\psi_1)^2 + \lambda_1\psi_1\frac{\partial\psi_1}{\partial z}\right)\right. \tag{5.48}$$

$$\left. -\alpha_0 + \sum_{n=0}^{\infty}\psi_n d^{(n)} 2\omega\frac{N^2}{2}\cos(2\omega t)\right] \qquad on\ z=0$$

Third order equations

The third order free surface conditions are given in equation (5.31) where, for the two-dimensional case

$$A_2 = -\nabla\phi_1\nabla\phi_2 - \zeta_1\frac{\partial^2\phi_2}{\partial z\partial t} - \zeta_2\frac{\partial^2\phi_1}{\partial z\partial t} - \zeta_1\nabla\phi_1\frac{\partial}{\partial z}\{\nabla\phi_1\} - \frac{1}{2}\zeta_1^2\frac{\partial^3\phi_1}{\partial z^2\partial t} \quad on\ z=0 \tag{5.49}$$

and

$$B_2 = -\frac{\partial\phi_1}{\partial x}\frac{\partial\zeta_2}{\partial x} - \frac{\partial\phi_2}{\partial x}\frac{\partial\zeta_1}{\partial x}$$

$$-\zeta_1\frac{\partial^2\phi_1}{\partial x\partial z}\frac{\partial\zeta_1}{\partial x} + \zeta_1\frac{\partial^2\phi_2}{\partial z^2} + \zeta_2\frac{\partial^2\phi_1}{\partial z^2} + \frac{1}{2}\zeta_1^2\frac{\partial^3\phi_1}{\partial z^3} \qquad on\ z=0 \tag{5.50}$$

The combined free surface condition for the third order equations is then

$$\frac{\partial^2\phi_3}{\partial t^2}+\frac{\omega^2}{\lambda_1}\frac{\partial\phi_3}{\partial z}=f(x)\cos(\omega t)+N\alpha\psi_1\cos(\omega t)+N\alpha_0\cos(\omega t)\left\{\frac{\partial^2\psi_1}{\partial z^2}-\lambda_1\frac{\partial\psi_1}{\partial z}\right\} \tag{5.51}$$

$$+N^3\cos(\omega t)\left\{\frac{1}{4}\omega\nabla\psi_1\sum_{n=0}^{\infty}\nabla\psi_n d^{(n)}-\frac{1}{2}\omega\lambda_1\psi_1\sum_{n=0}^{\infty}\frac{\partial\psi_n}{\partial z}d^{(n)}+\frac{1}{2}\lambda_1\frac{\partial\psi_1}{\partial z}\left(-\frac{1}{2}(\nabla\psi_1)^2+\lambda_1\psi_1\frac{\partial\psi_1}{\partial z}\right)\right.$$

$$+\frac{1}{4}\lambda_1\frac{\partial\psi_1}{\partial z}\left(\frac{1}{2}(\nabla\psi_1)^2+\lambda_1\psi_1\frac{\partial\psi_1}{\partial z}\right)-\frac{1}{2}\omega\lambda_1\frac{\partial\psi_1}{\partial z}\sum_{n=0}^{\infty}\psi_n d^{(n)}-\frac{1}{4}\lambda_1\psi_1\nabla\psi_1\frac{\partial}{\partial z}\{\nabla\psi_1\}$$

$$+\frac{3}{8}\lambda_1^2\psi_1^2\frac{\partial^2\psi_1}{\partial z^2}+\frac{1}{4}\frac{\partial\psi_1}{\partial x}\left\{2\omega\sum_{n=0}^{\infty}\frac{\partial\psi_n}{\partial x}d^{(n)}+\frac{\partial}{\partial x}\left(-\frac{1}{2}(\nabla\psi_1)^2-\lambda_1\psi_1\frac{\partial\psi_1}{\partial z}\right)\right\}$$

$$+\frac{1}{2}\frac{\partial\psi_1}{\partial x}\frac{\partial}{\partial x}\left(-\frac{1}{2}(\nabla\psi_1)^2+\lambda_1\psi_1\frac{\partial\psi_1}{\partial z}\right)-\frac{1}{4}\omega\frac{\partial\psi_1}{\partial x}\sum_{n=0}^{\infty}\frac{\partial\psi_n}{\partial x}d^{(n)}+\frac{1}{4}\lambda_1\psi_1\frac{\partial\psi_1}{\partial x}\frac{\partial^2\psi_1}{\partial x\partial z}$$

$$+\frac{1}{4}\omega\psi_1\sum_{n=0}^{\infty}\frac{\partial^2\psi_n}{\partial z^2}d^{(n)}-\frac{1}{8}\lambda_1\psi_1^2\frac{\partial^3\psi_1}{\partial z^3}+\frac{1}{4}\frac{\partial^2\psi_1}{\partial z^2}\left\{-2\omega\sum_{n=0}^{\infty}\psi_n d^{(n)}+\frac{1}{2}(\nabla\psi_1)^2+\lambda_1\psi_1\frac{\partial\psi}{\partial z}\right.$$

$$\left.\left.+\frac{1}{2}\frac{\partial^2\psi_1}{\partial z^2}\left(\frac{1}{2}(\nabla\psi_1)^2-\lambda_1\psi_1\frac{\partial\psi_1}{\partial z}\right)\right\}\right\}$$

$$+N^3\cos(3\omega t)\left\{\frac{3}{4}\omega\nabla\psi_1\sum_{n=0}^{\infty}\nabla\psi_n d^{(n)}+\frac{3}{2}\omega\lambda_1\psi_1\sum_{n=0}^{\infty}\frac{\partial\psi_n}{\partial z}d^{(n)}-\frac{3}{4}\lambda_1\frac{\partial\psi_1}{\partial z}\left(\frac{1}{2}(\nabla\psi_1)^2+\lambda_1\psi_1\frac{\partial\psi_1}{\partial z}\right)\right.$$

$$+\frac{3}{2}\omega\lambda_1\frac{\partial\psi_1}{\partial z}\sum_{n=0}^{\infty}\psi_n d^{(n)}-\frac{3}{4}\lambda_1\psi_1\nabla\psi_1\frac{\partial}{\partial z}\{\nabla\psi_1\}-\frac{3}{8}\lambda_1^2\psi_1^2\frac{\partial^2\psi_1}{\partial z^2}$$

$$+\frac{1}{4}\frac{\partial\psi_1}{\partial x}\left\{2\omega\sum_{n=0}^{\infty}\frac{\partial\psi_n}{\partial x}d^{(n)}+\frac{\partial}{\partial x}\left(-\frac{1}{2}(\nabla\psi_1)^2-\lambda_1\psi_1\frac{\partial\psi_1}{\partial z}\right)\right\}+\frac{1}{4}\omega\frac{\partial\psi_1}{\partial x}\sum_{n=0}^{\infty}\frac{\partial\psi_n}{\partial x}d^{(n)}$$

$$-\frac{1}{4}\lambda_1\psi_1\frac{\partial\psi_1}{\partial x}\frac{\partial^2\psi_1}{\partial x\partial z}-\frac{1}{4}\omega\psi_1\sum_{n=0}^{\infty}\frac{\partial^2\psi_n}{\partial z^2}d^{(n)}+\frac{1}{8}\lambda_1\psi_1^2\frac{\partial^3\psi_1}{\partial z^3}$$

$$\left.+\frac{1}{4}\frac{\partial^2\psi_1}{\partial z^2}\left\{-2\omega\sum_{n=0}^{\infty}\psi_n d^{(n)}+\frac{1}{2}(\nabla\psi_1)^2+\lambda_1\psi_1\frac{\partial\psi_1}{\partial z}\right\}\right\}$$

In order to avoid infinite response, we have to set the cos(ωt) terms on the right hand side in this combined free surface condition equal to zero. This determines N, and the resulting equation is:

$$KN^3+\alpha\psi_1 N+f(x)=0 \tag{5.52}$$

where

$$K=\frac{\alpha_0}{N^2}\left\{\frac{\partial^2\psi_1}{\partial z^2}-\lambda_1\frac{\partial\psi_1}{\partial z}\right\}+\frac{1}{4}\omega\nabla\psi_1\sum_{n=0}^{\infty}\nabla\psi_n d^{(n)}-\frac{1}{2}\omega\lambda_1\psi_1\sum_{n=0}^{\infty}\frac{\partial\psi_n}{\partial z}d^{(n)}$$

$$+\frac{1}{2}\lambda_1\frac{\partial\psi_1}{\partial z}\left(-\frac{1}{2}(\nabla\psi_1)^2+\lambda_1\psi_1\frac{\partial\psi_1}{\partial z}\right)+\frac{1}{4}\lambda_1\frac{\partial\psi_1}{\partial z}\left(\frac{1}{2}(\nabla\psi_1)^2+\lambda_1\psi_1\frac{\partial\psi_1}{\partial z}\right)$$

$$-\frac{1}{2}\omega\lambda_1\frac{\partial\psi_1}{\partial z}\sum_{n=0}^{\infty}\psi_n d^{(n)}-\frac{1}{4}\lambda_1\psi_1\nabla\psi_1\frac{\partial}{\partial z}\{\nabla\psi_1\}+\frac{3}{8}\lambda_1^2\psi_1^2\frac{\partial^2\psi_1}{\partial z^2}$$

$$+\frac{1}{4}\frac{\partial\psi_1}{\partial x}\left\{2\omega\sum_{n=0}^{\infty}\frac{\partial\psi_n}{\partial x}d^{(n)}+\frac{\partial}{\partial x}\left(-\frac{1}{2}(\nabla\psi_1)^2-\lambda_1\psi_1\frac{\partial\psi_1}{\partial z}\right)\right\} \tag{5.53}$$

$$+\frac{1}{2}\frac{\partial\psi_1}{\partial x}\frac{\partial}{\partial x}\left(-\frac{1}{2}(\nabla\psi_1)^2+\lambda_1\psi_1\frac{\partial\psi_1}{\partial z}\right)-\frac{1}{4}\omega\frac{\partial\psi_1}{\partial x}\sum_{n=0}^{\infty}\frac{\partial\psi_n}{\partial x}d^{(n)}$$

$$+\frac{1}{4}\lambda_1\psi_1\frac{\partial\psi_1}{\partial x}\frac{\partial^2\psi_1}{\partial x\partial z}+\frac{1}{4}\omega\psi_1\sum_{n=0}^{\infty}\frac{\partial^2\psi_n}{\partial z^2}d^{(n)}-\frac{1}{8}\lambda_1\psi_1^2\frac{\partial^3\psi_1}{\partial z^3}$$

$$+\frac{1}{4}\frac{\partial^2\psi_1}{\partial z^2}\left\{-2\omega\sum_{n=0}^{\infty}\psi_n d^{(n)}+\frac{1}{2}(\nabla\psi_1)^2+\lambda_1\psi_1\frac{\partial\psi_1}{\partial z}\right\}+\frac{1}{2}\frac{\partial^2\psi_1}{\partial z^2}\left(\frac{1}{2}(\nabla\psi_1)^2-\lambda_1\psi_1\frac{\partial\psi_1}{\partial z}\right)$$

Note that α_0, as given in equation (5.47) is proportional to N^2, so the first term in K is actually independent of N.

When the discriminant

$$\frac{1}{4}\left(\frac{f(x)}{K}\right)^2+\frac{1}{27}\left(\frac{\alpha\psi_1}{K}\right)^3<0 \tag{5.54}$$

there are three real roots of (5.52). When the discriminant is zero, there are three real roots, where at least two of them are equal. When the discriminant is greater than zero, there is only one real root. This implies that we are getting three solutions for the free surface elevation for those periods of oscillation which give negative values of the discriminant, and one solution for the ones which gives positive values of the discriminant. This is illustrated in Figure 6.10 and 6.11, where the free surface elevation in two-dimensional tanks is shown as function of period of oscillation.

5.1.6 Conservation of mass and the tank shape

To obtain conservation of mass in the tank, the integral over the free surface, equation (5.45) for the two-dimensional case, has to be equal to zero. To get α_0 as a constant, the integral of the time dependent cos(2ωt)-terms has to be zero, and the following condition has to be fulfilled.

$$\frac{N^2}{2}\cos(2\omega t)\int_x\left[-\frac{1}{2}(\nabla\psi_1)^2-\lambda_1\psi_1\frac{\partial\psi_1}{\partial z}+\sum_{n=0}^{\infty}\psi_n d^{(n)}2\omega\right]dx=0 \tag{5.55}$$

From the free surface condition (5.39), the expression (5.40) for A(x) and (5.46) for ϕ_2, it follows that

$$2\omega\sum_{n=0}^{\infty}\psi_n d^{(n)}=\frac{1}{2}(\nabla\psi_1)^2+\lambda_1\psi_1\frac{\partial\psi_1}{\partial z}+\frac{1}{2}\left(\frac{\partial\psi_1}{\partial x}\right)^2-\frac{1}{2}\psi_1\frac{\partial^2\psi_1}{\partial z^2}+\frac{\omega}{2\lambda_1}\sum_{n=0}^{\infty}\frac{\partial\psi_n}{\partial z}d^{(n)} \tag{5.56}$$

Then the condition (5.55) may be written as

$$\int_x\left[\frac{1}{2}\left(\frac{\partial\psi_1}{\partial x}\right)^2-\frac{1}{2}\psi_1\frac{\partial^2\psi_1}{\partial z^2}+\frac{\omega}{2\lambda_1}\sum_{n=0}^{\infty}\frac{\partial\psi_n}{\partial z}d^{(n)}\right]dx=0 \tag{5.57}$$

We have that the integral over the free surface

$$\int_x\frac{\partial\psi_n}{\partial z}dx=0 \tag{5.58}$$

and from Laplace equation that

$$\frac{\partial^2\psi_1}{\partial z^2}=-\frac{\partial^2\psi_1}{\partial x^2} \tag{5.59}$$

and hence the condition (5.57) may be written as

$$\int_x\left[\left(\frac{\partial\psi_1}{\partial x}\right)^2+\psi_1\frac{\partial^2\psi_1}{\partial x^2}\right]dx=\int_x\frac{\partial}{\partial x}\left\{\psi_1\frac{\partial\psi_1}{\partial x}\right\}dx=0 \tag{5.60}$$

The integral is to be taken over the free surface from the left to the right tank wall. It then follows that

$$\psi_1\frac{\partial\psi_1}{\partial x}\bigg|_{x(\text{left wall})}-\psi_1\frac{\partial\psi_1}{\partial x}\bigg|_{x(\text{right wall})}=0 \tag{5.61}$$

It should be noted that ψ_1 is antisymmetric and $\partial\psi_1/\partial x$ is symmetric about the centre of the tank. Hence, $\psi_1\,\partial\psi_1/\partial x$ cannot have the same values at the left and right tank walls, and then, $\psi_1\,\partial\psi_1/\partial x$ has to be equal to zero at the tank walls to fulfil equation (5.61). If

$\psi_1 = 0$ at the tank walls at z=0, it means that there are nodes with no free surface elevation at the walls associated with this eigenfunction. It is difficult to imagine that this can happen physically, but we cannot exclude that it can happen for a very special tank shape. For the above condition to be fulfilled, another possibility is then that

$$\frac{\partial \psi_1}{\partial x} = 0 \quad \textit{on the tank walls at } z = 0 \tag{5.62}$$

which means that the tank walls have to be vertical in the free surface line z=0. We have decided to use this as a limitation of the analysis.

5.2 Nonlinear solution for sloshing in a two-dimensional rectangular tank

In this chapter the general solution method in chapter 5.1 is used on a two-dimensional rectangular tank undergoing sway oscillations with small oscillation amplitude and frequency close to the first natural frequency. The results of this chapter are used to verify the combined analytical and numerical method in chapter 6.

The tank shape, dimensions and the coordinate system are shown in Figure 5.1. The half of the tank breadth, a, and the water depth, h, are assumed to be of O(1).

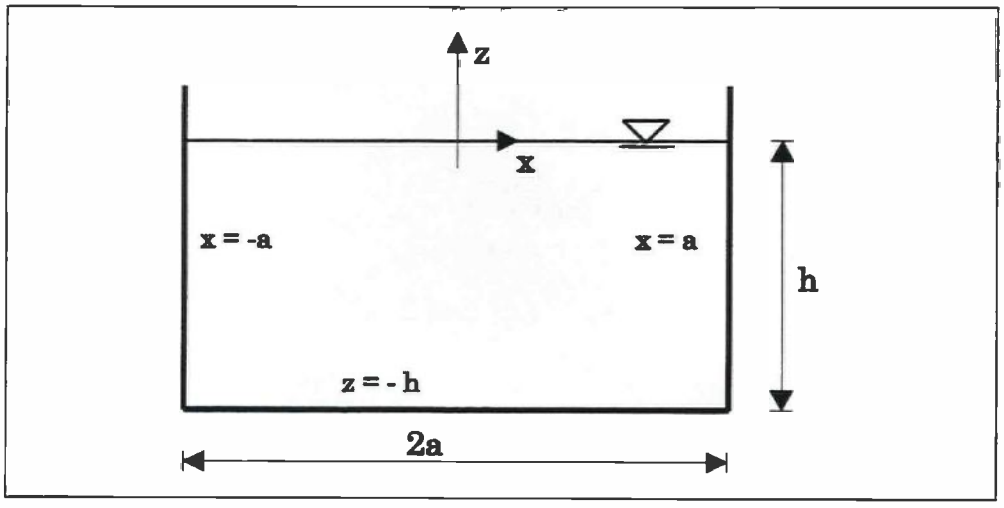

Figure 5.1 Coordinate system and tank dimensions for two-dimensional rectangular tank

5.2.1 Eigenfunctions and values

The eigenfunctions ψ_n and values λ_n may be obtained analytically for a rectangular tank from the following set of equations:

$$\frac{\partial^2\psi_n}{\partial x^2}+\frac{\partial^2\psi_n}{\partial z^2}=0 \qquad \textit{in the fluid domain} \tag{5.63}$$

and

$$\begin{aligned} &\frac{\partial\psi_n}{\partial x}=0 && \textit{on } x=\pm a \\ &\frac{\partial\psi_n}{\partial z}=0 && \textit{on } z=-h \\ &\frac{\partial\psi_n}{\partial z}=\lambda_n\psi_n && \textit{on } z=0 \end{aligned} \tag{5.64}$$

The boundary value problem is solved in chapter 4.1, and when the solution (4.7) is divided in to its antisymmetrical and symmetrical modes, the eigenfunctions have the form

$$\psi_n=\begin{cases} \sin\left(\frac{n\pi}{2a}x\right)\cosh\left(\frac{n\pi}{2a}(z+h)\right) & n = 1,3,5,... \\ \cos\left(\frac{n\pi}{2a}x\right)\cosh\left(\frac{n\pi}{2a}(z+h)\right) & n = 0,2,4,... \end{cases} \tag{5.65}$$

and the eigenvalues are

$$\lambda_n=\frac{n\pi}{2a}\tanh\left(\frac{n\pi}{2a}h\right) \tag{5.66}$$

The eigenfrequencies are related to the eigenvalues as

$$\sigma_n^2=\lambda_n g=g\frac{n\pi}{2a}\tanh\left(\frac{n\pi}{2a}h\right) \tag{5.67}$$

5.2.2 Forced sway oscillation near resonance

The tank is assumed to be oscillated harmonically with amplitude $\varepsilon_0\sin(\omega t)$ in transverse direction (sway), with the frequency, ω, near the lowest resonance frequency, σ_1.

$$\sigma_1^2=g\frac{\pi}{2a}\tanh\left(\frac{\pi}{2a}h\right) \tag{5.68}$$

The amplitude ε_0 is assumed to be small compared with the breadth 2a of the tank and in

the same manner as in Faltinsen (1974), we use that

$$\varepsilon = \frac{\varepsilon_0}{2a} \tag{5.69}$$

The total velocity potential is written as

$$\Phi_T = \Phi + \phi_c \tag{5.70}$$

where the velocity potential for the container motion is

$$\phi_c = 2a\omega\varepsilon x\cos(\omega t) \tag{5.71}$$

and the velocity potential for the fluid motion and the free surface elevation are taken to be correct to third order

$$\begin{aligned} \Phi &= \sum_{n=1}^{\infty} \phi_n \varepsilon^{n/3} = \phi_1\varepsilon^{1/3} + \phi_2\varepsilon^{2/3} + \phi_3\varepsilon \\ \zeta &= \sum_{n=1}^{\infty} \zeta_n \varepsilon^{n/3} = \zeta_1\varepsilon^{1/3} + \zeta_2\varepsilon^{2/3} + \zeta_3\varepsilon \end{aligned} \tag{5.72}$$

5.2.3 First order equations

The first eigenfunction is

$$\psi_1(x,z) = \sin\left(\frac{\pi}{2a}x\right)\cosh\left(\frac{\pi}{2a}(z+h)\right) \tag{5.73}$$

and the velocity potential of order $\varepsilon^{1/3}$ is then

$$\phi_1 = \sin\left(\frac{\pi}{2a}x\right)\cosh\left(\frac{\pi}{2a}(z+h)\right)N\cos(\omega t) \tag{5.74}$$

and the free surface elevation

$$\zeta_1 = \frac{\sigma_1^2}{\omega g}\sin\left(\frac{\pi}{2a}x\right)\cosh\left(\frac{\pi}{2a}h\right)N\sin(\omega t) \tag{5.75}$$

5.2.4 Second order equations

The combined free surface condition for the second order problem is

$$\frac{\partial^2\phi_2}{\partial t^2} + \frac{\omega^2}{\lambda_1}\frac{\partial\phi_2}{\partial z} = -\frac{N^2}{2}\sin(2\omega t)A(x)\omega \quad on\ z=0 \tag{5.76}$$

where

$$A(x) = -(\nabla\psi_1)^2 - 2\lambda_1\psi_1\frac{\partial\psi_1}{\partial z} - \left(\frac{\partial\psi_1}{\partial x}\right)^2 + \psi_1\frac{\partial^2\psi_1}{\partial z^2} \quad on\ z=0$$

$$= \left[-\left(\frac{\pi}{2a}\right)^2\sinh^2\left(\frac{\pi}{2a}h\right) - 2\frac{\sigma_1^2}{g}\left(\frac{\pi}{2a}\right)\cosh\left(\frac{\pi}{2a}h\right)\sinh\left(\frac{\pi}{2a}h\right)\right]\sin^2\left(\frac{\pi}{2a}x\right) \quad (5.77)$$

$$-\left(\frac{\pi}{2a}\right)^2\cosh^2\left(\frac{\pi}{2a}h\right)\cos^2\left(\frac{\pi}{2a}x\right) - \left(\frac{\pi}{2a}\right)^2\cosh^2\left(\frac{\pi}{2a}h\right)\cos\left(\frac{\pi}{a}x\right)$$

$$= C + D + (D - C - \frac{g}{\omega}F)\cos\left(\frac{\pi}{a}x\right)$$

C, D, and F are given by

$$C = -\frac{1}{2}\left(\frac{\pi}{2a}\right)^2\sinh^2\left(\frac{\pi}{2a}h\right) - \frac{\sigma_1^2}{g}\left(\frac{\pi}{2a}\right)\cosh\left(\frac{\pi}{2a}h\right)\sinh\left(\frac{\pi}{2a}h\right)$$

$$D = -\frac{1}{2}\left(\frac{\pi}{2a}\right)^2\cosh^2\left(\frac{\pi}{2a}h\right) \quad (5.78)$$

$$F = \frac{\omega}{g}\left(\frac{\pi}{2a}\right)^2\cosh^2\left(\frac{\pi}{2a}h\right)$$

which is in accordance with the solution given in Faltinsen (1974). The combined free surface condition is then

$$\frac{\partial^2\phi_2}{\partial t^2} + \frac{\omega^2}{\lambda_1}\frac{\partial\phi_2}{\partial z} = -\frac{N^2}{2}\sin(2\omega t)(C\omega + D\omega) - \frac{N^2}{2}\sin(2\omega t)(D\omega - C\omega - gF)\cos\left(\frac{\pi}{a}x\right) \quad (5.79)$$

When A(x) is written as

$$A(x) = \sum_{n=0}^{\infty}\alpha^{(n)}\psi_n(x, z=0) \quad (5.80)$$

it is seen from

$$A(x) = \alpha^{(0)}\psi_0 + \alpha^{(1)}\psi_1 + \alpha^{(2)}\psi_2 + \alpha^{(3)}\psi_3 + \ldots = C + D + (D - C - \frac{g}{\omega}F)\cos\left(\frac{\pi}{a}x\right) \quad (5.81)$$

where

$$\psi_0 = 1$$

$$\psi_1 = \sin\left(\frac{\pi}{2a}x\right)\cosh\left(\frac{\pi}{2a}(z+h)\right)$$

$$\psi_2 = \cos\left(\frac{\pi}{a}x\right)\cosh\left(\frac{\pi}{a}(z+h)\right) \tag{5.82}$$

$$\psi_3 = \sin\left(\frac{3\pi}{2a}x\right)\cosh\left(\frac{3\pi}{2a}(z+h)\right)$$

that

$$\alpha^{(0)} = \frac{C\omega + D\omega}{\omega}, \quad \alpha^{(1)} = 0, \quad \alpha^{(2)} = \frac{D\omega - C\omega - gF}{\omega\cosh\left(\frac{\pi}{a}h\right)}, \quad \alpha^{(3)} = \alpha^{(4)} = \ldots = 0 \tag{5.83}$$

When the second order potential ϕ_2 is written as

$$\phi_2 = \sum_{n=0}^{\infty} f_{n2}\psi_n(x,z) \tag{5.84}$$

we have that

$$f_{n2} = -\frac{N^2}{2}d^{(n)}\sin(2\omega t) \tag{5.85}$$

and

$$d^{(0)} = \frac{\alpha^{(0)}}{\omega\left(\frac{\lambda_0}{\lambda_1} - 4\right)} = \frac{C\omega + D\omega}{-4\omega^2} = A_0^{(2)}(C\omega + D\omega)$$

$$d^{(1)} = 0 \tag{5.86}$$

$$d^{(2)} = \frac{\alpha^{(2)}}{\omega\left(\frac{\lambda_2}{\lambda_1} - 4\right)} = \frac{D\omega - C\omega - gF}{-\omega^2 4\cosh\left(\frac{\pi}{a}h\right) + \frac{\omega^2}{\sigma_1^2}g\left(\frac{\pi}{a}\right)\sinh\left(\frac{\pi}{a}h\right)} = A_1^{(2)}(D\omega - C\omega - gF)$$

$$d^{(3)} = d^{(4)} = ,\ldots, = 0$$

if $\lambda_n \neq 4\lambda_1$, n=0,2, where

$$\lambda_0 = 0, \quad \lambda_1 = \frac{\pi}{2a}\tanh\left(\frac{\pi}{2a}h\right), \quad \lambda_2 = \frac{\pi}{a}\tanh\left(\frac{\pi}{a}h\right) \tag{5.87}$$

The homogeneous solution of the second order potential is $\phi_2^h = \alpha_0 t$, where

$$\int_{-a}^{a}\alpha_0 dx = \frac{N^2}{2}\cos(2\omega t)\int_{-a}^{a}\left(-\frac{1}{2}(\nabla\psi_1)^2 - \lambda_1\psi_1\frac{\partial\psi_1}{\partial z}\right)dx$$
$$+\frac{N^2}{2}\cos(2\omega t)2\omega\left[d^{(0)}\int_{-a}^{a}\psi_0 dx + d^{(2)}\int_{-a}^{a}\psi_2 dx\right]$$
$$+\frac{N^2}{2}\int_{-a}^{a}\left(-\frac{1}{2}(\nabla\psi_1)^2 + \lambda_1\psi_1\frac{\partial\psi_1}{\partial z}\right)dx \qquad (5.88)$$
$$\Downarrow$$
$$\alpha_0 = \frac{N^2}{2}\left(\frac{D+E}{2}\right)$$

The contribution from the integral of the cos(2ωt)-terms is equal to zero, and the constant E is given by

$$E = -\frac{1}{2}\left(\frac{\pi}{2a}\right)^2\sinh^2\left(\frac{\pi}{2a}h\right) + \frac{\sigma_1^2}{g}\left(\frac{\pi}{2a}\right)\cosh\left(\frac{\pi}{2a}h\right)\sinh\left(\frac{\pi}{2a}h\right) \qquad (5.89)$$

The total second order velocity potential is then

$$\phi_2 = \frac{N^2}{2}\left(\frac{E+D}{2}\right)t - A_0^{(2)}\frac{N^2}{2}\sin(2\omega t)(C\omega + D\omega)$$
$$-A_1^{(2)}\frac{N^2}{2}\sin(2\omega t)(D\omega - C\omega - gF)\cos\left(\frac{\pi}{a}x\right)\cosh\left(\frac{\pi}{a}(z+h)\right) \qquad (5.90)$$

and the second order free surface elevation

$$\zeta_2=\frac{\lambda_1}{\omega^2}\left[\frac{N^2}{2}\cos(2\omega t)\left(-\frac{1}{2}(\nabla\psi_1)^2-\lambda_1\psi_1\frac{\partial\psi_1}{\partial z}\right)+\frac{N^2}{2}\left(-\frac{1}{2}(\nabla\psi_1)^2+\lambda_1\psi_1\frac{\partial\psi_1}{\partial z}\right)\right.$$

$$\left.-\alpha_0+\left[\psi_0 d^{(0)}+\psi_2 d^{(2)}\right]2\omega\frac{N^2}{2}\cos(2\omega t)\right] \qquad on\ z=0 \tag{5.91}$$

$$=\frac{\sigma_1^2}{\omega^2 g}\cos(2\omega t)N^2\cos\left(\frac{\pi}{a}x\right)\left[\frac{D-C}{4}+A_1^{(2)}\omega(D\omega-C\omega-gF)\cosh\left(\frac{\pi}{a}h\right)\right]$$

$$+\frac{\sigma_1^2}{\omega^2 g}\frac{N^2}{2}\frac{D-E}{2}\cos\left(\frac{\pi}{a}x\right)$$

which is in accordance with the results obtained by Faltinsen (1974).

5.2.5 Third order equations

The combined free surface condition for the third order equations is obtained as

$$\frac{\partial^2\phi_3}{\partial t^2}+\frac{\omega^2}{\lambda_1}\frac{\partial\phi_3}{\partial z}=$$

$$\sin\left(\frac{\pi}{2a}x\right)\cos(\omega t)\left\{(K_1-K_2)N^3+\alpha\cosh\left(\frac{\pi}{2a}h\right)N+2a\omega^3\frac{8a}{\pi^2}\right\}$$

$$+\sin\left(\frac{\pi}{2a}x\right)\cos(3\omega t)(K_3-L_3)+\sin\left(\frac{3\pi}{2a}x\right)\cos(\omega t)(K_5-L_5) \tag{5.92}$$

$$+\sin\left(\frac{3\pi}{2a}x\right)\cos(3\omega t)(K_4-L_4)$$

$$+2a\omega^3\sum_{n=1}^{\infty}(-1)^n\frac{8a}{(2n+1)^2\pi^2}\sin\left(\frac{2n+1}{2a}\pi x\right)\cos(\omega t)$$

Here the f(x) is expanded in to a Fourier series:

$$f(x)=2a\omega^3 x=2a\omega^3\sum_{n=1}^{\infty}\frac{2}{a}\frac{4a^2}{(2n+1)^2\pi^2}(-1)^n\sin\left(\frac{2n+1}{2a}\pi x\right) \tag{5.93}$$

and the K and L terms are

$$K_1 = \frac{3\pi^2}{8a^2}\omega^2 A_1^{(2)}\left\{\frac{\pi^2}{16a^2}\cosh\left(\frac{\pi}{2a}h\right) - \frac{\sigma_1^2}{g}\frac{\pi}{8a}\sinh\left(\frac{\pi}{2a}h\right)\cosh\left(\frac{\pi}{a}h\right)\right\} \tag{5.94}$$
$$-\frac{5\pi^3}{256a^3}\sinh\left(\frac{\pi}{2a}h\right)\frac{\sigma_1^2}{g} + \frac{7\pi^3}{256a^3}\sinh\left(\frac{\pi}{2a}h\right)\cosh^2\left(\frac{\pi}{2a}h\right)\frac{\sigma_1^2}{g}$$

$$K_2 = -\frac{3\pi^4}{64a^4}\omega^2 A_1^{(2)}\cosh\left(\frac{\pi}{2a}h\right)\cosh\left(\frac{\pi}{a}h\right) \tag{5.95}$$
$$-\frac{3\pi^4}{512a^4}\cosh\left(\frac{\pi}{2a}h\right) - \frac{\sigma_1^2}{g}\frac{\pi^3}{256a^3}\sinh\left(\frac{\pi}{2a}h\right)\cosh^2\left(\frac{\pi}{2a}h\right)$$

$$K_3 = 3\omega N^3\left\{-\frac{3}{2}\left(\frac{\pi}{2a}\right)^4\omega A_1^{(2)}\left[-\frac{1}{4}\cosh\left(\frac{\pi}{2a}h\right)\cosh\left(\frac{\pi}{a}h\right) - \frac{3}{2}\sinh\left(\frac{\pi}{2a}h\right)\sinh\left(\frac{\pi}{a}h\right)\right.\right. \tag{5.96}$$
$$\left.\left. -\frac{1}{4}\tanh\left(\frac{\pi}{2a}h\right)\sinh\left(\frac{\pi}{2a}h\right)\cosh\left(\frac{\pi}{a}h\right)\right]\right.$$
$$\left. +\frac{\sigma_1^2}{\omega g}\left(\frac{\pi}{2a}\right)^3\sinh\left(\frac{\pi}{2a}h\right)\left[-\frac{3}{32}\sinh^2\left(\frac{\pi}{2a}h\right) - \frac{10}{32}\cosh^2\left(\frac{\pi}{2a}h\right)\right]\right\}$$

$$K_4 = 3\omega N^3\left\{-\frac{3}{2}\left(\frac{\pi}{2a}\right)^4\omega A_1^{(2)}\left[-\frac{1}{4}\cosh\left(\frac{\pi}{2a}h\right)\cosh\left(\frac{\pi}{a}h\right) + \frac{3}{4}\sinh\left(\frac{\pi}{2a}h\right)\sinh\left(\frac{\pi}{a}h\right)\right.\right. \tag{5.97}$$
$$\left.\left. +\frac{1}{4}\tanh\left(\frac{\pi}{2a}h\right)\sinh\left(\frac{\pi}{2a}h\right)\cosh\left(\frac{\pi}{a}h\right)\right]\right.$$
$$\left. +\frac{\sigma_1^2}{\omega g}\left(\frac{\pi}{2a}\right)^3\sinh\left(\frac{\pi}{2a}h\right)\frac{3}{32}\sinh^2\left(\frac{\pi}{2a}h\right)\right\}$$

$$K_5=\omega N^3\left\{-\frac{3}{2}\left(\frac{\pi}{2a}\right)^4\omega A_1^{(2)}\left[-\frac{1}{4}\cosh\left(\frac{\pi}{2a}h\right)\cosh\left(\frac{\pi}{a}h\right)-\frac{1}{4}\sinh\left(\frac{\pi}{2a}h\right)\sinh\left(\frac{\pi}{a}h\right)\right.\right.$$
$$\left.-\frac{1}{4}\tanh\left(\frac{\pi}{2a}h\right)\sinh\left(\frac{\pi}{2a}h\right)\cosh\left(\frac{\pi}{a}h\right)\right]$$
$$\left.+\frac{\sigma_1^2}{\omega g}\left(\frac{\pi}{2a}\right)^3\sinh\left(\frac{\pi}{2a}h\right)\left[-\frac{5}{32}\sinh^2\left(\frac{\pi}{2a}h\right)-\frac{1}{8}\cosh^2\left(\frac{\pi}{2a}h\right)\right]\right\} \tag{5.98}$$

$$L_3=N^3\left(\frac{\pi}{2a}\right)^4\cosh\left(\frac{\pi}{2a}h\right)\left[\frac{1}{16}\sinh^2\left(\frac{\pi}{2a}h\right)-\frac{1}{32}\cosh^2\left(\frac{\pi}{2a}h\right)\right] \tag{5.99}$$

$$L_4=N^3\left\{-\frac{3}{2}\left(\frac{\pi}{2a}\right)^4\omega^2A_1^{(2)}\frac{3}{2}\cosh\left(\frac{\pi}{2a}h\right)\cosh\left(\frac{\pi}{a}h\right)\right.$$
$$\left.+\left(\frac{\pi}{2a}\right)^4\cosh\left(\frac{\pi}{2a}h\right)\left[\frac{12}{32}\sinh^2\left(\frac{\pi}{2a}h\right)-\frac{3}{32}\cosh^2\left(\frac{\pi}{2a}h\right)\right]\right\} \tag{5.100}$$

$$L_5=-N^3\left(\frac{\pi}{2a}\right)^4\cosh\left(\frac{\pi}{2a}h\right)\frac{9}{32}\cosh^2\left(\frac{\pi}{2a}h\right) \tag{5.101}$$

Except for the L_3 term, where there is a plus sign before the 1/16 and the L_5 term, where there is not a $\sinh^2(\pi h/2a)$ term and there is 9 instead of 7 on the top of the bracket, these are the same expressions as the ones obtained in Faltinsen (1974). This is shown to be correct by comparing the values of the right hand side in the free surface condition (5.92), with the values obtained by putting the analytical obtained values of the eigenfunctions into equation (6.24). This should be exactly the same, which it is. If Faltinsens formulas for L_3 and L_5 are used, a small difference is obtained.

The unknown N is determined by setting the $\cos(\omega t)$ terms on the right hand side in the combined free surface condition equal to zero. The equation which determines N is then:

$$(K_1-K_2)N^3+\alpha\cosh\left(\frac{\pi}{2a}h\right)N+2a\omega^3\frac{8a}{\pi^2}=0 \tag{5.102}$$

The third order velocity potential, which satisfies the combined free surface condition (5.92) is given by

$$\phi_3 = A_0^{(3)}\sin\left(\frac{\pi}{2a}x\right)\cosh\left[\frac{\pi}{2a}(z+h)\right]\cos(3\omega t) + A_1^{(3)}\sin\left(\frac{3\pi}{2a}x\right)\cosh\left[\frac{3\pi}{2a}(z+h)\right]\cos(3\omega t)$$
$$+ A_2^{(3)}\sin\left(\frac{3\pi}{2a}x\right)\cosh\left[\frac{3\pi}{2a}(z+h)\right]\cos(\omega t)$$
$$+ \omega^3\cos(\omega t)\sum_{n=1}^{\infty}(-1)^n\sin\left(\frac{2n+1}{2a}\pi x\right)\cosh\left[\frac{2n+1}{2a}\pi(z+h)\right]\frac{16a^2B_n^{(3)}}{\pi^2(2n+1)^2} \qquad (5.103)$$

where the constants

$$A_0^{(3)} = \frac{K_3 - L_3}{-9\omega^2\cosh\left(\frac{\pi}{2a}h\right) + \frac{\omega^2}{\sigma_1^2}g\frac{\pi}{2a}\sinh\left(\frac{\pi}{2a}h\right)} \qquad (5.104)$$

$$A_1^{(3)} = \frac{K_4 - L_4}{-9\omega^2\cosh\left(\frac{3\pi}{2a}h\right) + \frac{\omega^2}{\sigma_1^2}g\frac{3\pi}{2a}\sinh\left(\frac{3\pi}{2a}h\right)} \qquad (5.105)$$

$$A_2^{(3)} = \frac{K_5 - L_5}{-\omega^2\cosh\left(\frac{3\pi}{2a}h\right) + \frac{\omega^2}{\sigma_1^2}g\frac{3\pi}{2a}\sinh\left(\frac{3\pi}{2a}h\right)} \qquad (5.106)$$

and

$$B_n^{(3)} = \frac{1}{-\omega^2\cosh\left(\frac{(2n+1)\pi}{2a}h\right) + \frac{\omega^2}{\sigma_1^2}g\frac{(2n+1)\pi}{2a}\sinh\left(\frac{(2n+1)\pi}{2a}h\right)} \qquad (5.107)$$

All terms in the velocity potential $\Phi = \phi_1\varepsilon^{1/3} + \phi_2\varepsilon^{2/3} + \phi_3\varepsilon$ are now determined.

5.3 Nonlinear solution for sloshing in a vertical circular cylindrical tank

In this chapter the response of the water inside a vertical circular cylindrical tank is determined. The analysis follows the work done by Hutton (1963) except for the constant term, α_0, in the second order potential, which he has not determined. His report contains some misprinting in some of the coefficients. These are pointed out in appendix F and appendix H, where the coefficients are presented. Misprints in subscripts and superscripts in Hutton's expressions are not commented.

The problem is solved to second order. The third order equations are used to find the generalized coordinates in the first and second order potential. Figure 4.4 illustrates the geometry and coordinate system which is used in the analysis.

5.3.1 Eigenfunctions and values

The eigenfunctions are obtained by solving Laplace equation

$$\frac{\partial^2\psi_{mn}}{\partial r^2}+\frac{1}{r}\cdot\frac{\partial\psi_{mn}}{\partial r}+\frac{1}{r^2}\cdot\frac{\partial^2\psi_{mn}}{\partial\theta^2}+\frac{\partial^2\psi_{mn}}{\partial z^2}=0 \tag{5.108}$$

in the fluid domain, with the boundary conditions

$$\begin{aligned}
&\frac{\partial\psi_{mn}}{\partial r}=0 && on\ r=a\\
&\frac{\partial\psi_{mn}}{\partial z}=0 && on\ z=-h\\
&\frac{\partial\psi_{mn}}{\partial z}=\frac{\sigma_{mn}^2}{g}\psi_{mn} && on\ z=0
\end{aligned} \tag{5.109}$$

in the same manner as in chapter 4.2.1. We should note that the occurrence of rotary sloshing is taken into account, and then, the solution is no longer symmetric about θ=0, and both $\sin(m\theta)$ and $\cos(m\theta)$ terms have to be taken in to account. Then, the eigenfunctions have the form

$$\psi_{mn}=\left[A_{mn}(t)\cos(m\theta)+B_{mn}(t)\sin(m\theta)\right]J_{mn}\left(\frac{\xi_{mn}}{a}r\right)\frac{\cosh\left(\frac{\xi_{mn}}{a}(z+h)\right)}{\cosh\left(\frac{\xi_{mn}}{a}h\right)} \tag{5.110}$$

where the functions A_{mn} and B_{mn} are dependent only upon time and are called the generalized coordinates of the mn'th mode. The eigenfrequencies are given by

$$\sigma_{mn}^2 = \frac{\xi_{mn}}{a} g \tanh\left(\frac{\xi_{mn}}{a} h\right) \tag{5.111}$$

where ξ_{mn} are the roots of $J'_m(\xi_{mn}) = 0$.

5.3.2 Forced sway oscillation near resonance

The tank is assumed to be oscillated harmonically with small amplitudes, ε_0 , in transverse (sway) direction in the vicinity of the lowest natural frequency, σ_{11} , of the water inside the tank. The tank is oscillated in the xz-plane only and the motion is $x_b(t)=\varepsilon_0 \sin(\omega t)$. The r,θ,z coordinate system moves with the tank with the plane z=0 in the undisturbed water plane.

The total velocity potential, Φ_T, satisfies the Laplace equation in the fluid domain. The dynamic free surface condition is given in equation (3.9) and the kinematic free surface condition in equation (3.11) on the instantaneous free surface $z=\zeta(r,\theta,t)$. The boundary condition on the tank bottom is

$$\frac{\partial \Phi_T}{\partial z} = 0 \quad on\ z = -h \tag{5.112}$$

and the boundary condition at the tank wall

$$\frac{\partial \Phi_T}{\partial r} = v_r \quad on\ r = a \tag{5.113}$$

where v_r is the container velocity in r direction. The tank velocity is

$$\dot{x}_b = \varepsilon_0 \omega \cos(\omega t) = \varepsilon \cos(\omega t) \tag{5.114}$$

where the frequency of oscillation ω is near the first resonance frequency

$$\omega^2 = \sigma_{11}^2 + \omega^2 \nu \varepsilon^{2/3} \tag{5.115}$$

Note that we have used that $\varepsilon = \varepsilon_0 \omega$, which is in accordance with Hutton (1963). The first natural frequency is

$$\sigma_{11} = \sqrt{g \frac{\xi_{11}}{a} \tanh\left(\frac{\xi_{11}}{a} h\right)} = \sqrt{g \frac{\xi_{11}}{a} \alpha_{11}} \tag{5.116}$$

where ξ_{11} corresponds to the first zero of $J_1'(\xi_{11})$, that is ξ_{11} =1.84119.

The velocity potential Φ_T is written as the sum of the disturbance potential Φ and a function accounting for the tank motion

$$\Phi_T(r,\theta,z,t) = \dot{x}_b \cdot r \cdot \cos\theta + \Phi(r,\theta,z,t) \tag{5.117}$$

Terms of order $\varepsilon_0\Phi$, ε_0^2 and $\varepsilon_0\zeta$ are neglected, and then, the total boundary value problem is

$$\frac{\partial^2\Phi}{\partial r^2}+\frac{1}{r}\cdot\frac{\partial\Phi}{\partial r}+\frac{1}{r^2}\cdot\frac{\partial^2\Phi}{\partial\theta^2}+\frac{\partial^2\Phi}{\partial z^2}=0 \quad \textit{in the fluid domain} \tag{5.118}$$

$$\frac{\partial\Phi}{\partial z}=0 \quad on\ z=-h \tag{5.119}$$

$$\frac{\partial\Phi}{\partial r}=0 \quad on\ r=a \tag{5.120}$$

$$g\cdot\zeta+\frac{\partial\Phi}{\partial t}+\frac{1}{2}\left[\left(\frac{\partial\Phi}{\partial r}\right)^2+\frac{1}{r^2}\left(\frac{\partial\Phi}{\partial\theta}\right)^2+\left(\frac{\partial\Phi}{\partial z}\right)^2\right]=-\ddot{x}_b\cdot r\cdot\cos\theta \quad on\ z=\zeta(r,\theta,t) \tag{5.121}$$

$$\frac{\partial\zeta}{\partial t}+\frac{\partial\Phi}{\partial r}\cdot\frac{\partial\zeta}{\partial r}+\frac{1}{r^2}\cdot\frac{\partial\Phi}{\partial\theta}\cdot\frac{\partial\zeta}{\partial\theta}-\frac{\partial\Phi}{\partial z}=0 \quad on\ z=\zeta(r,\theta,t) \tag{5.122}$$

Note that the only nonlinear character of this boundary value problem enters through the free-surface boundary conditions on $z = \zeta$. Since the free-surface height ζ is an unknown in the problem the two free-surface conditions are combined in appendix C to one equation that does not contain ζ

$$B_1+B_2+B_3+O(\zeta^4)=0 \quad on\ z=0 \tag{5.123}$$

where the terms B_1, B_2, and B_3 depend only upon the velocity potential function Φ and its derivatives, all evaluated on the undisturbed free-surface $z = 0$, and upon the prescribed tank displacement $x_b(t)$.

The solution of the boundary value problem is limited to the case where ε is small and the driving frequency ω is close to or equal to the first mode frequency $\bar{\sigma}_1$. The velocity potential is written as

$$\Phi=\varepsilon^{1/3}\Phi_1+\varepsilon^{2/3}\Phi_2+\varepsilon\Phi_3 \tag{5.124}$$

where

$$\begin{aligned}\Phi_1 &= \Psi_1(r,\theta,z,\tau)\cos(\omega t)+\chi_1(r,\theta,z,\tau)\sin(\omega t)\\ \Phi_2 &= \alpha_0 t+\Psi_2(r,\theta,z)\cos(2\omega t)+\chi_2(r,\theta,z)\sin(2\omega t)\\ \Phi_3 &= \Psi_3(r,\theta,z)\cos(3\omega t)+\chi_3(r,\theta,z)\sin(3\omega t)\end{aligned} \tag{5.125}$$

and

$$\tau = \frac{1}{2}\varepsilon^{2/3}\omega t \tag{5.126}$$

Ψ_n and χ_n satisfy Laplace equation and only Ψ_1 and χ_1 depend upon time. This time dependence is due to the stability investigation of the solution in chapter 5.3.7 Neglecting

the higher order terms, the terms B_1, B_2, and B_3 may be written as

$$B_1 = \varepsilon^{1/3}[\phi_{1tt}+g\phi_{1z}]+\varepsilon^{2/3}[\phi_{2tt}+g\phi_{2z}]+\varepsilon[\phi_{3tt}+g\phi_{3z}-r\omega^2\cos\theta\cos(\omega t)] \tag{5.127}$$

$$\begin{aligned} B_2 = {} & \varepsilon^{2/3}[2\phi_{1r}\phi_{1rt}+\frac{2}{r^2}\phi_{1\theta}\phi_{1\theta t}+2\phi_{1z}\phi_{1zt}-\frac{1}{g}\phi_{1tz}\phi_{1t}-\phi_{1zz}\phi_{1t}] \\ & + \varepsilon\ [2\phi_{1r}\phi_{2rt}+2\phi_{2r}\phi_{1rt}+\frac{2}{r^2}\phi_{1\theta}\phi_{2\theta t}+\frac{2}{r^2}\phi_{2\theta}\phi_{1\theta t}+2\phi_{1z}\phi_{2zt} \\ & +2\phi_{2z}\phi_{1zt}-\frac{1}{g}\phi_{1tz}\phi_{2t}-\frac{1}{g}\phi_{2tz}\phi_{1t}-\phi_{1zz}\phi_{2t}-\phi_{2zz}\phi_{1t}] \end{aligned} \tag{5.128}$$

$$\begin{aligned} B_3 = \varepsilon\ & [\phi_{1r}^2\phi_{1rr}+\frac{1}{r^4}\phi_{1\theta}^2\phi_{1\theta\theta}+\phi_{1z}^2\phi_{1zz}-\frac{1}{r^3}\phi_{1r}\phi_{1\theta}^2+2\phi_{1r}\phi_{1z}\phi_{1rz}+\frac{2}{r^2}\phi_{1r}\phi_{1\theta}\phi_{1r\theta} \\ & +\frac{2}{r^2}\phi_{1z}\phi_{1\theta}\phi_{1\theta z}-\frac{1}{g}\frac{1}{2}\phi_{1tz}\phi_{1r}^2-\frac{1}{g}\frac{1}{2}\frac{1}{r^2}\phi_{1tz}\phi_{1\theta}^2-\frac{1}{g}\frac{1}{2}\phi_{1tz}\phi_{1z}^2-\frac{1}{2}\phi_{1zz}\phi_{1r}^2 \\ & -\frac{1}{2}\frac{1}{r^2}\phi_{1zz}\phi_{1\theta}^2-\frac{1}{2}\phi_{1zz}\phi_{1z}^2-\frac{2}{g}(\phi_{1rz}\phi_{1rt}+\phi_{1r}\phi_{1rzt}+\frac{1}{r^2}\phi_{1\theta z}\phi_{1\theta t}+\frac{1}{r^2}\phi_{1\theta}\phi_{1\theta zt} \\ & +\phi_{1zz}\phi_{1zt}+\phi_{1z}\phi_{1zzt})+\phi_{1t}+\frac{1}{g^2}\phi_{1tz}\phi_{1t}\phi_{1tz}+\frac{1}{g}\phi_{1zz}\phi_{1t}\phi_{1tz} \\ & +\frac{1}{g^2}\frac{1}{2}\phi_{1tzz}\phi_{1t}^2+\frac{1}{g}\frac{1}{2}\phi_{1zzz}\phi_{1t}^2] \end{aligned} \tag{5.129}$$

where $\phi = \Phi(r,\theta,z=0,\tau)$, and the subscripts t, r, θ and z represent the time, r, θ and z derivatives respectively.

The terms of which $\varepsilon^{1/3}$, $\varepsilon^{2/3}$ and ε are the coefficients are now set equal to zero.

5.3.3 First order equations

Setting the coefficient of the $\varepsilon^{1/3}$ terms in the combined free surface equation equal to zero gives

$$\phi_{1tt}+g\phi_{1z} = 0 \qquad on\ z = 0 \tag{5.130}$$

and using the relation (5.115) and equation (5.125), equation (5.130) gives

$$(g\Psi_{1z}-\sigma_{11}^2\Psi_1)\cos(\omega t)+(g\chi_{1z}-\sigma_{11}^2\chi_1)\sin(\omega t)=0 \qquad on\ z=0 \tag{5.131}$$

For these first order term to vanish for all time, it is necessary that

$$\Psi_{1z} = \frac{\sigma_{11}^2}{g}\Psi_1 \qquad and \qquad \chi_{1z} = \frac{\sigma_{11}^2}{g}\chi_1 \qquad on\ z=0 \tag{5.132}$$

Equation (5.131) will be satisfied identically by choosing, in accordance with the shape of the eigenfunctions

$$\Psi_1=[f_1(\tau)\cos\theta+f_3(\tau)\sin\theta]J_1\left(\frac{\xi_{11}}{a}r\right)\frac{\cosh\left[\frac{\xi_{11}}{a}(z+h)\right]}{\cosh\left(\frac{\xi_{11}}{a}h\right)}$$

$$\chi_1=[f_2(\tau)\cos\theta+f_4(\tau)\sin\theta]J_1\left(\frac{\xi_{11}}{a}r\right)\frac{\cosh\left[\frac{\xi_{11}}{a}(z+h)\right]}{\cosh\left(\frac{\xi_{11}}{a}h\right)} \qquad (5.133)$$

regardless of the values of the generalized coordinates f_i.

5.3.4 Second order equations

For the second order terms in the free surface equation to vanish, the coefficient of $\varepsilon^{2/3}$ must be zero.

$$\phi_{2t}+g\phi_{2z}=-2\phi_{1r}\phi_{1rt}-\frac{2}{r^2}\phi_{1\theta}\phi_{1\theta t}-2\phi_{1z}\phi_{1zt}+\frac{1}{g}\phi_{1tz}\phi_{1t}+\phi_{1zz}\phi_{1t} \qquad (5.134)$$

When the relations

$$\chi_1\Psi_{1z}=\chi_{1z}\Psi_1 \quad \text{and} \quad \chi_1\Psi_{1zz}=\chi_{1zz}\Psi_1 \qquad (5.135)$$

are used, the following three equations are obtained , when the constant term, the cos(2ωt) and the sin(2ωt) terms are individually set equal to zero.

$$\alpha_{0z}=0$$

$$4\sigma_{11}^2\Psi_2-g\Psi_{2z}=2\sigma_{11}(\chi_{1r}\Psi_{1r}+\frac{1}{r^2}\chi_{1\theta}\Psi_{1\theta}+\frac{3\alpha_{11}^2-1}{2a^2}\xi_{11}^2\chi_1\Psi_1) \qquad (5.136)$$

$$4\sigma_{11}^2\chi_2-g\chi_{2z}=\sigma_{11}[\chi_{1r}^2-\Psi_{1r}^2+\frac{1}{r^2}\chi_{1\theta}^2-\frac{1}{r^2}\Psi_{1\theta}^2+\frac{3\alpha_{11}^2-1}{2a^2}\sigma_{11}^2(\chi_1^2-\Psi_1^2)]$$

The functions Ψ_2 and χ_2 are selected to satisfy equations (5.136). α_0 is a constant, and the first of the equations (5.136) is satisfied identically. If Ψ_2 and χ_2 are taken to be

$$\Psi_2 = \sum_{n=1}^{\infty} \hat{A}_{0n} J_0\left(\frac{\xi_{0n}}{a} r\right) \frac{\cosh\left[\frac{\xi_{0n}}{a}(z+h)\right]}{\cosh\left(\frac{\xi_{0n}}{a} h\right)}$$

$$+ \sum_{n=1}^{\infty} [\hat{A}_{2n}\cos(2\theta) + \hat{B}_{2n}\sin(2\theta)] J_2\left(\frac{\xi_{2n}}{a} r\right) \frac{\cosh\left[\frac{\xi_{2n}}{a}(z+h)\right]}{\cosh\left(\frac{\xi_{2n}}{a} h\right)}$$

$$\chi_2 = \sum_{n=1}^{\infty} \hat{C}_{0n} J_0\left(\frac{\xi_{0n}}{a} r\right) \frac{\cosh\left[\frac{\xi_{0n}}{a}(z+h)\right]}{\cosh\left(\frac{\xi_{0n}}{a} h\right)} \qquad (5.137)$$

$$+ \sum_{n=1}^{\infty} [\hat{C}_{2n}\cos(2\theta) + \hat{D}_{2n}\sin(2\theta)] J_2\left(\frac{\xi_{2n}}{a} r\right) \frac{\cosh\left[\frac{\xi_{2n}}{a}(z+h)\right]}{\cosh\left(\frac{\xi_{2n}}{h}\right)}$$

where $J'_0(\xi_{0n})=J'_2(\xi_{2n})=0$, then equations (5.136) can be satisfied by choosing the suitable generalized coordinates in ψ_2 and χ_2. These generalized coordinates can be expressed in terms of f_1, f_2, f_3 and f_4 by introducing equations (5.133) and (5.137) into (5.136) and use the following orthogonality relations

$$\int_0^a r J_0(\lambda_{0m} r) J_0(\lambda_{0n} r) dr = \begin{cases} 0 & , m \neq n \\ \frac{a^2}{2} J_0^2(\lambda_{0n} a) & , m = n \end{cases}$$

$$\int_0^a r J_2(\lambda_{2m} r) J_2(\lambda_{2n} r) dr = \begin{cases} 0 & , m \neq n \\ \frac{\lambda_{2n}^2 a^2 - 4}{2\lambda_{2n}^2} J_2^2(\lambda_{2n} a) & , m = n \end{cases} \qquad (5.138)$$

where $\lambda_{0n}= \xi_{0n}/a$ and $\lambda_{2n}= \xi_{2n}/a$. This is performed in appendix D, and gives the following expressions for the generalized coordinates

$$\begin{aligned}
\hat{A}_{0n} &= \Omega_{0n}(f_1 f_2 + f_3 f_4) \\
\hat{A}_{2n} &= \Omega_{2n}(f_1 f_2 - f_3 f_4) \\
\hat{B}_{2n} &= \Omega_{2n}(f_1 f_4 + f_2 f_3) \\
\hat{C}_{0n} &= \Omega_{0n}\frac{1}{2}(f_2^2 + f_4^2 - f_1^2 - f_3^2) \\
\hat{C}_{2n} &= \Omega_{2n}\frac{1}{2}(f_2^2 + f_3^2 - f_1^2 - f_4^2) \\
\hat{D}_{2n} &= \Omega_{2n}(f_2 f_4 - f_1 f_3)
\end{aligned} \tag{5.139}$$

where Ω_{0n} and Ω_{2n} are given in appendix D. The roots of $J'_0(\xi_{0n})=0$ and $J'_2(\xi_{2n})=0$ are given in appendix H. The constant α_0 is determined from

$$\int_0^{2\pi}\int_0^a \zeta\, r\, dr\, d\theta = 0 \tag{5.140}$$

in appendix E to be

$$\alpha_0 = (f_1^2 + f_2^2 + f_3^2 + f_4^2)(\alpha_{11}^2 - 1)\frac{[\xi_{11}^2 - 1]J_1^2(\xi_{11})}{8a^2} \tag{5.141}$$

5.3.5 Third order equations

The coefficients of ε in the combined free surface condition give the third order terms. Third order terms arise from each of the boundary value terms B_1, B_2 and B_3. For the third order terms, it is required that the first harmonic terms vanish. This determines the generalized coordinates f_1, f_2, f_3 and f_4. The first harmonic terms, $B_1^{FH\varepsilon}$, $B_2^{FH\varepsilon}$ and $B_3^{FH\varepsilon}$, are given in appendix F.

First, the equation $B_1^{FH\varepsilon} + B_2^{FH\varepsilon} + B_3^{FH\varepsilon}$ is multiplied by $J_1 \cdot \cos\theta \cdot r \cdot dr \cdot d\theta$ and integrated over the free surface, $0 \le r \le a$ and $0 \le \theta \le 2\pi$. Then, the equation $B_1^{FH\varepsilon} + B_2^{FH\varepsilon} + B_3^{FH\varepsilon}$ is multiplied by $J_1 \cdot \sin\theta \cdot r \cdot dr \cdot d\theta$ and integrated over the free surface. Both of these integrated equations have $\sin(\omega t)$ and $\cos(\omega t)$ terms. Requiring that the coefficients of each of the $\sin(\omega t)$ and $\cos(\omega t)$ terms vanish in these two equations gives the nonlinear differential equations that the generalized coordinates f_1, f_2, f_3 and f_4 must satisfy

$$\begin{aligned}
\frac{df_1}{d\tau} &= -\nu f_2 - K_1 f_2 (f_1^2 + f_2^2 + f_3^2 + f_4^2) + K_2 f_3 (f_2 f_3 - f_1 f_4) \\
\frac{df_2}{d\tau} &= F_1 + \nu f_1 + K_1 f_1 (f_1^2 + f_2^2 + f_3^2 + f_4^2) + K_2 f_4 (f_2 f_3 - f_1 f_4) \\
\frac{df_3}{d\tau} &= -\nu f_4 - K_1 f_4 (f_1^2 + f_2^2 + f_3^2 + f_4^2) - K_2 f_1 (f_2 f_3 - f_1 f_4) \\
\frac{df_4}{d\tau} &= \nu f_3 + K_1 f_3 (f_1^2 + f_2^2 + f_3^2 + f_4^2) - K_2 f_2 (f_2 f_3 - f_1 f_4)
\end{aligned} \tag{5.142}$$

where K_1, K_2 and F_1, which are constants depending upon tank geometry only, are defined in appendix F.

5.3.6 Steady-state harmonic solutions

The form of the set of first order differential equations (5.142) is identical with that of the set of differential equations derived by J.W. Miles (1962) for the undamped spherical pendulum. So, the steady-state solutions of equations (5.142) are the same as the two obtained by Miles for the spherical pendulum.

The two steady-state harmonic solutions of the boundary value problem expressed in equation (5.118), (5.119), (5.120) and (5.123) correspond to the zeros of $df_i/d\tau$ for i = 1, 2, 3, 4.

The first solution, called planar motion or lateral sloshing, is a steady-state fluid motion with a constant peak wave height and a single, stationary nodal diameter perpendicular to the direction of excitation. The second solution, called nonplanar motion or rotary sloshing, is a steady-state fluid motion with a constant peak wave height and a single nodal diameter that rotates at a constant rate around the container.

For the planar motion, the solution is

$$\begin{aligned}
f_1 &= \gamma \\
f_2 &= f_3 = f_4 = 0
\end{aligned} \tag{5.143}$$

and γ is governed by a cubic equation

$$K_1 \gamma^2 + F_1 \frac{1}{\gamma} + \nu = 0 \tag{5.144}$$

For the nonplanar motion, the solution is

$$\begin{aligned}
f_1 &= \gamma \\
f_2 &= f_3 = 0 \\
f_4^2 &= \zeta^2 = \gamma^2 + \frac{F_1}{K_2} \frac{1}{\gamma}
\end{aligned} \tag{5.145}$$

with

$$K_4\gamma^2 - K_3\frac{1}{\gamma} - \nu = 0 \tag{5.146}$$

where

$$K_3 = \frac{K_1}{K_2}F_1 \quad , \qquad K_4 = K_2 - 2K_1 \tag{5.147}$$

This solution is real, and hence exist, for $\gamma>0$ when $\gamma^3+F_1/K_2>0$ and for $\gamma<0$ when $\gamma^3+F_1/K_2<0$.

5.3.7 Stability of steady-state harmonic solutions

Now, a particular steady-state harmonic solution of equation (5.142) is denoted by the superscript (o), and the stability of such a solution is investigated by imposing a small perturbation from this steady-state solution and examining the subsequent motion. If the motion following the perturbation decreases with time, the solution is stable. If the motion increases with time, the solution is unstable. The generalized coordinates are written as

$$f_i(\tau) = f_i^{(o)} + c_i e^{\lambda\tau} \tag{5.148}$$

where $f_i^{(o)}$ are constants corresponding to the steady-state amplitudes of the harmonic solutions of equations (5.142) and the perturbation c_i are assumed to be small, i=1,2,3,4. Stable f_i solutions correspond to values of λ with negative real part, and unstable solutions correspond to values of λ with positive real part.

Introducing equation (5.148) into the equations (5.142), neglecting products of c_i, and imposing the condition that the $f_i^{(o)}$ are solutions of equations (5.142) leads to the following set of homogeneous algebraic equations:

$$\begin{bmatrix} d_{11}+\lambda & d_{12} & d_{13} & d_{14} \\ d_{21} & d_{22}-\lambda & d_{23} & d_{24} \\ d_{31} & d_{32} & d_{33}+\lambda & d_{34} \\ d_{41} & d_{42} & d_{43} & d_{44}-\lambda \end{bmatrix} \begin{bmatrix} c_1 \\ c_2 \\ c_3 \\ c_4 \end{bmatrix} = \begin{bmatrix} 0 \\ 0 \\ 0 \\ 0 \end{bmatrix} \tag{5.149}$$

where the d_{ij}, i,j=1,2,3,4, are given in appendix G.

Since equation (5.149) is a homogeneous set of equations in c_i, nontrivial solutions will exist only if the determinant of the coefficients is zero. Setting this determinant equal to zero gives the allowable values of λ. The question of stability is then reduced to an examination of the roots of the resulting equation in λ.

Planar motion solution

For the steady state planar motion

$$f_1^{(0)}=\gamma, \quad f_2^{(0)}=f_3^{(0)}=f_4^{(0)}=0 \tag{5.150}$$

where

$$\nu=-F_1\frac{1}{\gamma}-K_1\gamma^2 \tag{5.151}$$

Introducing this into equation (5.149) and setting the determinant of the coefficients of c_i equal to zero gives

$$\lambda^4+(M_1+M_2)\lambda^2+M_1M_2=0 \tag{5.152}$$

where

$$\begin{aligned} M_1&=(\nu+K_1\gamma^2)(\nu+3K_1\gamma^2)\\ M_2&=(\nu+K_1\gamma^2)(\nu+K_1\gamma^2-K_2\gamma^2) \end{aligned} \tag{5.153}$$

The d_{ij}, i,j=1,2,3,4 for the planar motion, are given in appendix G. The roots of equation (5.152) are

$$\lambda_1^2 = -M_1 = -(\nu+K_1\gamma^2)(\nu+3K_1\gamma^2) = -F_1\frac{1}{\gamma}\left(F_1\frac{1}{\gamma}-2K_1\gamma^2\right) \tag{5.154}$$

$$\lambda_2^2 = -M_2 = -(\nu+K_1\gamma^2)(\nu+K_1\gamma^2-K_2\gamma^2) = -F_1\frac{1}{\gamma}\left(F_1\frac{1}{\gamma}+K_2\gamma^2\right) \tag{5.155}$$

The boundary between stable and unstable planar motion corresponds to $\lambda_1 = 0$ and $\lambda_2 = 0$. From $\lambda_1^2 = 0$, it is found that

$$\gamma = \left(\frac{F_1}{2K_1}\right)^{1/3} \quad and \quad \gamma = \pm\infty \tag{5.156}$$

and from $\lambda_2^2 = 0$ that

$$\gamma = -\left(\frac{F_1}{K_2}\right)^{1/3} \quad and \quad \gamma = \pm\infty \tag{5.157}$$

Independent of the values of F_1 and K_2 is $\lambda_2^2 > 0$ when $\gamma < -(F_1/K_2)^{1/3}$. Then the motion is unstable. When $\gamma > (F_1/2K_1)^{1/3}$ is $\lambda_1^2 > 0$, independent of the values of F_1 and K_1 , and the motion is unstable. So, the motion is stable when

$$-\left(\frac{F_1}{K_2}\right)^{1/3} < \gamma < \left(\frac{F_1}{2K_1}\right)^{1/3} \tag{5.158}$$

Nonplanar motion solution

The steady state nonplanar motion was given as

$$f_1^{(0)}=\gamma, \quad f_2^{(0)}=f_3^{(0)}=0, \quad f_4^{(0)^2}=\zeta^2=\gamma^2+\frac{F_1}{K_2}\frac{1}{\gamma} \tag{5.159}$$

where

$$\nu=-K_3\frac{1}{\gamma}+K_4\gamma^2 \tag{5.160}$$

ζ have to be real, so $\zeta^2 > 0$. This indicates that the solution is not valid when γ lies in the range

$$-\frac{F_1}{K_2}<\gamma^3<0 \tag{5.161}$$

Introducing equation (5.159) and (5.160) into equation (5.149) and setting the determinant of the coefficients of c_i equal to zero gives

$$\lambda^4+(M_3+M_4)\lambda^2+M_5M_6=0 \tag{5.162}$$

where

$$\begin{aligned} M_3+M_4 &= 4K_2^2\gamma\left(\gamma^3+\frac{3K_2-2K_1}{4K_2^2}F_1\right) \\ M_5M_6 &= 4K_2^2(K_2-2K_1)F_1\frac{1}{\gamma}\left(\gamma^3+\frac{F_1}{K_2}\right)\left(\gamma^3+\frac{K_1F_1}{2K_2(K_2-2K_1)}\right) \end{aligned} \tag{5.163}$$

The d_{ij}, i,j=1,2,3,4 for the nonplanar motion and the M_3, M_4, M_5 and M_6, are given in appendix G.

Regarding equation (5.162) as quadratic in λ^2 and using Descartes rule of signs gives that if $\gamma^3<-F_1/K_2$ the equation (5.162) has one positive root. This implies that (since $\zeta^2 < 0$ if $-F_1/K_2 < \gamma < 0$) there can be no stable harmonic motions corresponding to $\gamma<0$. If $\gamma>0$ there are no positive real roots to (5.162) but the roots are complex if $(M_3+M_4)^2-4M_5M_6<0$.

The nonplanar motion is stable only for the values of γ which gives $(M_3+M_4)^2-4M_5M_6>0$.

5.3.8 Summary

For a given tank displacement amplitude ε_0 and frequency ω, the tank velocity amplitude ε is found from

$$\varepsilon = \varepsilon_0 \omega \tag{5.164}$$

and the transformed frequency ν from

$$\nu = \left(1 - \frac{\sigma_1^2}{\omega^2}\right)\varepsilon^{-2/3} \tag{5.165}$$

For the planar motion γ is governed by

$$K_1\gamma^2 + F_1\frac{1}{\gamma} + \nu = 0 \tag{5.166}$$

and for the nonplanar motion by

$$K_4\gamma^2 - K_3\frac{1}{\gamma} - \nu = 0 \tag{5.167}$$

The velocity potential is given by

$$\Phi = \varepsilon^{1/3}\Phi_1 + \varepsilon^{2/3}\Phi_2 + \varepsilon\Phi_3 \tag{5.168}$$

The contribution due to Φ_3 are not derived, so the velocity potential, correct to second order, is

$$\begin{aligned}
\Phi = \varepsilon^{1/3}\{ & [f_1(\tau)\cos\theta + f_3(\tau)\sin\theta]J_1(\lambda_{11}r)\frac{\cosh[\lambda_{11}(z+h)]}{\cosh(\lambda_{11}h)}\cos(\omega t) \\
& + [f_2(\tau)\cos\theta + f_4(\tau)\sin\theta]J_1(\lambda_{11}r)\frac{\cosh[\lambda_{11}(z+h)]}{\cosh(\lambda_{11}h)}\sin(\omega t)\} \\
+ \varepsilon^{2/3}\{ & \alpha_0 t + \sum_{n=1}^{\infty}\hat{A}_{0n}J_0(\lambda_{0n}r)\frac{\cosh[\lambda_{0n}(z+h)]}{\cosh(\lambda_{0n}h)}\cos(2\omega t) \\
& + \sum_{n=1}^{\infty}[\hat{A}_{2n}\cos(2\theta) + \hat{B}_{2n}\sin(2\theta)]J_2(\lambda_{2n}r)\frac{\cosh[\lambda_{2n}(z+h)]}{\cosh(\lambda_{2n}h)}\cos(2\omega t) \\
& + \sum_{n=1}^{\infty}\hat{C}_{0n}J_0(\lambda_{0n}r)\frac{\cosh[\lambda_{0n}(z+h)]}{\cosh(\lambda_{0n}h)}\sin(2\omega t) \\
& + \sum_{n=1}^{\infty}[\hat{C}_{2n}\cos(2\theta) + \hat{D}_{2n}\sin(2\theta)]J_2(\lambda_{2n}r)\frac{\cosh[\lambda_{2n}(z+h)]}{\cosh(\lambda_{2n}h)}\sin(2\omega t)\}
\end{aligned} \tag{5.169}$$

Stable motion

For the steady state harmonic planar motion

$$\begin{aligned} f_1&=\gamma \\ f_2&=f_3=f_4=0 \end{aligned} \tag{5.170}$$

and for the steady state nonplanar, that is rotating, motion

$$\begin{aligned} f_1&=\gamma \\ f_2&=f_3=0 \\ f_4^2&=\zeta^2=\gamma^2+\frac{F_1}{K_2}\frac{1}{\gamma} \end{aligned} \tag{5.171}$$

Unstable motion

For the unstable motion it may be interesting to study how the solution develops in time. How long time does it take before the disturbance, c_i, begins to influence the result. For the unstable motion

$$f_i(\tau)=f_i^{(o)}+c_i e^{\lambda\tau} \tag{5.172}$$

where $f_i^{(o)}$ are the steady-state amplitudes of the harmonic motions and c_i the small perturbation, i=1,2,3,4.

For planar unstable motion

$$\begin{aligned} f_1(\tau)&=\gamma+c_1 e^{\lambda\tau} \\ f_2(\tau)&=c_2 e^{\lambda\tau} \\ f_3(\tau)&=c_3 e^{\lambda\tau} \\ f_4(\tau)&=c_4 e^{\lambda\tau} \end{aligned} \tag{5.173}$$

and the set of homogeneous algebraic equations (5.149) becomes

$$\begin{bmatrix} \lambda & \nu+K_1\gamma^2 & 0 & 0 \\ \nu+3K_1\gamma^2 & -\lambda & 0 & 0 \\ 0 & 0 & \lambda & \nu+(K_1-K_2)\gamma^2 \\ 0 & 0 & \nu+K_1\gamma^2 & -\lambda \end{bmatrix} \begin{bmatrix} c_1 \\ c_2 \\ c_3 \\ c_4 \end{bmatrix} = \begin{bmatrix} 0 \\ 0 \\ 0 \\ 0 \end{bmatrix} \tag{5.174}$$

For $\lambda_1^2=-(\nu+K_1\gamma^2)(\nu+3K_1\gamma^2)$, we get

$$c_2=-\frac{\lambda_1}{(\nu+K_1\gamma^2)}c_1, \quad c_3=c_4=0 \tag{5.175}$$

and for $\lambda_2^2=-(\nu+K_1\gamma^2)(\nu+(K_1-K_2)\gamma^2)$, we get

$$c_4=\frac{(\nu+K_1\gamma^2)}{\lambda_2}c_3, \quad c_1=c_2=0 \tag{5.176}$$

For the unstable rotating motion

$$\begin{aligned} f_1(\tau)&=\gamma+c_1e^{\lambda\tau}\\ f_2(\tau)&=c_2e^{\lambda\tau}\\ f_3(\tau)&=c_3e^{\lambda\tau}\\ f_4(\tau)&=\zeta+c_4e^{\lambda\tau} \end{aligned} \tag{5.177}$$

and the set of homogeneous algebraic equations (5.149) becomes

$$\begin{bmatrix} \lambda & \nu+K_1(\gamma^2+\zeta^2) & K_2\gamma\zeta & 0\\ \nu+3K_1\gamma^2+(K_1-K_2)\zeta^2 & -\lambda & 0 & 2(K_1-K_2)\gamma\zeta\\ 2(K_1-K_2)\gamma\zeta & 0 & \lambda & \nu+3K_1\zeta^2+(K_1-K_2)\gamma^2\\ 0 & K_2\gamma\zeta & \nu+K_1(\gamma^2+\zeta^2) & -\lambda \end{bmatrix} \begin{bmatrix} c_1\\ c_2\\ c_3\\ c_4 \end{bmatrix} = \begin{bmatrix} 0\\ 0\\ 0\\ 0 \end{bmatrix} \tag{5.178}$$

5.3.9 Stability analysis for sloshing in vertical circular cylindrical tank

As an example a circular cylindrical tank with diameter 2a equal to 1.0 meter and water depth h equal to 0.5 meter is chosen. The eigenfrequency of the water inside the tank (from linear theory) is then 1.072 seconds. This tank dimensions give

$F_1 = 0.719090$
$K_1 = 0.509537$
$K_2 = 1.280300$

The values of other parameters are given in appendix H. In the evaluation of the coefficients K_1 and K_2 the infinite series terms are approximated by their first five terms. To indicate what errors this finite series approximation might cause it is seen, in appendix H, that the values of the last two terms in the calculation of $\hat{G}_1$ and $\hat{G}_2$, which contribute to K_1 and K_2, were less that a half percent of the values of the first two terms.

Planar motion

The amplitude-frequency relation for the planar motion is

$$\nu = -0.719090\frac{1}{\gamma} - 0.509537\gamma^2 \qquad (5.179)$$

The boundary between stable and unstable motion corresponds to $\lambda=0$. From $\lambda_1^2 = 0$ it is found that

$$\gamma = \pm\infty \text{ and } \gamma = (F_1 / 2K_1)^{1/3} = 0.890278$$

$K_1 > 0$, so these values correspond to

$$\nu = -\infty \text{ and } \nu = -3K_1 (F_1 / 2K_1)^{2/3} = -1.211570$$

From $\lambda_2^2 = 0$ it is found that

$$\gamma = \pm\infty \text{ and } \gamma = -(F_1 / K_2)^{1/3} = -0.825069$$

which corresponds to

$$\nu = -\infty \text{ and } \nu = (K_2 - K_1)(F_1 / K_2)^{2/3} = 0.524689$$

So, the motion is stable when

$$-0.825069 < \gamma < 0.890278$$

Figure 5.2 shows the regions for stable and unstable planar motions as function of the transformed frequency ν and the velocity potential function steady-state amplitude γ.

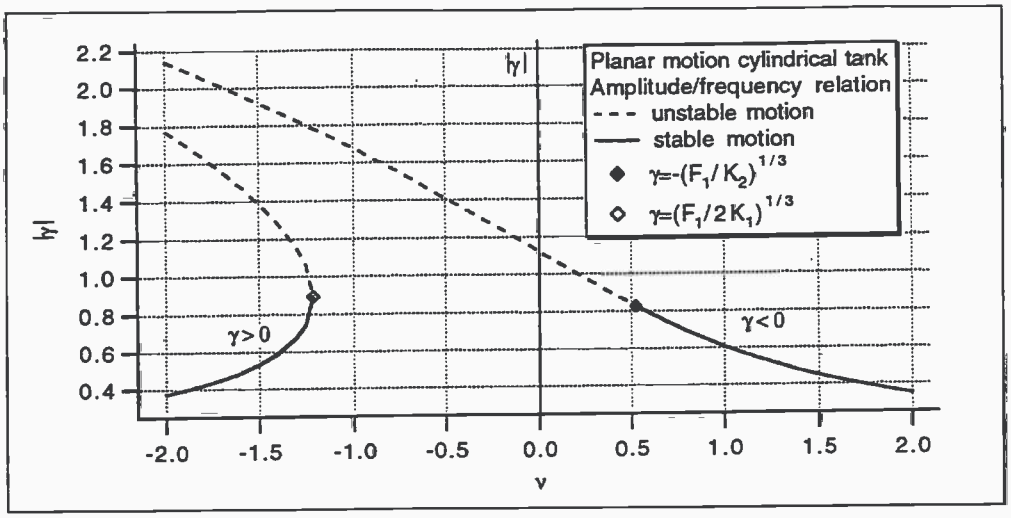

Figure 5.2 **Planar motion amplitude/frequency relation, γ-ν, for circular cylindrical tank with diameter 1.0 meter and water depth 0.5 meter.**

Figure 5.3 shows the regions for stable and unstable planar motion as function of the angular forcing frequency of tank motion, ω [rad/s], and the tank displacement amplitude, ε_0 [m].

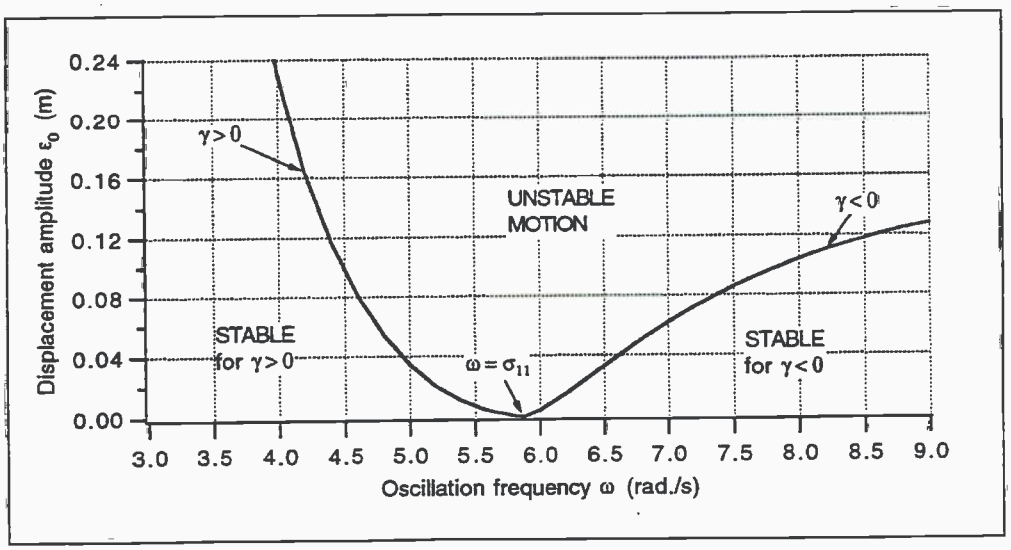

Figure 5.3 **Regions for stable and unstable planar motions as function of the angular forcing frequency of tank motion and the tank displacement amplitude.**

It is seen from Figure 5.3, that the planar motion is not stable for a oscillation frequency equal to the first natural frequency. When the oscillation frequency is in the vicinity of the first natural frequency, the motion is stable only for very small oscillation amplitudes. For small ω, that is, long oscillation periods, the motion is stable even for large amplitudes of oscillation.

Rotational sloshing / nonplanar motion

The amplitude-frequency relation for the nonplanar motion is

$$\nu = -0.286185\frac{1}{\gamma} + 0.261226\gamma^2 \tag{5.180}$$

and

$$\zeta^2 = \gamma^2 + 0.561657\frac{1}{\gamma} \tag{5.181}$$

The table below shows the regions for stable and unstable nonplanar motions.

$0.524689 < \nu < \infty$ $-0.825069 < \gamma < 0$	The nonplanar solution does not exist, since $\zeta^2 < 0$.
$0.524689 < \nu < \infty$ $-\infty < \gamma < -0.825069$ $0 < \lvert\zeta\rvert < \infty$	The nonplanar motion is unstable.
$-\infty < \nu < -0.359849$ $0 < \gamma < 0.621241$ $1.135794 < \lvert\zeta\rvert < \infty$	The nonplanar motion is unstable.
$-0.359849 < \nu < \infty$ $0.621241 < \gamma < \infty$ $1.135794 < \lvert\zeta\rvert < \infty$	Stable nonplanar motion.

Table 5.1 Regions for stable and unstable nonplanar motion for cylindrical tank with 2a=1.0 m, h=0.5 m.

Figure 5.4 shows the regions for stable and unstable nonplanar motions as a function of the transformed frequency ν and the velocity potential function steady-state amplitude γ and ζ. Figure 5.5 shows the regions for stable and unstable planar motion as a function of the angular forcing frequency of thank motion, ω [rad/s], and the tank displacement amplitude, ε_0 [m].

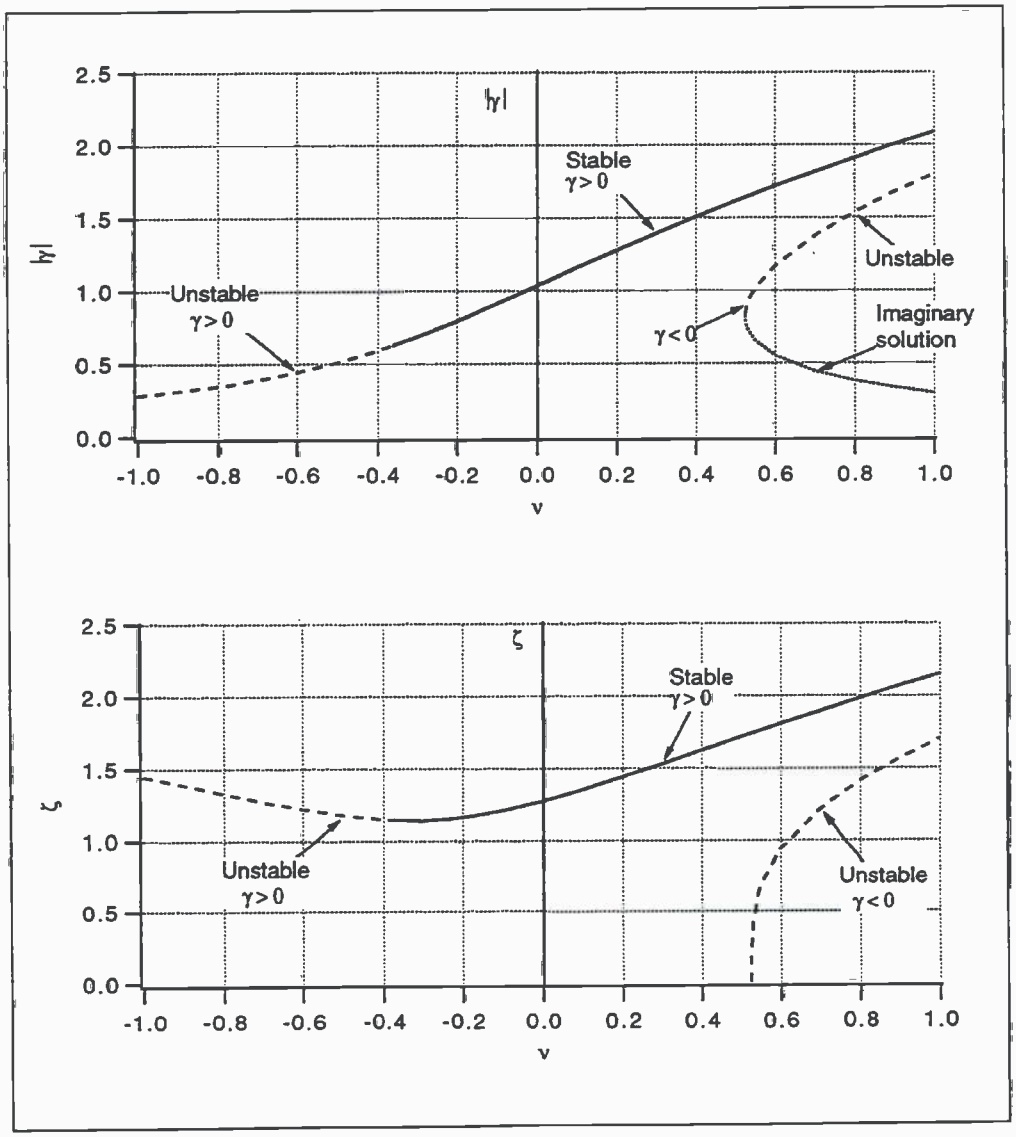

Figure 5.4 **Amplitude/frequency relations, γ-ν and ζ-ν, for rotational sloshing in circular cylindrical tank with 2a = 1.0 m and h = 0.5 m.**

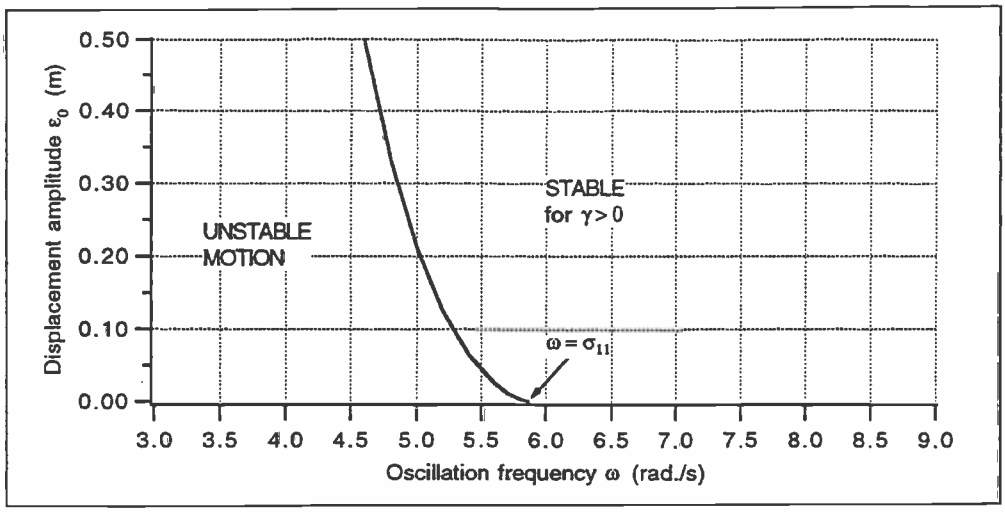

Figure 5.5 Regions for stable and unstable rotational sloshing as function of the angular forcing frequency of the tank motion and the tank displacement amplitude.

It is seen from Figure 5.5 that the rotational sloshing motion is stable for frequencies larger than the first eigenfrequency, and for smaller frequencies when the amplitude of tank motion is large.

The unstable velocity potential for planar sloshing

If the amplitude of oscillation of the tank is taken to be 0.025 meter and the oscillation frequency is in the vicinity of the first natural frequency, it is seen from Figure 5.3, that the planar motion is unstable. The first natural frequency is equal to 5.860954 rad./sec., and the frequency of oscillation is taken to be 5.7 rad./sec., that is a period equal to 1.1 sec. This gives

$$\nu = -0.209928$$

The values of K_1, K_2 and F_1 are the same as before. For the planar motion

$$\gamma = -1.243681.$$

From

$$\lambda_1^2 = -(\nu + K_1 \gamma^2)(\nu + 3 K_1 \gamma^2) = -1.2457$$

the solution is imaginary.

From

$$\lambda_2^2 = -(\nu + K_1\gamma^2)(\nu + (K_1 - K_2)\gamma^2) = 0.8107$$

the following values are obtained for unstable planar motion

$$\lambda_2 = 0.9004$$

$$c_1 = 0$$
$$c_2 = 0$$
$$c_4 = 0.6422c_3$$

and

$$f_1(\tau) = f_1^{(0)} = -1.2437$$
$$f_2(\tau) = 0$$
$$f_3(\tau) = c_3 e^{0.9004\tau}$$
$$f_4(\tau) = 0.6422c_3 e^{0.9004\tau}$$
$$\tau = 0.5\varepsilon^{2/3}\omega t = 0.2437t$$

The potential is then given by

$$\begin{aligned}
\Phi = \varepsilon^{1/3}\{ & [f_1^{(0)}\cos\theta + C_3 e^{\lambda_2\tau}\sin\theta] J_1(\lambda_{11}r)\frac{\cosh[\lambda_{11}(z+h)]}{\cosh(\lambda_{11}h)}\cos(\omega t) \\
& + [C_4 e^{\lambda_2\tau}\sin\theta] J_1(\lambda_{11}r)\frac{\cosh[\lambda_{11}(z+h)]}{\cosh(\lambda_{11}h)}\sin(\omega t)\} \\
+\varepsilon^{2/3}\{ & \alpha_0 t + \sum_{n=1}^{\infty}\Omega_{0n}C_3C_4 e^{2\lambda_2\tau} J_0(\lambda_{0n}r)\frac{\cosh[\lambda_{0n}(z+h)]}{\cosh(\lambda_{0n}h)}\cos(2\omega t) \\
& + \sum_{n=1}^{\infty}[-\Omega_{2n}C_3C_4 e^{2\lambda_2\tau}\cos(2\theta) + \Omega_{2n}f_1^{(0)}C_4 e^{\lambda_2\tau}\sin(2\theta)] \\
& \qquad J_2(\lambda_{2n}r)\frac{\cosh[\lambda_{2n}(z+h)]}{\cosh(\lambda_{2n}h)}\cos(2\omega t) \\
& + \sum_{n=1}^{\infty}\frac{1}{2}\Omega_{0n}(e^{2\lambda_2\tau}(C_4^2 - C_3^2) - f_1^{(0)2}) J_0(\lambda_{0n}r)\frac{\cosh[\lambda_{0n}(z+h)]}{\cosh(\lambda_{0n}h)}\sin(2\omega t) \\
& + \sum_{n=1}^{\infty}[\frac{1}{2}\Omega_{2n}(e^{2\lambda_2\tau}(C_3^2 - C_4^2) - f_1^{(0)2})\cos(2\theta) + \Omega_{2n}(-f_1^{(0)}C_3 e^{\lambda_2\tau})\sin(2\theta)] \\
& \qquad J_2(\lambda_{2n}r)\frac{\cosh[\lambda_{2n}(z+h)]}{\cosh(\lambda_{2n}h)}\sin(2\omega t)\}
\end{aligned} \tag{5.182}$$

The disturbance c_3 is assumed to be small. If c_3 is taken to be 0.1 times ε_0, that is 0.0025 m, the velocity potential in the point r = a = 0.5 m, z = 0 and θ = 0 is

$$\Phi = -0.37798\cos(5.7t) - 0.66664\sin(11.4t) - 0.01635t + 0.000002792e^{0.4388t}\cos(11.4t) - 0.000001277e^{0.4388t}\sin(11.4t) \quad (5.183)$$

where the last two terms represent the contribution from the disturbance. If

$$\Phi_{undist.} = -0.37798\cos(5.7t) - 0.66664\sin(11.4t) - 0.01635t \quad (5.184)$$

and

$$\Phi_{dist.} = 0.000002792e^{0.4388t}\cos(11.4t) - 0.000001277e^{0.4388t}\sin(11.4t) \quad (5.185)$$

the following values for the velocity potential as a function of time are obtained.

t [sec.]	0.0	T	1.5T	2T	2.5T	3T
$\Phi_{undist.}$	-0.3780	-0.3960	0.3509	0.3419	0.3329	-0.4320
$\Phi_{dist.}$	0.0000028	0.0000045	0.0000058	0.0000073	0.0000094	0.000012
Φ	-0.3780	-0.3960	0.3509	0.3419	0.3329	-0.4320

t [sec.]	3.5T	4T	6T	8T	9T	10T
$\Phi_{undist.}$	0.3149	-41.73	30.86	41.79	31.84	-4.38
Φ_{dist}	0.000015	-0.0044	0.0047	0.036	0.0081	-0.076
Φ	0.3149	-41.73	30.86	41.83	31.85	-4.46

Table 5.2 **Steady-state velocity potential $\Phi_{undist.}$, velocity potential due to a small disturbance $\Phi_{dist.}$ and total velocity potential Φ as function of time for a tank with diameter 1.0 m and water depth 0.5 m. T is the period of oscillation equal to 1.1 sec. and the oscillation amplitude is 0.025 m.**

It is seen from the table that, with the chosen disturbance, the tank may oscillate 8 to 10 times before the disturbance get any minor influence on the velocity potential.

5.4 Summary and conclusions

A general nonlinear solution for sloshing inside rigid tanks undergoing harmonic sway oscillations is outlined and used on a two-dimensional rectangular tank and a vertical circular cylindrical tank. The solutions are based on a perturbation scheme where the amplitude of the forced motions of the tank is of the same order of magnitude as the perturbation parameter. The solutions are valid for small oscillations of the containers with periods in the vicinity of the first natural period. It is shown that conservation of mass is not satisfied for a general tank shape. If the tank walls are vertical at the free surface, the conservation of mass condition is satisfied.

For periods of oscillation larger than a certain period, the nonlinear boundary value problem has three solutions, and then, three values of the velocity potential and the free-surface elevation are obtained. In addition, for the cylindrical tank, both lateral and rotational sloshing may occur. For the cylindrical tank, the stability of the solutions is studied. It is seen from Figure 5.3, that stable planar sloshing is possible except in a narrow frequency band around the first natural frequency, σ_{11}, and from Figure 5.5 that stable rotational sloshing is possible for frequencies above σ_{11}.

6 COMBINED NUMERICAL AND ANALYTICAL SOLUTION FOR SLOSHING IN TWO-DIMENSIONAL TANKS WITH ARBITRARY TANK SHAPE

In this chapter a new method is developed. This approach combines the possibility to use a numerical boundary element formulation to determine the eigenfrequencies and functions for the liquid motion in arbitrary shaped tanks, with the nonlinear analytical solution method described in chapter 5 to determine the nonlinear velocity potential. It is important to note that conservation of mass requires vertical tank walls at the liquid free surface (see chapter 5.1.6.) This limits the number of tank shapes where this combined method may be used. The method for determination of the linear eigenfrequencies and functions, described in chapter 6.2, may be used for other tank shapes too, where the walls are not vertical in the free surface.

The general formulation of the problem is the same as for the nonlinear analytical solutions in chapter 5. The tank is assumed to be oscillated harmonically with small amplitudes $\varepsilon_0 \sin(\omega t)$ in transverse/sway direction with frequency, ω, near the lowest resonance frequency, σ_1.

$$\omega^2 = \sigma_1^2 + \varepsilon^{2/3}\,\alpha \tag{6.1}$$

and $\varepsilon = \varepsilon_0/2a$. The total velocity potential is written correctly to third order as

$$\Phi_T = \Phi + \phi_C = \phi_1 \varepsilon^{1/3} + \phi_2 \varepsilon^{2/3} + \phi_3 \varepsilon + \phi_C \tag{6.2}$$

where, in accordance with the analytical solutions, the velocity potentials are assumed to have the form:

$$\begin{aligned} \phi_1 &= \varphi_1 N \cos(\omega t) \\ \phi_2 &= \alpha_0 t + \varphi_2 \frac{N^2}{2} \sin(2\omega t) \\ \phi_3 &= \varphi_3^{(3)} N^3 \cos(3\omega t) + \varphi_3^{(1)} N^3 \cos(\omega t) + \varphi_3^{(0)} \cos(\omega t) \end{aligned} \tag{6.3}$$

and the velocity potential for the tank motion is $\phi_C = 2a\omega x\varepsilon \cos(\omega t)$, where ϕ_C is of order ε. For a general shaped tank, it is not possible to determine the linear eigenfunctions and frequencies analytically. Therefore a boundary element formulation is used to find the eigenfrequencies and solve the equations for the velocity potentials.

To verify the method, comparisons are made with results from analytical solutions. But the number of tank shapes where the analytical solution has been obtained is small.

The eigenfrequencies and functions for a rectangular tank are given in chapter 5.2.1. In Lamb (1945) art.258.1 the eigenfrequencies and functions are given for two-dimensional oscillations of water across a channel whose section consists of two straight lines inclined at 45° to the vertical, (V-shaped tank). In art. 258.2 the first symmetrical eigenfrequency and function are

given for a V-shaped tank with 60° inclination to the vertical. In Lamb, this tank is also referred to as a tank with 30° inclination to the horizontal. For a canal of circular cross section only the first eigenfrequency is given in Lamb (1945) art. 259. One should note that the solutions for the V-shaped tanks may only be used to verify the routine for determination of eigenfunctions and frequencies. They cannot be used to determine the nonlinear velocity potential, due to the conservation of mass condition.

The nonlinear velocity potential for a rectangular tank is given in chapter 5.2. The nonlinear solution may be used for different non-shallow water depths within the limitation that h and 2a are of order O(1). In Faltinsen (1974) also the solution for infinite water depth is presented.

6.1 Boundary element formulation

A boundary element method will be used as a part of the solution. The theoretical formulation is based on Green's second identity. We can write the velocity potential Φ at a point (x_1, z_1) as

$$\Phi(x_1,z_1) = \frac{1}{2\pi}\oint_S \left(\Psi \frac{\partial \Phi}{\partial n} - \Phi \frac{\partial \Psi}{\partial n} \right) ds(x,z,) \tag{6.4}$$

S is the surface enclosing the fluid domain, $S=S_B+S_F$. S_B is the mathematical surface of the rigid walls, where body boundary conditions are to be satisfied, and S_F is the mathematical free surface, where free surface conditions are to be satisfied, as shown in Figure 6.1. **n** is the unit normal vector and it is positive into the fluid domain. Ψ is given by

$$\Psi(x_1,z_1;x,z) = \ln\sqrt{(x-x_1)^2+(z-z_1)^2} \tag{6.5}$$

In the numerical approximation, the free surface S_F and the wetted body surface S_B are divided into a number N_{EL} of straight line segments, with constant velocity potential $\Phi(i)$ and normal velocity component $\partial\Phi(i)/\partial n$ over each element. This means that

$$2\pi\Phi(x_1,z_1) = \sum_{i=1}^{N_{EL}} \frac{\partial\Phi(i)}{\partial n} \int_{\delta s_i} \Psi(x_1,z_1;x,z)\,ds - \sum_{i=1}^{N_{EL}} \Phi(i) \int_{\delta s_i} \frac{\partial\Psi(x_1,z_1;x,z)}{\partial n}\,ds \tag{6.6}$$

Here δs_i is the length of element number i.

Letting the field point (x_1,z_1) approach the midpoint on each element, N_{EL} linear equations are obtained.

$$
\begin{aligned}
2\pi\,\Phi(1) &= \sum_{i=1}^{N_{EL}} \frac{\partial \Phi(i)}{\partial n} \int_{\delta s_i} \Psi(1,i)\,ds + \sum_{i=1}^{N_{EL}} \Phi(i) \int_{\delta s_i} \frac{\partial \Psi(1,i)}{\partial n}\,ds \\
&\vdots \\
2\pi\,\Phi(j) &= \sum_{i=1}^{N_{EL}} \frac{\partial \Phi(i)}{\partial n} \int_{\delta s_i} \Psi(j,i)\,ds + \sum_{i=1}^{N_{EL}} \Phi(i) \int_{\delta s_i} \frac{\partial \Psi(j,i)}{\partial n}\,ds \\
&\vdots \\
2\pi\,\Phi(N_{EL}) &= \sum_{i=1}^{N_{EL}} \frac{\partial \Phi(i)}{\partial n} \int_{\delta s_i} \Psi(N_{EL},i)\,ds + \sum_{i=1}^{N_{EL}} \Phi(i) \int_{\delta s_i} \frac{\partial \Psi(N_{EL},i)}{\partial n}\,ds
\end{aligned}
\tag{6.7}
$$

These equations may be rewritten as

$$
2\pi\,\Phi(J) = \sum_{I=1}^{N_{EL}} \frac{\partial \Phi(I)}{\partial n} B(J,I) - \sum_{I=1}^{N_{EL}} \Phi(I) A(J,I) \tag{6.8}
$$

where the influence matrixes A(J,I) and B(J,I) are defined as follows:

$$
A(j,i) = \int_{\delta s_i} \frac{\partial \Psi(j,i)}{\partial n}\,ds \qquad B(j,i) = \int_{\delta s_i} \Psi(j,i)\,ds \tag{6.9}
$$

This formulation is used several times later in the text.

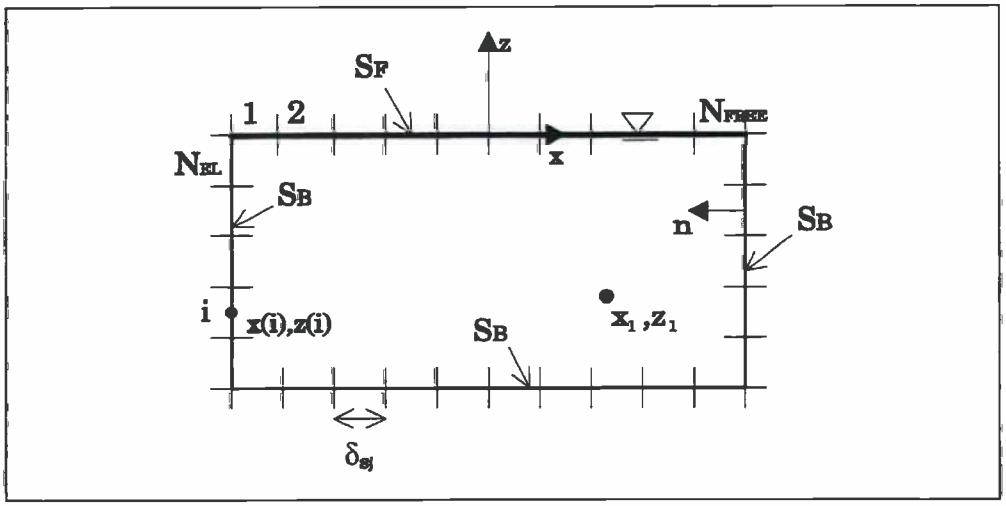

Figure 6.1 **Coordinate system and element distribution. N_{EL} is the total number of elements, N_{FREE} the number of elements on the free surface. S_F is the mathematical free surface and S_B the rigid body surface. $\vec{n}$ is the unit normal vector, δ_{sj} is the element length and x(i) and z(i) are the coordinates of the midpoint of element number i.**

6.2 The eigenvalue problem

Finding the linear eigenvalues and functions means to find non-trivial solutions of a boundary value problem for the fluid motion inside the tank when there are no forcing from either the tank wall or the free surface, and the fluid motion satisfies the linearized free surface conditions. So, the eigenfrequencies or eigenvalues are determined by setting the normal velocities $\partial\psi_n(i)/\partial n$ equal to zero at the rigid parts of the body. At the free surface the normal velocities are written in terms of the velocity potentials or eigenfunctions $\psi_n(i)$ by using the free surface condition for the eigenfunctions:

$$\frac{\partial \psi_n(i)}{\partial z} = \lambda_n \psi_n(i) = \frac{\sigma_n^2}{g}\psi_n(i) \qquad \text{at the mean free surface } z = 0 \tag{6.10}$$

where i is the element number. At the free surface $\partial\psi_n(i)/\partial z = -\partial\psi_n(i)/\partial n$ and the velocities on the free surface are then given by

$$\frac{\partial \psi_n(i)}{\partial n} = -\frac{\sigma_n^2}{g}\psi_n(i) \tag{6.11}$$

The system of equations is then

$$2\pi\psi_n(J) + \sum_{I=1}^{N_{EL}} \psi_n(I)A(J,I) = \frac{\sigma_n^2}{g}\sum_{I=1}^{N_{EL}} -\psi_n(I)B(J,I)\gamma_J \tag{6.12}$$

where γ_J is equal to 1.0 for free surface elements and equal to zero for rigid wall elements. When writing equation (6.12) in matrix form

$$\begin{bmatrix} 2\pi+A(1,1) & A(1,2) & .. & A(1,N_{EL}) \\ A(2,1) & 2\pi+A(2,2) & .. & A(2,N_{EL}) \\ : & : & : & : \\ A(N_{EL},1) & A(N_{EL},2) & .. & 2\pi+A(N_{EL},N_{EL}) \end{bmatrix} \begin{bmatrix} \psi_n(1) \\ \psi_n(2) \\ : \\ \psi_n(N_{EL}) \end{bmatrix} = -\frac{\sigma_n^2}{g} \begin{bmatrix} B(1,1)\gamma_1 & B(1,2)\gamma_2 & .. & B(1,N_{EL})\gamma_{N_{EL}} \\ B(2,1)\gamma_1 & B(2,2)\gamma_2 & .. & B(2,N_{EL})\gamma_{N_{EL}} \\ : & : & : & : \\ B(N_{EL},1)\gamma_1 & B(N_{EL},2)\gamma_2 & .. & B(N_{EL},N_{EL})\gamma_{N_{EL}} \end{bmatrix} \begin{bmatrix} \psi_n(1) \\ \psi_n(2) \\ : \\ \psi_n(N_{EL}) \end{bmatrix} \tag{6.13}$$

this is recognised as a generalized eigenvalue problem on the form $\mathbf{Ax}=\lambda\mathbf{Bx}$. By solving this equation system, we find the eigenvalues $\lambda_n = \sigma_n^2/g$.

When the eigenfrequencies are obtained as $\sigma_n = \sqrt{g\lambda_n}$, the equation system for determination of the eigenfunctions is

$$\begin{bmatrix} 2\pi+A(1,1)+\frac{\sigma_n^2}{g}B(1,1)\gamma_1 & A(1,2)+\frac{\sigma_n^2}{g}B(1,2)\gamma_2 & .. & A(1,N_{EL})+\frac{\sigma_n^2}{g}B(1,N_{EL})\gamma_{N_{EL}} \\ A(2,1)+\frac{\sigma_n^2}{g}B(2,1)\gamma_1 & 2\pi+A(2,2)+\frac{\sigma_n^2}{g}B(2,2)\gamma_2 & .. & A(2,N_{EL})+\frac{\sigma_n^2}{g}B(2,N_{EL})\gamma_{N_{EL}} \\ \vdots & \vdots & \vdots & \vdots \\ A(N_{EL},1)+\frac{\sigma_n^2}{g}B(N_{EL},1)\gamma_1 & A(N_{EL},2)+\frac{\sigma_n^2}{g}B(N_{EL},2)\gamma_2 & .. & 2\pi+A(N_{EL},N_{EL})+\frac{\sigma_n^2}{g}B(N_{EL},N_{EL})\gamma_{N_{EL}} \end{bmatrix} \begin{bmatrix} \psi_n(1) \\ \psi_n(2) \\ \vdots \\ \psi_n(N_{EL}) \end{bmatrix} = 0 \qquad (6.14)$$

Since σ_n^2/g is an eigenvalue, the determinant of this matrix is equal to zero. To be able to determine $\psi_n(i)$ we have to introduce another constraint. We do that by choosing the velocity potential in element N_{EL}, $\psi_n(N_{EL})$, equal to 1.0.

This is done in the following way; By Gauss elimination, an upper triangular matrix is obtained. When the last row contains only zeros, the potential $\psi_n(N_{EL})$ is set equal to 1.0, and the other potentials are then determined by back substitution.

6.3 First order velocity potential

The first eigenfrequency is $\sigma_1 = \sqrt{g\lambda_1}$ and the first order potential is given by equation (6.3) where the $\varphi_1(i)$ is equal to the first eigenfunctions $\psi_1(i)$.

6.4 Second order problem

The second order velocity potential has to satisfy the condition $\partial\phi_2(i)/\partial n = 0$ on the rigid walls, and the combined free surface condition

$$\frac{\partial^2\phi_2(i)}{\partial t^2} + \frac{\omega^2}{\lambda_1}\frac{\partial\phi_2(i)}{\partial z} = -\frac{N^2}{2}\sin(2\omega t)\,\omega A(x(i)) \qquad (6.15)$$

at the mean free surface z=0. Here

$$A(x(i)) = -\left(\nabla\varphi_1(i)\right)^2 - 2\lambda_1\varphi_1(i)\frac{\partial\varphi_1(i)}{\partial z} - \left(\frac{\partial\varphi_1(i)}{\partial x}\right)^2 + \varphi_1(i)\frac{\partial^2\varphi_1(i)}{\partial z^2} \qquad (6.16)$$

When the second order potential is written as in equation (6.3), the condition to be satisfied on the free surface is

$$-4\omega^2\varphi_2(i) + \frac{\omega^2}{\lambda_1}\frac{\partial\varphi_2(i)}{\partial z} = -\omega A(x(i)) \tag{6.17}$$

The normal velocities may then be written in terms of the velocity potential as

$$\frac{\partial\varphi_2(i)}{\partial n} = \frac{\lambda_1}{\omega}A(x(i)) - 4\lambda_1\varphi_2(i) \tag{6.18}$$

and together with equation (6.8), the system of equations to be solved for the second order potential is

$$\begin{bmatrix} 2\pi+A(1,1)+4\lambda_1 B(1,1)\gamma_1 & .. & A(1,N_{EL})+4\lambda_1 B(1,N_{EL})\gamma_{N_{EL}} \\ A(2,1)+4\lambda_1 B(2,1)\gamma_1 & .. & A(2,N_{EL})+4\lambda_1 B(2,N_{EL})\gamma_{N_{EL}} \\ : & : & : \\ A(N_{EL},1)+4\lambda_1 B(N_{EL},1)\gamma_1 & .. & 2\pi+A(N_{EL},N_{EL})+4\lambda_1 B(N_{EL},N_{EL})\gamma_{N_{EL}} \end{bmatrix} \begin{bmatrix} \varphi_2(1) \\ \varphi_2(2) \\ \vdots \\ \varphi_2(N_{EL}) \end{bmatrix} = \frac{\lambda_1}{\omega} \begin{bmatrix} \sum_{i=1}^{N_{FREE}} A(x(i))B(1,i) \\ \sum_{i=1}^{N_{FREE}} A(x(i))B(2,i) \\ \vdots \\ \sum_{i=1}^{N_{FREE}} A(x(i))B(N_{EL},i) \end{bmatrix} \tag{6.19}$$

where N_{FREE} is the number of elements on the free surface, as shown in Figure 6.1. The A(x(i)) terms contain the derivatives of the first order potential on each element on the free surface. How these derivatives are determined is shown in chapter 6.7.

The α_0 term is obtained from the conservation of mass condition, where the approximation of the surface shape has to satisfy

$$\int_{-a}^{a}\zeta_2 dx = 0 \tag{6.20}$$

From the dynamic free surface condition together with equation (6.3), the surface elevation is given by

$$\zeta_2 = \frac{\lambda_1}{\omega^2}\left\{-\alpha_0 + \frac{N^2}{2}\left[-\frac{1}{2}(\nabla\varphi_1)^2 + \lambda_1\varphi_1\frac{\partial\varphi_1}{\partial z}\right] + \frac{N^2}{2}\left[-2\omega\varphi_2 - \frac{1}{2}(\nabla\varphi_1)^2 - \lambda_1\varphi_1\frac{\partial\varphi_1}{\partial z}\right]\cos(2\omega t)\right\}$$

From chapter 5.1.6, it is seen that the integral of the cos(2ωt)-term is equal to zero. Then, the constant α_0 is given by

$$\alpha_0 = \frac{N^2}{2}\frac{1}{2a}\int_{-a}^{a}\left[-\frac{1}{2}(\nabla\varphi_1)^2 + \lambda_1\varphi_1\frac{\partial\varphi_1}{\partial z}\right]dx = \frac{N^2}{2}\bar{\alpha}_0 \tag{6.22}$$

6.5 Third order problem

The third order potential has to satisfy the condition $\partial\phi_3(i)/\partial n=0$ on the rigid walls and the combined free surface condition

$$\frac{\partial^2\phi_3}{\partial t^2}+\frac{\omega^2}{\lambda_1}\frac{\partial\phi_3}{\partial z}=N^3\cos(\omega t)A31(x)+N\cos(\omega t)\varphi_1(x)\alpha+f(x)\cos(\omega t)+N^3\cos(3\omega t)A33(x) \tag{6.23}$$

where, in the first term on the right hand side

$$\begin{aligned}A31(x)=&-\frac{1}{4}\omega\nabla\varphi_1\nabla\varphi_2+\frac{1}{2}\omega\lambda_1\varphi_1\frac{\partial\varphi_2}{\partial z}+\frac{1}{2}\lambda_1\frac{\partial\varphi_1}{\partial z}\left(-\frac{1}{2}(\nabla\varphi_1)^2+\lambda_1\varphi_1\frac{\partial\varphi_1}{\partial z}\right)\\&+\frac{1}{4}\lambda_1\frac{\partial\varphi_1}{\partial z}\left(\frac{1}{2}(\nabla\varphi_1)^2+\lambda_1\varphi_1\frac{\partial\varphi_1}{\partial z}\right)+\frac{1}{2}\omega\lambda_1\frac{\partial\varphi_1}{\partial z}\varphi_2-\frac{1}{4}\lambda_1\varphi_1\nabla\varphi_1\frac{\partial}{\partial z}(\nabla\varphi_1)\\&+\frac{3}{4}\frac{1}{2}\lambda_1^2\varphi_1^2\frac{\partial^2\varphi_1}{\partial z^2}+\frac{1}{4}\frac{\partial\varphi_1}{\partial x}\left[-2\omega\frac{\partial\varphi_2}{\partial x}+\frac{\partial}{\partial x}\left(-\frac{3}{2}(\nabla\varphi_1)^2+\lambda_1\varphi_1\frac{\partial\varphi_1}{\partial z}\right)\right]\\&+\frac{1}{4}\omega\frac{\partial\varphi_1}{\partial x}\frac{\partial\varphi_2}{\partial x}+\frac{1}{4}\lambda_1\varphi_1\frac{\partial\varphi_1}{\partial x}\frac{\partial^2\varphi_1}{\partial x\partial z}+\frac{1}{4}\left(-\omega\varphi_1\frac{\partial^2\varphi_2}{\partial z^2}-\frac{\lambda_1}{2}\varphi_1^2\frac{\partial^3\varphi_1}{\partial z^3}\right)\\&+\frac{1}{4}\frac{\partial^2\varphi_1}{\partial z^2}\left(+2\omega\varphi_2+\frac{1}{2}(\nabla\varphi_1)^2+\lambda_1\varphi_1\frac{\partial\varphi_1}{\partial z}\right)+\frac{1}{2}\frac{\partial^2\varphi_1}{\partial z^2}\left(\frac{1}{2}(\nabla\varphi_1)^2-\lambda_1\varphi_1\frac{\partial\varphi_1}{\partial z}\right)\\&+\tilde{\alpha}_0\left(\frac{\partial^2\varphi_1}{\partial z^2}-\lambda_1\frac{\partial\varphi_1}{\partial z}\right)\end{aligned} \tag{6.24}$$

The second term on the right hand side of equation (6.23) is due to the difference between the first natural frequency and the frequency of oscillation, as given in equation (6.1). The third term is due to the oscillation of the tank

$$f(x)=2a\omega^3x \tag{6.25}$$

The last term in equation (6.23) is

$$
\begin{aligned}
A33(x) = &-\frac{3}{4}\omega\nabla\varphi_1\nabla\varphi_2 - \frac{3}{2}\omega\lambda_1\varphi_1\frac{\partial\varphi_2}{\partial z} - \frac{3}{4}\lambda_1\frac{\partial\varphi_1}{\partial z}\left(\frac{1}{2}(\nabla\varphi_1)^2 + \lambda_1\varphi_1\frac{\partial\varphi_1}{\partial z}\right) \\
&- \frac{3}{2}\omega\lambda_1\frac{\partial\varphi_1}{\partial z}\varphi_2 - \frac{3}{4}\lambda_1\varphi_1\nabla\varphi_1\frac{\partial}{\partial z}(\nabla\varphi_1) - \frac{3}{4}\frac{1}{2}\lambda_1^2\varphi_1^2\frac{\partial^2\varphi_1}{\partial z^2} \\
&+ \frac{1}{4}\frac{\partial\varphi_1}{\partial x}\left[-2\omega\frac{\partial\varphi_2}{\partial x} + \frac{\partial}{\partial x}\left(-\frac{1}{2}(\nabla\varphi_1)^2 - \lambda_1\varphi_1\frac{\partial\varphi_1}{\partial z}\right)\right] - \frac{1}{4}\omega\frac{\partial\varphi_1}{\partial x}\frac{\partial\varphi_2}{\partial x} \\
&- \frac{1}{4}\lambda_1\varphi_1\frac{\partial\varphi_1}{\partial x}\frac{\partial^2\varphi_1}{\partial x\partial z} - \frac{1}{4}\left(-\omega\varphi_1\frac{\partial^2\varphi_2}{\partial z^2} - \frac{\lambda_1}{2}\varphi_1^2\frac{\partial^3\varphi_1}{\partial z^3}\right) \\
&+ \frac{1}{4}\frac{\partial^2\varphi_1}{\partial z^2}\left(+2\omega\varphi_2 + \frac{1}{2}(\nabla\varphi_1)^2 + \lambda_1\varphi_1\frac{\partial\varphi_1}{\partial z}\right)
\end{aligned}
\tag{6.26}
$$

Now, A31(x) and f(x) are written as

$$
\begin{aligned}
A31(x) &= \sum_{n=1}^{\infty} a_n\psi_n(x) \\
f(x) &= \sum_{n=1}^{\infty} e_n\psi_n(x)
\end{aligned}
\qquad on\ z = 0 \tag{6.27}
$$

The coefficients a_n and e_n may be determined by use of the orthogonality condition

$$
\int_{S_r}\psi_n\psi_m\,ds = 0 \qquad for\ n \neq m \tag{6.28}
$$

which is shown from Greens theorem in appendix I. a_n and e_n are then determined as

$$
a_n = \frac{\int_{-a}^{a} A31(x)\psi_n(x)\,dx}{\int_{-a}^{a}\psi_n(x)\psi_n(x)\,dx}, \qquad e_n = \frac{2a\omega^3\int_{-a}^{a} x\psi_n(x)\,dx}{\int_{-a}^{a}\psi_n(x)\psi_n(x)\,dx} \tag{6.29}
$$

N is determined by setting the terms proportional to $\varphi_1\cos(\omega t)$ on the right hand side of the combined free surface condition (6.23) equal to zero. This means

$$
a_1N^3 + \alpha N + e_1 = 0 \tag{6.30}
$$

Where a_1 and e_1 are given by equation (6.29).

When the discriminant

$$
\left(\frac{1}{2}\frac{e_1}{a_1}\right)^2 + \left(\frac{1}{3}\frac{\alpha}{a_1}\right)^3 < 0 \tag{6.31}
$$

there are three real roots of equation (6.30). When the discriminant is equal to zero, there are

three real roots, where at least two of them are equal. When the discriminant is greater than zero, there is only one real root.

6.5.1 Third order velocity potential

When the third order velocity potential is written as in equation (6.3), three equations are obtained from the free surface condition, which, together with the conditions on the rigid walls $\partial\varphi_3^{(3)}/\partial n=0$, $\partial\varphi_3^{(1)}/\partial n=0$ and $\partial\varphi_3^{(0)}/\partial n=0$, determine $\varphi_3^{(3)}$, $\varphi_3^{(1)}$ and $\varphi_3^{(0)}$ separately.

$$-9\omega^2\varphi_3^{(3)}+\frac{\omega^2}{\lambda_1}\frac{\partial\varphi_3^{(3)}}{\partial z}=A33(x) \qquad on\ z=0 \tag{6.32}$$

$$-\omega^2\varphi_3^{(1)}+\frac{\omega^2}{\lambda_1}\frac{\partial\varphi_3^{(1)}}{\partial z}=A31(x)-a_1\varphi_1(x)=\sum_{n=2}^{\infty}a_n\psi_n(x) \qquad on\ z=0 \tag{6.33}$$

$$-\omega^2\varphi_3^{(0)}+\frac{\omega^2}{\lambda_1}\frac{\partial\varphi_3^{(0)}}{\partial z}=f(x)-e_1\varphi_1(x)=\sum_{n=2}^{\infty}e_n\psi_n(x) \qquad on\ z=0 \tag{6.34}$$

The cos(3ωt)-term, $\varphi_3^{(3)}$, may be determined in the same manner as the second order potential, by the equation system

$$\begin{bmatrix} 2\pi+A(1,1)+9\lambda_1B(1,1)\gamma_1 & .. & A(1,N_{EL})+9\lambda_1B(1,N_{EL})\gamma_{N_{EL}} \\ A(2,1)+9\lambda_1B(2,1)\gamma_1 & .. & A(2,N_{EL})+9\lambda_1B(2,N_{EL})\gamma_{N_{EL}} \\ \vdots & \vdots & \vdots \\ A(N_{EL},1)+9\lambda_1B(N_{EL},1)\gamma_1 & .. & 2\pi+A(N_{EL},N_{EL})+9\lambda_1B(N_{EL},N_{EL})\gamma_{N_{EL}} \end{bmatrix}\begin{bmatrix} \varphi_3^{(3)}(1) \\ \varphi_3^{(3)}(2) \\ \vdots \\ \varphi_3^{(3)}(N_{EL}) \end{bmatrix}=-\frac{\lambda_1}{\omega^2}\begin{bmatrix} \sum_{i=1}^{N_{FREE}}A33(x(i))B(1,i) \\ \sum_{i=1}^{N_{FREE}}A33(x(i))B(2,i) \\ \vdots \\ \sum_{i=1}^{N_{FREE}}A33(x(i))B(N_{EL},i) \end{bmatrix} \tag{6.35}$$

For the $\varphi_3^{(1)}$ and $\varphi_3^{(0)}$ problems, the matrix on the left hand side will be equal to the matrix on the left hand side of equation (6.14) with $\sigma_n^2=\sigma_1^2$. For this matrix the determinant is equal to zero, and it is not possible to find $\varphi_3^{(1)}$ and $\varphi_3^{(0)}$ in the same way as φ_2 and $\varphi_3^{(3)}$.

Now, the potentials are written as sums of the eigenfunctions

$$\begin{aligned}\varphi_3^{(0)}(x,z)&=\sum_{n=2}^{\infty}B_n^{(0)}\psi_n(x,z)\\ \varphi_3^{(1)}(x,z)&=\sum_{n=2}^{\infty}B_n^{(1)}\psi_n(x,z)\end{aligned} \tag{6.36}$$

the sums start with n=2, since the terms containing the first eigenfunction have already been taken care of. The expressions (6.36) are then put into equations (6.33) and (6.34). When the free surface condition (6.10) for the eigenfunctions is used, the following expressions are obtained

$$-\omega^2\sum_{n=2}^{\infty}B_n^{(0)}\psi_n+\omega^2\frac{\sigma_n^2}{\sigma_1^2}\sum_{n=2}^{\infty}B_n^{(0)}\psi_n=\sum_{n=2}^{\infty}e_n\psi_n \qquad on\ z=0 \tag{6.37}$$

$$-\omega^2\sum_{n=2}^{\infty}B_n^{(1)}\psi_n+\omega^2\frac{\sigma_n^2}{\sigma_1^2}\sum_{n=2}^{\infty}B_n^{(1)}\psi_n=\sum_{n=2}^{\infty}a_n\psi_n \qquad on\ z=0 \tag{6.38}$$

Now, equation (6.37) and (6.38) are multiplied by ψ_m and integrated over the free surface. When the orthogonality condition (6.28) is used, $B_n^{(0)}$ and $B_n^{(1)}$ are given by

$$B_n^{(0)}=\frac{e_n}{\omega^2\left(\frac{\sigma_n^2}{\sigma_1^2}-1\right)}, \qquad B_n^{(1)}=\frac{a_n}{\omega^2\left(\frac{\sigma_n^2}{\sigma_1^2}-1\right)} \tag{6.39}$$

and the velocity potentials for each element

$$\varphi_3^{(0)}(i)=\sum_{n=2}^{\infty}\frac{e_n}{\omega^2\left(\frac{\sigma_n^2}{\sigma_1^2}-1\right)}\psi_n(i), \qquad \varphi_3^{(1)}(i)=\sum_{n=2}^{\infty}\frac{a_n}{\omega^2\left(\frac{\sigma_n^2}{\sigma_1^2}-1\right)}\psi_n(i) \tag{6.40}$$

6.6 Free surface elevation

The free surface elevation inside the tank is obtained from the dynamic free surface condition. For each element the elevation is given by

$$\zeta(i)=\zeta_1(i)\,\varepsilon^{1/3}+\zeta_2(i)\,\varepsilon^{2/3}+\zeta_3(i)\,\varepsilon \tag{6.41}$$

where the first, second and third order wave elevation are given by

$$\zeta_1(i)=\frac{\sigma_1^2}{\omega g}N\varphi_1(i)\sin(\omega t) \tag{6.42}$$

$$\zeta_2(i)=\frac{\sigma_1^2}{\omega g}\left\{-\alpha_0-2\omega\frac{N^2}{2}\varphi_2(i)\cos(2\omega t)-\frac{N^2}{2}\cos^2(\omega t)\left[\left(\frac{\partial\varphi_1(i)}{\partial x}\right)^2+\left(\frac{\partial\varphi_1(i)}{\partial z}\right)^2\right]+\frac{\sigma_1^2}{g}N^2\sin^2(\omega t)\varphi_1(i)\frac{\partial\varphi_1(i)}{\partial z}\right\} \tag{6.43}$$

and

$$\zeta_3(i) = \frac{\sigma_1^2}{\omega^2 g}\Bigg\{ 3\omega\varphi_3^{(3)}(i)N^3\sin(3\omega t) + \omega\varphi_3^{(1)}(i)N^3\sin(\omega t) + \omega\varphi_3^{(0)}(i)\sin(\omega t)$$
$$+\frac{\alpha}{\lambda_1}\zeta_1(i) - \frac{N^3}{2}\cos(\omega t)\sin(2\omega t)\left[\frac{\partial\varphi_1(i)}{\partial x}\frac{\partial\varphi_2(i)}{\partial x} + \frac{\partial\varphi_1(i)}{\partial z}\frac{\partial\varphi_2(i)}{\partial z}\right]$$
$$-\zeta_1(i)\omega\frac{\partial\varphi_2(i)}{\partial z}N^2\cos(2\omega t) + \zeta_2(i)\omega\frac{\partial\varphi_1(i)}{\partial z}N\sin(\omega t) \qquad (6.44)$$
$$-\zeta_1(i)\left(\frac{\partial\varphi_1(i)}{\partial x}\right)^2 N^2\lambda_1\cos^2(\omega t) + \zeta_1(i)\frac{\partial\varphi_1(i)}{\partial z}\frac{\partial^2\varphi_1(i)}{\partial x^2}N^2\cos^2(\omega t)$$
$$-\frac{1}{2}\zeta_1^2(i)\omega\frac{\partial^2\varphi_1(i)}{\partial x^2}N\sin(\omega t) + 2a\omega^2 x(i)\sin(\omega t)\Bigg\}$$

on z = 0.

6.7 The derivatives of the potentials

The derivatives of the potentials at z=0 are obtained by the following method. The potential in each element is written as a series

$$\varphi(i) = A + Bx(i) + Cx^2(i) \qquad (6.45)$$

The constants A, B and C for element number i, which is not next to the wall, are determined by using the values of the potentials in element number i-1 and i+1. The x derivatives are then obtained from

$$\frac{\partial\varphi(i)}{\partial x} = B + 2Cx(i)$$
$$\frac{\partial^2\varphi(i)}{\partial x^2} = 2C \qquad (6.46)$$

In z-direction the first derivatives are obtained from the free surface conditions

$$\frac{\partial\varphi_1(i)}{\partial z} = \frac{\sigma_1^2}{g}\varphi_1(i)$$
$$\frac{\partial\varphi_2(i)}{\partial z} = \frac{4\sigma_1^2}{g}\varphi_2(i) - \frac{\sigma_1^2}{\omega g}A(x(i)) \qquad (6.47)$$

and the second derivatives from the Laplace equation.

$$\frac{\partial^2\varphi(i)}{\partial z^2} = -\frac{\partial^2\varphi(i)}{\partial x^2} = -2C \qquad (6.48)$$

For the elements near the wall x=-a, the following method to determine the derivatives has been found to give good results compared with the analytical solution. The constants A, B

and C are determined from the φ values in element number k-1 and k, together with the condition $\partial\varphi/\partial x=0$ at the wall. The element number k, used to determine the derivatives in the elements near the wall, is dependent on the number of elements on the free surface. The derivatives in element number 1 to k-1 are then determined from

$$\begin{aligned}\frac{\partial\varphi(i)}{\partial x} &= B(k-1) + 2C(k-1)x(i) = C(k-1)(2a + 2x(i)) \\ \frac{\partial^2\varphi(i)}{\partial x^2} &= 2C(k-1)\end{aligned} \tag{6.49}$$

where B is determined from the wall condition $\partial\varphi/\partial x = 0$ at x = - a. Similarly is done for the elements near the right wall, x=a.

6.8 Verification of the method

In order to verify the calculation procedure comparisons are made with results from the nonlinear analytical solution given in chapter 5.2 and Faltinsen (1974) for translational/sway motion of a two-dimensional rectangular tank with breadth 2a=1.0 m and water depth h=0.5 m. In all of the numerical results the element length is taken to be constant over both the free surface and the rigid body surface.

The calculations are performed in double precision on a IBM RS6000 computer.

6.8.1 The eigenperiods

The linear eigenperiods for the rectangular tank are given analytically from

$$T_n = \frac{2\pi}{\sqrt{\frac{n\pi}{2a} g \tanh\left(\frac{n\pi}{2a}h\right)}} \quad \text{(sec.)} \qquad n = 1,2,3,4,.... \tag{6.50}$$

and compared with the numerically obtained eigenperiods.

Numerically, the real generalized eigenvalue problem (6.13) is solved by use of the subroutines RGG, QHES, QZIT and QZVAL from the eigensystem subroutine package (EISPACK) in the SLATEC library.

In Table 6.1 the first 15 of the analytically obtained eigenperiods are compared with the eigenperiods obtained from the numerical method with 120, 240 and 500 elements on the free surface. The element length is taken to be constant over the surface S. With 120 elements on the free surface, the total number of elements is 360, and the element length is then equal to 0.00833333 meter. With 240 elements on the free surface, the total number of elements is 720, and the element length is 0.00416667 meter. With 500 elements on the free surface, the total number of elements is 1500 and the length of the elements is 0.002 meter.

It is seen from Table 6.1, that the values of the eigenfrequencies are getting closer to the analytical solution when the number of elements increases.

The most correct values are obtained for T_1 and the difference from the analytical solution is getting larger for increasing value of n. The reason for this is that the number of wave lengths over the tank breadth 2a, describing the eigenfunction or shape of the wave, is increasing for increasing n. For example, T_1 corresponds to a wave length equal to 4a, T_2 to a wave length equal to 2a, and T_3 to a wave length 4a/3. And hence, the number of elements describing each wave length are decreasing for increasing n.

In Figure 6.2 it is shown how the eigenperiods calculated from the numerical method are changing with increasing number of elements. It is seen that the numerical solutions converge to the analytical solution when the number of elements increases.

n	T_n analytical solution	T_n numerical solution N_{FREE} = 120	T_n numerical solution N_{FREE}= 240	T_n numerical solution N_{FREE}= 500
1	1.181816	1.181685	1.181772	1.181800132
2	0.801801	0.801625	0.801743	0.801780600
3	0.653499	0.653285	0.653431	0.653475
4	0.565903	0.565640	0.565821	0.565875
5	0.506157	0.505845	0.506061	0.506126
6	0.462056	0.461689	0.461945	0.462020
7	0.427781	0.427357	0.427654	0.427741
8	0.400152	0.399668	0.400008	0.400107
9	0.377267	0.376721	0.377106	0.377218
10	0.357907	0.357296	0.357727	0.357853
11	0.341251	0.340574	0.341052	0.341191
12	0.326723	0.325978	0.326505	0.326658
13	0.313905	0.313091	0.313667	0.313835
14	0.302487	0.301602	0.302228	0.302411
15	0.292230	0.291274	0.291950	0.292149

Table 6.1 **Comparison between analytically and numerically obtained eigenperiods for a rectangular tank with breadth 2a=1.0 m and water depth h=0.5 m. Numerical results are given for the cases with 120, 240 and 500 elements on the free surface.**

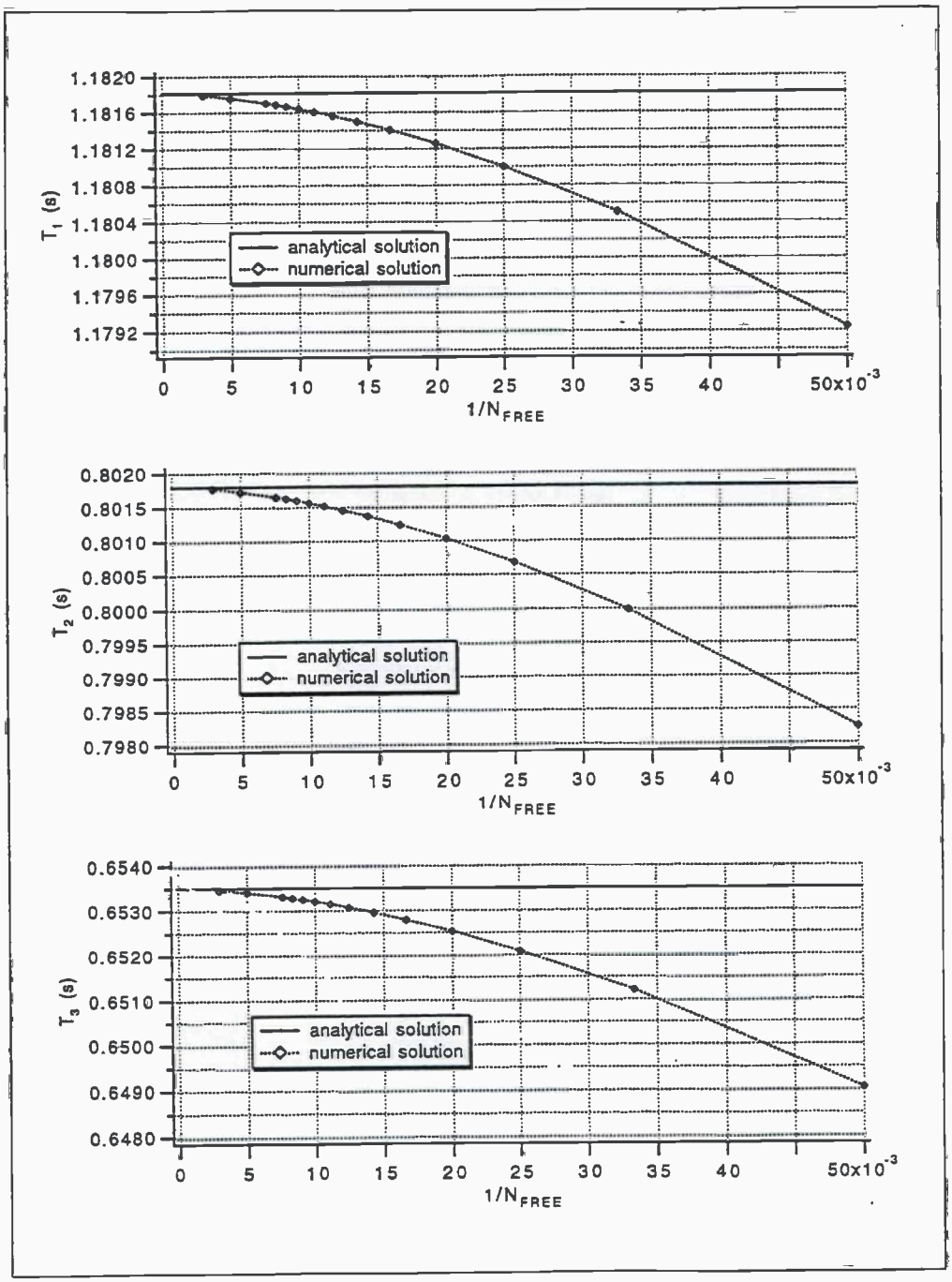

Figure 6.2 **First, second and third eigenperiods as function of $1/N_{FREE}$ for rectangular tank with 2a=1.0 m and h=0.5 m.**

6.8.2 The velocity potentials

The parts of the velocity potentials independent of time, that is, φ_1 , φ_2 , $\bar{\alpha}_0$, $\varphi_3^{(3)}$, $\varphi_3^{(1)}$ and $\varphi_3^{(0)}$, are compared with the results from the nonlinear analytical method.

To be able to compare the numerically obtained values with the results from the analytical solutions, the analytical solutions have to be multiplied by a constant D. The value of this constant is determined from the condition that φ_1 is equal to 1.0 in element number N_{EL}.

$$\varphi_1 = D\sin\left(\frac{\pi}{2a}x(N_{EL})\right)\cosh\left[\frac{\pi}{2a}(z(N_{EL})+h)\right] = 1.0 \qquad (6.51)$$

For the rectangular tank in the examples h=0.5 m, $x(N_{EL})$ = -a = -0.5 m and $z(N_{EL})$ = - δ_s /2.

The first order potential φ_1 has to be multiplied by D, the second order potential φ_2 and $\bar{\alpha}_0$ by D^2. The third order terms $\varphi_3^{(3)}$ and $\varphi_3^{(1)}$ have to be multiplied by D^3. $\varphi_3^{(0)}$ is due to the tank motion and is the same for the analytical and numerical solutions.

In the examples below, the numerical obtained results are compared with the potential from the analytical solution for the cases with 120, 240 and 500 elements on the free surface. The difference in the analytical values for the different number of elements is due to the different D values for the cases.

N_{FREE} = 120	N_{EL} = 360	δ_s= 0.00833333	D = -0.403344750
N_{FREE} = 240	N_{EL} = 920	δ_s= 0.00416667	D = -0.400934956
N_{FREE} = 500	N_{EL} = 1500	δ_s= 0.00200000	D = -0.399686469

The second and third order velocity potentials φ_2 and φ_3 are dependent on the oscillation frequency ω. In the examples ω is chosen to be equal to the first eigenfrequency σ_1.

Derivation near the wall and the value of k

The element number k, used in the interpolation to find the derivatives in the elements near the wall, is dependent on the element size or the number of elements on the free surface. To be able to do a good choice of k, the constant $\bar{\alpha}_0$, the integral over the free surface of the cos(2ωt)-terms in the second order free surface elevation, equation (6.21), and the second order potential in element number 1, 2 and 3 are compared with the analytical solutions for different element number k.

(k-1), k	$\bar{\alpha}_0$	integral	φ_2 el. 1	φ_2 el. 2	φ_2 el. 3
3-4	-0.400592	-0.00043660	-0.578826	-0.579754	-0.583471
4-5	-0.400635	-0.00041307	-0.582676	-0.583005	-0.585103
5-6	-0.400669	-0.00037901	-0.584725	-0.584882	-0.586555
6-7	-0.400694	-0.00036424	-0.585867	-0.585965	-0.587490
7-8	-0.400708	-0.00035629	-0.586393	-0.586473	-0.587950
8-9	-0.400707	-0.00035637	-0.586389	-0.586469	-0.587947
9-10	-0.400688	-0.00036684	-0.585851	-0.585942	-0.587449
10-11	-0.400642	-0.00039111	-0.584727	-0.584836	-0.586393
11-12	-0.400561	-0.00043357	-0.582933	-0.583066	-0.584694
analytical	-0.401414	0.00000000	-0.589599	-0.590278	-0.591634

Table 6.2 **Values of $\bar{\alpha}_0$, the integral over the free surface of the cos(2ωt)-term in ζ_2, and second order velocity potential in element number 1, 2 and 3 for different values of k in equation (6.49), for 120 elements on the free surface.**

(k-1), k	$\bar{\alpha}_0$	integral	φ_2 el. 1	φ_2 el. 2	φ_2 el. 3
5-6	-0.396501	-0.00010191	-0.578757	-0.578717	-0.579263
6-7	-0.396508	-0.00009696	-0.579702	-0.579611	-0.580026
7-8	-0.396514	-0.00009315	-0.580319	-0.580205	-0.580562
8-9	-0.396519	-0.00009014	-0.580736	-0.580611	-0.580940
9-10	-0.396523	-0.00008709	-0.581015	-0.580885	-0.581199
10-11	-0.396526	-0.00008617	-0.581187	-0.581055	-0.581362
11-12	-0.396528	-0.00008529	-0.581269	-0.581136	-0.581441
12-13	-0.396528	-0.00008531	-0.581267	-0.581134	-0.581439
13-14	-0.396526	-0.00008641	-0.581184	-0.581051	-0.581358
14-15	-0.396521	-0.00008881	-0.581015	-0.580884	-0.581194
15-16	-0.396514	-0.00009279	-0.580758	-0.580627	-0.580942
analytical	-0.396632	0.00000000	-0.582576	-0.582744	-0.583080

Table 6.3 **Values of $\bar{\alpha}_0$, the integral over the free surface of the cos(2ωt)-term in ζ_2, and second order velocity potential in element number 1, 2 and 3 for different values of k in equation (6.49), for 240 elements on the free surface.**

(k-1), k	$\hat{\alpha}_0$	integral	φ_2 el. 1	φ_2 el. 2	φ_2 el. 3
11-12	-0.394168	-0.00002138	-0.578084	-0.577986	-0.578045
12-13	-0.394169	-0.00002090	-0.578197	-0.578097	-0.578153
13-14	-0.394170	-0.00002049	-0.578284	-0.578184	-0.578238
14-15	-0.394170	-0.00002014	-0.578351	-0.578250	-0.578303
15-16	-0.394171	-0.00001985	-0.578400	-0.578299	-0.578351
16-17	-0.394171	-0.00001963	-0.578434	-0.578334	-0.578385
17-18	-0.394171	-0.00001949	-0.578455	-0.578354	-0.578405
18-19	-0.394172	-0.00001943	-0.578463	-0.578362	-0.578413
19-20	-0.394172	-0.00001947	-0.578459	-0.578358	-0.578409
20-21	-0.394171	-0.00001961	-0.578442	-0.578341	-0.578393
21-22	-0.394171	-0.00001987	-0.578414	-0.578313	-0.578365
analytical	-0.394166	0.00000000	-0.578930	-0.578969	-0.579046

Table 6.4 **Values of $\hat{\alpha}_0$, the integral over the free surface of the cos(2ωt)-term in ζ_2, and second order velocity potential in element number 1, 2 and 3 for different values of k in equation (6.49), for 500 elements on the free surface.**

The best results for the case with 120 elements on the free surface are obtained when the interpolation is taken from element number 7 and 8 to the wall. That is a distance equal to 0.05833 m from the wall. For the case with 240 elements on the free surface the best results are obtained when the interpolation is taken from element number 11 and 12 to the wall, which is a distance equal to 0.04583 m from the wall. For 500 elements on the free surface the best results are when the interpolation is taken from element number 18 and 19 to the wall. That is a distance equal to 0.036 m from the wall.

It is seen that when the element number increases, one may go closer to the wall to get the best approximation for the elements near the wall. A reason for this is that the error in the first order potential near the wall is getting less when the number of elements increases.

In the calculations below, the following values of k are used:

N_{FREE}=120: k=8
N_{FREE}=240: k=12
N_{FREE}=500: k=19

It is seen from the tables that this k-values are the ones which gives the smallest value of the integral over the free surface of the cos(2ωt) terms. So, to find which value of k to choose when the results are not known, one may choose the k which gives the smallest value of the integral.

The first and second order potentials

In the tables below, the numerical velocity potentials at some x-values on the free surface are compared with the potential from the analytical solution for the cases with 120, 240 and 500 elements on the free surface. The given x-values are the midpoint of the elements.The first order potential is antisymmetrical about origo, x=0, and the second order symmetrical about origo. The difference in the analytical values of the potentials for the different number of elements is due to the different D values for the two cases.

At the intersection between the walls and z=0, both the free surface condition and the boundary condition at the wall have to be satisfied. This is not possible in the numerical approximation, and then, the largest errors occur in the elements near the walls.

For the case with N_{FREE} = 120 elements, the largest error in φ_1 occur in the first and last elements on the free surface, and is equal to 0.1 percent. The maximum error in φ_2 is 0.64 percent and it occurs in element number 2 and N_{FREE} - 1. When the number of elements are increased to N_{FREE} = 240, the largest error in φ_1 is reduced to 0.05 percent in element number 1 and N_{FREE}. In φ_2 it is reduced to 0.28 percent. For the case with 500 elements on the free surface, the errors in the potentials are decreased even more. For φ_1 to 0.025 percent and for φ_2 to 0.11 percent.

x-value	el.	analytical φ_1	numerical φ_1	analytical φ_2	numerical φ_2
-0.495833	1	1.011977	1.010961	-0.589599	-0.586393
-0.487500	2	1.011284	1.011328	-0.590278	-0.586447
-0.479167	3	1.009897	1.010172	-0.591634	-0.587950
-0.470833	4	1.007818	1.008203	-0.593664	-0.590395
-0.462500	5	1.005049	1.005501	-0.596363	-0.593711
-0.420833	10	0.980924	0.981520	-0.619551	-0.620040
-0.337500	20	0.830218	0.883661	-0.707870	-0.710820
-0.254167	30	0.724943	0.725507	-0.830891	-0.834530
-0.170833	40	0.517461	0.517880	-0.955651	-0.957973
-0.087500	50	0.274715	0.274942	-1.048720	-1.048921
-0.004167	60	0.013248	0.013259	-1.085160	-1.084283

Table 6.5 Comparison between analytical and numerical results for the first and second order potential for N_{FREE} = 120 elements. The given x-values are the midpoints of the elements. Oscillation frequency $\omega = \sigma_1$=5.317 rad/s.

x-value	el.	analytical φ_1	numerical φ_1	analytical φ_2	numerical φ_2
-0.497917	1	1.005995	1.005484	-0.582576	-0.581269
-0.493750	2	1.005823	1.005834	-0.582744	-0.581136
-0.489583	3	1.005479	1.005600	-0.583080	-0.581441
-0.485417	4	1.004962	1.005135	-0.583583	-0.581988
-0.481250	5	1.004273	1.004477	-0.584253	-0.582750
-0.460417	10	0.998249	0.998521	-0.590092	-0.589466
-0.418750	20	0.973421	0.973732	-0.613786	-0.614117
-0.335417	40	0.874510	0.874820	-0.702259	-0.703432
-0.252083	60	0.716002	0.716268	-0.824289	-0.825714
-0.168750	80	0.508700	0.508894	-0.947178	-0.948145
-0.085417	100	0.266731	0.266834	-1.037998	-1.038228
-0.002083	120	0.006584	0.006587	-1.072414	-1.072281

Table 6.6 **First and second order potential for N_{FREE} = 240 elements. Oscillation frequency $\omega = \sigma_1$=5.317 rad/s.**

x-value	el.	analytical φ_1	numerical φ_1	analytical φ_2	numerical φ_2
-0.499000	1	1.002880	1.002632	-0.578930	-0.578463
-0.497000	2	1.002840	1.002841	-0.578967	-0.578362
-0.495000	3	1.002761	1.002814	-0.579046	-0.578413
-0.493000	4	1.002642	1.002719	-0.579161	-0.578525
-0.491000	5	1.002484	1.002575	-0.579315	-0.578686
-0.481000	10	1.001099	1.001220	-0.580658	-0.580172
-0.461000	20	0.995367	0.995506	-0.586197	-0.586159
-0.421000	40	0.972156	0.972306	-0.608301	-0.608483
-0.301000	100	0.813199	0.813335	-0.745667	-0.746209
-0.201000	150	0.592027	0.592129	-0.896102	-0.896606
-0.101000	200	0.312903	0.312958	-1.018362	-1.018589
-0.001000	250	0.003151	0.003151	-1.065748	-1.065815

Table 6.7 **First and second order potential for N_{FREE} = 500 elements. Oscillation frequency $\omega = \sigma_1$=5.317 rad/s.**

When φ_2 is calculated, the values of φ_1 , or more correctly, the first eigenfunction ψ_1 , and its derivatives, are used. The errors in φ_2 are larger than in φ_1 because the errors contributing to the total error in φ_2 are the errors in the calculation of the first eigenperiod and in φ_1 together with the errors due to the differentiation of φ_1 and products of φ_1 .

The third order potential

In the calculation of $\varphi_3^{(3)}$, the errors contributing to the total error are the errors in the calculation of φ_1 and φ_2 and in the derivatives. For $\varphi_3^{(1)}$ and $\varphi_3^{(0)}$, which are determined as series of the eigenfunctions ψ_n , the errors are due to errors in the determination of the eigenvalues and functions and that a finite number of terms in the infinite series are used. For $\varphi_3^{(1)}$, also the errors in A31(x), which are dependent on the errors in φ_1 , φ_2 and their derivatives, contribute.

In Table 6.8 and Table 6.9, the cos(3ωt) terms in the third order velocity potential are compared with the analytical solutions for the cases where the number of elements on the free surface are 240 and 500. It is seen from the tables that the differences between the numerical and the analytical results are decreasing when the number of elements is increased.

x-value	el.	analytical $\varphi_3^{(3)}$	numerical $\varphi_3^{(3)}$
-0.497917	1	0.659986	0.664725
-0.493750	2	0.659844	0.664744
-0.489583	3	0.659560	0.664389
-0.485417	4	0.659135	0.663910
-0.481250	5	0.658568	0.663309
-0.460417	10	0.653626	0.657222
-0.418750	20	0.633442	0.634232
-0.335417	40	0.555903	0.555842
-0.252083	60	0.440266	0.439485
-0.168750	80	0.302152	0.301244
-0.085417	100	0.154305	0.153246
-0.002083	120	0.003770	0.003733

Table 6.8 **Comparison between analytical and numerical results for the cos(3ωt) terms in the third order potential for N_{FREE} = 240 elements. The frequency of oscillation $\omega = \sigma_1 = 5.317$ rad/s.**

x-value	el.	analytical $\varphi_3^{(3)}$	numerical $\varphi_3^{(3)}$
-0.499000	1	0.653860	0.655445
-0.497000	2	0.653804	0.655543
-0.495000	3	0.653739	0.655485
-0.493000	4	0.653642	0.655390
-0.491000	5	0.653512	0.655266
-0.481000	10	0.652380	0.654209
-0.461000	20	0.647706	0.647774
-0.421000	40	0.628943	0.629637
-0.301000	100	0.507085	0.506701
-0.201000	150	0.354004	0.354051
-0.101000	200	0.180588	0.180100
-0.001000	250	0.001793	0.001779

Table 6.9 **Comparison between analytical and numerical results for the cos(3ωt) terms in the third order potential for N_{FREE} = 500 elements. The frequency of oscillation ω = σ_1=5.317 rad/s.**

The cos(ωt)-terms in the third order potential, $\varphi_3^{(1)}$ and $\varphi_3^{(0)}$ are dependent on the number of terms in the series in equation (6.36). The third order potential are antisymmetrical, and hence, the symmetric values of a_n and e_n, that is n=2,4,6,8,.., should be very small compared with the antisymmetrical values of a_n and e_n for n=1,3,5,7,... From Table 6.10 it is seen that this is the case.

Analytically $\varphi_3^{(1)}$ contains only the a_3 term in the series and then all a_n except a_1 and a_3 should be equal to zero. From the Table 6.10 it is seen that this is not the case numerically. And then, the error in the calculation of $\varphi_3^{(1)}$ is increasing for increasing number of terms in the series. $\varphi_3^{(0)}$ contains all terms from n=2 to infinity, and the solution converges to the analytical solution when the number of terms in the series increases. This is shown in Table 6.11 for the values of $\varphi_3^{(1)}$ and $\varphi_3^{(0)}$ in element number 1. It is important to note that the series starts with n=2, so, for example, a number of terms equal to 2 means that the series contain the n=2 and n=3 terms.

In Table 6.12 the values of $\varphi_3^{(1)}$ and $\varphi_3^{(0)}$ are compared with the analytical solution in some of the elements for 240 elements on the free surface and 10 terms in the series. In Table 6.13 the values are compared for 500 elements on the free surface and 20 terms in the series. The results will depend upon the number of terms in the series. With the chosen number of terms, it is seen, from the tables, that the results are getting much better when the number of elements on the free surface is increased from 240 to 500.

n	a_n	e_n
1	1.616020E+01	-6.052729E+01
2	-3.914852E-10	1.902466E-12
3	2.256034E+00	-6.632353E+00
4	-3.3570577E-09	-1.413592E-13
5	-5.6359547E-02	-2.358021E+00
6	-4.5735175E-09	-5.555860E-13
7	-8.4406658E-02	-1.189114E+00
8	-6.0708755E-09	2.423802E-13
9	-1.1058246E-01	-7.115725E-01
10	-6.9747117E-09	1.360966E-12
11	-1.3178293E-01	-4.715756E-01

Table 6.10 **The first 11 values of a_n and e_n for N_{FREE}=240 elements and frequency of oscillation $\omega = \sigma_1$=5.317 rad/s.**

Number of terms	$\varphi_3^{(0)}$	$\varphi_3^{(1)}$
2	-0.105173	0.035775
4	-0.124465	0.035314
8	-0.134077	0.034391
10	-0.135692	0.033927
20	-0.138240	0.032452
30	-0.138809	0.032554
40	-0.139028	0.033116
50	-0.139136	0.033156
60	-0.139199	0.032865
90	-0.139285	0.033014
120	-0.139318	0.032908
Analytical solution	-0.139545	0.037457

Table 6.11 **Numerical values of $\varphi_3^{(0)}$ and $\varphi_3^{(1)}$ in element number 1 for different number of terms in the series and N_{FREE}=240 elements and frequency of oscillation $\omega = \sigma_1$=5.317 rad/s.**

x-value	el.	analytical $\varphi_3^{(1)}$	numerical $\varphi_3^{(1)}$	analytical $\varphi_3^{(0)}$	numerical $\varphi_3^{(0)}$
-0.497917	1	0.037457	0.033927	-0.139545	-0.135692
-0.493750	2	0.037399	0.033946	-0.138779	-0.135611
-0.489583	3	0.037284	0.033891	-0.137474	-0.134930
-0.485417	4	0.037111	0.033795	-0.135724	-0.133845
-0.481250	5	0.036881	0.033663	-0.133590	-0.132385
-0.460417	10	0.034887	0.032431	-0.118527	-0.119965
-0.418750	20	0.027006	0.026584	-0.075553	-0.076745
-0.335417	40	0.000736	0.001181	0.018627	0.019103
-0.252083	60	-0.024966	-0.024899	0.081797	0.081576
-0.168750	80	-0.037457	-0.036079	0.094886	0.095070
-0.085417	100	-0.027006	-0.026099	0.061864	0.061798
-0.002083	120	-0.000736	-0.000693	0.001632	0.001681

Table 6.12 **cos(ωt) terms in the third order potential for N_{FREE} = 240 elements, frequency of oscillation ω =σ_1=5.317 rad/s and n=10 terms in the series.**

x-value	el.	analytical $\varphi_3^{(1)}$	numerical $\varphi_3^{(1)}$	analytical $\varphi_3^{(0)}$	numerical $\varphi_3^{(0)}$
-0.499000	1	0.037113	0.035245	-0.139637	-0.138417
-0.497000	2	0.037099	0.035267	-0.139431	-0.138456
-0.495000	3	0.037073	0.035266	-0.139073	-0.138266
-0.493000	4	0.037033	0.035257	-0.138582	-0.137948
-0.410000	5	0.036981	0.035245	-0.137973	-0.137515
-0.481000	10	0.036521	0.035102	-0.133453	-0.133745
-0.461000	20	0.034635	0.034147	-0.119031	-0.119546
-0.421000	40	0.027293	0.027450	-0.078115	-0.077807
-0.301000	100	-0.011136	-0.010995	0.050200	0.050068
-0.201000	150	-0.035188	-0.034823	0.095916	0.095808
-0.101000	200	-0.030230	-0.029926	0.070825	0.070763
-0.001000	250	-0.000350	-0.000350	0.000783	0.000777

Table 6.13 **cos(ωt) terms in the third order potential for N_{FREE} = 500 elements, frequency of oscillation ω =σ_1= 5.317 rad/s and n=20 terms in the series.**

The constants and the integral over the free surface

Other interesting parameters to compare with the analytical solution are the value of the constant $\bar{\alpha}_0$, the integral over the free surface, and the constants a_1 and e_1 in the equation (6.30) for determination of N.

The integral over the free surface of the cos(2ωt)-term in the second order free surface elevation, equation (6.20) and (6.21), is analytically equal to zero. In the numerical solution the integral is equal to -0.00035629 for the case with 120 elements on the free surface, -0.00008529 for 240 elements on the free surface, and -0.00001943 for 500 elements on the free surface. From the Figure 6.3 it is seen that the integral converges to zero, when the number of elements is increased.

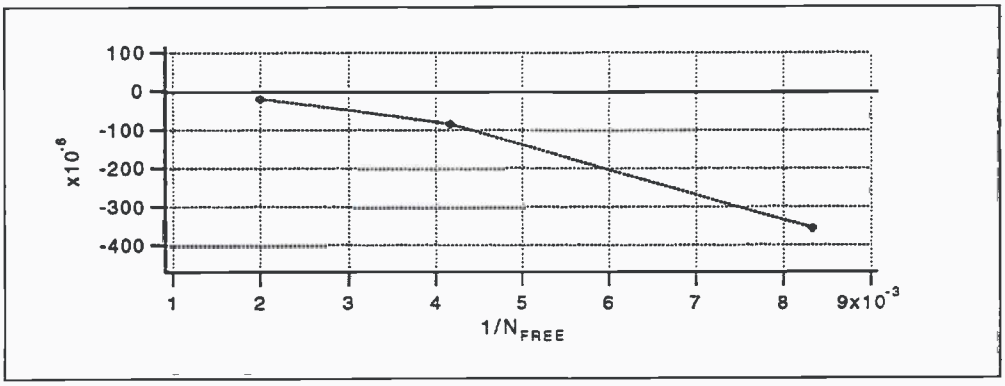

Figure 6.3 The integral over the free surface of the cos(2ωt) terms in ζ_2, equation (6.21).The integral converges to zero, when the N_{FREE} is increased.

The condition of conservation of mass requires also that the integral of the total free surface elevation over the free surface is equal to zero.

$$\int_{-a}^{a} \zeta \, dx = 0 \tag{6.52}$$

When the tank is oscillated with a period equal to the first natural period and with amplitude of oscillation equal to 0.025 m, the integral over the free surface for 240 elements on the free surface is equal to 0.8964E-06 and for 500 elements on the free surface equal to 0.2056E-06. Both these values are very small, and the condition of conservation of mass must be considered as fulfilled.

The constant $\bar{\alpha}_0$ is independent of the oscillation frequency and has the following values for the numerical and analytical solutions

	numerical $\bar{\alpha}_0$	analytical $\bar{\alpha}_0$
$N_{FREE} = 120$	-0.400708	-0.401414
$N_{FREE} = 240$	-0.396528	-0.396632
$N_{FREE} = 500$	-0.394172	-0.394166

Table 6.14 The value of the constant in the second order potential.

In the same manner as for the velocity potential, the difference in the analytical values is due to the difference in the value of D for the three cases. To be able to compare the analytical and numerical results, the analytical value of $\bar{\alpha}_0$ is multiplied with D^2. It is seen that the error in the value for the case with $N_{FREE} = 120$ elements is much larger (0.18 percent) than the value when $N_{FREE} = 240$ elements (0.026 percent). For 500 elements on the free surface, the error is reduced to 0.0015 percent.

The numerical obtained equation for N, equation (6.30), may be compared with the analytical solution by writing the analytical equation from chapter 5.2 on the form

$$\frac{(K_1 - K_2)C^2}{\cosh\left(\frac{\pi}{2a}h\right)}N^3 + \alpha N + \frac{2a\omega^3\frac{8a}{\pi^2}}{\cosh\left(\frac{\pi}{2a}h\right)C} = 0 \qquad (6.53)$$

a_1 should be equal to the term in front of N^3 and e_1 equal to the last term. The obtained values are

	Analytical solution N_{FREE} = 120	Numerical solution N_{FREE} = 120	Analytical solution N_{FREE} = 240	Numerical solution N_{FREE} = 240	Analytical solution N_{FREE} = 500	Numerical solution N_{FREE} = 500
a_1	16.335519	16.382851	16.140908	16.160199	16.040541	16.048877
e_1	-60.178747	-60.159715	-60.540448	-60.527286	-60.729556	-60.722395

Table 6.15 The numerical and analytical values of a_1 and e_1 for oscillation frequency $\omega = \sigma_1$=5.317 rad/s.

When the number of elements on the free surface is increased from 120 to 240, the error in a_1 decreases from 0.29 percent to 0.12 percent, and the error in e_1 decreases from 0.032 to 0.022 percent. When the number of elements on the free surface is increased further, to 500, the error in a_1 is decreased to 0.052 percent and in e_1 to 0.012 percent.

The free surface elevation

In Figure 6.4 the free surface elevation for the case with 120 elements on the free surface is shown. The tank is undergoing forced sway oscillation with amplitude ε_0 equal to 0.025 meter and period of oscillation T equal to the first natural period, which, for N_{FREE}=120 is equal to 1.181684612 sec.

The first figure shows the free surface elevation in element number 1 as function of time over one cycle of oscillation. In the second figure the free surface elevation is shown as a function of the x-coordinate for the time instant t = T/4. The numerical results are plotted in the same figures as the analytical results, and it is seen that the difference between the two results is so small that it is difficult to detect it in the figure.

6.8.3 Conclusions

The values of the eigenperiods T_n and the velocity potentials for the two-dimensional rectangular tank converge to the nonlinear analytical solution when the number of elements increases. Conservation of mass converges also with increasing number of elements.

Quite many elements have to be used in the two-dimensional boundary element method. Good agreement between the numerical and analytical results are obtained when 120 elements are used on the free surface.

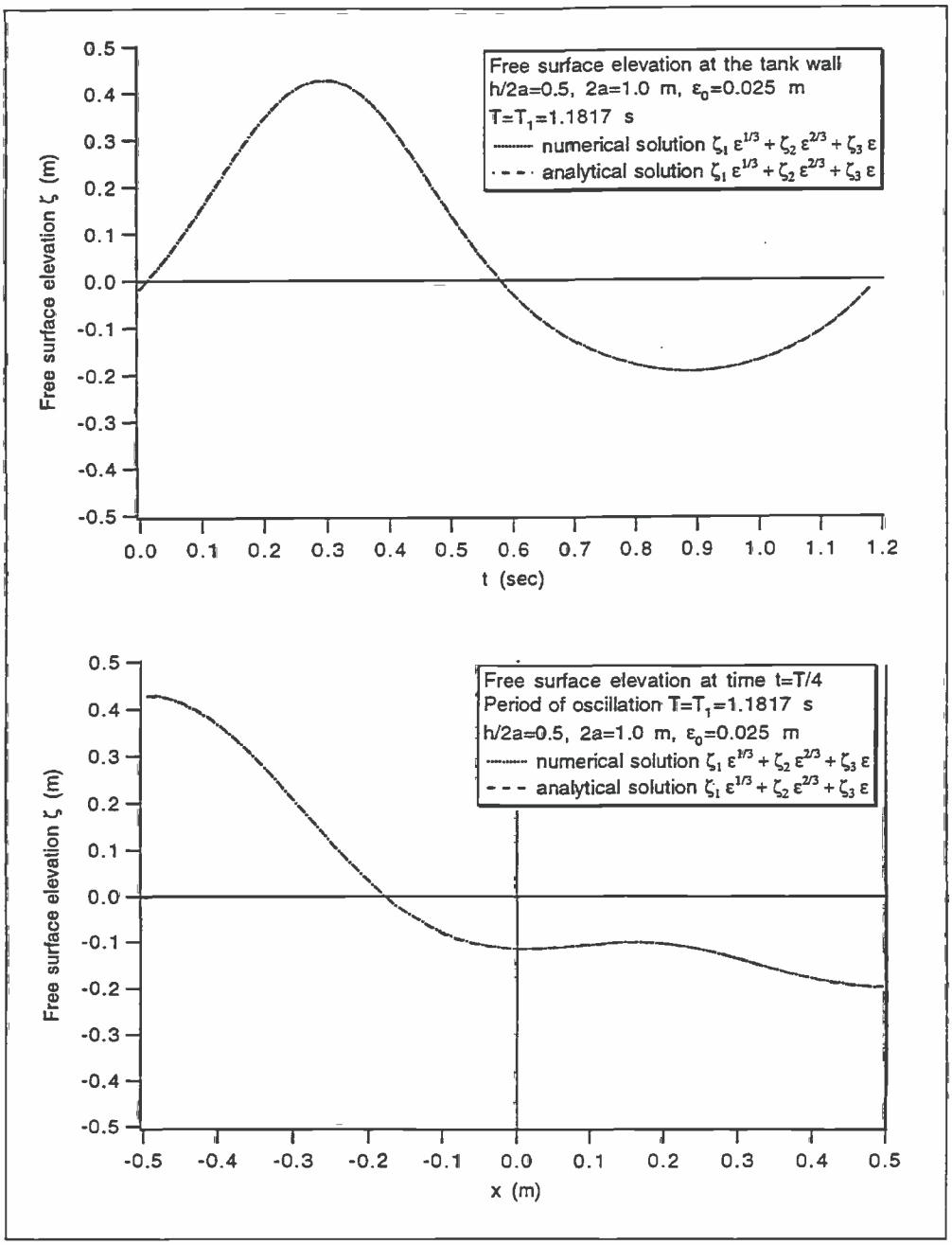

Figure 6.4 **Free surface elevation in a rectangular tank undergoing sway oscillations with amplitude 0.025 m and period equal to the first natural period. N_{FREE}=120.**

6.9 Different tank shapes

To complete the verification of the method, the numerical solutions for other tank shapes are compared with analytical solutions for those cases where the analytical solution is known.

For the rectangular tank the analytical solution may be used for different non-shallow water depths, within the limitation that h and 2a are of O(1).

For a canal with circular cross section only the first eigenfrequency is given in Lamb (1945) art.259. For a half full circular tank the walls are vertical in z=0, and then, the nonlinear analytical/numerical method may be used to find not only the eigenfunctions and frequencies, but also the velocity potential and free surface elevation.

For V-shaped tanks, only the eigenfunctions and frequencies may be found. In Lamb (1945) art.258.1 the eigenfrequencies and functions are given for a V-shaped tank with 45° inclination of the walls, and in art. 258.2 the first symmetrical eigenfrequency and function are given for a V-shaped tank with 30° inclination to the horizontal.

6.9.1 Rectangular tank with different water depths

The eigenperiods for the rectangular tank are given analytically from equation (6.50). When the water depth is increased to two times or more of the tank breadth, the tanh(kh) term will be approximately equal to 1.0 and the following approximation may be used to find the eigenperiods

$$T_n = \frac{2\pi}{\sqrt{\frac{n\pi}{2a}g}} \qquad n = 1,2,3,4,..... \tag{6.54}$$

In Figure 6.5, it is illustrated how the first, second and third eigenperiod change for different ratios between the tank breadth and the water depth. The tank breadth, 2a, is taken to be equal to 1.0 m. Both analytical and numerical results are shown. In the numerical approximation two sets of cases are shown. The cases where the number of elements on the free surface are 500 and the element length is equal to 0.002 m, and the cases where N_{FREE} is equal to 120 and the element length is 0.008333 m.

The figure gives a good illustration of how the eigenperiods change with water depth, and when they are getting independent of the water depth. It is seen that there is very good agreement between the numerical and analytical results for T_1 and T_2. The numerically obtained values for T_3 from the case with 120 elements on the free surface, have slightly smaller values that the analytical results, but the shape of the curve is the same.

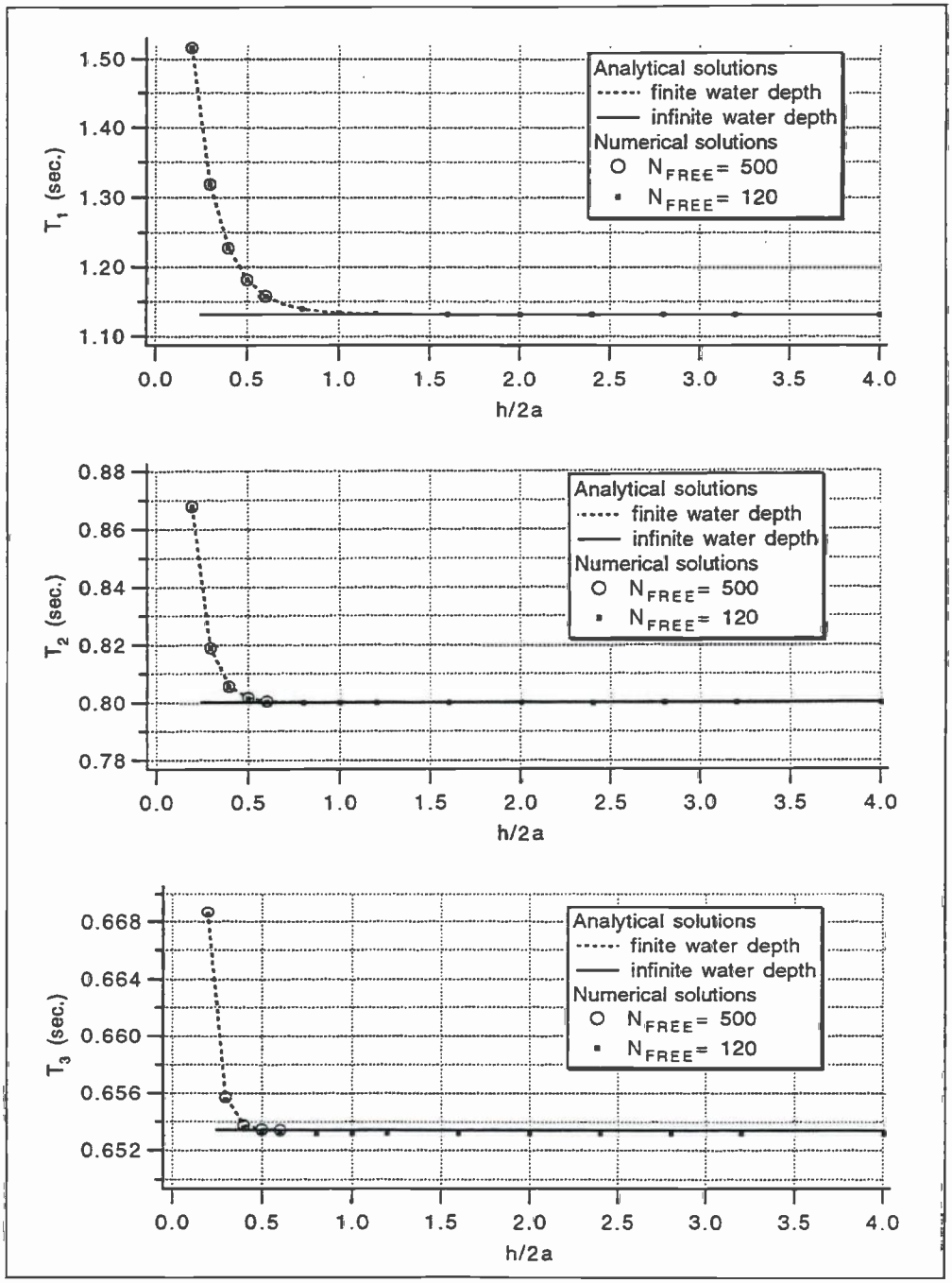

Figure 6.5 **First, second and third eigenperiod as function of water depth for a rectangular tank with 2a=1.0 m.**

In the tables below, the numerical and analytical solutions for the first 10 eigenperiods for breadth/depth relation 0.3 and 0.6 are compared. As expected, 500 elements on the free surface give better results than 120.

n	T_n analytical solution	T_n numerical solution N_{FREE}=120	T_n numerical solution N_{FREE}=500
1	1.318942	1.318804	1.318926
2	0.818973	0.818794	0.818953
3	0.655738	0.655523	0.655714
4	0.566202	0.565939	0.566174
5	0.506198	0.505886	0.506166
6	0.462062	0.461694	0.462026
7	0.427782	0.427358	0.427741
8	0.400153	0.399668	0.400108
9	0.377267	0.376721	0.377218
10	0.357907	0.357296	0.357853

Table 6.16 Eigenperiods for a rectangular tank with breadth 2a=1.0 m and water depth h=0.3 m.

n	T_n analytical solution	T_n numerical solution N_{FREE}=120	T_n numerical solution N_{FREE}=500
1	1.158202	1.158072	1.158187
2	0.800730	0.800555	0.800710
3	0.653454	0.653240	0.653431
4	0.565901	0.565638	0.565873
5	0.506157	0.505845	0.506126
6	0.462056	0.461689	0.462020
7	0.427881	0.427357	0.427741
8	0.400152	0.399668	0.400107
9	0.377267	0.376721	0.377218
10	0.357907	0.357296	0.357853

Table 6.17 Eigenperiods for a rectangular tank with breadth 2a=1.0 m and water depth h=0.6 m.

In table 6.18, the integral of the cos(2ωt) terms in the second order free surface elevation and the integral of the total free surface elevation are shown for different depth/breadth relations of the tank for 120 elements on the free surface.

h/2a	$\int_{-a}^{a} [\ ] \cos(2\omega t)\, dx$	$\int_{-a}^{a} \zeta\, dx$
0.2	-0.1324E-02	0.4024E-05
0.3	-0.6740E-03	0.9578E-05
0.4	-0.4529E-03	0.6680E-05
0.5	-0.3563E-03	0.3696E-05
0.6	-0.3101E-03	0.2890E-05
0.8	-0.2829E-03	0.2464E-05
1.0	-0.3097E-03	0.2653E-05
1.2	-0.4063E-03	0.3463E-05
1.6	-0.7452E-03	0.6338E-05
2.0	-0.1255E-02	0.1067E-04
2.4	-0.6607E-02	0.5611E-04
2.8	0.1235E-02	-0.1050E-04
3.2	0.4156E-03	-0.3535E-05
4.0	0.6796E-04	-0.5780E-06

Table 6.18 Integral of the cos(2ωt) terms in the second order free surface elevation and the integral of the total free surface elevation for different h/2a relations of the tank for N_{FREE}=120. Frequency of oscillation $\omega = \sigma_1$ for the actual tank depth. Oscillation amplitude is 0.025 m and the number of terms in the series approximating $\varphi_3^{(0)}$ and $\varphi_3^{(1)}$ are 5.

All the values in table 6.18 should be equal to zero. It is seen from the tables that the values are relatively small for all cases.

The free surface elevation for some water depths is shown in chapter 6.10.

6.9.2 Tank with circular cross section

In Lamb (1945) art. 259 two approximations for the first antisymmetrical eigenfrequency for a tank with circular cross section are given.

$$\sigma = \sqrt{\frac{8\pi}{48-3\pi^2}\frac{g}{a}} = 1.1690\sqrt{\frac{g}{a}} \tag{6.55}$$

and

$$\sigma = 1.1644\sqrt{\frac{g}{a}} \tag{6.56}$$

where a is the tank radius. The last one is said to be the closest approximation. For a tank radius equal to 0.5 meter the first approximation gives the eigenperiod 1.213432 sec. and the last 1.218227 sec.

The tank with circular cross section is shown in Figure 6.6. For this tank, the walls are vertical in the water line, and then, the nonlinear velocity potential and free surface elevation may be determined. The free surface elevation in a tank with cylindrical cross section is shown for different periods of oscillation in chapter 6.10.

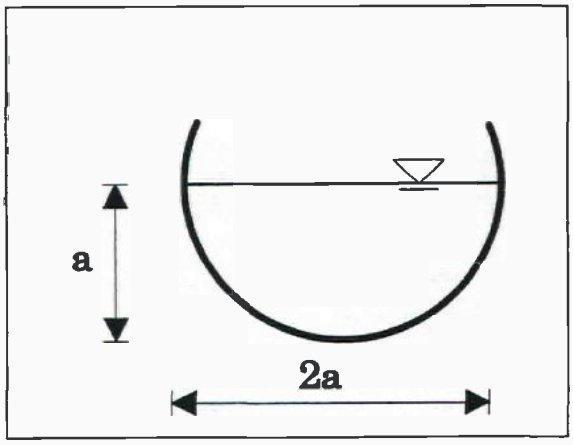

Figure 6.6 Tank with circular cross section. In the example a=0.5 m.

240 and 500 elements on the free surface are used in the numerical calculations. When the number of elements on the free surface is 240, the total number of elements is 617, and the element length 0.004167 meter. For N_{FREE} equal to 500, the total number of elements is 1285 and the length of the elements 0.002 meter. The case with oscillation period equal to the first natural period and forced sway amplitude equal to 0.025 meter is run. The element number from which the derivatives are interpolated to the wall is chosen to be the same as for the rectangular tank. That is 12 for 240 elements on the free surface and 19 for 500 elements on the free surface. The number of terms in the series for determination of $\varphi_3^{(1)}$ and $\varphi_3^{(0)}$ are 10 for 240 and 20 for 500 elements on the free surface.

In Table 6.18, the first, second and third eigenperiods are shown for different number of elements. It is seen that the first eigenperiod from the numerical solutions converges to a

value which is slightly larger than the best of the approximations given in Lamb (1945).

	T_1 (sec.)	T_2 (sec.)	T_3 (sec.)
N_{FREE} = 120	1.218132	0.814307	0.657523
N_{FREE} = 240	1.218226	0.814432	0.657672
N_{FREE} = 500	1.218256	0.814471	0.657717
N_{FREE} = 580	1.218258	0.814474	0.657721

Table 6.18 The first, second and third eigenperiod for a half cylindrical tank with radius 0.5 m.

Since the analytical solutions for the eigenfunctions and velocity potentials are not known for this tank shape, other criteria than similarity with analytical solutions have to be used to verify the goodness of the results. The integral of the free surface elevation over the free surface will give an indication of the errors in the calculation of the free surface elevation, since the criterion for conservation of mass gives that this integral should be equal to zero. For oscillation frequency equal to the first natural frequency and amplitude equal to 0.025 meter the integral over the free surface is equal to 0.4232E-05 for 240 elements on the free surface and 0.2266E-05 for 500 elements on the free surface. Both these values are small, and conservation of mass is fulfilled.

The integral over the free surface of the $\cos(2\omega t)$ term in the second order free surface elevation is -0.3404E-03 for 240 elements on the free surface and -0.1812E-03 for 500 elements on the free surface.

6.9.3 V-shaped tank with 45 degrees inclination

The eigenfrequencies and functions obtained numerically for the two-dimensional oscillations of water across a channel whose section consists of two straight lines inclined at 45° to the vertical, as shown in Figure 6.7, are compared with the analytical results given in Lamb (1945) art. 258.1.

Analytical expressions

The symmetrical eigenfrequencies and eigenfunctions are given by

$$\sigma_n^2 = k_n g \frac{\sinh(k_n h)}{\cosh(k_n h)}, \quad \psi_n = A[\cosh(k_n x)\cos(k_n(z+h)) + \cos(k_n x)\cosh(k_n(z+h))] \tag{6.57}$$

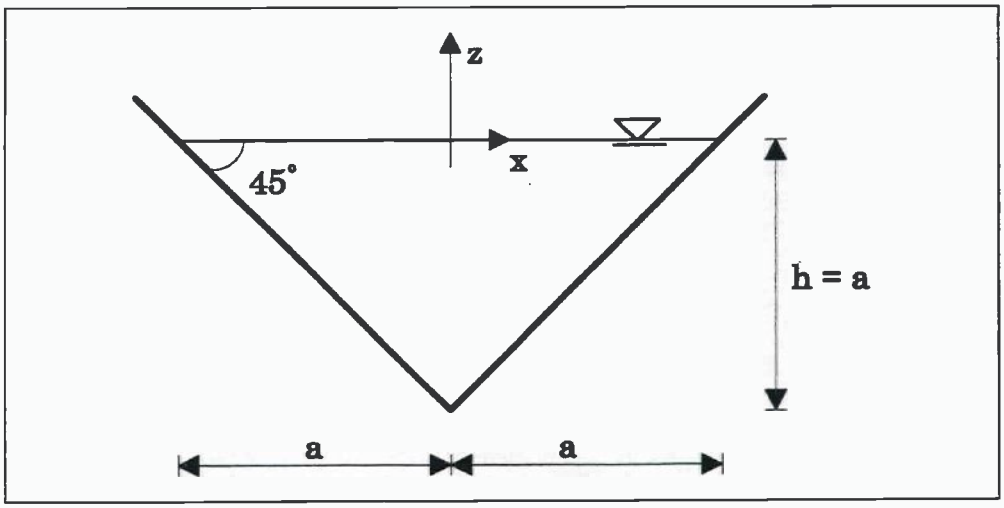

Figure 6.7 Coordinate system for V-shaped tank. In the example 2a is taken to be 1.0 meter.

and the antisymmetrical eigenfrequencies and eigenfunctions by

$$\sigma_n^2 = k_n g \frac{\cosh(k_n h)}{\sinh(k_n h)}, \quad \psi_n = -A[\sinh(k_n x)\sin(k_n(z+h)) + \sin(k_n x)\sinh(k_n(z+h))] \tag{6.58}$$

where k_n are the roots of

$$\cos(2kh)\cosh(2kh) = 1 \tag{6.59}$$

The first antisymmetrical mode, is the one corresponding to kh=0. The surface of this mode is always a plane, with one node in x=0. When $Ak^2=B$ and k is small, the eigenfrequency and eigenfunction are given by

$$\sigma_1^2 = \frac{g}{h}, \quad \psi_1 = -2Bx(z+h) \tag{6.60}$$

The other roots are, from Abramowitz and Stegun (table 4.18):

n	2	3	4	5	6	n > 6
2kh	4.7300407	7.8532046	10.9956078	14.1371655	17.2787596	[2n+1]π/2

Table 6.19 Roots of cos(2kh)cosh(2kh)=1.

where the ones for n=2,4,6, . . are symmetrical and the ones for n=1,3,5, . . . are antisymmetrical.

Numerical results

Calculations are done for a tank with breadth at the free surface, 2a, equal to 1.0 meter and water depth equal to 0.5 meter. The number of elements on the free surface is chosen to be 500 and 240. For 500 elements on the free surface, the total number of elements is 1206 and element length 0.002 meter. For 240 elements, the total number of elements is 578 and the element length is 0.004167 meter on the free surface and 0.004184 m on the side walls.

n	kh	T_n (sec.) analytical	T_n (sec.) numerical N_{FREE} =500	T_n (sec.) numerical N_{FREE} =240
1	0.000000	1.418503	1.418448	1.418319
2	2.365020	0.930564	0.930475	0.930296
3	3.926602	0.715579	0.715480	0.715295
4	5.497804	0.604983	0.604886	0.604691
5	7.068583	0.533536	0.533435	0.533233
6	8.639380	0.482602	0.482496	0.482284
7	10.210176	0.443929	0.443820	0.443598
8	11.780973	0.413276	0.413161	0.412930
9	13.351769	0.388205	0.388086	0.387842
10	14.922565	0.367205	0.367082	0.366825
11	16.493361	0.349282	0.349154	0.348885

Table 6.20 Eigenperiods for a 45 degrees V-shaped tank with 2a=1.0 m.

It is seen that there is good agreement between the analytical and the numerical results for the eigenperiods. As expected, the results are getting closer to the analytical when the number of elements is increased. For increasing eigenperiod number n, the results are getting poorer.

In the tables 6.21 and 6.22, the values of the first, second, third and fourth eigenfunctions in some of the elements on the free surface, are compared with the analytical solutions given in Lamb. The first and third eigenfunctions are antisymmetrical about x=0. The second and fourth eigenfunctions are symmetrical about x=0. For the first eigenfunction, the difference between the analytical and numerical solution is 0.014 percent in element number 1, and it increases to 0.18 percent in element number 120. For the second eigenfunction the error is 0.032 percent in element number 1 and 0.40 in element 120.

From table 6.22 it is seen that the results are poorer for the third and fourth eigenfunctions than for the first and second. This should be expected since the approximation for the eigenfunctions are poorer for increasing n. For the third eigenfunction maximum error is 0.9 percent and for the fourth eigenfunction 2.6 percent.

x-value	el.	analytical ψ_1	numerical ψ_1	analytical ψ_2	numerical ψ_2
-0.497917	1	1.001752	1.001615	1.004076	1.003760
-0.493750	2	0.993369	0.994149	0.984443	0.986299
-0.489583	3	0.984986	0.987773	0.964811	0.967205
-0.485417	4	0.976604	0.969412	0.945179	0.947835
-0.481250	5	0.968221	0.961075	0.925548	0.928354
-0.460417	10	0.926306	0.927626	0.827432	0.830420
-0.418750	20	0.842478	0.843797	0.631908	0.634541
-0.335417	40	0.674820	0.675952	0.251548	0.252891
-0.252083	60	0.507163	0.508041	-0.092695	-0.092765
-0.168750	80	0.339506	0.340104	-0.369931	-0.371230
-0.085417	100	0.171849	0.172154	-0.551235	-0.553371
-0.002083	120	0.004191	0.004199	-0.616227	-0.618668

Table 6.21 **First and second eigenfunctions for 45 degrees V-shaped tank with 240 elements on the free surface.**

x-value	el.	analytical ψ_3	numerical ψ_3	analytical ψ_4	numerical ψ_4
-0.497917	1	1.006903	1.006371	1.009671	1.008932
-0.493750	2	0.973381	0.976607	0.962331	0.966975
-0.489583	3	0.939861	0.944013	0.914996	0.920965
-0.485417	4	0.906344	0.910928	0.867676	0.874238
-0.481250	5	0.872834	0.877643	0.820382	0.827224
-0.460417	10	0.705578	0.710437	0.585013	0.591551
-0.418750	20	0.376152	0.379628	0.132729	0.136180
-0.335417	40	-0.212047	-0.212445	-0.539608	-0.543317
-0.252083	60	-0.592756	-0.596289	-0.647317	-0.642385
-0.168750	80	-0.667101	-0.671647	-0.191368	-0.194165
-0.085417	100	-0.435542	-0.438664	0.437648	0.441133
-0.002083	120	-0.011516	-0.011600	0.734712	0.741335

Table 6.22 **Third and fourth eigenfunctions for 45 degrees V-shaped tank with 240 elements on the free surface.**

6.9.4 V-shaped tank with 30 degrees inclination

The first symmetrical eigenfrequency and eigenfunction for the oscillation inside a tank with side walls inclined 30 degrees to the horizontal are given in Lamb (1945) art. 258.2. With the coordinate system given in Figure 6.8, the eigenfrequency and function are given by

$$\sigma_2^2 = \frac{g}{h}, \quad \psi_2 = A(z+h)[(z+h)^2 - 3x^2] + 2Ah^3 \tag{6.61}$$

If $\varphi = \psi_2 \cos(\sigma_2 t)$, the form of the free surface corresponding to this symmetrical eigenfunction is

$$\zeta = \frac{1}{g}\frac{\partial \varphi}{\partial t}\bigg|_{z=0} = -\frac{3A}{\sigma_2}(h^2 - x^2)\sin(\sigma_2 t) \tag{6.62}$$

which has two nodes at x=-h and x=h.

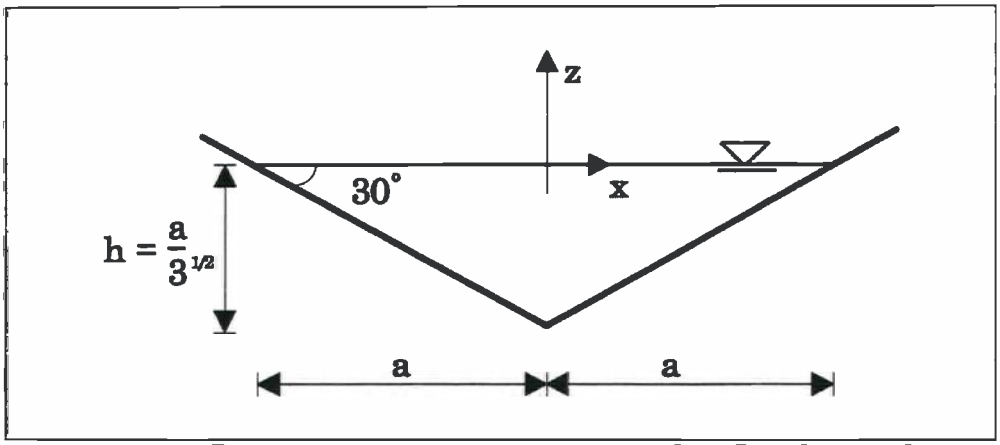

Figure 6.8 Coordinate system for V-shaped tank with 30 degree inclination to the horizontal. In the example 2a=1.0 m and h=0.288675 m.

With tank breadth equal to 1.0 meter the tank depth will be 0.288675 meter. The second eigenperiod, which is the first symmetrical, is 1.077830 sec. from the analytical solution. In the table below, the first five of the numerical obtained eigenperiods for 240 and 500 elements on the free surface are shown. When the number of elements on the free surface are 240, the total number of elements is 516. For 500 elements on the free surface, the total number is 1076. The second eigenperiod is getting closer to the analytical solution when the number of elements is increased.

n	T_n (sec.) analytical	T_n (sec.) numerical N_{FREE} =500	T_n (sec.) numerical N_{FREE} =240
1		1.681983	1.681704
2	1.077829	1.077669	1.077350
3		0.793408	0.793049
4		0.653492	0.653105
5		0.565595	0.565207

Table 6.23 Eigenperiods for a 30 degrees V-shaped tank with 2a=1.0 m.

The numerical obtained values of the symmetrical eigenfunction ψ_2 in some of the elements on the free surface are compared with the analytical solution in the table below.

x-value	el.	analytical ψ_2	numerical ψ_2
-0.497917	1	1.001995	1.001863
-0.493750	2	0.976840	0.979076
-0.489583	3	0.951897	0.954900
-0.485417	4	0.927165	0.930502
-0.481250	5	0.902644	0.906161
-0.460417	10	0.783213	0.786872
-0.418750	20	0.560199	0.563239
-0.335417	40	0.177591	0.178895
-0.252083	60	-0.120463	-0.120748
-0.168750	80	-0.333963	-0.335466
-0.085417	100	-0.462908	-0.465173
-0.002083	120	-0.507300	-0.509831

Table 6.24 Second eigenfunctions for a 30 degrees V-shaped tank with 240 elements on the free surface.

The value of ψ_2 changes sign between element number 51 and 52 and between element number 189 and 190. This gives the same x-value for the nodes as predicted in the analytical solution.

6.10 Free surface elevation in a rectangular tank and a tank with circular cross section

The maximum free surface elevation for the rectangular tank is studied for different depth/breadth relations, different periods of oscillation and different amplitudes of oscillations. For the tank with cylindrical cross section the free surface elevation is studied for different periods and amplitudes of oscillations. For all cases the tank breadth, 2a, is chosen to be 1.0 meter.

In the study of different depth/breadth ratios the number of elements on the free surface is 120, that is an element length equal to 0.008333 meter. For all other cases, the chosen number of elements on the free surface is 240, which gives an element length equal to 0.004167 meter.

6.10.1 Free surface elevation for rectangular tank as function of the depth/breadth ratio

In Figure 6.9 the maximum free surface elevation is shown as function of the depth/breadth ratio, h/2a, for rectangular tanks. The period of oscillation is chosen to be equal to the first natural period for the actual tank depth. It is seen from the figure that the solution blows up for depth/breadth ratios around 0.34, and that the smallest free surface elevation is obtained for a depth/breadth ratio equal to 0.8. For h/2a greater than approximately 0.5, it is seen that the depth of the tank has little influence on the free surface elevation.

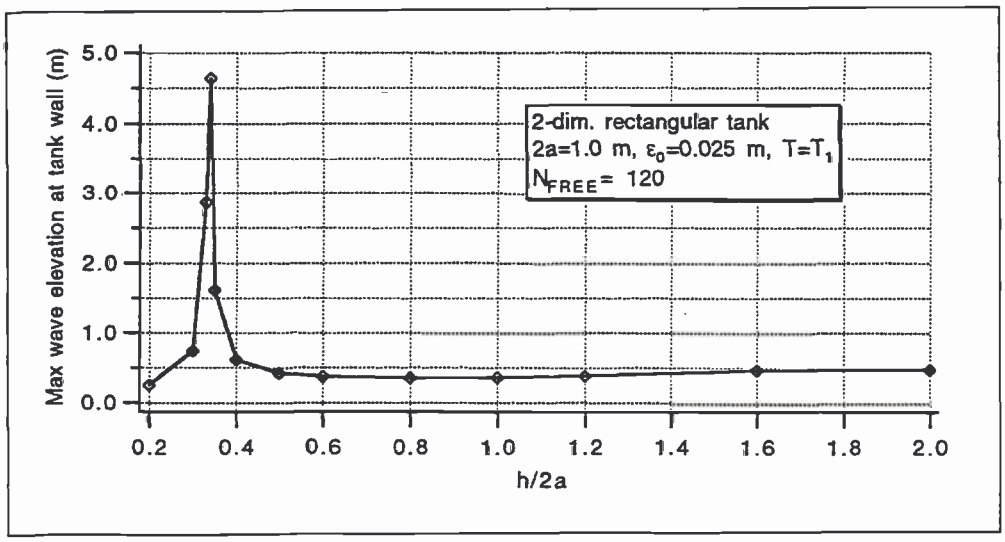

Figure 6.9 Maximum wave elevation as function of depth/breadth ratio for rectangular tanks. $\omega = \sigma_1$ and ε_0=0.025 m. N_{FREE}=120.

In Faltinsen, Olsen, Abramson and Bass (1974) a similar figure is shown for roll oscillation of the tank. When the frequency of oscillation ω is equal to the first natural frequency σ_1 and the depth/breadth ratio is in the vicinity of 0.34, the nonlinear theory, which is the basis for this numerical/analytical method, is not applicable. Analytically, the solution should become infinite when h/2a is equal to 0.34 and ω is equal to σ_1 , but since there are errors in the numerically obtained values, we get a large, but finite, value for the free surface elevation.

6.10.2 Free surface elevation as function of the period of oscillation

In Figure 6.10 the maximum free surface elevation for rectangular tanks with depth/breadth ratios 0.3, 0.35 and 0.5 is shown for different relations between the periods of oscillation and the natural periods. It is seen that the solution blows up around the first natural period for h/2a equal to 0.35.

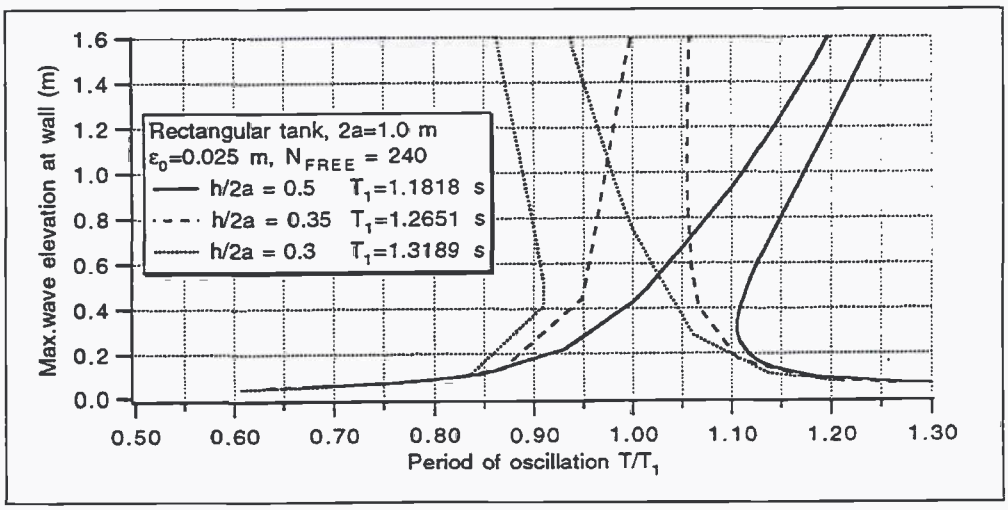

Figure 6.10 Maximum free surface elevation as function of period of oscillation for rectangular tank with h/2a=0.3, 0.35 and 0.5. ε_0=0.025 m. N_{FREE}=240.

For periods of oscillation above a certain period for h/2a greater than 0.34, there are three solutions of the system of equations. Which solution the physical system will select depends on how the frequency of oscillation is reached, and when it will jump down from the upper to the lower solution can not be predicted in this method. The physical system will never select the solution in the middle, since this is an unstable solution, (see Faltinsen (1974).)

In Figure 6.11 the maximum free surface elevation for a rectangular tank with h/2a=0.5 (2a=1.0 m) and a tank with circular cross section and a=0.5 m is shown for different ratios between the periods of oscillation and the natural periods. It is seen that the curves are fairly similar.

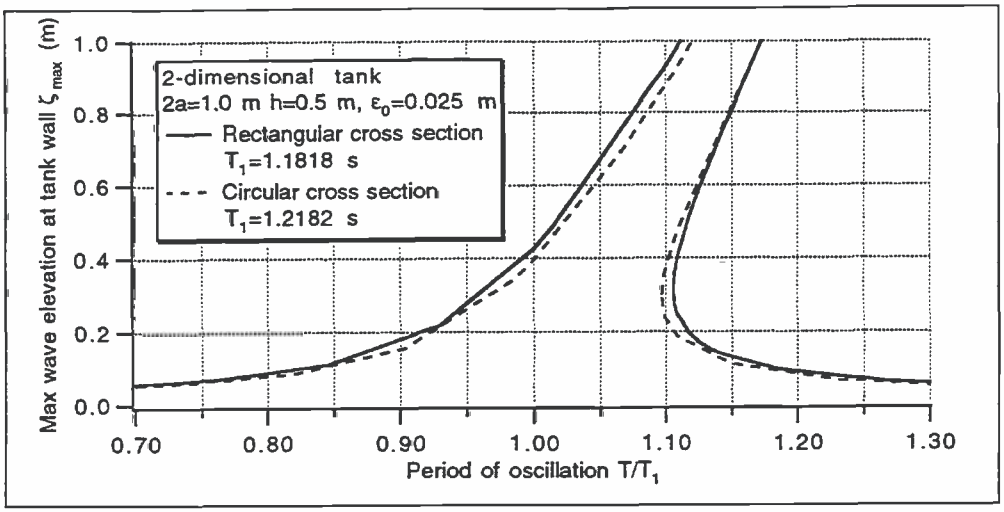

Figure 6.11 Maximum free surface elevation for rectangular tank with h/2a=0.5 and tank with circular cross section with a=0.5 m. N_{FREE}=240.

6.10.3 Free surface elevation as function of the amplitude of oscillation

In Figure 6.12 the maximum free surface elevation is shown for a rectangular tank and a tank with circular cross section for amplitudes of oscillation between 0.005 meter and 0.100 meter. For both tanks a=0.5 meter and for the rectangular tank h/2a=0.5. The frequency of oscillation is chosen to be equal to the first natural frequency, that is 1.18177 sec. for the rectangular tank and 1.21823 sec. for the tank with the cylindrical cross section. The nonlinearity of the solution is seen from this figure.

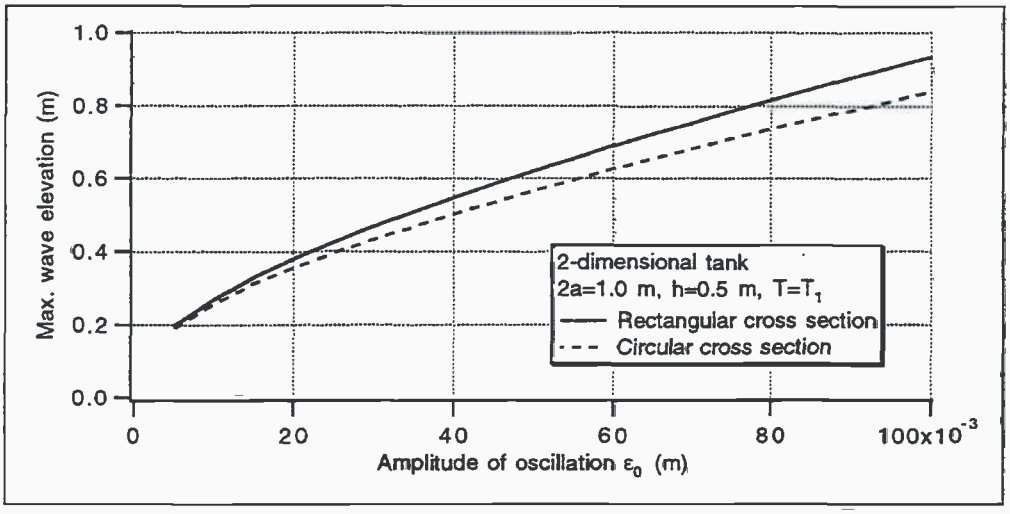

Figure 6.12 Maximum free surface elevation for rectangular tank with h/2a=0.5 and tank with circular cross section with a=0.5 m. N_{FREE}=240.

6.11 Discussions and conclusions

A nonlinear numerical method for calculation of sloshing in two-dimensional tanks, based on the analytical solution in chapter 5 and a boundary element method, is developed. It is assumed that the tank is oscillated harmonically in sway with amplitudes of oscillations small compared to the tank breadth and water depth. The frequencies of oscillation are assumed to be in the vicinity of the first resonance frequency. It is assumed that the tank breadth 2a and the water depth h are of the same order of magnitude.

The results are compared with analytical solutions. Quite many elements was necessary to use in the boundary element method to get satisfactory results. For calculation of the free surface elevation for a rectangular tank there is good agreement between the numerical and analytical results when 120 elements are used on the free surface.

In the same way as for the analytical method, the solution for a rectangular tank will blow up for tank breadth/depth ratios around 0.34 when the frequency of oscillation is equal to the first natural frequency. Similar results could be expected for other tank shapes, but has not been studied.

Advantages compared with the analytical solution is the possibility of finding the solution for tank shapes where it is not possible to determine the eigenfunctions and frequencies analytically. But, it is shown that the nonlinear method can only be used for tanks with vertical walls in the water line. It is not possible to calculate strong nonlinear waves, such as breaking waves and hydraulic jumps.

The eigenfunctions and frequencies can be determined for an arbitrary shaped tank, including tanks where the walls are not vertical in the free surface line.

For tanks with vertical walls in the free surface line, the velocity potential and free surface elevation can be determined for harmonic sway motions of the tank. To increase the practical use of the method, pressures and forces on the tank should be calculated, and roll motions of the tank included. This is not investigated numerically, but, in principle, it should not create any difficulties.

When the velocity potential is determined in all of the elements, the pressure on the tank walls may be determined from the Bernoulli equation. To do this, the x- and z-derivatives of the φ_1 and φ_2 velocity potentials in each of the wall elements have to be found.

When the pressure is determined in each of the elements, the forces may be determined by integrating the pressure over the tank walls. If the force is to be determined to third order, the contributions from both $z = -h$ to 0, and from $z = 0$ to the actual free surface, ζ, have to be taken into account. When integrating from $z = -h$ to 0 one may take the sum of the pressure in each element times the length of the element. The contribution from $z = 0$ to ζ may be determined by a Taylor series expansion of the pressure around $z = 0$. How to do this analytically is shown in Abramson (1966) chapter 3.3.

Extension of the method to forced roll motions of the tank, may be done in the same manner as in the nonlinear analytical solution in Faltinsen (1974). The same procedure as for the sway motion may be followed, but it will be more complex to find the particular solution of the velocity potential ϕ_c, associated with the tank motion. The first and second order velocity potentials will remain unchanged except for different constant proportionality factors.

Since this method gives three solutions for the velocity potential at some frequencies of oscillation, it is not known how to use the results for irregular motions of the tank.

Extension of the method to three-dimensional tanks should be possible, but it will require much memory in the computer, since large matrix systems are to be solved and the size of the matrixes is increasing with the number of elements as N_{EL}^2. In this method, it is assumed that the velocity potential is constant over each of the elements. This requires a fine discretization to obtain good results. To reduce the number of elements needed, one may try to use a higher order boundary element method, but this will require a different solution procedure than the one described above.

7 APPLICATION OF THE FINITE DIFFERENCE COMPUTER CODE FLOW-3D

From the literature survey in chapter 2.2 it appears that there exist different direct numerical solvers of Navier-Stokes equation with complete nonlinear free surface conditions where the authors claim they are able to solve the sloshing problem for a general tank shape with any forced tank motion. Based on the mathematical formulation of the boundary value problem, this is in principle possible. However, it appears from the publications that the computer codes have generally not been sufficiently verified and validated.

We decided to study in more detail the application of the commercial computer code "FLOW-3D, Computational Modelling Power for Scientists and Engineers" developed by Flow Science, Inc. Before the FLOW-3D code was chosen, the original SOLA-SURF code, as described in Hirt, Nichols and Romero (1975), (see chapter 2.2.1), was tried modified to handle sway motion of a rectangular tank. The modified code functioned for small oscillations far away from resonance. Around the first resonance frequency, however, the calculations had difficulties and the program stopped before the solution reached the steady-state. Newer versions of the SOLA codes have been developed after the original SOLA-SURF, but since the FLOW-3D code, which is based on the SOLA-VOF code, became available at SINTEF, the modified SOLA-SURF code was not tested out further.

Other reasons for choosing the FLOW-3D code was that this code has possibilities for calculations of sloshing in different tank shapes in two-and three-dimensions, all modes of motion, viscous flow, large fluid motions and breaking waves in the tank. It is not the intention with this work to verify the numerical methods used in the FLOW-3D code, but to find out if the code is suitable for practical sloshing calculations. The quality of the code is evaluated by comparing results from the calculations with published results from model tests and analytical solutions. In addition, a study of the influence on the solution of changing some of the numerical parameters in the code which may be set by the user, is performed.

The description of the FLOW-3D code is based on the user's manual (1991). The calculations of sway motions of the tank and the influence of numerical parameter values were carried out by the 1991 version of the code. The 1994 version of the code is used for the calculations of roll motions of the tank.

The FLOW-3D code and the methods used in the code are presented in chapter 7.1. Chapter 7.2 contains a study of how the values of some numerical parameters influence the numerical results. In chapter 7.3, some results from numerical calculations with use of the FLOW-3D code are presented and compared with analytical solutions, solutions from the nonlinear combined analytical and numerical method in chapter 6 and published results from model tests.

The FLOW-3D code is able to handle coupled motions of the computational reference frame. But, in the calculations presented here, the results are compared with analytical solutions and published results from model tests with either forced sway or roll oscillations of the tank. Calculation of other modes of motion are not performed.

In the numerical simulations, the fluid in the tanks is water with mass density 1000 kg/m^3 and kinematic viscosity 10^{-6} m^2/s. It is assumed that the flow is laminar.

7.1 Description of the code

The FLOW-3D code is a multi purpose commercial code that analyses fluid dynamics and thermal phenomena. Cartesian or cylindrical geometry may be used, and the computational mesh may contain moving obstacles and arbitrarily shaped obstacles, or represent arbitrarily shaped containers. Accelerations of the fluid may be arbitrary. It may contain two-fluid interfaces or free surfaces, with or without surface tension. The fluid may be viscous or non-viscous, incompressible, slightly compressible or fully compressible, Newtonian or non-Newtonian. The boundary conditions may be free-slip or no-slip walls with symmetry boundaries or specified velocity or pressure boundaries. The flow may be subsonic, transonic or supersonic. The mesh may contain power sources or porous baffles with flow losses. To follow the flow, marker particles may be used. Computations may also be done for cavitation and turbulent mixing, heat transfer, thermal conduction in solids and solidification/melting processes.

The governing basic equations used in the computer code for analysis of the sloshing problem are the mass continuity equation and the momentum equations (Navier-Stokes equations with some additional terms, which take care of mass sources and flow losses across porous baffle plates). The equations are formulated with area and volume porosity functions. This formulation is called FAVOR, for Fractional area / Volume Obstacle Representation method and it is described in Hirt and Sicilian (1985) and in Hirt (1993). The method is used to model complex geometric regions. For example, zero volume porosity regions, that is, the cell is blocked out and contains no fluid, are used to define obstacles.

The complete mass continuity equation is given in section II.B in the theory manual (1991) and the complete momentum equations in section II.C.

For application to fluid sloshing in moving containers the equations of motion have a formulation for a moving non-inertial reference frame. This is described in the quick reference guide to the 1994 version of the code.

Fluid configurations are defined in terms of a volume of fluid (VOF) function, $F(x,y,z,t)$, which represents the volume of fluid per unit volume. The time dependence of F is governed by the equation

$$\frac{DF}{Dt} = \frac{\partial F}{\partial t} + u\frac{\partial F}{\partial x} + v\frac{\partial F}{\partial y} + w\frac{\partial F}{\partial z} = 0 \qquad (7.1)$$

where u,v and w are the velocity components in x, y and z directions. This equation states that F does not change value when one follows a point that moves with the fluid. For a single fluid case, F represents the volume fraction in a cell occupied by fluid. Thus, fluid of constant density exists where F=1, and void regions correspond to locations where F=0. "Voids" are regions without fluid mass that have a uniform pressure assigned to them. Physically, they

represent regions filled with a vapour or gas whose density is insignificant with respect to the fluid density. By definition, a surface cell is a cell containing fluid, with F≠1 and having at least one adjacent cell that is empty and one that is full of fluid. A cell with a F-value less than unity, but with no empty neighbour, is considered a full cell in one-fluid problems.

It is also necessary to define where the fluid is located in a boundary cell. The normal direction to the boundary lies in the direction in which the value of F changes most rapidly. When both the normal direction and the value of F in a boundary cell are known, a line cutting the cell can be constructed that approximates the interface there. The VOF method is described in more detail in Hirt and Nichols (1981).

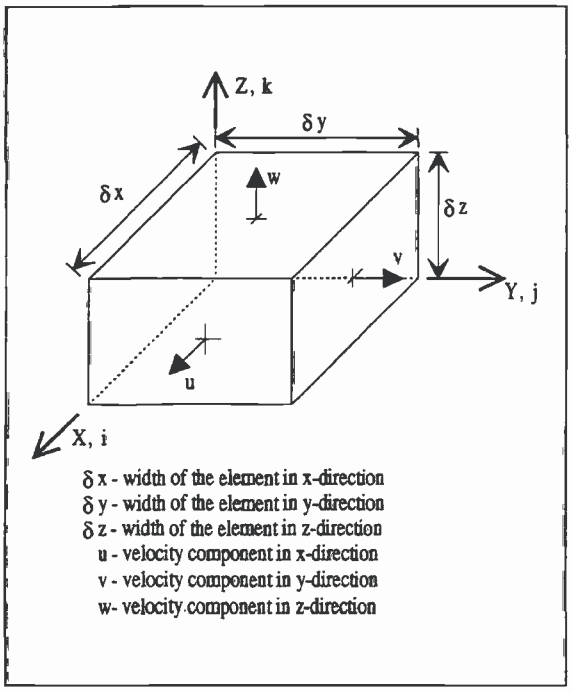

Figure 7.1 A rectangular mesh cell.

Generally, two different computational meshes may be used; a rectangular mesh or a cylindrical mesh. The rectangular finite-difference mesh, which is used here for numerically solving the governing equations, consists of rectangular cells of width δx_i, depth δy_j, and height δz_k, as shown in Figure 7.1 The active mesh region has IBAR cells in the x-direction labelled with the index i, JBAR cells in the y-direction labelled with the index j, and KBAR cells in the z-direction labelled with the index k. This region is surrounded by layers of fictitious or boundary cells used to set mesh boundary conditions.

With each cell there are associated local average values of all dependent variables. The velocity components and the fractional areas are located at the centre of the cell faces. All other variables, like pressure, fluid fraction, densities and viscosity are located at the centre of the cells.

Generally shaped tanks are made by blocking out the cells which contain no fluid, as shown for a LNG tank in Figure 7.2. Here the corners of the tank is made by blocking out cells in the corners of the rectangular mesh.

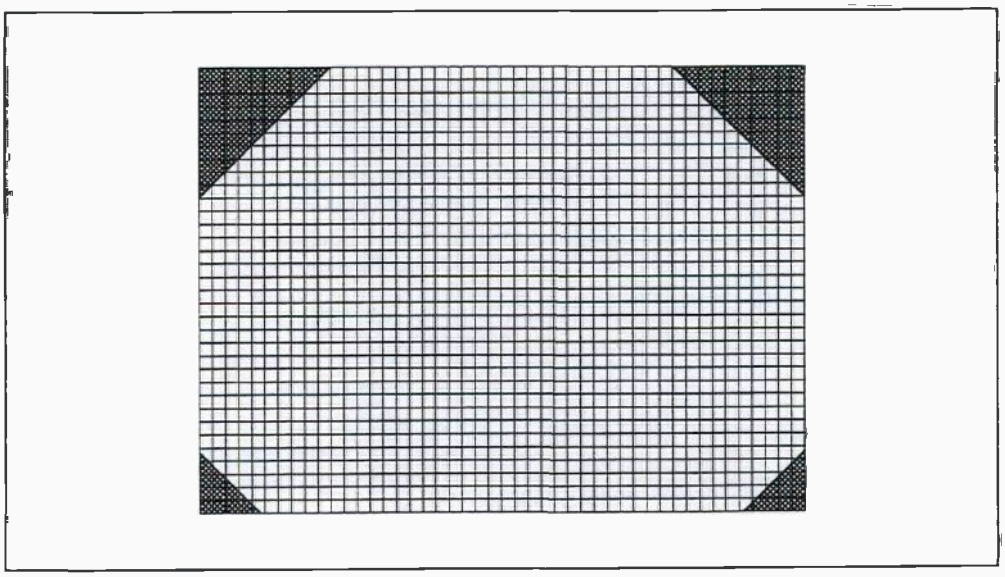

Figure 7.2 Computational mesh where the corners are blocked out to model a LNG tank

The basic procedure for advancing a solution through one increment in time consists of three steps:

1. Explicit approximations of the momentum equations are used to compute the first guess for new time-level velocities using the initial conditions or previous time-level values for velocities, accelerations and pressure.

2. To satisfy the continuity equation, the pressures are iteratively adjusted in each cell and the velocity changes induced by each pressure change are added to the velocities computed in step 1. An iteration is needed because the change in pressure needed in one cell will upset the balance in the six adjacent cells.

3. Finally, when there is a free surface or fluid interface, F is updated by using equation (7.1) to give the new fluid configuration.

Repetition of these steps will advance a solution through the desired time interval. At each step suitable boundary conditions must be imposed at all mesh, obstacle, and free-boundary surfaces.

For the sloshing problem, free surface boundary conditions have to be satisfied. The normal stress, i.e., specified pressure, condition at a free surface is satisfied by the pressure setting scheme. Tangential stresses at a free surface are zero because all velocity derivatives that involve velocity components outside the surface are set equal to zero.

In addition to the free-surface pressure boundary condition it is also necessary to set conditions at all mesh boundaries and surfaces of all internal obstacles. Free-slip boundaries are surfaces having zero tangential stresses. This condition is imposed by setting to zero all velocity derivatives that are computed using one or more velocity components from cell faces having a zero flow area (or a face outside the fluid in free-surface problems).

At the mesh boundaries the conditions may be set by using the layer of fictitious cells surrounding the mesh. Consider, for example, the boundary separating the i=1 and i=2 layer of cells. The i=1 cells are fictitious in the sense that variable values are set, not calculated, in these cells to satisfy boundary conditions. If the boundary is to be a vertical rigid wall, the normal velocity there must be zero, and the boundary conditions for incompressible flow are, for all j,k:

$$\begin{aligned} u_{1,j,k} &= 0.0 \\ p_{1,j,k} &= p_{2,j,k} \\ F_{1,j,k} &= F_{2,j,k} \end{aligned} \tag{7.2}$$

Here u is the velocity in x-direction, p is the pressure and F is the volume of fluid function. Tangential velocities in the fictitious cells are not used. They do not have to be set, because free-slip conditions are set automatically by ensuring that all velocity derivatives across the wall are zero.

No-slip wall conditions, including specified wall velocities, are imposed through the wall shear-stress model, described in the theory manual (see Sec.IV.D.4). The wall stresses are modeled by assuming a zero tangential velocity on the walls and edges of areas closed to flow. For moving boundaries, the tangential velocity is equal to the velocity of the boundary in a direction parallel to its surface.

The different types of boundary conditions are described in the theory manual Sec. IV.H.

There are several restrictions on time-step size that must be observed to avoid numerical instabilities. If the user requests the automatic time-step selection in the input data, the code will adjust the time steps to be as large as possible without violating the stability conditions or exceeding the user-supplied maximum time-step size. If the user selects the time-step size, the following criteria have to be satisfied. First, fluid must not be permitted to flow across more than one computational cell in one time step. This advective transport depends on the velocity and the fractional area / volume open to flow. For free surfaces the surface waves should not propagate more than one cell in one time step. When a nonzero value of dynamic viscosity is used, the restriction that no quantity should diffuse more than approximately one mesh cell in one time step, is introduced. To ensure stability, the parameter which controls the relative amounts of donor-cell and centred differencing used for the momentum advection terms, also has to be set correctly. A more detailed description of the stability criteria is given in sec.J in the theory manual.

7.2 Study of the influence of different parameter values in the FLOW-3D code

The FLOW-3D code contains several physical and numerical parameters which may be set by the user. The influence on the solution of changing the values of the convergence criterion, the weighting of upstream differencing, the element size and the boundary condition at the tank walls, are studied in this chapter. A complete list of input variables is given in the users manual.

7.2.1 The convergence criterion in the pressure iteration

The error in the volume of fluid inside the tank will increase as the numerical calculation goes on. The magnitude of the volume errors changes with the period of oscillation and the oscillation amplitude. Generally, the largest errors in the volume of fluid are obtained when the motions of the water inside the tank are large. This may be seen from Figure 7.3 where the volume error after 30 oscillations is shown as function of period of sway oscillation for the LNG tank model in Figure 7.13. It is seen from the figure that the volume error is large for the periods around resonance, where the free surface elevation and forces on the tank are large.

The amount of the volume error may be reduced by choosing a smaller value of the parameter EPSADJ than the default value, which is equal to 1.0. The EPSADJ parameter gives an automatic adjustment of the convergence criterion, EPSI, in the pressure iteration algorithm, step 2 on page 7.4. In this iteration, the code is trying to fulfil the continuity equation. The right hand side of the continuity equation is equal to zero. The pressure iteration will continue until the value of this right hand side is less or equal to EPSI. The convergence criterion EPSI has a small value, typically of order 10^{-3}. EPSI may be set by the user or set automatically by the code. When set automatically, the value of EPSI will change from time step to time step. When EPSADJ has a value smaller than 1.0, the convergence criteria get more strict.

When the default value of EPSADJ equal to 1.0 is used for the adjustment of the pressure iteration convergence criterion, it is seen from Figure 7.3 that the volume error is above 10 percent for oscillations around the resonance period. If a smaller value of EPSADJ is chosen, the convergence is getting better. For a value of EPSADJ equal to 0.01, the volume error reduces to less than 4 percent after 30 periods of oscillation.

In the calculations in Figure 7.3, the element size in x-direction is 0.0276 meter and in z-direction 0.02757 meter. A two-dimensional approach is used, where the front and the back walls of the computational mesh is symmetry planes. The weighting of upstream differencing, ALPHA, described in chapter 7.2.2, is equal to 0.5.

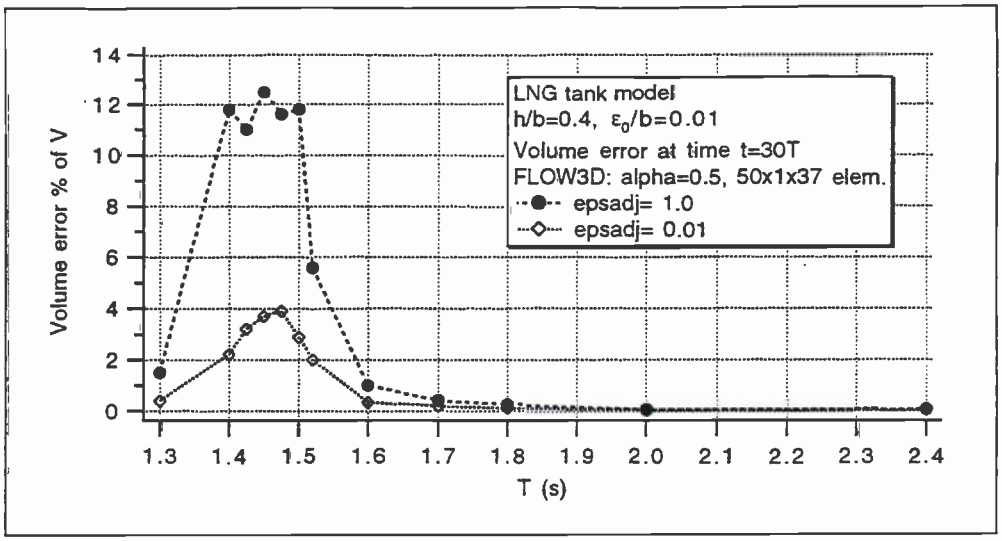

Figure 7.3 Volume error after 30 oscillations as function of period of oscillation for the LNG tank model in Figure 7.13.

In some cases with EPSADJ=1.0, the volume error became so large, that the resonance frequency changed and the violent sloshing in the tank suddenly became more calm. This phenomenon was observed for some of the cases where the water was hitting the tank top in the beginning of the calculations. This is illustrated in Figure 7.4, where the rectangular tank in Figure 7.11 was forced to oscillate harmonically in sway with amplitude of oscillation 0.05 meter, and frequency of oscillation 1.45 sec. The first natural period of the tank is 1.27 sec. After about 25 sec. of calculation, the volume of fluid inside the tank has increased from 0.035 m^3 to 0.043 m^3. This leads to an increase in the mean water depth from 0.35 m to 0.43 m, and then the first natural period is decreased to 1.21 sec. This was enough to change the amplitude of the surface elevation to about half the value it had in the first part of the calculation.

This illustrates the importance of having control of the volume errors in the computations. This may be done by adjusting the EPSADJ value down to a value which gives small volume changes during the calculations. The volume error, when the change in the fluid motion in Figure 7.4 occurred, was 23 percent.

When the free surface elevation is to be determined, it is necessary to account for the increase in the still water level due to the volume error.

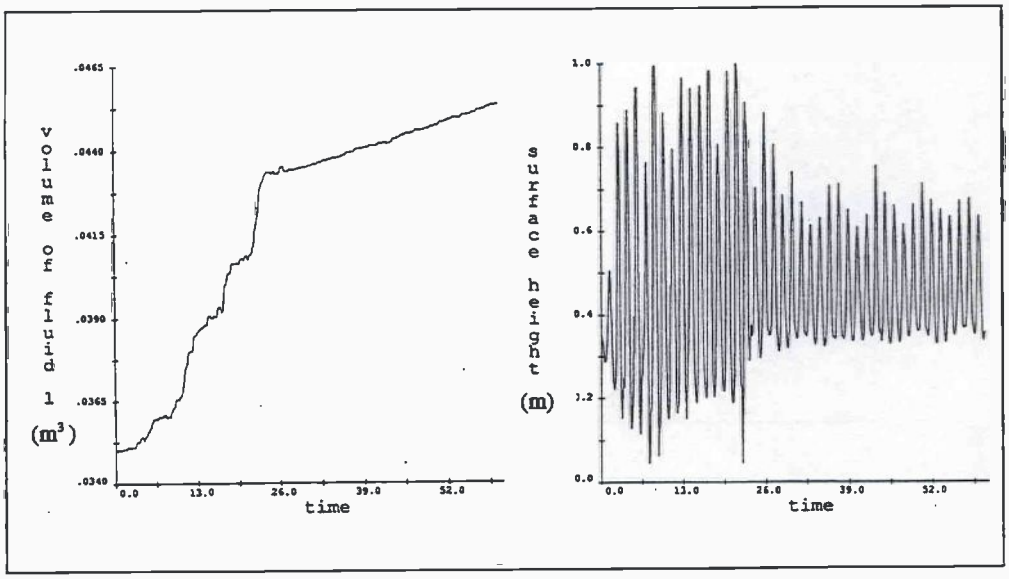

Figure 7.4 Volume of fluid (left) and free surface elevation (right) as function of time for rectangular tank 1x0.1x1 m³, h/b=0.35, ε_0/b=0.05 and T=1.45s.

7.2.2 ALPHA, the weighting of upstream values

The ALPHA parameter controls the weightening of upstream and central differencing in the approximation of the advective flux terms in Navier-Stokes equation. The value of ALPHA may be between 0.0 and 1.0. Normally, the default value 1.0, which means fully upstream differencing and a first order approximation of the advective flux terms, is used. If the value 0.0 is chosen, only central differencing, which gives a second order approximation of the advective flux terms, is used, but then the solution will be unstable.

In Figure 7.5 the total horizontal force for sway motion of the LNG tank model in Figure 7.13 is shown for ALPHA equal to 1.0 and 0.5. It is seen that the force is generally getting larger for ALPHA equal to 0.5 than for ALPHA equal to 1.0. The width of the peak around resonance is also larger for ALPHA equal to 0.5. From Figure 7.6, Figure 7.7 and Figure 7.8 it is seen that also the free surface elevation is getting larger when the value of ALPHA is decreased.

In Figure 7.5 the force is made nondimensional by dividing by the water density, ρ, gravitational acceleration, g, tank breadth b, and tank length perpendicular to the paper plane, l. In the numerical approximation l is taken to be 0.1 meter. The calculation is made two-dimensional by assuming that the front and back walls are symmetry planes.

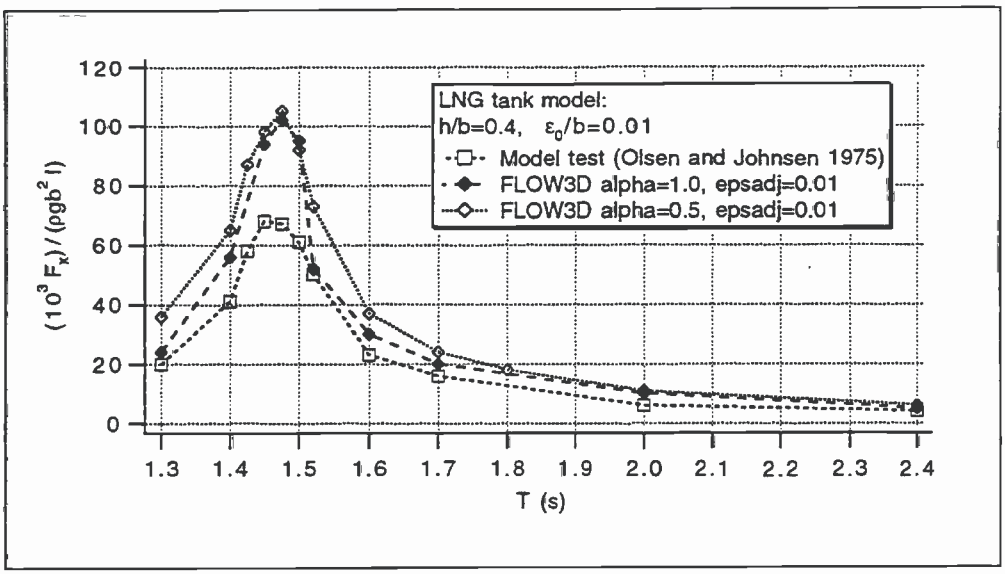

Figure 7.5 Total force in x-direction as function of period of oscillation for the LNG tank model in Figure 7.13.

7.2.3 Element size

How the number of elements or element size will influence on the results is studied for a two-dimensional rectangular tank with height 1.0 meter, breadth 1.0 meter, water depth/tank breadth ratio equal to 0.35 and amplitude of forced sway oscillation equal to 0.05 meter. The lowest natural period for the water in the tank is 1.27 sec.

In Figure 7.6 the free surface elevation and total force in x-direction are shown as function of element size for a period of oscillation equal to 1.0 sec. For ALPHA equal to 0.75 and 1.0, the solution for the free surface elevation approaches the model test result from Olsen and Johnsen (1975) when the number of elements is increased. The value of the force is higher than in the model tests, but for ALPHA equal to 0.75 and 1.0, the values lie between the theoretical and the experimental results. For ALPHA=1.0 the element size has relatively small influence on the results. The volume error is large, 16 percent of the original volume, after a computational time equal to 30 sec. for an element size equal to 0.05 meter. When the element size is decreased to 0.02 meter, the volume error decreases to 4 percent.

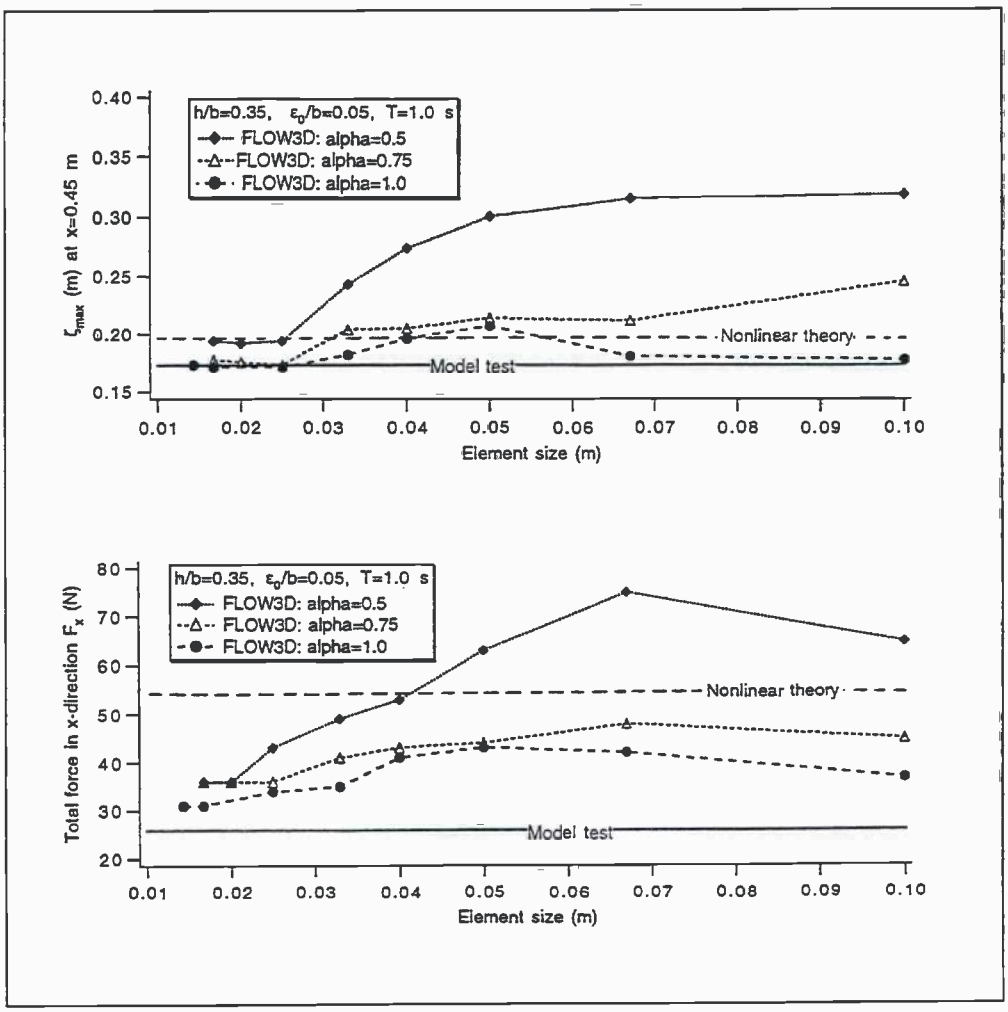

Figure 7.6 Free surface elevation and horizontal force as function of element size for 1 m x 0.1 m x 1 m tank. Model tests and theoretical results from Olsen and Johnsen (1975).

Figure 7.7 shows the free surface elevation and total force in x-direction as function of element size for T=1.8 sec. It should be noted that the values of the free surface elevation, and hence the differences between the solutions, are small. For ALPHA=1.0, the values of the forces are between the results from linear theory and the model test results for element sizes less than 0.06 meter. The largest volume error occurs for element sizes around 0.04 meter and is 4.5 percent for ALPHA=0.5.

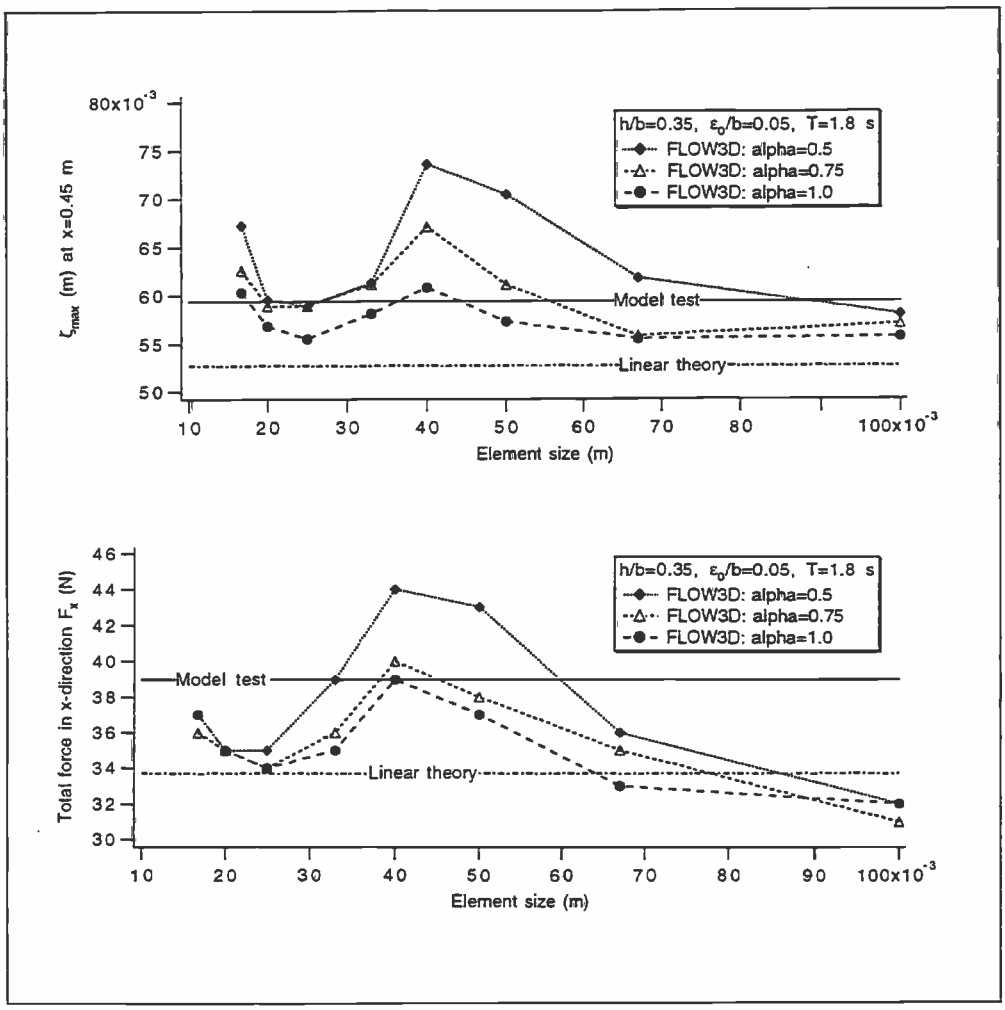

Figure 7.7 Free surface elevation and horizontal force as function of element size for 1 m x 0.1 m x 1 m tank. Model tests results from Olsen and Johnsen (1975).

Figure 7.8 shows the free surface elevation as function of element size for a period of oscillation equal to 1.2 sec. The tank height is chosen equal to 1.4 meter, to avoid the water from hitting the tank top. It is seen that ALPHA equal to 0.5 gives good results compared with the model tests. For the other two ALPHA values, the free surface elevation is smaller than in the model tests. The volume error is between 5 and 17 percent.

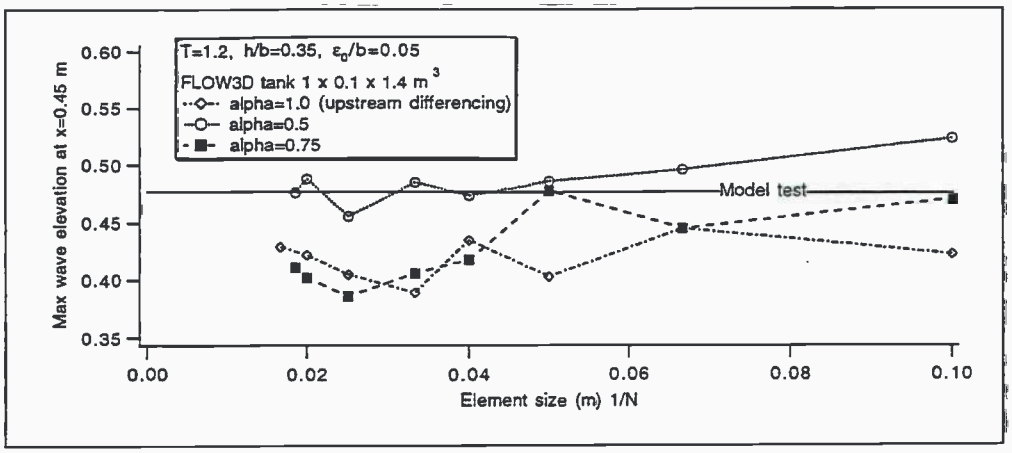

Figure 7.8 Free surface elevation as function of element size for a rectangular tank. Model test results from Olsen and Johnsen (1975).

It may be difficult to conclude based on these results. As all calculations are done with EPSADJ equal to 1.0, relatively large volume errors occur for some cases. One could argue that this is a bad choice in those cases, but the results demonstrate sensitivity to element size.

7.2.4 Boundary condition at the tank walls

The free surface elevation is shown in Figure 7.9 for a three-dimensional rectangular tank, where the front and back walls of the computational mesh are taken to be real tank walls with free- or no-slip boundary conditions. No-slip condition implies that viscous effects in the boundary layer along the wall is accounted for. The tank dimensions are 1.0 x 0.1 x 1.5 m^3. The water depth is 0.5 meter and the tank is oscillated in roll with amplitude of oscillation 0.1 rad. The number of elements in x-, y- and z-direction is respectively 30, 3 and 45. It is seen from Figure 7.9 that free-slip condition on the walls gives a slightly higher free-surface elevation for the periods around resonance than the no-slip condition. Away from resonance, the free-surface elevation is the same for the two cases.

If the same case is run with a two-dimensional tank, i.e., the front and back walls are taken to be symmetry planes, no-slip versus free-slip boundary conditions on the tank bottom and walls have little influence on the solution.

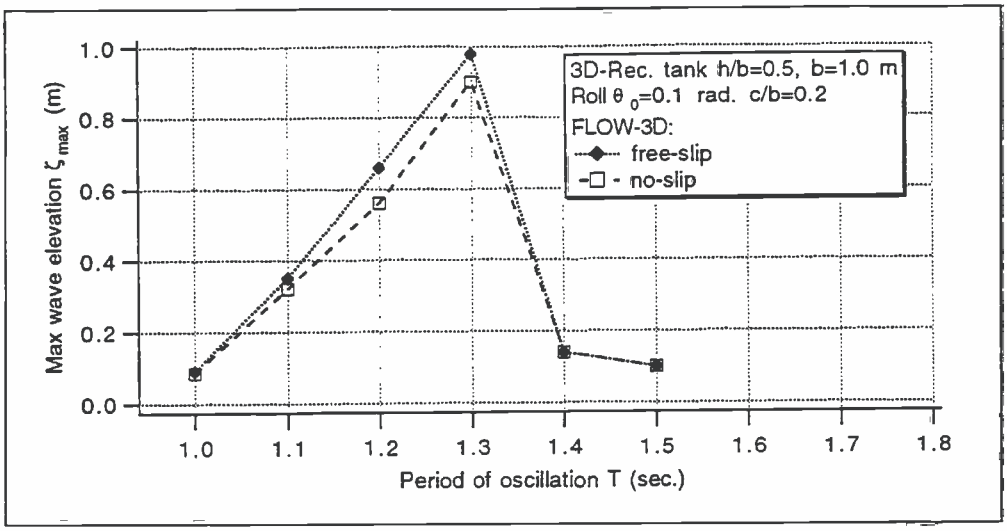

Figure 7.9 Free surface elevation in 3D-rectangular tank. Comparison between free-slip and no-slip boundary condition on the tank walls.

7.3 Numerical results

In this chapter some results from calculations with the FLOW-3D code are compared with published results from model tests or analytical solutions.

7.3.1 Translational motion of rectangular tank

For translational oscillations of a rectangular tank, the free surface elevation for different periods of oscillations are calculated for water depth/tank breadth ratios 0.5 and 0.35.

Tank with depth/breadth ratio 0.5

For harmonical oscillations of a rectangular tank in sway motion for a tank with breadth equal to 1.0 meter and water depth 0.5 meter, the results from FLOW-3D are compared with the results from the nonlinear numerical/analytical method in chapter 6. The first natural period from linear theory is 1.18 sec. for these tank dimensions.

To compare the results from FLOW-3D with the results from the nonlinear numerical/analytical method, the code is run for a two-dimensional tank. This is done by choosing the minimum y-side (front) and maximum y-side (back) of the mesh to be symmetry planes. The boundary conditions on the tank bottom and walls are taken to be free-slip.

In FLOW-3D the number of elements in the mesh are taken to be 20 in x-direction, which gives an element size Δx=0.05 m. In z-direction the element size is Δz=0.05 m and the tank height is chosen to be so large that the water is not hitting the tank top. The reason for this is that there is no "tank top" in the analytical/numerical solution to limit the wave elevation. To avoid too large volume errors before the solution reaches the steady state, the convergence criterion parameter EPSADJ is chosen equal to 0.01. ALPHA is equal to 1.0 in the computations.

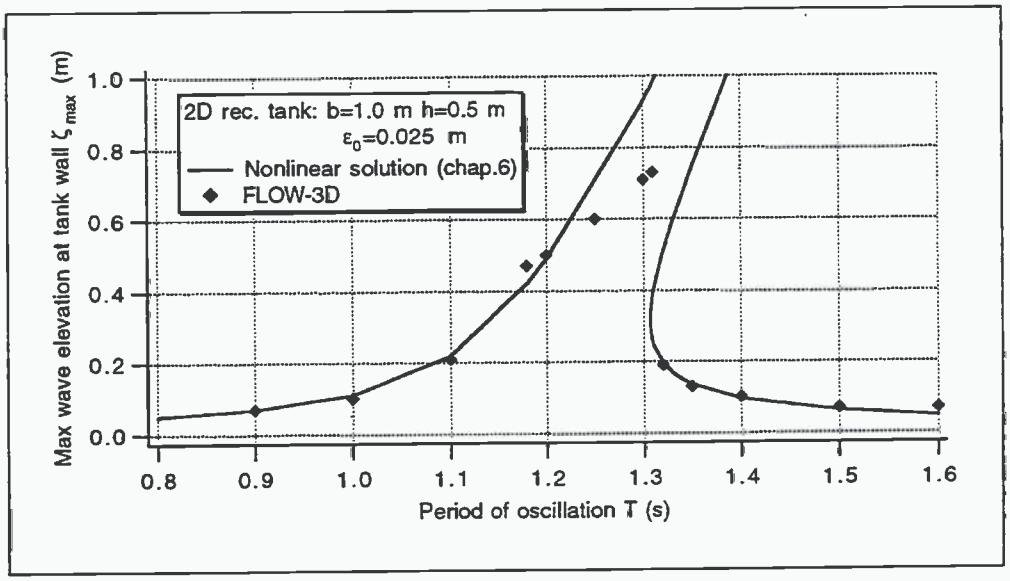

Figure 7.10 Maximum wave elevation at tank wall as function of period of oscillation. Nonlinear solution has N_{FREE}=240. FLOW-3D has element size 0.05 m.

It is seen from Figure 7.10 that it is good agreement between the numerical and the analytical results, except for some periods around resonance. One reason for the difference in the results may be the difference in damping in the two solutions. The analytical/numerical method is based on potential theory where there is no damping. In FLOW-3D there will be a small damping due to the viscosity of the water together with the numerical damping. Another reason may be that the response is so large that the nonlinear solution in chapter 6 does not account for all nonlinearities.

Tank with depth/breadth ratio 0.35

In Olsen and Johnsen (1975) results from model tests for a tank with depth/breadth ratio 0.35 are presented. The model and its dimensions are shown in the Figure 7.11. The description of the model is taken from Faltinsen (1974). The breadth of the tank and the distance from the top to the bottom of the tank are both 1.0 m. The length of the tank in the direction perpendicular to the paper plane is 0.1 m. The wave amplitude recorder A1, is placed 50 mm

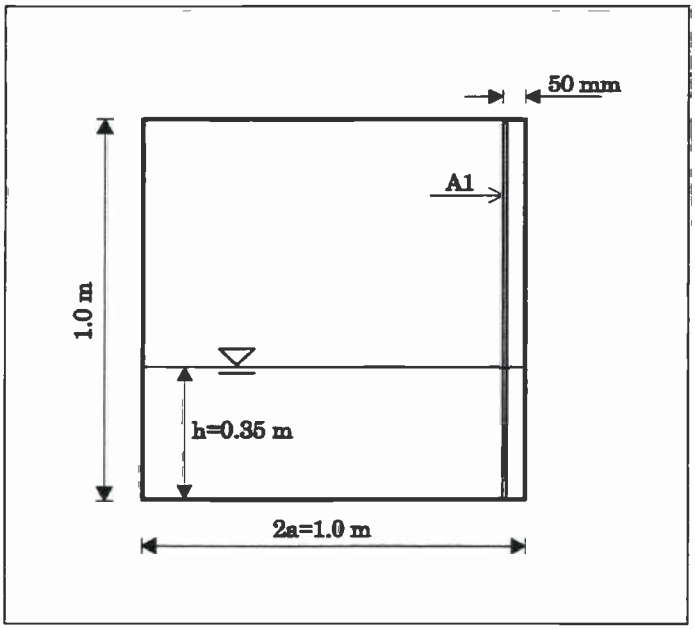

Figure 7.11 Rectangular tank model.

from the tank wall. All dimensions given above are inside dimensions. The first natural period based on linear theory is equal to 1.27 sec.

In figure 27 in Olsen and Johnsen (1975) the maximum free surface elevation is given for a forced sway amplitude equal to 0.05 meter, and in figure 30, the total force in x-direction is presented.

In the FLOW-3D approximation of the problem a two-dimensional tank with height 1.0 m and breadth 1.0 m is used, with element size $\Delta x = \Delta z = 0.025$ m. That is 40 x 40 elements in x and z direction respectively. The front and back side of the mesh are taken to be symmetry planes. The ALPHA value is equal to 0.5, and EPSADJ is 1.0.

In Figure 7.12 the maximum wave elevation at x = 0.45 m and the total force in x-direction are compared with results from model tests and analytical solutions.

It is seen from Figure 7.12 that the water will hit the tank top both in the model tests and in the numerical simulations. For some of the periods, 1.45, 1.47 and 1.7 sec. the difference between the maximum wave amplitude obtained from the model tests and from FLOW-3D is large. However this is in period ranges where small differences in the period cause large differences in the wave elevation.

Results based on the linear theory in chapter 4.1.2 and the nonlinear theory in chapter 5.2.2 are also presented. They show less good agreement with the experiments than FLOW-3D. However, for this water depth/breadth ratio the nonlinear theory predicts very large values of the response around the linear resonance frequency. Actually it predicts infinite values at resonance when h/b=0.34. It indicates that the assumed perturbation procedure in the nonlinear theory should have been different for this particular h/b-ratio.

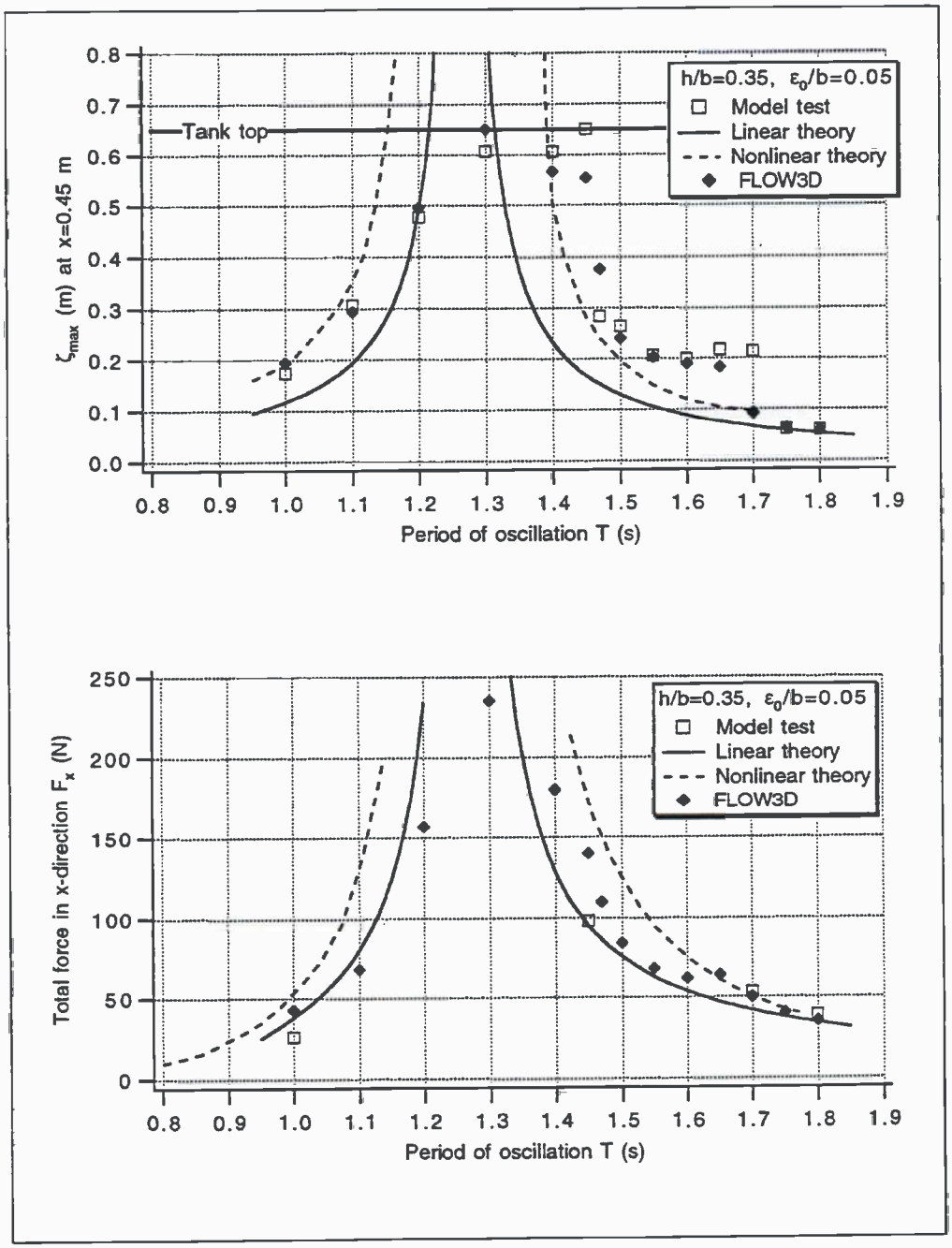

Figure 7.12 **Maximum wave elevation and total horizontal force for rectangular tank with breadth 1.0 m, height 1.0 m. Model tests from Olsen and Johnsen (1975).**

7.3.2 Translational motion of LNG tank model

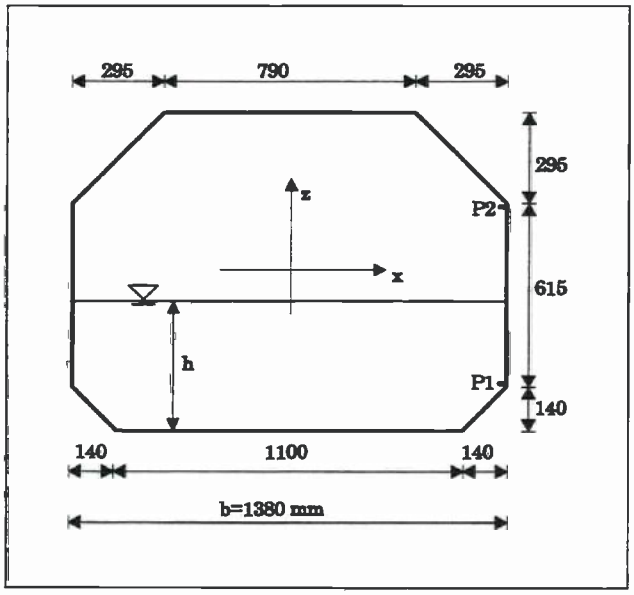

Figure 7.13 LNG tank model

In figure 32 in Olsen and Johnsen (1975), the amplitude of the total force in x-direction as function of the period of forced sway oscillation is given for sloshing in a model of a LNG tank. The water depth is 0.552 m, that is h / b = 0.4 and the amplitude of the forced sway oscillation, ε_0, is 0.0138 m, or ε_0 / b = 0.01. The model and its dimensions are described in Faltinsen et. al. (1974), and is here shown in Figure 7.13.

In the FLOW-3D approximation a two-dimensional tank with 50 x 37 elements is used. The element size is then Δx=0.02760 m and Δz=0.02757 m. The corners of the tank are modelled with correct shape as regions in the mesh which are blocked and contain no fluid. This is shown in Figure 7.14, where the velocity vector field for a period of oscillation equal to 1.4 sec. is shown. To prevent a large volume error in FLOW-3D when the wave motion is large and the waves are breaking or hitting the tank top, the EPSADJ (adjustment of the pressure iteration convergence criterion) is chosen to be 0.01 to give a finer convergence of the pressure iterations. The weighting of upstream differencing, ALPHA is equal to 1.0 in the computations.

In Figure 7.15 results from numerical calculations are compared with model tests. It is seen from the figure, that the numerical approximation generally gives higher values of the force in x-direction than the model tests. The first natural period for a tank with breadth equal to 1.38 meter and h/b=0.4 is 1.442 sec. based on linear theory for a rectangular tank. From the analytical/numerical method in chapter 6, the period is obtained as 1.443 sec. It is seen from the figure that the maximum forces are obtained around these periods, but the agreement between the numerical obtained forces and the experiments is not satisfactory around resonance.

The values of the forces from FLOW-3D are steady-state values. The necessary time of computation to reach steady-state varies with period of oscillation. It is seen from Figure 7.16 and Figure 7.17 that for example for T = 1.4 sec. the steady-state solution is approximately obtained after about 50 sec. and for 1.7 sec. it takes more than 150 sec. to reach steady-state.

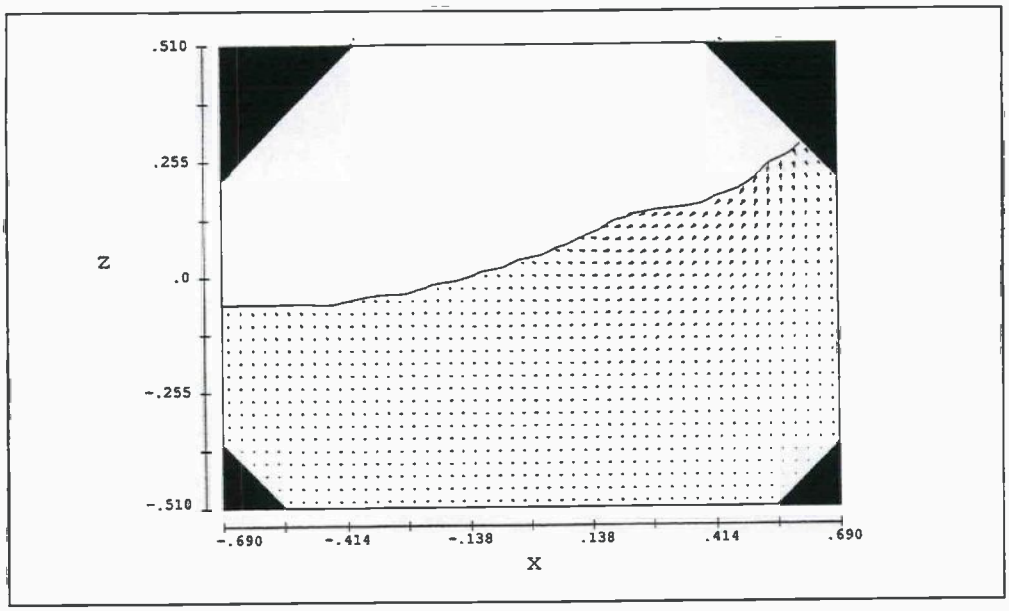

Figure 7.14 FLOW-3D approximation of the LNG tank. Velocity vector field for T=1.4 sec. ε_0/b=0.01.

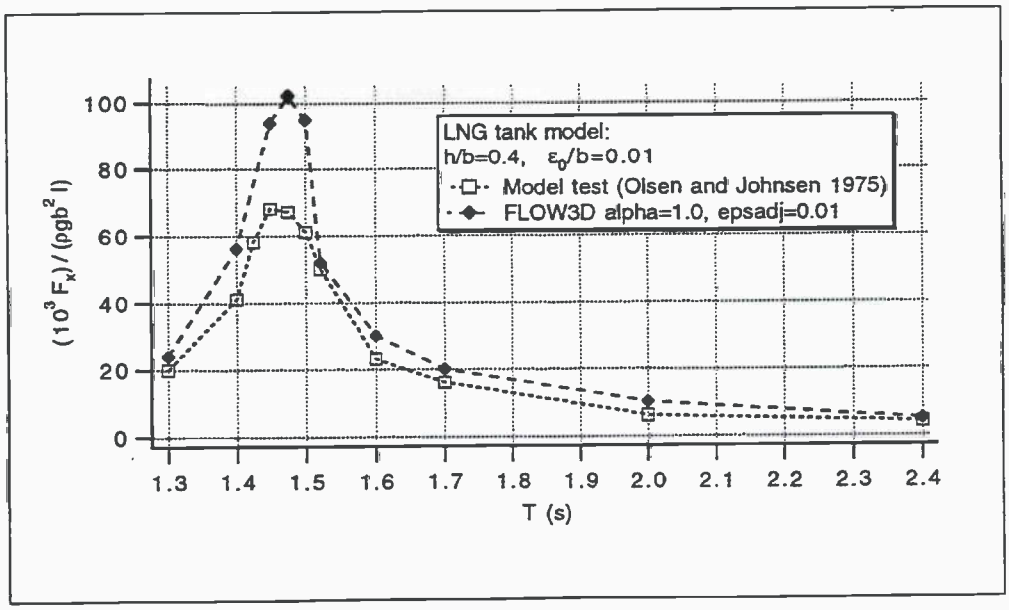

Figure 7.15 Comparison between numerical calculations and model tests for LNG tank with b=1.38 m, h/b=0.4 and ε_0 /b=0.01.

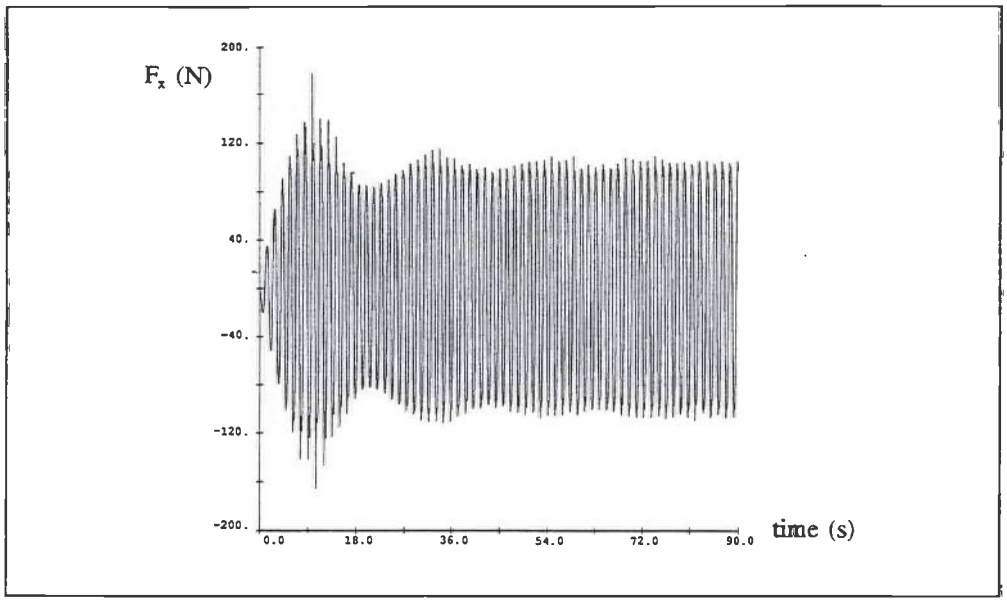

Figure 7.16 **Total force in x-direction as function of time for LNG tank with b=1.38 m, h/b=0.4, ε_0 /b=0.01 and period of oscillation 1.4 sec.**

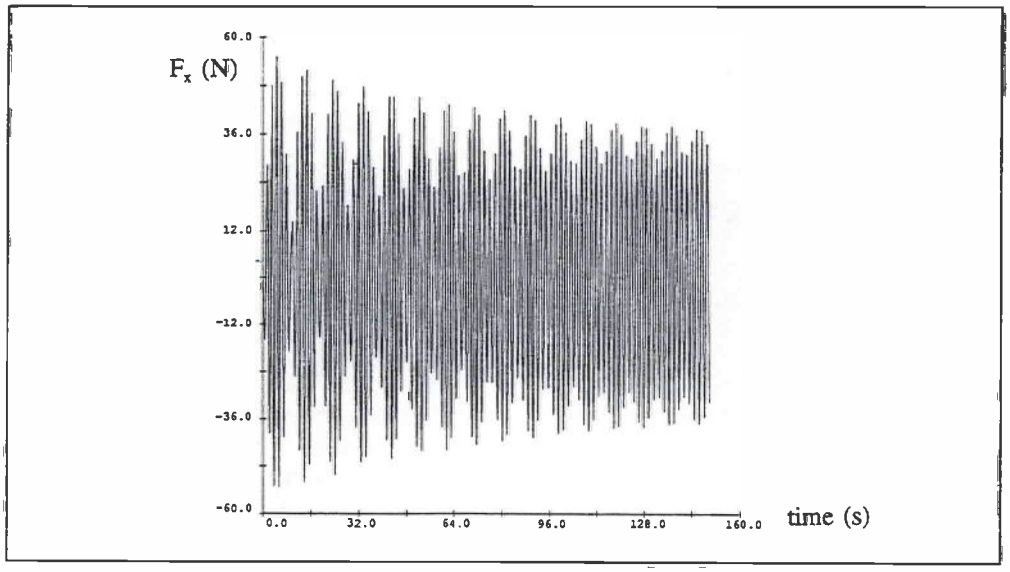

Figure 7.17 **Total force in x-direction as function of time for LNG tank with b=1.38 m, h/b=0.4, ε_0 /b=0.01 and period of oscillation 1.7 sec.**

7.3.3 Roll motion of rectangular tank

For roll oscillations of a rectangular tank, the free surface elevation for different periods of oscillations is calculated for water depth/tank breadth ratios 0.5, 0.35 and 0.2.

Tank with depth/breadth ratio 0.5

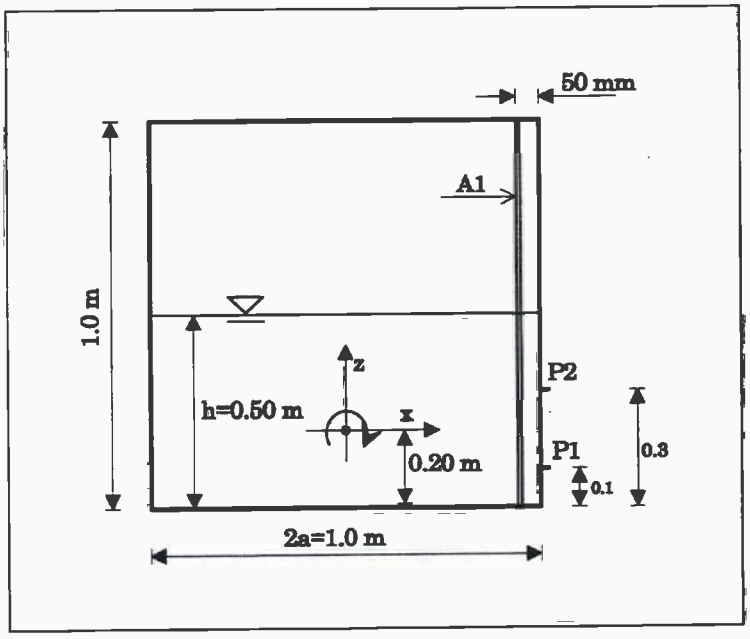

In Faltinsen (1974) the pressure and free surface elevation from nonlinear theory are given for a rectangular tank which is forced to oscillate harmonically in roll. Results from model tests as well as from nonlinear analytical theory are given for amplitudes of oscillation $\theta_0 = 0.1$ rad. and $\theta_0 = 0.2$ rad. In figure 19 in Olsen and Johnsen (1975), more results for $\theta_0 = 0.1$ rad. are given.

Figure 7.18 Tank model

The tank model and its dimensions are shown in Figure 7.18. The axis of oscillation is 0.2 m above the tank bottom and the water depth is 0.5 m.

In the FLOW-3D approximation, the element size is $\Delta x = \Delta z = 0.05$ m, and the tank height is so high that the water is not hitting the tank top. The front and back walls are taken to be symmetry planes and there are free slip conditions on the walls. The convergence criterion parameter EPSADJ is equal to 0.01 and the weighting of upstream values ALPHA is equal to 1.0.

The first natural period is obtained from linear theory to be equal to 1.18 sec.

In Figure 7.19 the free surface elevation as function of period of oscillation is shown for $\theta_0 = 0.1$ rad. and in Figure 7.20 for $\theta_0 = 0.2$ rad. The asymptotic values given in the figures are the quasistatic solutions when the tank is rotated 0.1 and 0.2 rad. respectively.

It is seen from the figures that there is reasonable good agreement between the numerical results from FLOW-3D and the results from model tests and the nonlinear theory. The best agreement is obtained for periods longer than the resonance period. It is seen that the maximum wave elevation is obtained for a longer period than the first natural period from linear theory. For $\theta_0 = 0.1$ rad. maximum wave elevation is obtained at a period equal to 1.32 sec. and for $\theta_0 = 0.2$ rad.for a period equal to 1.4 sec. The reason for this must be the nonlinearity in the sloshing problem.

In Figure 7.21, the free surface elevation at the wall as function of time for steady state condition, is shown for the case with oscillation period 1.2 sec. and $\theta_0 = 0.1$ rad. The shape and the magnitude of the elevation is similar for the numerical results from FLOW-3D and the model tests from Faltinsen (1974), where a beating effect is observed. The phase between the tank motion and the free surface elevation is also similar. However there are differences in the simulated and experimental time records (see for instance the first two periods of oscillation). On the other hand we have no control of what the initial conditions were in the experiments. We should also note the different time scales in the model test results and the numerical results shown in Figure 7.21. In the model tests the tank was oscillated for approximately 5 minutes before the measurements started. t=0 corresponds to the time instance when the measurements start. For the numerical calculations the results are shown for t=38 to 45 sec.

In the model tests, the pressure was measured at the tank wall 0.1 meter and 0.3 meter above the bottom of the tank. In Figure 7.22 the pressure in the pressure gauges P1 and P2 are shown for T=1.2 sec. and $\theta_0 = 0.1$ rad. In the model tests, the maximum dynamic pressure (given as $p/\rho gb$) was measured to be 0.14 in P1 and 0.16 in P2. The minimum dynamic pressure was -0.12 in P1 and -0.17 in P2. From FLOW-3D the total pressure was calculated to vary between 3180 and 6060 Pa in P1 and between 560 and 4080 Pa in P2. This corresponds to a nondimensional dynamic pressures between -0.1 and 0.19 in P1 and between -0.17 and 0.19 in P2. It is also seen from the figure that the shape of the pressure curves is fairly similar for the numerical and the experimental results.

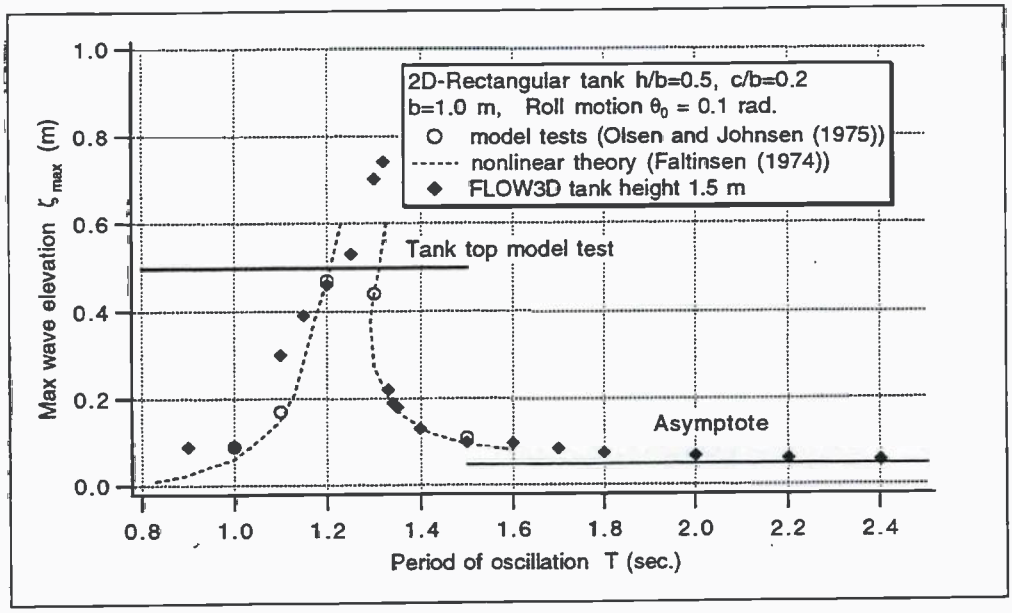

Figure 7.19 **Maximum free surface elevation at tank wall in rectangular tank with b=1.0 m, h/b=0.5, θ_0 =0.1 rad. as function of period of oscillation.**

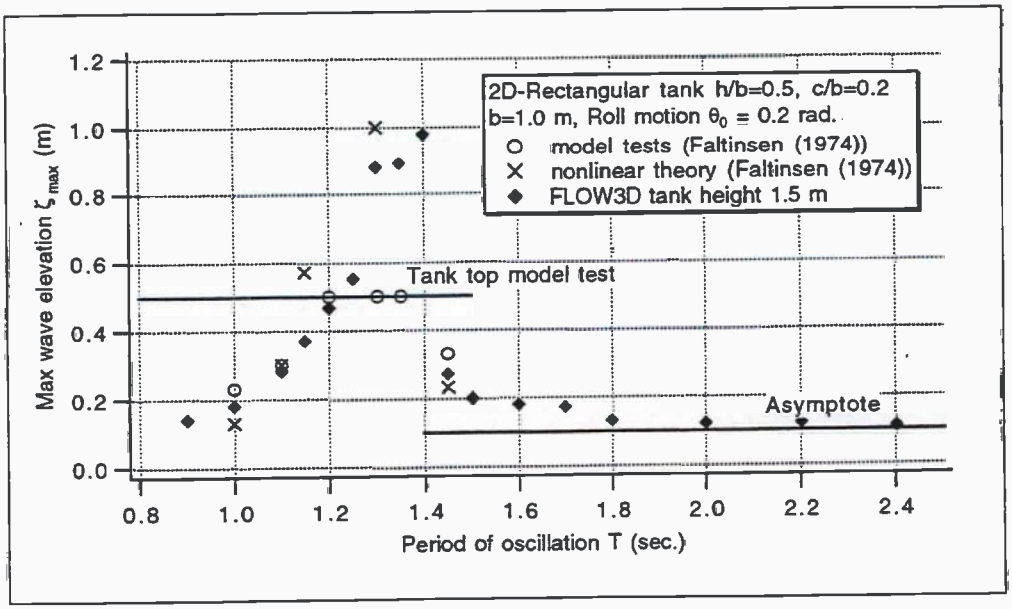

Figure 7.20 **Maximum free surface elevation at tank wall in rectangular tank with b=1.0 m, h/b=0.5, θ_0=0.2 rad as function of period of oscillation.**

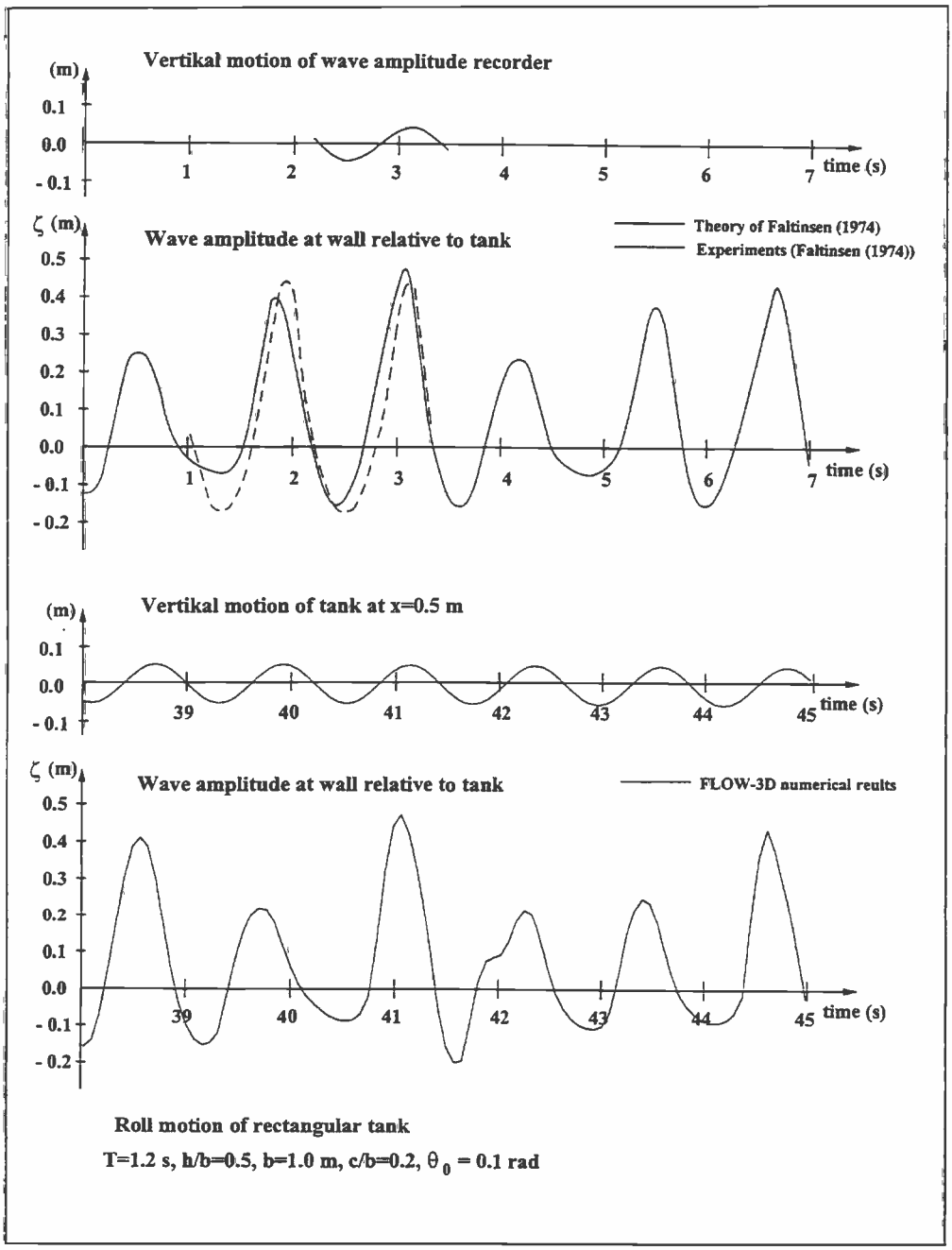

Figure 7.21 Free surface elevation as function of time. Numerical results (bottom), and model tests and theory (top). Note: the time instants are not the same.

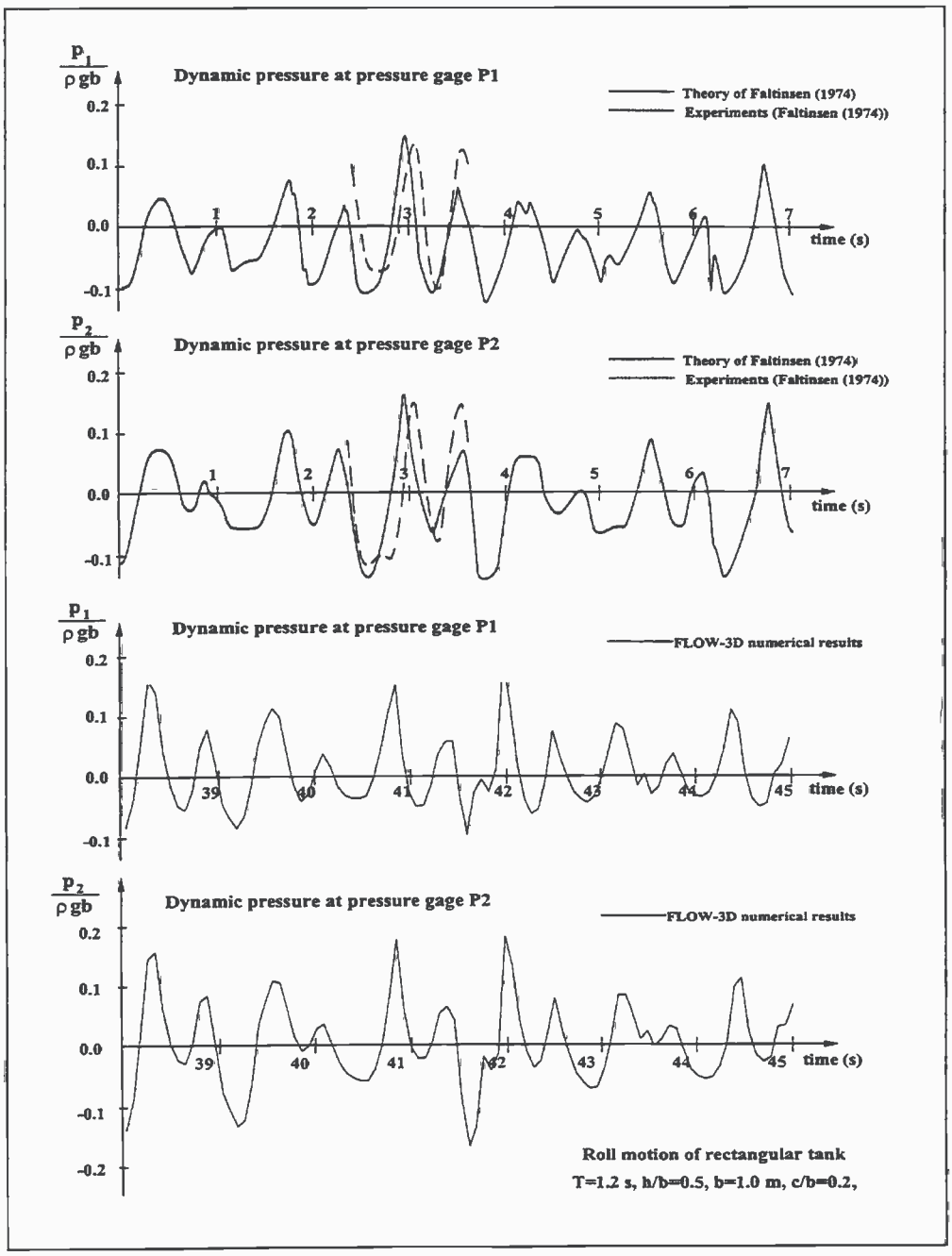

Figure 7.22 **Pressure in P1 and P2 as function of time. Numerical results (bottom), and model tests and theory (top). Note: the time instants are not the same.**

Tank with depth/breadth ratio 0.35

In Olsen and Johnsen (1975), figure 10, results from model tests with the tank in Figure 7.18 are given for a water depth/breadth ratio equal to 0.35 and an amplitude of oscillation θ_0 equal to 0.1 rad.

The first natural period for this water depth and tank breadth is calculated to be equal to 1.27 sec. from linear theory.

In Figure 7.23 the free surface elevation as function of period of oscillation from Olsen and Johnsen (1975) is compared with numerical results from FLOW-3D. In the FLOW-3D approximation the same parameters are used as for the case with water depth 0.5 m.

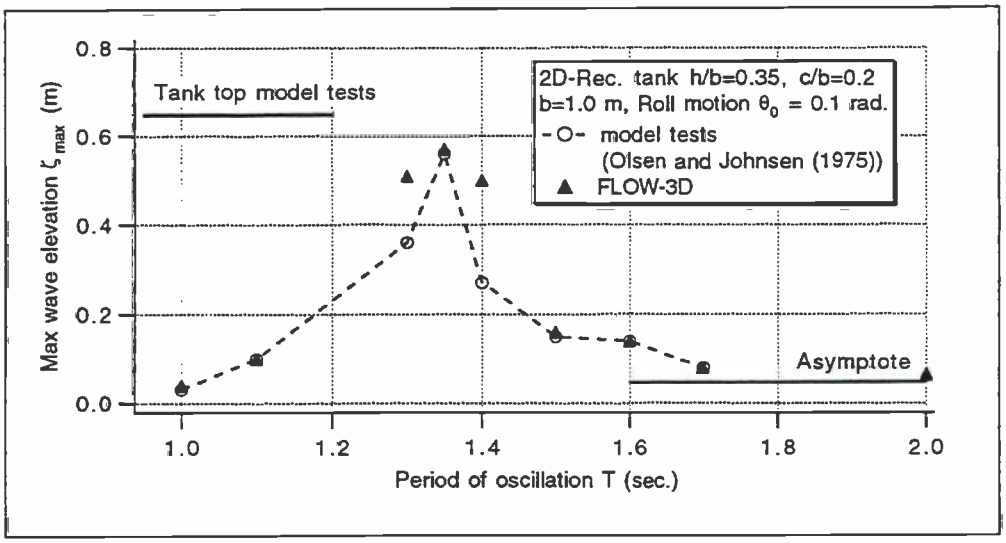

Figure 7.23 Maximum free surface elevation at tank wall in rectangular tank with b=1.0 m, h/b=0.35, θ_0=0.1 rad. as function of period of oscillation.

It is seen from Figure 7.23, that the maximum wave elevation is obtained at the same period of oscillation both in the model tests and in the numerical calculations. It is obtained at a period equal to 1.35 sec. which is longer than the first natural period obtained from linear theory. In the vicinity of the maximum response, FLOW-3D predicts larger values for the free surface elevation than the model test. There is very good agreement between the numerical results and the results from the model tests away from resonance.

Tank with depth/breadth ratio 0.2

In Olsen and Johnsen (1975), figure 10, results from model tests with the tank in Figure 7.18 are given for a depth/breadth relation equal to 0.2 and an amplitude of oscillation θ_0 equal to 0.1 rad.

From linear theory the first natural period for this water depth and tank breadth is equal to 1.52 sec.

In Figure 7.24 the free surface elevation as function of period of oscillation from Olsen and Johnsen (1975) is compared with numerical results from FLOW-3D. In the FLOW-3D approximation a two-dimensional tank with element size $\Delta x = \Delta z = 0.025$ m is used. EPSADJ is taken to be equal to 0.01 and ALPHA equal to 1.0.

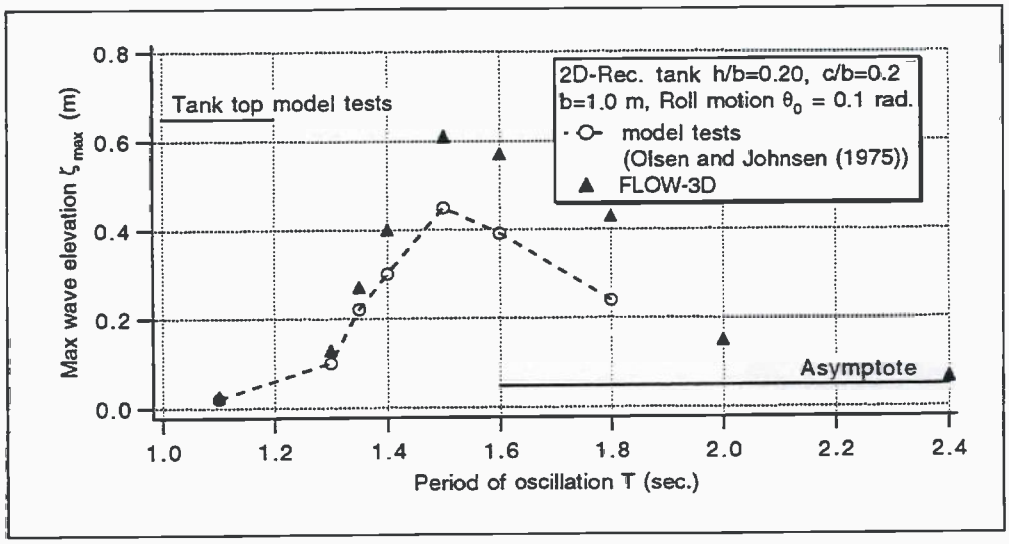

Figure 7.24 Maximum free surface elevation at tank wall in rectangular tank with b=1.0 m, h/b=0.2, θ_0=0.1 rad. as function of period of oscillation.

It is seen from the figure that the agreement is not satisfactory. In a broad period range around resonance, the wave elevations obtained from FLOW-3D is clearly higher than the wave elevations measured in the model tests. Far away from resonance the numerical results are approaching the asymptotic solution, that is the quasistatic solution when the tank is rotated 0.1 rad. For periods much smaller than the resonance period, there is good agreement between the numerical and experimental results. The maximum free surface elevation is obtained in vicinity of the first natural period calculated from linear theory.

7.3.4 Shallow water depth

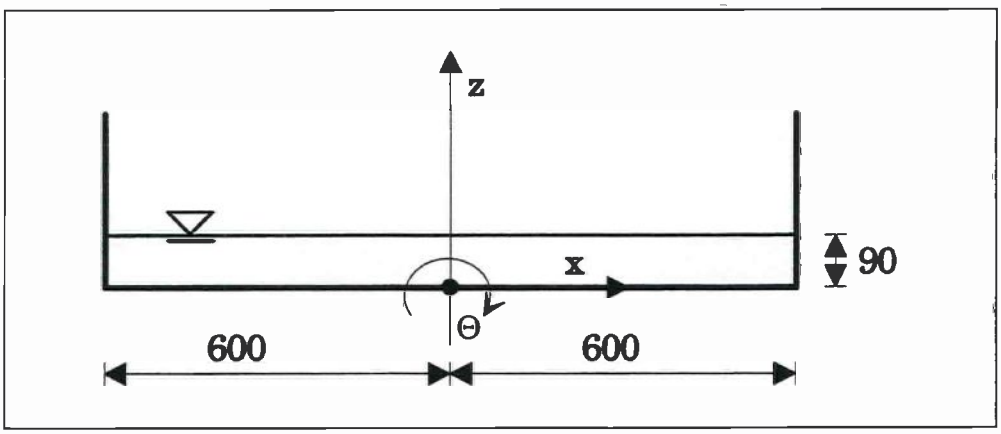

Figure 7.25 Model tank with shallow water

In Verhagen and Wijngaarden (1965) results from model tests and nonlinear theory are given for sloshing in shallow water. The tank breadth is 1.2 meter and the water depth is 0.09 meter. The roll axis is located at the tank bottom, and the amplitudes of oscillation are 1,2,3 and 4 degrees. From linear shallow water theory, the first natural frequency for this tank dimensions is 2.46 rad/sec which corresponds to a period of 2.55 sec. From nonlinear theory a hydraulic jump is assumed to be formed for oscillation frequencies less than 5.04 rad./sec. for an amplitude of the forced oscillation equal to 2 degrees and less than 6.13 rad./ sec. for an amplitude equal to 4 degrees. The tank and its dimensions are shown in Figure 7.25.

In the FLOW-3D approximation the element size is $\Delta x = \Delta z = 0.015$ meter, with 80 elements in x-direction. The tank is two-dimensional, with front and back walls as symmetry planes. The convergence criterion, EPSADJ, is taken to be 0.01, to prevent too large volume errors. ALPHA is equal to 1.0.

In Figure 7.26, the shape of the free surface and the velocity vector field are shown for some time instants for oscillations at the first natural frequency with amplitude 2 degrees. It is clearly seen from the figure how a bore is travelling back and forth between the walls of the container with a period like the oscillation period.

Figure 7.27 shows the free surface elevation in x = 0.3 meter during one period of oscillation with amplitude 4 degrees and period equal to the first natural period. The free surface elevation is measured when steady-state is obtained. The results from FLOW-3D are compared with results from model tests and theory given in Verhagen and Wijngaarden (1965). It is seen that there is good agreement between the numerical results and the results from model tests.

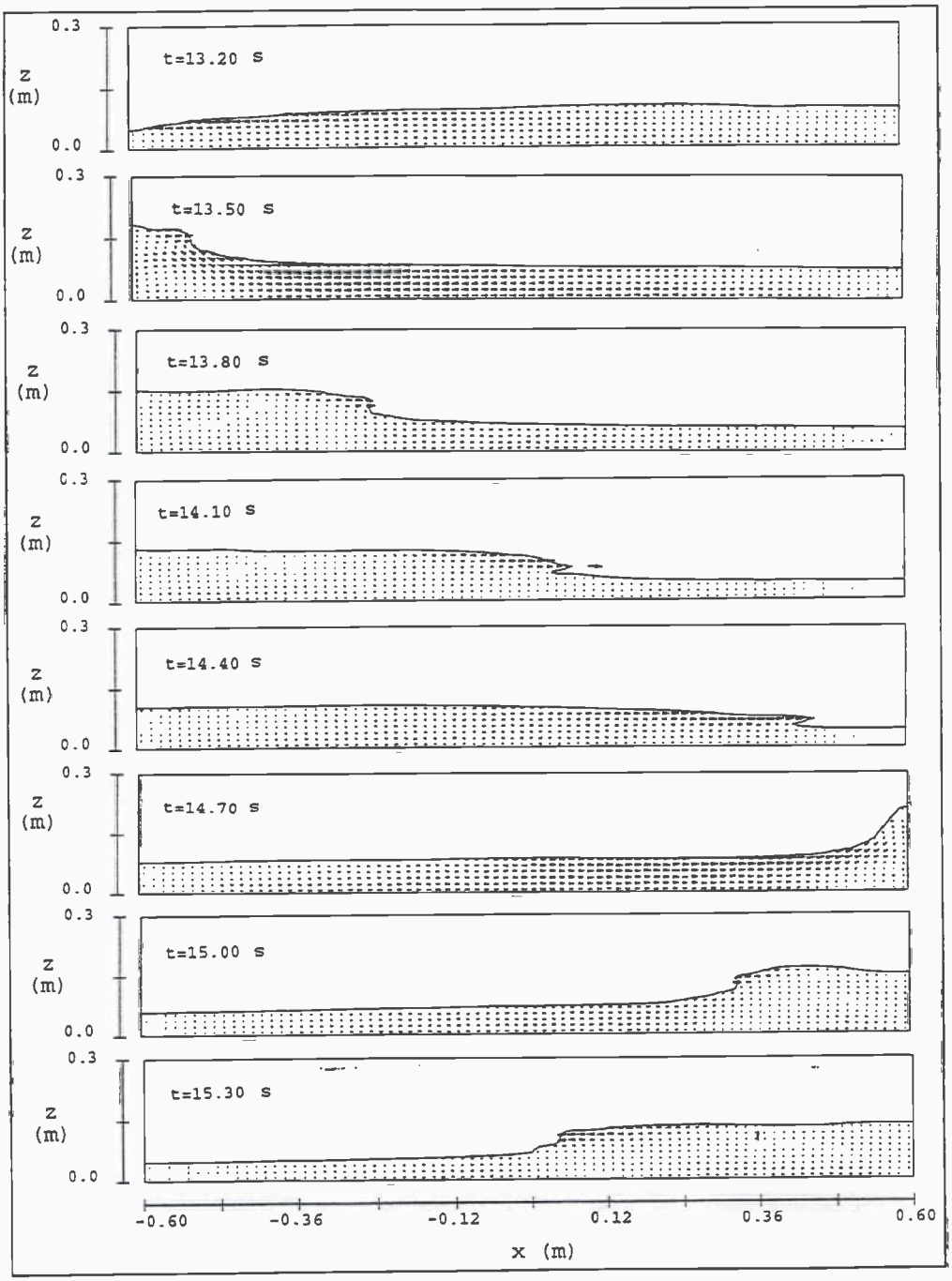

Figure 7.26 Liquid motion predicted by FLOW-3D in a rectangular tank with h/b=0.075, forced to roll with $T=T_1=2.55$ sec. and $\theta_0=2$ degrees.

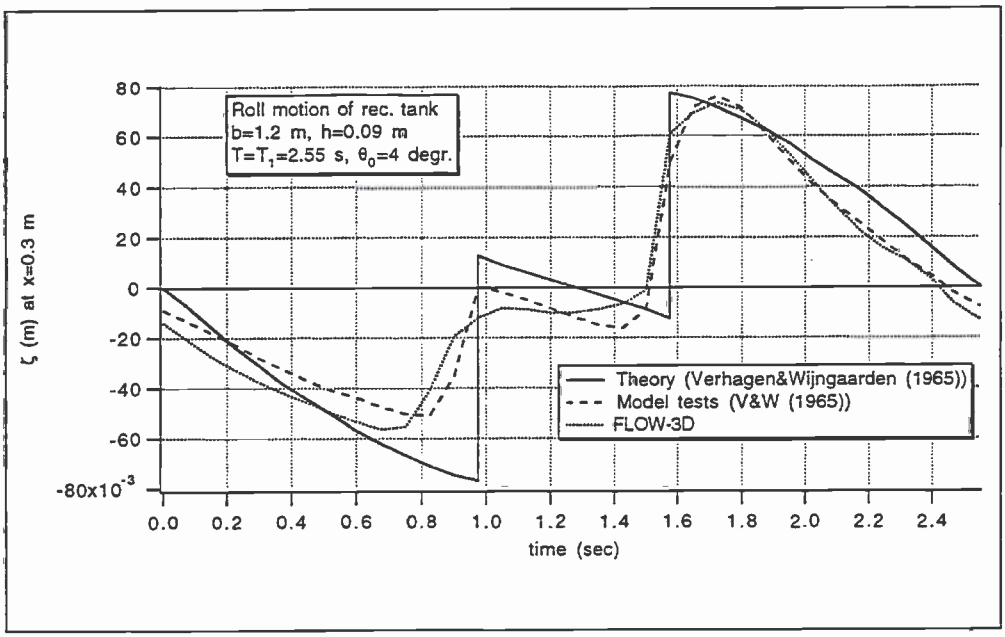

Figure 7.27 Free surface elevation during one period of oscillation (steady-state condition) in x=0.3 m from FLOW-3D and Verhagen and Wijngaarden (1965).

7.4 Discussions and conclusions

The finite difference code FLOW-3D is used to calculate sloshing in two-dimensional tanks with different water depths. The tanks are either oscillated harmonically in sway or roll motion. The results are compared with published results from model tests and theory.

The comparative study shows that it is difficult to conclude about the ability of the computer code to estimate sloshing in moving containers. Some of the results from FLOW-3D are in good agreement with analytical and experimental results and some are not.

When comparing with model test results it is important to note that according to Faltinsen (1974), it was difficult to determine from the test recordings what actually was zero response for the wave amplitude in roll motion, and that they did not know how close to sinusoidal the excitation of the tank actually was. This is also the case for the results given in Olsen and Johnsen (1975), which are the same tests as reported by Faltinsen (1974). In addition, the size of the errors in the model test results are not given. It should be noted that the analytical solutions idealize the problem and contain no effect of viscosity, damping or breaking waves. The numerical method incorporates these effects. However, due to the violent fluid motion that occurs around resonance in a tank, it may be that the numerical method does not represent a sufficient detailed reproduction of the flow.

For sway oscillations of the rectangular tank, the results seems to be satisfactory, but for the LNG tank with chambered corners, the numerically obtained forces are up to 50 percent higher than the ones from the model test for periods around resonance.

For roll motion of the rectangular tank, there is reasonably good agreement for the depth/breadth ratios 0.5 and 0.35, however not for 0.2, where the numerically obtained free surface elevation is up to 60 percent larger than in the model tests. For the shallow water case, there is good agreement between the numerical results and the results in Verhagen and Wijngaarden (1965), so one cannot conclude that the disagreement for h/b=0.2 is due to the small water depth.

In the case of the rolling tank in chapter 7.3.3, the compared pressures gave good agreement.

The FLOW-3D code contains numerous options for physical and numerical parameters. The physical parameters are set to describe the actual problem, and which values to choose are fairly clear. Concerning the numerical parameters however, it is not so clear. To some extent the solution will depend on the value of the numerical parameters. For example, for sway oscillations with period 1.0 sec. and amplitude 0.05 meter of a rectangular tank with h/b=0.35, it is shown in Figure 7.6 that for an element size of 0.05 meter, ALPHA equal to 0.5 gives a free surface elevation 2.5 times the value obtained if ALPHA is equal to 1.0. The total horizontal force obtained for ALPHA equal to 0.5 is 1.8 times the value obtained for ALPHA equal to 1.0. For the same element size, approximately the same relations are obtained for the periods of oscillation of 1.8 and 1.2 sec. in Figure 7.7 and Figure 7.8. If the element size is halved to 0.025 meter, the free surface elevation for T=1.0 sec. and ALPHA = 1.0 is halved and the force reduced by approximately 40 percent.

It is important that a steady-state solution is obtained before the values of free surface elevation, forces etc. are read from the time history plots. For some periods of oscillation the necessary number of oscillations to reach steady-state was large and in some cases the volume error became too large before steady-state was reached. To solve the large volume error problem, a value smaller than 1.0 of EPSADJ, which controls the pressure convergence criteria, may be chosen. With an appropriate small value of EPSADJ, the computation may be run to steady-state with minor volume errors.

8 CONCLUSIONS AND RECOMMENDATIONS FOR FURTHER WORK

A literature survey shows that extensive analytical, numerical and experimental studies of the sloshing problem have been carried out for the last 40 years. Generally, the problem of liquid sloshing is a nonlinear phenomenon and it is difficult to handle either analytically or numerically. It is important to be aware of the limitations of the chosen calculation method.

Analytical solutions are mostly based on potential theory and they are limited to a small class of tank shapes where it is possible to find the analytical solutions of the governing equations.

Linear solutions are valid for small oscillations far away from the resonance frequencies. At oscillation frequencies equal to the resonance frequencies, the linear theory predicts an infinite response amplitude of the fluid. The resonance frequencies are defined as the ones predicted from linear theory.

Nonlinear solutions can be constructed based on the perturbation method by Moiseev (1958). They hold for small oscillations of the tank with frequency of oscillation in the vicinity of the first natural frequency. The water depth and tank breadth are of the same order of magnitude. To fulfil the conservation of mass condition, it is shown that it is necessary that the tank has vertical walls in the free surface. A two-dimensional rectangular tank and a vertical circular cylindrical tank are studied analytically. In the two-dimensional tank only planar sloshing may occur due to the harmonic oscillations of the tank. But for the circular cylindrical tank, in addition, rotational sloshing may be activated. Regions for stable and unstable sloshing motions in a tank with given dimensions are established. It is important to be aware of these three-dimensional effects when dealing with three-dimensional numerical tools or model tests. Misprints in earlier published results for a rectangular tank and a vertical circular cylindrical tank are pointed out.

A nonlinear theoretical solution based on Moiseev's idea is not restricted to rectangular or circular cylindrical tanks. However for a more general tank shape we have to rely on a combined analytical and numerical method. This is shown in details for a two-dimensional tank and forced harmonic sway oscillation. The method is limited to tanks with vertical walls in the free surface.

In the nonlinear combined analytical and numerical method a boundary element method is used to determine the eigenfunctions and eigenvalues of the problem. These are used in the nonlinear analytical free surface conditions following from Moiseev's idea. The velocity potential and free surface elevation for each boundary value problem in the perturbation scheme are determined by the boundary element method.

A low order panel method is used and it is shown by convergence studies that quite many elements are needed for sufficient agreement with the analytical solution for a rectangular tank. As an example, 120 elements on the free surface is needed to get satisfactory

prediction of the free surface elevation.

Advantages of using this combined analytical and numerical method are that one is able to examine sloshing in many class of tanks and being able to have good control of numerical errors. But, the method cannot predict impact pressure, overturning waves, and viscous losses due to for instance baffles. Neither can it predict hydraulic jumps that occur in shallow water. The method is based on forced harmonic motion of the tank, and it is not obvious how to generalize it to irregular forced motion of the tank. For the frequencies where there are three solutions of the nonlinear problem, one may choose to pick out one of the response amplitudes for each frequency and use this in an analysis of irregular motion. But if the spectrum for the tank motion contains much energy in this area, the solution will be sensitive to the choice of response amplitude.

Both finite difference, boundary element and finite element methods have been used in different publications to study the sloshing problem. It would be impossible to test all the direct numerical methods reported in the literature survey. We have studied the commercial code FLOW-3D, which solves the Navier-Stokes equations by use of a finite difference code. The numerical methods used in the code have been tested out by others, so the intention has therefore not been to verify the numerical code, but to study the suitability of the program to estimate sloshing. The effect of changing numerical parameters is studied, but most of the work is concentrated on calculating the fluid motions inside tanks for cases where the analytical solution is known or there exist model tests results to compare with. The comparisons gave variable results. For some of the cases there was good agreement between the numerical results and model tests, for other cases not. To some extent, the numerical results were dependent on the choice of numerical parameters like the element size, the convergence criterium in the pressure iteration routine and the method for numerical differencing used in the momentum equation. These are topics which are hardly discussed in the papers presenting the numerical methods reported in the literature survey.

Concerning the results from the parameter study with FLOW-3D, new convergence studies should be carried out to study the effect of the element size. A finer pressure iteration convergence criterion should then be used to prevent large errors in the fluid volume.

FLOW-3D may be used for calculations of sloshing in general shaped tanks, and the combined analytical and numerical method for tank shapes where the walls are vertical in the free surface. Based on the combined analytical and numerical method, the liquid response inside two-dimensional tanks with rectangular and cylindrical cross sections is shown in Figure 6.11. The figure shows relatively small influence of the tank shape. The sensitivity of the FLOW-3D results to the tank shape should also be studied. In FLOW-3D the tank top and ceiling have to be modelled, and will influence on the solution for the cases where the fluid is hitting the tank top. The accuracy of the solution for such cases should be studied.

The accuracy of the calculation of pressure and forces on the tank are important for tank design. Pressure and forces are not studied with the nonlinear analytical and numerical method. But, the pressure may be determined in each of the elements, and the force by

integrating the pressure. Pressure in the cells of the computational mesh and forces and moments on the tank may be determined in the FLOW-3D program. In the case of the rectangular tank where pressure was studied, there was good agreement between the computational results and model tests. However, further studies should be performed before we can give a final conclusion about the programs ability to determine the pressure in the tank. The forces are obtained by integrating the pressure. Good results are obtained for a rectangular tank, but for a LNG tank with inclined corners (Figure 7.13), the results were poor.

Velocities and accelerations of the water in the tanks are important for fish rearing tanks and containers for transportation of living fish. From the FLOW-3D program we may get plots of the velocity vector field at specified time instants. These plots give a visualisation of the situation inside the tank. In addition time series of velocities and accelerations in the mesh cells may be obtained. The validity of these results are not studied in this work.

Only two-dimensional flow is studied numerically in this work. But, if the FLOW-3D program or a three-dimensional version of the combined analytical and numerical method are to be used to study three-dimensional sloshing, it is important to be aware of the possibility of rotational sloshing and instable solutions, as detected in the nonlinear analytical solution for the circular cylindrical tank. The occurrence of instabilities and rotational sloshing may be used to verify if the FLOW-3D program gives good estimation of three-dimensional effects in the sloshing problem. For the combined analytical and numerical method a stability analysis like the one shown in chapter 5.3 has to be included as part of the program.

References

Abramson, H.N.: " The Dynamic Behaviour of Liquids in Moving Containers, With Applications to Space Vehicle Technology", NASA SP-106, 1966.

Abramson, H.N., Chu, W.H. and Kana, D.D.:"Some Studies of Nonlinear Lateral Sloshing in Rigid Containers", Journal of Applied Mechanics, Transactions of the ASME, December 1966, pp.777-784.

Anderson, D.A., Tannehill, J.C. and Pletcher, R.H.:"Computational fluid mechanics and heat transfer", McGraw-Hill Book Company, 1984.

Arai, M.:"Experimental and Numerical Studies of Sloshing Pressure in Liquid Cargo Tanks" Journal of The Society of Naval Architects of Japan, Vol. 155, 1984, pp.114-121.

Arai, M.:"Experimental and Numerical Studies of Sloshing in Liquid Cargo tanks with Internal structures", IHI Eng. Rev. Vol. 19 No. 2 April 1986.

Arai, M., Cheng, L.Y. and Inoue, Y.:"3D Numerical Simulation of Impact Load due to Liquid cargo Sloshing", Journal of The Society of Naval Architects of Japan, Vol. 171, 1992, pp. 177-184.

Arai, M., Cheng, L.Y., Inoue, I., Sasaki, H. and Yamagishi, N.: "Numerical Analysis of Liquid Sloshing in Tanks of FPSO", Proceedings 2nd ISOPE, San Francisco, 1992, pp. 383-390.

Barron, R. and Roy Chng, S.W.: "Dynamic Analysis and Measurements of Sloshing of Fluid in Containers", Transactions of the ASME, Journal of Dynamic Systems, Measurements and Control, Vol. 111, March 1989, pp.83-90.

Bass, P.L., Bowles, E.B and Cox, P.A.:"Liquid Dynamic Loads in LNG Cargo Tanks", Transactions of SNAME, Vol. 88, 1980, pp. 103-126.

Bass, P.L., Bowles, E.B., Trudell, R.W., Navickas, J., Peck, J.C., Yoshimura, N., Endo, S. and Pots, B.F.M.:"Modelling Criteria for Scaled LNG Sloshing Experiments", Journal of Fluids Engineering, Vol. 107, June 1985, pp.272-280.

Bosch, J.J.van den and Vugts, J.H.: "Roll damping by free surface tanks", Report 83 S of the Netherlands Ship Research Centre TNO, April 1966.

Case, K.M. and Parkinson, W.C.:"Damping of surface waves in an incompressible liquid", Journal of Fluid Mechanics 1957, pp 172-184.

Chakrabarti, S.K.: "Internal Waves in a Large Offshore Storage Tank", Journal of Energy Resources Technology, Vol. 115, June 1993, pp.133-141.

Demirbilek, Z.:"Energy Dissipation in Sloshing Waves in a Rolling Rectangular Tank -I. Mathematical Theory", Ocean Engng. Volume 10, No. 5, 1983, pp 347-358.

Demirbilek, Z.:"Energy Dissipation in Sloshing Waves in a Rolling Rectangular Tank -II. Solution method and Analysis of Numerical Technique", Ocean Engng. Volume 10, No. 5, 1983, pp 359-374.

Demirbilek, Z.:"Energy Dissipation in Sloshing Waves in a Rolling Rectangular Tank -III. Results and Applications", Ocean Engng. Volume 10, No. 5, 1983, pp 375-382.

Dick, E.:"Introduction to finite element techniques in computational fluid dynamics", Lecture notes, Introduction to computational fluid dynamics, von Karman Institute for Fluid Dynamics, 18-22 January 1993.

Faltinsen, O. M.:"A Nonlinear Theory of Sloshing in Rectangular Tanks", Journal of Ship Research, Volume 18, Number 4, December 1974, pp. 224-241.

Faltinsen, O. M.:"A Numerical Nonlinear Method of Sloshing in Tanks with Two-Dimensional Flow", Journal of Ship Research, Volume 22, Number 3, September 1978, pp. 193-202.

Faltinsen, O.M., Olsen, H.A., Abramson, H.N. and Bass, R.L.:"Liquid slosh in LNG carriers", Det norske Veritas, Publication No. 85, Sept. 1974.

Hamlin, N.A., Lou, Y.K., Maclean, W.M., Seibold, F. and Chandras, L.M.: "Liquid Sloshing in Slack Ship Tanks - Theory, Observations and Experiments", Tr. SNAME, New York, N.Y., 19-22 November, 1986.

Hara, F. and Shibata, H.:"Experimental Study on Active Suppression by Gas Bubble Injection for Earthquake Induced Sloshing in Tanks", International Journal of JSME, Vol.30, No.260, 1987, pp. 318-323.

Harlow, F. H. and Welch, J.., "Numerical Calculation of Time-Dependent Viscous Incompressible Flow of Fluid with Free Surface", The Physics of Fluids, Volume 8, Number 12, December 1965, pp. 2182 - 2189.

Harlow, Francis H. and Welch, J.Eddie, "Numerical Study of Large-Amplitude Free Surface Motions", The Physics of Fluids, Volume 9, Number 5, May 1966, pp. 842 - 851.

Hirt,C.W., Nichols,B.D. and Romero,N.C.: "SOLA - A Numerical Solution Algorithm for Transient Fluid Flows", Los Alamos Scientific Laboratory Report LA-5852, 1975.

Hirt,C.W. and Nichols,B.D.:"Volume of Fluid (VOF) Method for the Dynamics of Free Boundaries", Journal of Computational Physics, Volume 39, 1981, pp.201 - 225.

Hirt,C.W. and Sicilian J.M.:"A porosity Technique for the Definition of Obstacles in Rectangular Cell Meshes" Proc. Fourth Intern. Conf. Ship. Hydro., National Academy of Science, Washington, DC, Sept. 1985.

Hirt,C.W.:"SOLA: A Basic Solution Algorithm for Flow Analysis", "Applications of SOLA to Confined Flows" and "Applications of SOLA to Free Surface Flows", von Karman Institute for Fluid Dynamics, Lecture Series 1986-07, Introduction to Numerical Solution of Industrial Flows, 12-16 May, 1986.

Hirt,C.W.:"Volume-Fraction Techniques: Powerful Tools for Wind Engineering", Journal of Wind Engineering and Industrial Aerodynamics, vol. 46-47, 1993, pp. 327-339.

Huerta, A. and Liu, W. K.:"Viscous flow with large free surface motion" Computer Methods in Applied Mechanics and Engineering, 69, 1988, pp. 227-324.

Hutton, R.E.: "An Investigation of Resonant, Nonlinear Nonplanar Free Surface Oscillations of a Fluid", NASA TN D-1870, 1963.

Ikegawa, M.:"Finite element analysis of fluid motion in a container", in Finite Element Methods in Flow Problems (Eds. J.T.Oden, O.C.Zienkiewicz, R.H.Gallagher and C.Taylor), UAH Press, Huntsville, 1974, pp. 737-738.

Keulegan, G.H.:"Energy dissipation in standing waves in rectangular basins", J.Fluid Mech.6, 1959, pp 33-50.

Kvålsvold, J.:"Hydroelastic modelling of wetdeck slamming on multihull vessels" Dr.ing. Thesis, Department of Marine Hydrodynamics, The Norwegian Institute of Technology, 1994.

Lamb, H.: "Hydrodynamics", 6th Edn. Dover, New Your, 1945.

Lepelletier, T.G. and Raichlen, F.: "Nonlinear Oscillations in Rectangular Tanks", Journal of Engineering Mechanics, Vol. 114, no. 1, January 1988, pp. 1-23.

Mikelis,N.E., Miller,J.K. and Taylor K.V.:"Sloshing in Partially Filled Tanks and its Effect on Ship Motions: Numerical Simulation and Experimental Verification",The Naval Architect, RINA, October 1984, pp. 267-282.

Mikelis,N.E. and Robinson,D.W.:"Sloshing in Arbitrary Shaped Tanks", Journal of The Society of Naval Architects of Japan, Vol 158, 1985, pp.246-255.

Miles, J.W; "Stability of forced oscillations of a spherical pendulum", Quart. Appl. Math, vol 20, p. 21-32, April 1962.

Moiseev, N.N.:"On the Theory of Nonlinear Vibrations of a Liquid of Finite Volume", Applied Mathematics and Mechanics (PMM), Vol. 22, No. 5, 1958.

Nakayama,T. and Washizu, K.:"Nonlinear analysis of liquid motion in a container subjected to forced pitching oscillations", International Journal for Numerical Methods in Engineering, Vol. 15, 1980, pp. 1207-1220.

Nakayama,T. and Washizu, K.:"The boundary element method applied to the analysis of two-dimensional nonlinear sloshing problems", International Journal for numerical methods in engineering, Vol.17, 1981, pp. 1631-1646.

Navickas, J., et.al.:"Sloshing of Fluids at High-Fill Levels in Closed Tanks", ASME-winter meeting, Washington, DC, 1981, pp. 191-198.

Olsen, H. and Johnsen, K.R.:"Nonlinear sloshing in rectangular tanks. A pilot study on the applicability of analytical models", Det norske Veritas Report No. 74-72-S, Vol. II., 24.July 1975.

Penney, W.G. and Price, A.T.:"Finite Periodic Stationary Gravity Waves in a Perfect Liquid", Philosophical Transactions of the Royal Society (London), Vol. A 244, 1952, pp. 254-284.

Ramaswamy, B., Kawahara, M. and Nakayama, T.:"Lagrangian finite element method for the analysis of two-dimensional sloshing problems", International Journal for Numerical Methods in Fluids, Vol.6, 1986, pp. 659-670.

Schilling,U. and Siekmann, J.:"Numerical Calculation of the Translational Forced Oscillations of a Sloshing Liquid in Axially Symmetric Tanks", Israel Journal of Technology, Vol.20, 1982, pp. 201-205.

Seminar on Liquid Sloshing, Det norske Veritas, Oslo 20-21. May 1976.

Shiojiri,H. and Hagiwara,Y.: "Development of a computational method for nonlinear sloshing by BEM" Pressure Vessels and Piping, Volume 191. ASME, New York, 1990, pp. 149 - 154.

Stephens, D.G., Leonard, H.W. and Perry, T.W. Jr.:"Investigation of the Damping of Liquids in Right-Circular Cylindrical tanks, Including the Effects of a Time-Variant Liquid Depth", NASA TN D-1367, July 1962.

Su, T.-C. and Wang, Y.: " Numerical Simulation of Three-Dimensional Large Amplitude Liquid Sloshing in Cylindrical Tanks Subjected to Arbitrary Excitations" Pressure Vessels and Piping, Volume 191. ASME, New York, 1990, pp. 127 - 148.

Sudo, S., Hashimoto, H., Kazunari, K. and Shibuya, T.: "Nonlinear Response of Liquid Surface in Lateral Sloshing", JSME International Journal, Series II, Vol. 32, No.3, 1989.

Timin, Tsai and Esmail M.N.: "A comparative study of central and upwind difference schemes using the primitive variables" International Journal for Numerical Methods in Fluids, vol. 3, 1983.

Torrey, M.D., Mjolsness, R.C. and Stein, L.R.:"NASA-VOF3D: A Three-Dimensional Computer Program for Incompressible Flows with Free Surfaces", Report LA11009-MS, UC-32, July 1987.

Tozawa, S. and Sueoka, H.: "Experimental and Numerical Studies on Sloshing in Partially Filled Tank" The Proceedings of the Fourth International Symposium on Practical Design of Ships and Mobile Units (1989) pp. 57.1 - 57.8.

Verhagen, J.H.G., and van Wijngaarden, L.: "Nonlinear oscillations of fluid in a Container", Journal of Fluid Mechanics, Vol. 22, part 4, 1965, pp. 737 - 751.

Washizu, K. and Ikegawa, M.:"Some applications of finite-element method to fluid mechanics", Theoretical and Applied Mechanics (Proc. 22nd Japan National Congr. for Applied Mechanics), University of Tokyo Press, Tokyo, 1974, pp. 143-154.

Washizu, K., Nakayama, T. and Ikegawa, M.:"Applications of the finite element method to some free surface fluid problems", Finite Element in Water Resources (Eds. W.G.Gray, G.F.Pinder and C.A.Brebbia), Pentech Press, London, 1978, pp. 4.247-4.266.

Welch, J.E., Harlow, F.H., Shannon,J.P. and Daly, B.J.: "The MAC Method, a Computing Technique for Solving Viscous, Incompressible, Transient Fluid-Flow Problems Involving Free Surfaces." Los Alamos Scientific Laboratory, Report LA-3425, 1965.

Appendix A The total velocity potential for roll motion of the two-dimensional rectangular tank

The total velocity potential is $\Phi_T=\Phi+\phi_c$ where ϕ_c is the velocity potential for the container motion given in the main text, chapter 4.1.3, and Φ is the velocity potential for the liquid moving relative to the container. The total velocity potential must satisfy the free surface condition

$$\frac{\partial^2\Phi_T}{\partial t^2}+g\frac{\partial\Phi_T}{\partial z}=0 \quad \text{at the mean free surface } z=0 \tag{A.1}$$

Assuming that the time dependence of the velocity potential is $\Phi(x,z,t)=\phi(x,z)\cos(\omega t)$, and putting the total velocity potential into the free surface boundary condition, the following equation is obtained

$$-\omega^2\Phi+g\frac{\partial\Phi}{\partial z}=\omega^3\Theta_0\cos(\omega t)\sum_{n=0}^{\infty}\frac{(-1)^n}{(2n+1)^3\pi^3}\left\{\frac{16a^2\sin\left(\frac{2n+1}{2a}\pi x\right)}{\sinh\left(\frac{2n+1}{2a}\pi h\right)}+\frac{4h^2(-1)^n\sinh\left(\frac{2n+1}{h}\pi x\right)}{\cosh\left(\frac{2n+1}{h}\pi a\right)}\right\}$$

A Fourier-series expansion of $\sinh[\pi x(2n+1)/h]$ is needed in the analysis. This is done by defining a function f(x) as

$$f(x)=\begin{cases}\sinh\left[\frac{2n+1}{h}\pi x\right] & \text{for } -a\le x\le a\\ \sinh\left[\frac{2n+1}{h}\pi(2a-x)\right] & \text{for } a\le x\le 2a\\ \sinh\left[\frac{2n+1}{h}\pi(-2a-x)\right] & \text{for } -2a\le x\le -a\end{cases} \tag{A.3}$$

We can then write

$$f(x)=\sum_{k=1}^{\infty}K_k\sin\left(\frac{k\pi}{2a}x\right) \tag{A.4}$$

To find K_k the following integrals are needed

$$\int_{-2a}^{2a}f(x)\sin\left(\frac{m\pi}{2a}x\right)dx=\begin{cases}0 & \text{for } m=2\nu\\ 4\int_0^a\sinh\left(\frac{2n+1}{h}\pi x\right)\sin\left(\frac{m\pi}{2a}x\right)dx & \text{for } m=2\nu+1\end{cases} \tag{A.5}$$

where, for m=2ν+1

$$\int_{-2a}^{2a} f(x)\sin\left(\frac{m\pi}{2a}x\right)dx = 4(-1)^{\nu}\frac{\left(\frac{2n+1}{h}\pi\right)\cosh\left(\frac{2n+1}{h}\pi a\right)}{\left(\frac{2n+1}{h}\pi\right)^2+\left(\frac{2\nu+1}{2a}\pi\right)^2} \tag{A.6}$$

and

$$\int_{-2a}^{2a} \sin^2\left(\frac{m\pi}{2a}x\right)dx = 2a \tag{A.7}$$

The constants K_k are determined as

$$K_k = \frac{2}{a}(-1)^{\nu}\frac{\left(\frac{2n+1}{h}\pi\right)\cosh\left(\frac{2n+1}{h}\pi a\right)}{\left(\frac{2n+1}{h}\pi\right)^2+\left(\frac{2\nu+1}{2a}\pi\right)^2} \tag{A.8}$$

and

$$f(x) = \sum_{\nu=0}^{\infty}\frac{2}{a}(-1)^{\nu}\frac{\left(\frac{2n+1}{h}\pi\right)\cosh\left(\frac{2n+1}{h}\pi a\right)}{\left(\frac{2n+1}{h}\pi\right)^2+\left(\frac{2\nu+1}{2a}\pi\right)^2}\sin\left(\frac{2\nu+1}{2a}\pi x\right) \tag{A.9}$$

We can then write:

$$\sum_{n=0}^{\infty}\frac{4h^2\sinh\left[\frac{2n+1}{h}\pi x\right]}{\pi^3(2n+1)^3\cosh\left[\frac{2n+1}{h}\pi a\right]} = \frac{8h}{\pi^2 a}\sum_{\nu=0}^{\infty}(-1)^{\nu}\sin\left(\frac{2\nu+1}{2a}\pi x\right)\sum_{n=0}^{\infty}\frac{1}{(2n+1)^2}\left[\frac{1}{\left(\frac{2n+1}{h}\pi\right)^2+\left(\frac{2\nu+1}{2a}\pi\right)^2}\right]$$

and have to study

$$\sum_{n=0}^{\infty}\frac{1}{(2n+1)^2}\left[\frac{1}{\left(\frac{2n+1}{h}\pi\right)^2+\left(\frac{2\nu+1}{2a}\pi\right)^2}\right] = \frac{1}{2}\sum_{n=-\infty}^{\infty}\frac{1}{4\left(\frac{2n+1}{2}\right)^2}\left[\frac{1}{4\left(\frac{2n+1}{2h}\pi\right)^2+\left(\frac{2\nu+1}{2a}\pi\right)^2}\right] \tag{A.11}$$

$$= \sum_{n=-\infty}^{\infty} f\left(\frac{2n+1}{2}\right) = \{\sum \textit{ of residues of } \pi\tan(\pi z)f(z) \textit{ at all poles of } f(z)\ \}$$

(see for example Spiegel: Complex variables)

$$f(z) = \frac{h^2}{32z^2\pi^2}\frac{1}{z^2+\frac{(2\nu+1)^2h^2}{16a^2}} \tag{A.12}$$

The poles are located at

$$z=0$$
$$z=z_1=i\frac{(2\nu+1)h}{4a} \tag{A.13}$$
$$z=z_2=-i\frac{(2\nu+1)h}{4a}$$

and the residues

$$Res(\pi\tan(\pi z)f(z))_{z=0}=\frac{a^2}{2(2\nu+1)^2}$$

$$Res(\pi\tan(\pi z)f(z))_{z=z_1}=\frac{-\tanh\left(\pi\frac{2\nu+1}{4a}h\right)}{\left(\frac{2\nu+1}{2a}\right)^3 8\pi h} \tag{A.14}$$

$$Res(\pi\tan(\pi z)f(z))_{z=z_2}=Res(\pi\tan(\pi z)f(z))_{z=z_1}$$

So

$$\sum_{n=0}^{\infty}\frac{4h^2\sinh\left[\frac{2n+1}{h}\pi x\right]}{\pi^3(2n+1)^3\cosh\left[\frac{2n+1}{h}\pi a\right]}=\sum_{\nu=0}^{\infty}(-1)^{\nu}\sin\left(\frac{2\nu+1}{2a}\pi x\right)\frac{8a}{\pi^2(2\nu+1)^2}\left[\frac{h}{2}-\frac{2a\tanh\left(\pi\frac{2\nu+1}{4a}h\right)}{(2\nu+1)\pi}\right]$$

and the boundary condition on z=0 is

$$-\omega^2\Phi+g\frac{\partial\Phi}{\partial z}=\omega^3\Theta_0\cos(\omega t)\sum_{\nu=0}^{\infty}(-1)^{\nu}\sin\left(\frac{2\nu+1}{2a}\pi x\right)\frac{8a}{\pi^2(2\nu+1)^2}$$
$$\cdot\left[\frac{h}{2}-\frac{2a\tanh\left(\pi\frac{2\nu+1}{4a}h\right)}{(2\nu+1)\pi}+\frac{2a}{\pi(2\nu+1)\sinh\left(\frac{2\nu+1}{2a}\pi h\right)}\right] \tag{A.16}$$

Using then

$$\tanh\left(\frac{2\nu+1}{4a}h\pi\right)=\frac{\cosh\left(\frac{2\nu+1}{2a}\pi h\right)-1}{\sinh\left(\frac{2\nu+1}{2a}\pi h\right)}\quad\text{and}\quad\sigma_\nu^2=\frac{2\nu+1}{2a}\pi g\tanh\left(\frac{2\nu+1}{2a}\pi h\right) \tag{A.17}$$

the boundary condition on z=0 may be written as:

$$-\omega^2\Phi+g\frac{\partial\Phi}{\partial z}=\omega^3\Theta_0\cos(\omega t)\sum_{\nu=0}^{\infty}(-1)^{\nu}\sin\left(\frac{2\nu+1}{2a}\pi x\right)\frac{8a}{\pi^2(2\nu+1)^2}\left\{\frac{h}{2}-\frac{4a\tanh\left(\pi\frac{2\nu+1}{4a}h\right)}{(2\nu+1)\pi}+\frac{g}{\sigma_{\nu}^2}\right\}$$

If the velocity potential for the liquid is written as

$$\Phi=\sum_{n=0}^{\infty}K_n\sin\left(\frac{2n+1}{2a}\pi\ x\right)\cosh\left(\frac{2n+1}{2a}\pi\,(z+h)\right)\cos(\omega t) \tag{A.19}$$

and is put into the boundary condition on z=0, K_n is found to be

$$K_n=\frac{\omega^3\Theta_0(-1)^n\frac{8a}{\pi^2(2n+1)^2}\left[\frac{h}{2}-\frac{4a\tanh\left(\frac{2n+1}{4a}\pi h\right)}{(2n+1)\pi}+\frac{g}{\sigma_n^2}\right]}{-\omega^2\cosh\left(\frac{2n+1}{2a}\pi h\right)+g\pi\frac{2n+1}{2a}\sinh\left(\frac{2n+1}{2a}\pi h\right)} \tag{A.20}$$

and the velocity potential for the liquid is then

$$\Phi=\omega\Theta_0\cos(\omega t)\frac{8a(-1)^n}{\pi^2(2n+1)^2}\left[\frac{h}{2}-\frac{4a\tanh\left(\frac{2n+1}{4a}\pi h\right)}{(2n+1)\pi}+\frac{g}{\sigma_n}\right]$$
$$\left(\frac{\omega^2}{\sigma_n^2-\omega^2}\right)\sin\left(\frac{2n+1}{2a}\pi x\right)\frac{\cosh\left(\frac{2n+1}{2a}\pi\,(z+h)\right)}{\cosh\left(\frac{2n+1}{2a}\pi h\right)} \tag{A.21}$$

where

$$\sigma_n^2=\frac{2n+1}{2a}\pi g\tanh\left(\frac{2n+1}{2a}\pi h\right) \tag{A.22}$$

Appendix B Third order free surface condition for general tank shape

The third order free surface conditions, terms of order ε, are

$$\frac{\partial \phi_3}{\partial t} + \frac{\omega^2}{\lambda_1}\zeta_3 = \frac{\alpha}{\lambda_1}\zeta_1 + A_2 + \frac{1}{\omega}f(x,y)\sin(\omega t) \quad on\ z=0$$

$$\frac{\partial \zeta_3}{\partial t} = \frac{\partial \phi_3}{\partial z} + B_2 \quad on\ z=0 \tag{B.1}$$

where

$$A_2 = -\nabla\phi_1\nabla\phi_2 - \zeta_1\frac{\partial^2\phi_2}{\partial z\partial t} - \zeta_2\frac{\partial^2\phi_1}{\partial z\partial t} - \zeta_1\nabla\phi_1\frac{\partial}{\partial z}\{\nabla\phi_1\} - \frac{1}{2}\zeta_1^2\frac{\partial^3\phi_1}{\partial z^2\partial t} \quad on\ z=0 \tag{B.2}$$

and

$$B_2 = -\frac{\partial\phi_1}{\partial x}\frac{\partial\zeta_2}{\partial x} - \frac{\partial\phi_2}{\partial x}\frac{\partial\zeta_1}{\partial x} - \frac{\partial\phi_1}{\partial y}\frac{\partial\zeta_2}{\partial y} - \frac{\partial\phi_2}{\partial y}\frac{\partial\zeta_1}{\partial y}$$

$$-\zeta_1\frac{\partial}{\partial z}\left\{\frac{\partial\phi_1}{\partial x}\frac{\partial\zeta_1}{\partial x} + \frac{\partial\phi_1}{\partial y}\frac{\partial\zeta_1}{\partial y}\right\} + \zeta_1\frac{\partial^2\phi_2}{\partial z^2} + \zeta_2\frac{\partial^2\phi_1}{\partial z^2} + \frac{1}{2}\zeta_1^2\frac{\partial^3\phi_1}{\partial z^3} \quad on\ z=0 \tag{B.3}$$

The combined free surface condition is then

$$\frac{\partial^2\phi_3}{\partial t^2} + \frac{\omega^2}{\lambda_1}\frac{\partial\phi_3}{\partial z} = \frac{\partial A_2}{\partial t} - \frac{\omega^2}{\lambda_1}B_2 + \frac{\alpha}{\lambda_1}\frac{\partial\zeta_1}{\partial t} + f(x,y)\cos(\omega t) \quad on\ z=0 \tag{B.4}$$

$$= \nabla\psi_1\sum_{n=0}^{\infty}\nabla\psi_n d^{(n)}\left\{\frac{1}{4}N(M^2+N^2)\omega\cos(\omega t) + \frac{1}{4}M(M^2+N^2)\omega\sin(\omega t)\right.$$

$$\left. -\frac{3}{4}N(3M^2-N^2)\omega\cos(3\omega t) - \frac{3}{4}M(M^2-3N^2)\omega\sin(3\omega t)\right\}$$

$$+\lambda_1\psi_1\sum_{n=0}^{\infty}\frac{\partial\psi_n}{\partial z}d^{(n)}\left\{-\frac{1}{2}N(M^2+N^2)\omega\cos(\omega t) - \frac{1}{2}M(M^2+N^2)\omega\sin(\omega t)\right.$$

$$\left. -\frac{3}{2}N(3M^2-N^2)\omega\cos(3\omega t) - \frac{3}{2}M(M^2-3N^2)\omega\sin(3\omega t)\right\}$$

$$+\lambda_1\frac{\partial\psi_1}{\partial z}\alpha_0\{-N\cos(\omega t) - M\sin(\omega t)\}$$

$$+\frac{\lambda_1}{\omega}\frac{\partial\psi_1}{\partial z}\left(-\frac{1}{2}(\nabla\psi_1)^2+\lambda_1\psi_1\frac{\partial\psi_1}{\partial z}\right)$$

$$\cdot\left\{\frac{1}{2}N(M^2+N^2)\omega\cos(\omega t)+\frac{1}{2}M(M^2+N^2)\omega\sin(\omega t)\right\}$$

$$+\frac{\lambda_1}{\omega}\frac{1}{2}\frac{\partial\psi_1}{\partial z}\left(\frac{1}{2}(\nabla\psi_1)^2+\lambda_1\psi_1\frac{\partial\psi_1}{\partial z}\right)$$

$$\cdot\left\{\frac{1}{2}N(M^2+N^2)\omega\cos(\omega t)+\frac{1}{2}M(M^2+N^2)\omega\sin(\omega t)\right.$$

$$\left.+\frac{3}{2}N(3M^2-N^2)\omega\cos(3\omega t)+\frac{3}{2}M(M^2-3N^2)\omega\sin(3\omega t)\right\}$$

$$+\lambda_1\frac{\partial\psi_1}{\partial z}\sum_{n=0}^{\infty}\psi_n d^{(n)}\left\{-\frac{1}{2}N(M^2+N^2)\omega\cos(\omega t)-\frac{1}{2}M(M^2+N^2)\omega\sin(\omega t)\right.$$

$$\left.-\frac{3}{2}N(3M^2-N^2)\omega\cos(3\omega t)-\frac{3}{2}M(M^2-3N^2)\omega\sin(3\omega t)\right\}$$

$$+\frac{\lambda_1}{\omega}\psi_1\nabla\psi_1\frac{\partial}{\partial z}\{\nabla\psi_1\}\left\{-\frac{1}{4}N(M^2+N^2)\omega\cos(\omega t)-\frac{1}{4}M(M^2+N^2)\omega\sin(\omega t)\right.$$

$$\left.+\frac{3}{4}N(3M^2-N^2)\omega\cos(3\omega t)+\frac{3}{4}M(M^2-3N^2)\omega\sin(3\omega t)\right\}$$

$$+\frac{1}{2}\frac{\lambda_1^2}{\omega}(\psi_1)^2\frac{\partial^2\psi_1}{\partial z^2}\left\{\frac{3}{4}N(M^2+N^2)\omega\cos(\omega t)+\frac{3}{4}M(M^2+N^2)\omega\sin(\omega t)\right.$$

$$\left.+\frac{3}{4}N(3M^2-N^2)\omega\cos(3\omega t)+\frac{3}{4}M(M^2-3N^2)\omega\sin(3\omega t)\right\}$$

$$+\frac{\partial\psi_1}{\partial x}\left\{2\omega\sum_{n=0}^{\infty}\frac{\partial\psi_n}{\partial x}d^{(n)}+\frac{\partial}{\partial x}\left(-\frac{1}{2}(\nabla\psi_1)^2-\lambda_1\psi_1\frac{\partial\psi_1}{\partial z}\right)\right\}$$

$$\cdot\left\{\frac{1}{4}N(M^2+N^2)\cos(\omega t)+\frac{1}{4}M(M^2+N^2)\sin(\omega t)\right.$$

$$\left.-\frac{1}{4}N(3M^2-N^2)\cos(3\omega t)-\frac{1}{4}M(M^2-3N^2)\sin(3\omega t)\right\}$$

$$+\frac{\partial\psi_1}{\partial x}\frac{\partial}{\partial x}\left(-\frac{1}{2}(\nabla\psi_1)^2+\lambda_1\psi_1\frac{\partial\psi_1}{\partial z}\right)$$

$$\cdot\left\{\frac{1}{2}N(M^2+N^2)\cos(\omega t)+\frac{1}{2}M(M^2+N^2)\sin(\omega t)\right\}$$

$$+\frac{\partial\psi_1}{\partial y}\left\{2\omega\sum_{n=0}^{\infty}\frac{\partial\psi_n}{\partial y}d^{(n)}+\frac{\partial}{\partial y}\left(-\frac{1}{2}(\nabla\psi_1)^2-\lambda_1\psi_1\frac{\partial\psi_1}{\partial z}\right)\right\}$$

$$\cdot\left\{\frac{1}{4}N(M^2+N^2)\cos(\omega t)+\frac{1}{4}M(M^2+N^2)\sin(\omega t)\right.$$

$$\left.-\frac{1}{4}N(3M^2-N^2)\cos(3\omega t)-\frac{1}{4}M(M^2-3N^2)\sin(3\omega t)\right\}$$

$$+\frac{\partial\psi_1}{\partial y}\frac{\partial}{\partial y}\left(-\frac{1}{2}(\nabla\psi_1)^2+\lambda_1\psi_1\frac{\partial\psi_1}{\partial z}\right)$$

$$\cdot\left\{\frac{1}{2}N(M^2+N^2)\cos(\omega t)+\frac{1}{2}M(M^2+N^2)\sin(\omega t)\right\}$$

$$+\omega\left\{\frac{\partial\psi_1}{\partial x}\sum_{n=0}^{\infty}\frac{\partial\psi_n}{\partial x}d^{(n)}+\frac{\partial\psi_1}{\partial y}\sum_{n=0}^{\infty}\frac{\partial\psi_n}{\partial y}d^{(n)}\right\}$$

$$\cdot\left\{-\frac{1}{4}N(M^2+N^2)\cos(\omega t)-\frac{1}{4}M(M^2+N^2)\sin(\omega t)\right.$$

$$\left.-\frac{1}{4}N(3M^2-N^2)\cos(3\omega t)-\frac{1}{4}M(M^2-3N^2)\sin(3\omega t)\right\}$$

$$+\lambda_1\psi_1\left(\frac{\partial\psi_1}{\partial x}\frac{\partial^2\psi_n}{\partial x\partial z}+\frac{\partial\psi_1}{\partial y}\frac{\partial^2\psi_n}{\partial y\partial z}\right)$$

$$\cdot\left\{\frac{1}{4}N(M^2+N^2)\cos(\omega t)+\frac{1}{4}M(M^2+N^2)\sin(\omega t)\right.$$

$$\left.+\frac{1}{4}N(3M^2-N^2)\cos(3\omega t)+\frac{1}{4}M(M^2-3N^2)\sin(3\omega t)\right\}$$

$$+\left\{\omega\psi_1\sum_{n=0}^{\infty}\frac{\partial^2\psi_n}{\partial^2 z}d^{(n)}-\frac{\lambda_1}{2}\psi_1^2\frac{\partial^3\psi_1}{\partial z^3}\right\}$$

$$\cdot\left\{\frac{1}{4}N(M^2+N^2)\cos(\omega t)+\frac{1}{4}M(M^2+N^2)\sin(\omega t)\right.$$

$$\left.+\frac{1}{4}N(3M^2-N^2)\cos(3\omega t)+\frac{1}{4}M(M^2-3N^2)\sin(3\omega t)\right\}$$

$$+\frac{\partial^2\psi_1}{\partial z^2}\left(\frac{1}{2}(\nabla\psi_1)^2-\lambda_1\psi_1\frac{\partial\psi_1}{\partial z}\right)$$

$$\cdot\left\{\frac{1}{2}N(M^2+N^2)\cos(\omega t)+\frac{1}{2}M(M^2+N^2)\sin(\omega t)\right\}$$

$$+\frac{\partial^2\psi_1}{\partial z^2}\left\{-2\omega\sum_{n=0}^{\infty}\psi_n d^{(n)}+\frac{1}{2}(\nabla\psi_1)^2+\lambda_1\psi_1\frac{\partial\psi_1}{\partial z}\right\}$$

$$\cdot\left\{\frac{1}{4}N(M^2+N^2)\cos(\omega t)+\frac{1}{4}M(M^2+N^2)\sin(\omega t)\right.$$

$$\left.-\frac{1}{4}N(3M^2-N^2)\cos(3\omega t)-\frac{1}{4}M(M^2-3N^2)\sin(3\omega t)\right\}$$

$$+\frac{\partial^2\psi_1}{\partial z^2}\alpha_0\{N\cos(\omega t)+M\sin(\omega t)\}$$

$$+\alpha\psi_1\{N\cos(\omega t)+M\sin(\omega t)\}+f(x,y)\cos(\omega t)$$

at the free surface z = 0.

Appendix C Nonlinear combined free surface condition for vertical circular cylindrical tank

The kinematic free-surface condition may be written as

$$\frac{\partial}{\partial t}(z-\zeta)+\nabla\Phi\cdot\nabla(z-\zeta)=0 \tag{C.1}$$

Since ζ is no longer an independent variable, we get

$$\frac{\partial\zeta}{\partial t}+\frac{\partial\Phi}{\partial r}\frac{\partial\zeta}{\partial r}+\frac{1}{r^2}\frac{\partial\Phi}{\partial\theta}\frac{\partial\zeta}{\partial\theta}+\frac{\partial\Phi}{\partial z}\frac{\partial\zeta}{\partial z}-\frac{\partial\Phi}{\partial z}=0 \qquad on\ z=\zeta \tag{C.2}$$

By inserting the dynamic free-surface condition

$$\zeta=\frac{1}{g}\left[-\ddot{x}_b r\cos\theta-\frac{\partial\Phi}{\partial t}-\frac{1}{2}\left[\left(\frac{\partial\Phi}{\partial r}\right)^2+\frac{1}{r^2}\left(\frac{\partial\Phi}{\partial\theta}\right)^2+\left(\frac{\partial\Phi}{\partial z}\right)^2\right]\right] \qquad on\ z=\zeta \tag{C.3}$$

into equation (C.2) we find that

$$\begin{aligned}&\Phi_{tz}+g\Phi_z+2\Phi_r\Phi_{rz}+\frac{2}{r^2}\Phi_\theta\Phi_{\theta z}+2\Phi_z\Phi_{zz}+\Phi_r^2\Phi_{rz}+\Phi_z^2\Phi_{zz}+\\&\frac{1}{r^4}\Phi_\theta^2\Phi_{\theta\theta}-\frac{1}{r^3}\Phi_r\Phi_\theta^2+\frac{2}{r^2}\Phi_r\Phi_{r\theta}\Phi_\theta+\frac{2}{r^2}\Phi_z\Phi_{z\theta}\Phi_\theta+2\Phi_r\Phi_z\Phi_{rz}\\&=-\ddot{x}_b r\cos\theta+\ddot{x}_b\left(\frac{1}{r}\Phi_\theta\sin\theta-\Phi_r\cos\theta\right) \qquad on\ z=\zeta\end{aligned} \tag{C.4}$$

Here the subscripts t, r, θ and z represent the time, r, θ and z derivatives, respectively. The dots above x_b represent the time derivative.

Since the potential functions must be evaluated on $z=\zeta$, equation (C.4) depends upon ζ implicitly and equation (C.3) depends upon ζ both implicitly and explicitly. The wave height ζ can be eliminated between equation (C.3) and (C.4) if these two equations are first expanded in a Taylor series in ζ about $z=0$.

The notation

$$\phi_k\equiv\Phi_k(r,\theta,z=0,t) \tag{C.5}$$

is introduced, where the subscript k represents any order of partial differentiation.

The Taylor series expansions of equation (C.4) and (C.3) may be written in the forms

$$a_0+a_1\zeta+a_2\zeta^2+a_3\zeta^3+\cdots=0 \tag{C.6}$$

$$b_0+b_1\zeta+b_2\zeta^2+b_3\zeta^3+\cdots=0 \tag{C.7}$$

respectively, where

$$
\begin{aligned}
a_0 &= a_{00} + a_{01} + a_{02} \\
a_1 &= a_{11} + a_{12} + a_{13} \\
a_2 &= a_{22} + a_{23} + a_{24}
\end{aligned}
\tag{C.8}
$$

$$
\begin{aligned}
a_{00} &= \phi_{tt} + g\phi_z + r\,\ddot{x}_b \cos\theta \\
a_{01} &= 2\phi_r\phi_{rt} + \frac{2}{r^2}\phi_\theta\phi_{\theta t} + 2\phi_z\phi_{zt} + \ddot{x}_b\left(\phi_r\cos\theta - \frac{1}{r}\phi_\theta\sin\theta\right) \\
a_{02} &= \phi_r^2\phi_{rr} + \phi_z^2\phi_{zz} + \frac{1}{r^4}\phi_\theta^2\phi_{\theta\theta} - \frac{1}{r^3}\phi_r\phi_\theta^2 \\
&\quad + \frac{2}{r^2}\phi_r\phi_{r\theta}\phi_\theta + \frac{2}{r^2}\phi_z\phi_{z\theta}\phi_\theta + 2\phi_r\phi_z\phi_{rz} \\
a_{11} &= \phi_{ttz} + g\phi_{zz} \\
a_{12} &= 2\left(\phi_{rz}\phi_{rt} + \phi_r\phi_{rtz} + \frac{1}{r^2}\phi_{\theta z}\phi_{\theta t} + \frac{1}{r^2}\phi_\theta\phi_{\theta zt} + \phi_{zz}\phi_{zt} + \phi_z\phi_{zzt}\right) \\
&\quad + \ddot{x}_b\left(\phi_{rz}\cos\theta - \frac{1}{r}\phi_{\theta z}\sin\theta\right) \\
a_{22} &= \frac{1}{2}\left(\phi_{ttzz} + g\phi_{zzz}\right) \\
a_{m+1,n+1} &= \frac{1}{(m+1)!}\cdot\frac{\partial a_{mn}}{\partial z}
\end{aligned}
\tag{C.9}
$$

and

$$
\begin{aligned}
b_0 &= b_{00} + b_{01} \\
b_1 &= g + b_{11} + b_{12} \\
b_2 &= b_{22} + b_{23}
\end{aligned}
\tag{C.10}
$$

$$
\begin{aligned}
b_{00} &= \phi_t + \ddot{x}_b\, r\cos\theta \\
b_{01} &= \frac{1}{2}\left(\phi_r^2 + \frac{1}{r^2}\phi_\theta^2 + \phi_z^2\right) \\
b_{11} &= \phi_{tz} \\
b_{12} &= \phi_r\phi_{rz} + \frac{1}{r^2}\phi_\theta\phi_{\theta z} + \phi_z\phi_{zz} \\
b_{22} &= \frac{1}{2}\phi_{tzz} \\
b_{m+1,n+1} &= \frac{1}{(m+1)!}\cdot\frac{\partial b_{mn}}{\partial z}
\end{aligned}
\tag{C.11}
$$

If the terms from equations (C.10) and (C.11) are put into equation (C.7) and the products of ζ and ϕ are neglected in equation (C.7), it is seen that the potential functions are of the same

order as the wave height. Then the first approximation becomes

$$\zeta = -\frac{1}{g}\phi_t \tag{C.12}$$

Hence, a term such as $b_2\zeta^2$ in equation (C.7) is of order ζ^3. Solving equation (C.7) for ζ gives

$$\zeta = -\frac{b_0}{b_1} - \frac{b_2}{b_1}\zeta^2 - \cdots = -\frac{b_0}{b_1} + O(\zeta^3) \tag{C.13}$$

and upon substituting equation (C.13) into (C.6), the results becomes

$$a_0 - \frac{a_1 b_0}{b_1} + a_2\frac{b_0^2}{b_1^2} + O(\zeta^4) = 0 \tag{C.14}$$

Now

$$\begin{aligned} \frac{a_1 b_0}{b_1} &= \frac{a_1 b_0}{g + (b_{11} + b_{12})} = \frac{a_1 b_0}{g} \cdot \frac{1}{1 + \dfrac{b_{11} + b_{12}}{g}} \\ &= \frac{a_{11}b_{00} + a_{11}b_{01} + a_{12}b_{00}}{g} - \frac{a_{11}b_{00}b_{11}}{g^2} + O(\zeta^4) \end{aligned} \tag{C.15}$$

when the bracket $1/(1+(b_{11}+b_{12})/g)$ is expanded in series $1/(1+a)=1-a+a^2-...$

Similarly we can write

$$\begin{aligned} a_2\frac{b_0^2}{b_1^2} &= \frac{(a_{22} + a_{23} + a_{24})(b_{00} + b_{01})^2}{(g + b_{11} + b_{12})^2} \\ &= \left(\frac{a_{22}b_{00}^2}{g^2}\right) + O(\zeta^4) \end{aligned} \tag{C.16}$$

so that the combined free surface condition equation (C.14) becomes

$$B_1 + B_2 + B_3 + O(\zeta^4) = 0 \qquad on\ z = 0 \tag{C.17}$$

Here

$$\begin{aligned} B_1 &= a_{00} \\ B_2 &= a_{01} - \frac{a_{11}b_{00}}{g} \\ B_3 &= a_{02} - \frac{a_{11}b_{01} + a_{12}b_{00}}{g} + \frac{a_{11}b_{00}b_{11} + a_{22}b_{00}^2}{g^2} \end{aligned} \tag{C.18}$$

Appendix D The second order equations for nonlinear sloshing in a vertical circular cylindrical tank

From the first order equations it is determined that

$$\Psi_1=[f_1(\tau)\cos\theta+f_3(\tau)\sin\theta]\cdot J_1(\lambda_{11}r)\cdot\frac{\cosh[\lambda_{11}(z+h)]}{\cosh(\lambda_{11}h)}$$
$$\chi_1=[f_2(\tau)\cos\theta+f_4(\tau)\sin\theta]\cdot J_1(\lambda_{11}r)\cdot\frac{\cosh[\lambda_{11}(z+h)]}{\cosh(\lambda_{11}h)} \qquad (D.1)$$

where $\lambda_{11}=\xi_{11}/a$, and from the second order equations that

$$\Psi_2=\sum_{n=1}^{\infty}\hat{A}_{0n}J_0(\lambda_{0n}r)\frac{\cosh[\lambda_{0n}(z+h)]}{\cosh(\lambda_{0n}h)}$$
$$+\sum_{n=1}^{\infty}[\hat{A}_{2n}\cos(2\theta)+\hat{B}_{2n}\sin(2\theta)]J_2(\lambda_{2n}r)\frac{\cosh[\lambda_{2n}(z+h)]}{\cosh(\lambda_{2n}h)}$$
$$\chi_2=\sum_{n=1}^{\infty}\hat{C}_{0n}J_0(\lambda_{0n}r)\frac{\cosh[\lambda_{0n}(z+h)]}{\cosh(\lambda_{0n}h)} \qquad (D.2)$$
$$+\sum_{n=1}^{\infty}[\hat{C}_{2n}\cos(2\theta)+\hat{D}_{2n}\sin(2\theta)]J_2(\lambda_{2n}r)\frac{\cosh[\lambda_{2n}(z+h)]}{\cosh(\lambda_{2n}h)}$$

where $J'_0(\lambda_{0n}a) = J'_2(\lambda_{2n}a) = 0$, and

$$\alpha_{0z}=0$$
$$4\sigma_{11}^2\Psi_2-g\Psi_{2z}=2\sigma_{11}(\chi_{1r}\Psi_{1r}+\frac{1}{r^2}\chi_{1\theta}\Psi_{1\theta}+\frac{3\alpha_{11}^2-1}{2}\lambda_{11}^2\chi_1\Psi_1) \qquad (D.3)$$
$$4\sigma_{11}^2\chi_2-g\chi_{2z}=\sigma_{11}[\chi_{1r}^2-\Psi_{1r}^2+\frac{1}{r^2}\chi_{1\theta}^2-\frac{1}{r^2}\Psi_{1\theta}^2+\frac{3\alpha_{11}^2-1}{2}\lambda_{11}^2(\chi_1^2-\Psi_1^2)]$$

The generalized coordinates $\hat{A}_{0n}$, $\hat{A}_{2n}$, B_{0n}, B_{2n}, $\hat{C}_{0n}$ $\hat{C}_{2n}$ and D_{2n} can be expressed in terms of f_1, f_2, f_3 and f_4. First the equations (D.1) and (D.2) are introduced into (D.3) and then we use

$$\sigma_{11}^2=g\lambda_{11}\tanh(\lambda_{11}h)$$
$$\sigma_{0n}^2=g\lambda_{0n}\tanh(\lambda_{0n}h) \qquad (D.4)$$
$$\sigma_{2n}^2=g\lambda_{2n}\tanh(\lambda_{2n}h)$$

and

$$\cos^2\theta = \frac{1}{2} + \frac{1}{2}\cos(2\theta)$$
$$\sin^2\theta = \frac{1}{2} - \frac{1}{2}\cos(2\theta) \qquad \text{(D.5)}$$
$$\sin\theta\cos\theta = \frac{1}{2}\sin(2\theta)$$

This gives

$$\begin{aligned}
&\sum_{n=1}^{\infty} \hat{A}_{0n} J_0(\lambda_{0n} r)(4\sigma_{11}^2 - \sigma_{0n}^2) + \\
&\sum_{n=1}^{\infty} [\hat{A}_{2n}\cos(2\theta) + \hat{B}_{2n}\sin(2\theta)] J_2(\lambda_{2n} r)(4\sigma_{11}^2 - \sigma_{2n}^2) \\
&= (f_1 f_2 + f_3 f_4)\sigma_{11}[\lambda_{11}^2 J_1'^2(\lambda_{11} r) + \frac{1}{r^2} J_1^2(\lambda_{11} r) + K_0 \lambda_{11}^2 J_1^2(\lambda_{11} r)] \\
&\quad + (f_1 f_2 - f_3 f_4)\sigma_{11}[\lambda_{11}^2 J_1'^2(\lambda_{11} r) - \frac{1}{r^2} J_1^2(\lambda_{11} r) + K_0 \lambda_{11}^2 J_1^2(\lambda_{11} r)]\cos(2\theta) \\
&\quad + (f_1 f_4 + f_2 f_3)\sigma_{11}[\lambda_{11}^2 J_1'^2(\lambda_{11} r) - \frac{1}{r^2} J_1^2(\lambda_{11} r) + K_0 \lambda_{11}^2 J_1^2(\lambda_{11} r)]\sin(2\theta)
\end{aligned} \qquad \text{(D.6)}$$

and

$$\begin{aligned}
&\sum_{n=1}^{\infty} \hat{C}_{0n} J_0(\lambda_{0n} r)(4\sigma_{11}^2 - \sigma_{0n}^2) + \\
&\sum_{n=1}^{\infty} [\hat{C}_{2n}\cos(2\theta) + \hat{D}_{2n}\sin(2\theta)] J_2(\lambda_{2n} r)(4\sigma_{11}^2 - \sigma_{2n}^2) \\
&= \frac{1}{2}(f_2^2 + f_4^2 - f_1^2 - f_3^2)\sigma_{11}[\lambda_{11}^2 J_1'^2(\lambda_{11} r) + \frac{1}{r^2} J_1^2(\lambda_{11} r) + K_0 \lambda_{11}^2 J_1^2(\lambda_{11} r)] \\
&\quad + \frac{1}{2}(f_2^2 + f_3^2 - f_1^2 - f_4^2)\sigma_{11}[\lambda_{11}^2 J_1'^2(\lambda_{11} r) - \frac{1}{r^2} J_1^2(\lambda_{11} r) + K_0 \lambda_{11}^2 J_1^2(\lambda_{11} r)]\cos(2\theta) \\
&\quad + (f_2 f_4 - f_1 f_3)\sigma_{11}[\lambda_{11}^2 J_1'^2(\lambda_{11} r) - \frac{1}{r^2} J_1^2(\lambda_{11} r) + K_0 \lambda_{11}^2 J_1^2(\lambda_{11} r)]\sin(2\theta)
\end{aligned} \qquad \text{(D.7)}$$

where

$$K_0 = \frac{3\alpha_{11}^2 - 1}{2} \qquad \text{(D.8)}$$

According to Abramson (1966), K_0 should be multiplied by λ_{11}^2. But, we have obtained the same result as the one given in Hutton (1963).

Then the following orthogonality relations are used:

$$\int_0^a rJ_0(\lambda_{0m}r)J_0(\lambda_{0n}r)dr = \begin{cases} 0 & ,m\neq n \\ \frac{a^2}{2}J_0^2(\lambda_{0n}a) & ,m=n \end{cases}$$

$$\int_0^a rJ_2(\lambda_{2m}r)J_2(\lambda_{2n}r)dr = \begin{cases} 0 & ,m\neq n \\ \frac{\lambda_{2n}^2a^2-4}{2\lambda_{2n}^2}J_2^2(\lambda_{2n}a) & ,m=n \end{cases} \qquad (D.9)$$

First the equations (D.6) and (D.7) are multiplied by $rJ_0(\lambda_{0m}r)$ and integrated from 0 to a. This gives the following expressions for the generalized coordinates

$$\begin{aligned} \hat{A}_{0n} &= \Omega_{0n}(f_1f_2+f_3f_4) \\ \hat{C}_{0n} &= \Omega_{0n}\frac{1}{2}(f_2^2+f_4^2-f_1^2-f_3^2) \end{aligned} \qquad (D.10)$$

where

$$\Omega_{0n} = \frac{I_{01}^n+I_{02}^n+K_0I_{03}^n}{(4\sigma_{11}^2-\sigma_{0n}^2)\frac{a^2}{2\sigma_{11}}J_0^2(\lambda_{0n}a)} \qquad (D.11)$$

And then, equation (D.6) and (D.7) are multiplied by $rJ_2(\lambda_{2m}r)$ and integrated from 0 to a, which gives

$$\begin{aligned} \hat{A}_{2n} &= \Omega_{2n}(f_1f_2-f_3f_4) \\ \hat{B}_{2n} &= \Omega_{2n}(f_1f_4+f_2f_3) \\ \hat{C}_{2n} &= \Omega_{2n}\frac{1}{2}(f_2^2+f_3^2-f_1^2-f_4^2) \\ \hat{D}_{2n} &= \Omega_{2n}(f_2f_4-f_1f_3) \end{aligned} \qquad (D.12)$$

where

$$\Omega_{2n} = \frac{I_{21}^n-I_{22}^n+K_0I_{23}^n}{(4\sigma_{11}^2-\sigma_{2n}^2)\frac{\lambda_{2n}^2a^2-4}{2\lambda_{2n}^2\sigma_{11}}J_2^2(\lambda_{2n}a)} \qquad (D.13)$$

The integrals are

$$I_{01}^{n}=\int_{0}^{a\lambda_{11}} uJ_0\left(\frac{\lambda_{0n}}{\lambda_{11}}u\right)\left[\frac{d}{du}J_1(u)\right]^2 du$$

$$I_{02}^{n}=\int_{0}^{a\lambda_{11}} \frac{1}{u}J_0\left(\frac{\lambda_{0n}}{\lambda_{11}}u\right) J_1^2(u)\,du \qquad \text{(D.14)}$$

$$I_{03}^{n}=\int_{0}^{a\lambda_{11}} uJ_0\left(\frac{\lambda_{0n}}{\lambda_{11}}u\right) J_1^2(u)\,du$$

and

$$I_{21}^{n}=\int_{0}^{a\lambda_{11}} uJ_2\left(\frac{\lambda_{2n}}{\lambda_{11}}u\right)\left[\frac{d}{du}J_1(u)\right]^2 du$$

$$I_{22}^{n}=\int_{0}^{a\lambda_{11}} \frac{1}{u}J_2\left(\frac{\lambda_{2n}}{\lambda_{11}}u\right) J_1^2(u)\,du \qquad \text{(D.15)}$$

$$I_{23}^{n}=\int_{0}^{a\lambda_{11}} uJ_2\left(\frac{\lambda_{2n}}{\lambda_{11}}u\right) J_1^2(u)\,du$$

The values of these integrals are independent of the circular cylindrical tank dimensions, and given in appendix H.

Appendix E Determination of the constant in the second order velocity potential for sloshing in a vertical circular cylindrical tank

The constant α_0 is determined from the condition that the total amount of water inside the tank should be constant.

$$\int_0^{2\pi}\int_0^a \zeta r dr d\theta = 0 \tag{E.1}$$

The integral of the first order free surface elevation is equal to zero, and then the condition is

$$\int_0^{2\pi}\int_0^a \zeta_2 r dr d\theta = 0 \tag{E.2}$$

The second order free surface elevation is given by

$$\zeta_2 = \frac{\sigma_{11}^2}{\omega^2 g}\left\{-\frac{\partial\phi_2}{\partial t} - \frac{1}{2}\left(\frac{\partial\phi_1}{\partial r}\right)^2 - \frac{1}{2}\frac{1}{r^2}\left(\frac{\partial\phi_1}{\partial\theta}\right)^2 \frac{1}{2}\left(\frac{\partial\phi_1}{\partial z}\right)^2 - \zeta_1\frac{\partial^2\phi_1}{\partial z\partial t}\right\} \tag{E.3}$$

where the velocity potentials are given on z=0. From equation (E.3) and (E.2), the condition becomes

$$\begin{aligned}\int_0^{2\pi}\int_0^a \frac{\partial\phi_2}{\partial t} r dr d\theta = &-\frac{1}{2}\int_0^{2\pi}\int_0^a\left(\frac{\partial\phi_1}{\partial r}\right)^2 r dr d\theta - \frac{1}{2}\int_0^{2\pi}\int_0^a \frac{1}{r}\left(\frac{\partial\phi_1}{\partial\theta}\right)^2 dr d\theta \\ &-\frac{1}{2}\int_0^{2\pi}\int_0^a\left(\frac{\partial\phi_1}{\partial z}\right)^2 r dr d\theta - \int_0^{2\pi}\int_0^a \zeta_1\frac{\partial^2\phi_1}{\partial z\partial t} r dr d\theta\end{aligned} \tag{E.4}$$

or

$$\begin{aligned}&\int_0^{2\pi}\int_0^a \frac{\partial\phi_2}{\partial t} r dr d\theta = \\ &-\frac{\pi}{8}[\lambda_{11}^2 a^2 - 1] J_1^2(\lambda_{11} a) \\ &\left\{(f_1^2+f_2^2+f_3^2+f_4^2) + (f_1^2+f_3^3-f_2^2-f_4^2)\cos(2\omega t) + 2(f_1 f_2 + f_3 f_4)\sin(2\omega t)\right\} \\ &+\frac{\pi}{8}[\lambda_{11}^2 a^2 - 1] J_1^2(\lambda_{11} a)\alpha_{11}^2 \\ &\left\{(f_1^2+f_2^2+f_3^2+f_4^2) - 3(f_1^2+f_3^2-f_2^2-f_4^2)\cos(2\omega t) - 6(f_1 f_2 + f_3 f_4)\sin(2\omega t)\right\}\end{aligned} \tag{E.5}$$

when the integrals of the first order potential are calculated. The time derivative of the

second order potential is

$$\frac{\partial \phi_2}{\partial t} = \alpha_0 + \Psi_2(-2\omega)\sin(2\omega t) + \chi_2(2\omega)\cos(2\omega t) \tag{E.6}$$

where Ψ_2 and χ_2 are given by equation (D.2). The integrals of the terms in the second order potential are

$$\int_0^{2\pi}\int_0^a \hat{A}_{0n} J_0(\lambda_{0n} r)\, r\, dr\, d\theta = \begin{cases} 0 & \text{for } n = 2,3,4,5,\ldots \\ \hat{A}_{01} a^2 \pi & \text{for } n = 1 \end{cases} \tag{E.7}$$

$$\int_0^{2\pi}\int_0^a \hat{A}_{2n} J_2(\lambda_{2n} r)\cos(2\theta)\, r\, dr\, d\theta = 0 \qquad \text{for all values of } n \tag{E.8}$$

$$\int_0^{2\pi}\int_0^a \hat{B}_{2n} J_2(\lambda_{2n} r)\sin(2\theta)\, r\, dr\, d\theta = 0 \qquad \text{for all values of } n \tag{E.9}$$

$$\int_0^{2\pi}\int_0^a \hat{C}_{0n} J_0(\lambda_{0n} r)\, r\, dr\, d\theta = \begin{cases} 0 & \text{for } n = 2,3,4,5,\ldots \\ \hat{C}_{01} a^2 \pi & \text{for } n = 1 \end{cases} \tag{E.10}$$

$$\int_0^{2\pi}\int_0^a \hat{C}_{2n} J_2(\lambda_{2n} r)\cos(2\theta)\, r\, dr\, d\theta = 0 \qquad \text{for all values of } n \tag{E.11}$$

$$\int_0^{2\pi}\int_0^a \hat{D}_{2n} J_2(\lambda_{2n} r)\sin(2\theta)\, r\, dr\, d\theta = 0 \qquad \text{for all values of } n \tag{E.12}$$

when $\lambda_{01}a = 0.0$ and then $J_0(\lambda_{01}a)=1.0$. The constants $\hat{A}_{01}$ and $\hat{C}_{01}$ are given in appendix D, and when the analytical expressions for the integrals on the top of the brackets are used, the constants are obtained as

$$\hat{A}_{01} = (f_1 f_2 + f_3 f_4)\frac{\frac{1}{4}[\lambda_{11}^2 a^2 - 1]J_1^2(\lambda_{11}a)[1+3\alpha_{11}^2]}{2\sigma_{11}a^2} \tag{E.13}$$

and

$$\hat{C}_{01} = (f_2^2 + f_4^2 - f_1^2 - f_3^2)\frac{\frac{1}{4}[\lambda_{11}^2 a^2 - 1]J_1^2(\lambda_{11}a)[1+3\alpha_{11}^2]}{4\sigma_{11}a^2} \tag{E.14}$$

when $\sigma_{01} = 0.0$. The total integral of the second order potential is then

$$\int_0^{2\pi}\int_0^{a}\frac{\partial\phi_2}{\partial t}r\,dr\,d\theta = \pi\ \alpha_0 a^2 - 2\omega\hat{A}_{01}a^2\pi\sin(2\omega t) + 2\omega\hat{C}_{0n}a^2\pi\cos(2\omega t) \qquad \text{(E.15)}$$

which should be equal to the integral obtained in equation (E.5). This determines the constant α_0. When the approximation $\omega = \sigma_{11}$ is used, α_0 is obtained as

$$\alpha_0 = (f_1^2 + f_2^2 + f_3^2 + f_4^2)(\alpha_{11}^2 - 1)\frac{[\lambda_{11}^2 a^2 - 1]J_1^2(\lambda_{11}a)}{8a^2} \qquad \text{(E.16)}$$

Appendix F Third order equations for nonlinear sloshing in a vertical circular cylindrical tank

The coefficients of ε give the third order terms. Using equation (5.115) and (5.125) in equation (5.127) gives the first harmonic terms of B_1 of order ε.

$$B_1^{FH\varepsilon}=\sigma_{11}^2[(\chi_{1\tau}-\nu\Psi_1-r\cos\theta)\cos(\omega t)-(\chi_{1\tau}+\nu\chi_1)\sin(\omega t)] \tag{F.1}$$

Equations (5.115), (5.125) and (5.128) give the first harmonic terms of B_2 of order ε.

$$\begin{aligned}B_2^{FH\varepsilon}=&\sigma_{11}[\Psi_{1r}\chi_{2r}-\chi_{1r}\Psi_{2r}+\frac{1}{r^2}(\Psi_{1\theta}\chi_{2\theta}-\chi_{1\theta}\Psi_{2\theta})-\lambda_{11}\alpha_{11}(\Psi_1\chi_{2z}-\chi_1\Psi_{2z})\\&+\frac{1}{2}(\Psi_1\chi_{2zz}-\chi_1\Psi_{2zz})-\lambda_{11}^2(\alpha_{11}^2-1)(\chi_1\Psi_2-\Psi_1\chi_2)]\cos(\omega t)\\&-\sigma_{11}[\chi_{1r}\chi_{2r}+\Psi_{1r}\Psi_{2r}+\frac{1}{r^2}(\chi_{1\theta}\chi_{2\theta}+\Psi_{1\theta}\Psi_{2\theta})-\lambda_{11}\alpha_{11}(\chi_1\chi_{2z}+\Psi_1\Psi_{2z})\\&+\frac{1}{2}(\chi_1\chi_{2zz}+\Psi_1\Psi_{2zz})+\lambda_{11}^2(\alpha_{11}^2-1)(\Psi_1\Psi_2+\chi_1\chi_2)]\sin(\omega t)\end{aligned} \tag{F.2}$$

where the following relations are used

$$\begin{aligned}\cos(\omega t)\sin(2\omega t)&=\frac{1}{2}\sin(\omega t)+\frac{1}{2}\sin(3\omega t)\\\cos(\omega t)\cos(2\omega t)&=\frac{1}{2}\cos(\omega t)+\frac{1}{2}\cos(3\omega t)\\\sin(\omega t)\sin(2\omega t)&=\frac{1}{2}\cos(\omega t)-\frac{1}{2}\cos(3\omega t)\\\sin(\omega t)\cos(2\omega t)&=-\frac{1}{2}\sin(\omega t)+\frac{1}{2}\sin(3\omega t)\end{aligned} \tag{F.3}$$

α_0 is a constant, so α_{0r} is equal to 0, and

$$\begin{aligned}\chi_{1z}&=\frac{\sigma_{11}^2}{g}\chi_1=\lambda_{11}\alpha_{11}\chi_1\\\Psi_{1z}&=\frac{\sigma_{11}^2}{g}\Psi_1=\lambda_{11}\alpha_{11}\Psi_1\\\chi_{1zz}&=\lambda_{11}^2\chi_1\\\Psi_{1zz}&=\lambda_{11}^2\Psi_1\end{aligned} \tag{F.4}$$

Equations (5.115), (5.125) and (5.129) give the first harmonic terms of B_3 of order ε.

$$B_3^{FH\varepsilon}=(T_I+T_{II}+T_{III}+T_{IV})\cos(\omega t)+(T_V+T_{VI}+T_{VII}+T_{VIII})\sin(\omega t) \tag{F.5}$$

where

$$
\begin{aligned}
T_I=&\frac{3}{4}\Psi_{1r}^2\Psi_{1rr}+\frac{1}{4}\chi_{1r}^2\Psi_{1rr}+\frac{1}{2}\Psi_{1r}\chi_{1r}\chi_{1rr}+\frac{3}{4}\frac{1}{r^4}\Psi_{1\theta}^2\Psi_{1\theta\theta}+\frac{1}{4}\frac{1}{r^4}\chi_{1\theta}^2\Psi_{1\theta\theta}+\frac{1}{2}\frac{1}{r^4}\Psi_{1\theta}\chi_{1\theta}\chi_{1\theta\theta}\\
&+\frac{3}{4}\Psi_{1z}^2\Psi_{1zz}+\frac{1}{4}\chi_{1z}^2\Psi_{1zz}+\frac{1}{2}\Psi_{1z}\chi_{1z}\chi_{1zz}-\frac{3}{4}\frac{1}{r^3}\Psi_{1\theta}^2\Psi_{1r}-\frac{1}{4}\frac{1}{r^3}\chi_{1\theta}^2\Psi_{1r}-\frac{1}{2}\frac{1}{r^3}\Psi_{1\theta}\chi_{1\theta}\chi_{1r}\\
&+\frac{3}{2}\Psi_{1r}\Psi_{1z}\Psi_{1rz}+\frac{1}{2}[\chi_{1r}\chi_{1z}\Psi_{1rz}+\Psi_{1r}\chi_{1z}\chi_{1rz}+\chi_{1r}\Psi_{1z}\chi_{1rz}]\\
&+\frac{3}{2}\frac{1}{r^2}\Psi_{1r}\Psi_{1\theta}\Psi_{1r\theta}+\frac{1}{2}\frac{1}{r^2}[\chi_{1r}\chi_{1\theta}\Psi_{1r\theta}+\Psi_{1r}\chi_{1\theta}\chi_{1r\theta}+\chi_{1r}\Psi_{1\theta}\chi_{1r\theta}]
\end{aligned}
\tag{F.6}
$$

$$
\begin{aligned}
T_{II}=&\frac{3}{2}\frac{1}{r^2}\Psi_{1z}\Psi_{1\theta}\Psi_{1\theta z}+\frac{1}{2}\frac{1}{r^2}[\chi_{1z}\chi_{1\theta}\Psi_{1\theta z}+\Psi_{1z}\chi_{1\theta}\chi_{1\theta z}+\chi_{1z}\Psi_{1\theta}\chi_{1\theta z}]\\
&+\frac{3}{8}\frac{1}{g}\Psi_{1r}^2\Psi_{1z}\omega^2-\frac{1}{2}\frac{1}{g}[-\frac{1}{2}\Psi_{1r}\chi_{1r}\chi_{1z}\omega^2-\frac{1}{4}\chi_{1r}^2\Psi_{1z}\omega^2]\\
&+\frac{3}{8}\frac{1}{g}\frac{1}{r^2}\Psi_{1\theta}^2\Psi_{1z}\omega^2-\frac{1}{2}\frac{1}{g}\frac{1}{r^2}[-\frac{1}{2}\Psi_{1\theta}\chi_{1\theta}\chi_{1z}\omega^2-\frac{1}{4}\chi_{1\theta}^2\Psi_{1z}\omega^2]\\
&+\frac{3}{8}\frac{1}{g}\Psi_{1z}^3\omega^2-\frac{1}{2}\frac{1}{g}[-\frac{1}{2}\Psi_{1z}\chi_{1z}^2\omega^2-\frac{1}{4}\chi_{1z}^2\Psi_{1z}\omega^2]\\
&-\frac{3}{8}\Psi_{1r}^2\Psi_{1zz}-\frac{1}{2}[\frac{1}{2}\Psi_{1r}\chi_{1r}\chi_{1zz}+\frac{1}{4}\chi_{1r}^2\Psi_{1zz}]\\
&-\frac{3}{8}\frac{1}{r^2}\Psi_{1\theta}^2\Psi_{1zz}-\frac{1}{2}\frac{1}{r^2}[\frac{1}{2}\Psi_{1\theta}\chi_{1\theta}\chi_{1zz}+\frac{1}{4}\chi_{1\theta}^2\Psi_{1zz}]
\end{aligned}
\tag{F.7}
$$

$$
\begin{aligned}
T_{III}=&-\frac{3}{8}\Psi_{1z}^2\Psi_{1zz}-\frac{1}{2}[\frac{1}{2}\Psi_{1z}\chi_{1z}\chi_{1zz}+\frac{1}{4}\chi_{1z}^2\Psi_{1zz}]\\
&-\frac{3}{2}\frac{1}{g}\Psi_{1rz}\chi_{1r}\chi_1\omega^2-\frac{1}{2}\frac{1}{g}[-\chi_{1rz}\Psi_{1r}\chi_1\omega^2+\Psi_{1rz}\Psi_{1r}\Psi_1\omega^2-\chi_{1rz}\chi_{1r}\Psi_1\omega^2]\\
&-\frac{3}{2}\frac{1}{g}\Psi_{1r}\chi_{1rz}\chi_1\omega^2-\frac{1}{2}\frac{1}{g}[-\chi_{1r}\Psi_{1rz}\chi_1\omega^2+\Psi_{1r}\Psi_{1rz}\Psi_1\omega^2-\chi_{1r}\chi_{1rz}\Psi_1\omega^2]\\
&-\frac{3}{2}\frac{1}{r^2}\frac{1}{g}\Psi_{1\theta z}\chi_{1\theta}\chi_1\omega^2-\frac{1}{2}\frac{1}{r^2}\frac{1}{g}\omega^2[-\chi_{1\theta z}\Psi_{1\theta}\chi_1+\Psi_{1\theta z}\Psi_{1\theta}\Psi_1-\chi_{1\theta z}\chi_{1\theta}\Psi_1]\\
&-\frac{3}{2}\frac{1}{r^2}\frac{1}{g}\Psi_{1\theta}\chi_{1\theta z}\chi_1\omega^2-\frac{1}{2}\frac{1}{r^2}\frac{1}{g}\omega^2[-\chi_{1\theta}\Psi_{1\theta z}\chi_1+\Psi_{1\theta}\Psi_{1\theta z}\Psi_1-\chi_{1\theta}\chi_{1\theta z}\Psi_1]
\end{aligned}
\tag{F.8}
$$

$$
\begin{aligned}
T_{IV}=&-\frac{3}{2}\frac{1}{g}\Psi_{1zz}\chi_{1z}\chi_1\omega^2-\frac{1}{2}\frac{1}{g}\omega^2[-\chi_{1zz}\Psi_{1z}\chi_1+\Psi_{1zz}\Psi_{1z}\Psi_1-\chi_{1zz}\chi_{1z}\Psi_1]\\
&-\frac{3}{2}\frac{1}{g}\Psi_{1z}\chi_{1zz}\chi_1\omega^2-\frac{1}{2}\frac{1}{g}\omega^2[-\chi_{1z}\Psi_{1zz}\chi_1+\Psi_{1z}\Psi_{1zz}\Psi_1-\chi_{1z}\chi_{1zz}\Psi_1]\\
&-\frac{3}{4}\frac{1}{g^2}\Psi_{1z}\chi_1\chi_{1z}\omega^4+\frac{1}{4}\frac{1}{g^2}\omega^4[\chi_{1z}\Psi_1\chi_{1z}-\Psi_{1z}\Psi_1\Psi_{1z}+\chi_{1z}\chi_1\Psi_{1z}]\\
&+\frac{3}{4}\frac{1}{g}\Psi_{1zz}\chi_{1z}\chi_1\omega^2+\frac{1}{4}\frac{1}{g}\omega^2[-\chi_{1zz}\Psi_{1z}\chi_1+\Psi_{1zz}\Psi_{1z}\Psi_1-\chi_{1zz}\chi_{1z}\Psi_1]\\
&-\frac{3}{8}\frac{1}{g^2}\chi_1^2\Psi_{1zz}\omega^4+\frac{1}{2}\frac{1}{g^2}\omega^4[\frac{1}{2}\chi_1\Psi_1\chi_{1zz}-\frac{1}{4}\Psi_1^2\Psi_{1zz}]\\
&+\frac{3}{8}\frac{1}{g}\chi_1^2\Psi_{1zzz}\omega^2+\frac{1}{2}\frac{1}{g}\omega^2[-\frac{1}{2}\chi_1\Psi_1\chi_{1zzz}-\frac{1}{4}\Psi_1^2\Psi_{1zzz}]
\end{aligned}
\tag{F.9}
$$

$$
\begin{aligned}
T_V=&\frac{1}{2}\Psi_{1r}\chi_{1r}\Psi_{1rr}+\frac{1}{4}\Psi_{1r}^2\chi_{1rr}+\frac{3}{4}\chi_{1r}^2\chi_{1rr}+\frac{1}{2}\frac{1}{r^4}\Psi_{1\theta}\chi_{1\theta}\Psi_{1\theta\theta}+\frac{1}{4}\frac{1}{r^4}\Psi_{1\theta}^2\chi_{1\theta\theta}+\frac{3}{4}\frac{1}{r^4}\chi_{1\theta}^2\chi_{1\theta\theta}\\
&+\frac{1}{2}\Psi_{1z}\chi_{1z}\Psi_{1zz}+\frac{1}{4}\Psi_{1z}^2\chi_{1zz}+\frac{3}{4}\chi_{1z}^2\chi_{1zz}-\frac{1}{2}\frac{1}{r^3}\Psi_{1\theta}\chi_{1\theta}\Psi_{1r}-\frac{1}{4}\frac{1}{r^3}\Psi_{1\theta}^2\chi_{1r}-\frac{3}{4}\frac{1}{r^3}\chi_{1\theta}^2\chi_{1r}\\
&+\frac{3}{2}\chi_{1r}\chi_{1z}\chi_{1rz}+\frac{1}{2}[\Psi_{1r}\chi_{1z}\Psi_{1rz}+\chi_{1r}\Psi_{1z}\Psi_{1rz}+\Psi_{1r}\Psi_{1z}\chi_{1rz}]\\
&+\frac{3}{2}\frac{1}{r^2}\chi_{1r}\chi_{1\theta}\chi_{1r\theta}+\frac{1}{2}\frac{1}{r^2}[\Psi_{1r}\chi_{1\theta}\Psi_{1r\theta}+\chi_{1r}\Psi_{1\theta}\Psi_{1r\theta}+\Psi_{1r}\Psi_{1\theta}\chi_{1r\theta}]
\end{aligned}
\tag{F.10}
$$

$$
\begin{aligned}
T_{VI}=&\frac{3}{2}\frac{1}{r^2}\chi_{1z}\chi_{1\theta}\chi_{1\theta z}+\frac{1}{2}\frac{1}{r^2}[\Psi_{1z}\chi_{1\theta}\Psi_{1\theta z}+\chi_{1z}\Psi_{1\theta}\Psi_{1\theta z}+\Psi_{1z}\Psi_{1\theta}\chi_{1\theta z}]\\
&+\frac{3}{8}\frac{1}{g}\chi_{1r}^2\chi_{1z}\omega^2-\frac{1}{2}\frac{1}{g}[-\frac{1}{2}\Psi_{1r}\chi_{1r}\Psi_{1z}\omega^2-\frac{1}{4}\Psi_{1r}^2\chi_{1z}\omega^2]\\
&+\frac{3}{8}\frac{1}{r^2}\frac{1}{g}\chi_{1\theta}^2\chi_{1z}\omega^2-\frac{1}{2}\frac{1}{r^2}\frac{1}{g}[-\frac{1}{2}\Psi_{1\theta}\chi_{1\theta}\Psi_{1z}\omega^2-\frac{1}{4}\Psi_{1\theta}^2\chi_{1z}\omega^2]\\
&+\frac{3}{8}\frac{1}{g}\chi_{1z}^3\omega^2-\frac{1}{2}\frac{1}{g}[-\frac{1}{2}\Psi_{1z}^2\chi_{1z}\omega^2-\frac{1}{4}\Psi_{1z}^2\chi_{1z}\omega^2]\\
&-\frac{3}{8}\chi_{1r}^2\chi_{1zz}-\frac{1}{2}[\frac{1}{2}\Psi_{1r}\chi_{1r}\Psi_{1zz}+\frac{1}{4}\Psi_{1r}^2\chi_{1zz}]\\
&-\frac{3}{8}\frac{1}{r^2}\chi_{1\theta}^2\chi_{1zz}-\frac{1}{2}\frac{1}{r^2}[\frac{1}{2}\Psi_{1\theta}\chi_{1\theta}\Psi_{1zz}+\frac{1}{4}\Psi_{1\theta}^2\chi_{1zz}]
\end{aligned}
\tag{F.11}
$$

$$
\begin{aligned}
T_{VII}=&-\frac{3}{8}\chi_{1z}^2\chi_{1zz}-\frac{1}{2}[\frac{1}{2}\Psi_{1z}\chi_{1z}\Psi_{1zz}+\frac{1}{4}\Psi_{1z}^2\chi_{1zz}]\\
&-\frac{3}{2}\frac{1}{g}\chi_{1rz}\Psi_{1r}\Psi_1\omega^2-\frac{1}{2}\frac{1}{g}\omega^2[-\Psi_{1rz}\Psi_{1r}\chi_1+\chi_{1rz}\chi_{1r}\chi_1-\Psi_{1rz}\chi_{1r}\Psi_1]\\
&-\frac{3}{2}\frac{1}{g}\chi_{1r}\Psi_{1rz}\Psi_1\omega^2-\frac{1}{2}\frac{1}{g}\omega^2[-\Psi_{1r}\Psi_{1rz}\chi_1+\chi_{1r}\chi_{1rz}\chi_1-\Psi_{1r}\chi_{1rz}\Psi_1]\\
&-\frac{3}{2}\frac{1}{r^2}\frac{1}{g}\chi_{1\theta z}\Psi_{1\theta}\Psi_1\omega^2-\frac{1}{2}\frac{1}{r^2}\frac{1}{g}\omega^2[-\Psi_{1\theta z}\Psi_{1\theta}\chi_1+\chi_{1\theta z}\chi_{1\theta}\chi_1-\Psi_{1\theta z}\chi_{1\theta}\Psi_1]\\
&-\frac{3}{2}\frac{1}{r^2}\frac{1}{g}\chi_{1\theta}\Psi_{1\theta z}\Psi_1\omega^2-\frac{1}{2}\frac{1}{r^2}\frac{1}{g}\omega^2[-\Psi_{1\theta}\Psi_{1\theta z}\chi_1+\chi_{1\theta}\chi_{1\theta z}\chi_1-\Psi_{1\theta}\chi_{1\theta z}\Psi_1]\\
&-\frac{3}{2}\frac{1}{g}\chi_{1zz}\Psi_{1z}\Psi_1\omega^2-\frac{1}{2}\frac{1}{g}\omega^2[-\Psi_{1zz}\Psi_{1z}\chi_1+\chi_{1zz}\chi_{1z}\chi_1-\Psi_{1zz}\chi_{1z}\Psi_1]
\end{aligned}
\tag{F.12}
$$

$$
\begin{aligned}
T_{VIII}=&-\frac{3}{2}\frac{1}{g}\chi_{1z}\Psi_{1zz}\Psi_1\omega^2-\frac{1}{2}\frac{1}{g}\omega^2[-\Psi_{1z}\Psi_{1zz}\chi_1+\chi_{1z}\chi_{1zz}\chi_1-\Psi_{1z}\chi_{1zz}\Psi_1]\\
&-\frac{3}{4}\frac{1}{g^2}\chi_{1z}\Psi_1\Psi_{1z}\omega^4+\frac{1}{4}\frac{1}{g^2}\omega^4[\Psi_{1z}\Psi_1\chi_{1z}-\chi_{1z}\chi_1\chi_{1z}+\Psi_{1z}\chi_1\Psi_{1z}]\\
&+\frac{3}{4}\frac{1}{g}\chi_{1zz}\Psi_{1z}\Psi_1\omega^2+\frac{1}{4}\frac{1}{g}\omega^2[-\Psi_{1zz}\Psi_{1z}\chi_1+\chi_{1zz}\chi_{1z}\chi_1-\Psi_{1zz}\chi_{1z}\Psi_1]\\
&-\frac{3}{8}\frac{1}{g^2}\Psi_1^2\chi_{1zz}\omega^4+\frac{1}{2}\frac{1}{g^2}\omega^4[\frac{1}{2}\chi_1\Psi_1\Psi_{1zz}-\frac{1}{4}\chi_1^2\chi_{1zz}]\\
&+\frac{3}{8}\frac{1}{g}\Psi_1^2\chi_{1zzz}\omega^2+\frac{1}{2}\frac{1}{g}\omega^2[-\frac{1}{2}\chi_1\Psi_1\Psi_{1zzz}+\frac{1}{4}\chi_1^2\chi_{1zzz}]
\end{aligned}
\qquad \text{(F.13)}
$$

For the third order terms, it is only required that the first harmonic terms vanish. First the equation $B_1^{FH\varepsilon}+B_2^{FH\varepsilon}+B_3^{FH\varepsilon}$ is multiplied by $J_1\cos\theta r dr d\theta$ and integrated over the free surface. Then the equation is multiplied by $J_1\sin\theta r dr d\theta$ and integrated over the free surface. This gives the following integrals, when the expressions for Ψ_1, χ_1, Ψ_2 and χ_2 in terms of f_1, f_2, f_3, f_4, J_0, J_1 and J_2 from the first and second order equations are used.

$$
\begin{aligned}
\int_0^a\int_0^{2\pi} B_1^{FH\varepsilon}\cos\theta\, J_1(\lambda_{11}r)r\,dr\,d\theta=&\pi\sigma_{11}^2\left[\left(\frac{df_2}{d\tau}-\nu f_1\right)\frac{\lambda_{11}^2a^2-1}{2\lambda_{11}^2}J_1^2(\lambda_{11}a)-\frac{a}{\lambda_{11}^2}J_1(\lambda_{11}a)\right]\cos(\omega t)\\
&-\pi\sigma_{11}^2\left[\left(\frac{df_1}{d\tau}+\nu f_2\right)\frac{\lambda_{11}^2a^2-1}{2\lambda_{11}^2}J_1^2(\lambda_{11}a)\right]\sin(\omega t)
\end{aligned}
\qquad \text{(F.14)}
$$

$$
\begin{aligned}
\int_0^a\int_0^{2\pi} B_1^{FH\varepsilon}\sin\theta\, J_1(\lambda_{11}r)r\,dr\,d\theta=&\pi\sigma_{11}^2\left[\left(\frac{df_4}{d\tau}-\nu f_3\right)\frac{\lambda_{11}^2a^2-1}{2\lambda_{11}^2}J_1^2(\lambda_{11}a)\right]\cos(\omega t)\\
&-\pi\sigma_{11}^2\left[\left(\frac{df_3}{d\tau}+\nu f_4\right)\frac{\lambda_{11}^2a^2-1}{2\lambda_{11}^2}J_1^2(\lambda_{11}a)\right]\sin(\omega t)
\end{aligned}
\qquad \text{(F.15)}
$$

$$
\begin{aligned}
\int_0^a\int_0^{2\pi} B_2^{FH\varepsilon}J_1(\lambda_{11}r)r\cos\theta\,dr\,d\theta=&\pi\sigma_{11}\left[f_1(f_1^2+f_2^2+f_3^2+f_4^2)\hat{G}_1+f_4(f_2f_3-f_1f_4)\hat{G}_2\right]\cos(\omega t)\\
&+\pi\sigma_{11}\left[f_2(f_1^2+f_2^2+f_3^2+f_4^2)\hat{G}_1-f_3(f_2f_3-f_1f_4)\hat{G}_2\right]\sin(\omega t)
\end{aligned}
\qquad \text{(F.16)}
$$

$$
\begin{aligned}
\int_0^a\int_0^{2\pi} B_2^{FH\varepsilon}J_1(\lambda_{11}r)r\sin\theta\,dr\,d\theta=&\pi\sigma_{11}\left[f_3(f_1^2+f_2^2+f_3^2+f_4^2)\hat{G}_1-f_2(f_2f_3-f_1f_4)\hat{G}_2\right]\cos(\omega t)\\
&+\pi\sigma_{11}\left[f_4(f_1^2+f_2^2+f_3^2+f_4^2)\hat{G}_1+f_1(f_2f_3-f_1f_4)\hat{G}_2\right]\sin(\omega t)
\end{aligned}
\qquad \text{(F.17)}
$$

$$\int_0^a\int_0^{2\pi} B_3^{FH\varepsilon} J_1(\lambda_{11} r)\, r\cos\theta\, dr\, d\theta = -\frac{1}{4}\sigma_{11}^2\left[f_1(f_1^2+f_2^2+f_3^2+f_4^2)\hat{P}_1 + f_4(f_2f_3 - f_1f_4)\hat{P}_2\right]\cos(\omega t) - \frac{1}{4}\sigma_{11}^2\left[f_2(f_1^2+f_2^2+f_3^2+f_4^2)\hat{P}_1 - f_3(f_2f_3 - f_1f_4)\hat{P}_2\right]\sin(\omega t) \tag{F.18}$$

$$\int_0^a\int_0^{2\pi} B_3^{FH\varepsilon} J_1(\lambda_{11} r)\, r\sin\theta\, dr\, d\theta = -\frac{1}{4}\sigma_{11}^2\left[f_3(f_1^2+f_2^2+f_3^2+f_4^2)\hat{P}_1 - f_2(f_2f_3 - f_1f_4)\hat{P}_2\right]\cos(\omega t) - \frac{1}{4}\sigma_{11}^2\left[f_4(f_1^2+f_2^2+f_3^2+f_4^2)\hat{P}_1 + f_1(f_2f_3 - f_1f_4)\hat{P}_2\right]\sin(\omega t) \tag{F.19}$$

where

$$\hat{G}_1 = \frac{1}{2}\sum_{n=1}^{\infty}\{-\Omega_{0n} I_{04}^n - \frac{1}{2}\Omega_{2n} I_{24}^n - \Omega_{2n} I_{22}^n + [\alpha_{11}\alpha_{0n}\frac{\lambda_{0n}}{\lambda_{11}} - \frac{1}{2}\frac{\lambda_{0n}^2}{\lambda_{11}^2} + (1-\alpha_{11}^2)]\Omega_{0n} I_{03}^n + \frac{1}{2}[\alpha_{11}\alpha_{2n}\frac{\lambda_{2n}}{\lambda_{11}} - \frac{1}{2}\frac{\lambda_{2n}^2}{\lambda_{11}^2} + (1-\alpha_{11}^2)]\Omega_{2n} I_{23}^n\} \tag{F.20}$$

and

$$\hat{G}_2 = \sum_{n=1}^{\infty}\{-\Omega_{0n} I_{04}^n + \frac{1}{2}\Omega_{2n} I_{24}^n + \Omega_{2n} I_{22}^n + [\alpha_{11}\alpha_{0n}\frac{\lambda_{0n}}{\lambda_{11}} - \frac{1}{2}\frac{\lambda_{0n}^2}{\lambda_{11}^2} + (1-\alpha_{11}^2)]\Omega_{0n} I_{03}^n - \frac{1}{2}[\alpha_{11}\alpha_{2n}\frac{\lambda_{2n}}{\lambda_{11}} - \frac{1}{2}\frac{\lambda_{2n}^2}{\lambda_{11}^2} + (1-\alpha_{11}^2)]\Omega_{2n} I_{23}^n\} \tag{F.21}$$

In Hutton's report the I_{03}^n and I_{23}^n terms in (F.20) and (F.21) are multiplied by λ_{11}^2, but according to Abramson (1966), Hutton's expressions should be divided by λ_{11}^2, so according to Abramson (1966), the expressions in (F.20) and (F.21) should be correct.

$$\hat{P}_1 = -\frac{\lambda_{11}^2}{\sigma_{11}^2}\pi\frac{1}{8}(18I_1 - 3I_3 - 6I_4 - 9I_5 + 12I_6 - 6I_7 - 9\alpha_{11}^2 I_2 + 7\alpha_{11}^2 I_3 + 21\alpha_{11}^2 I_5 + 3\alpha_{11}^4 I_2) \tag{F.22}$$

$$\hat{P}_2 = -\frac{\lambda_{11}^2}{\sigma_{11}^2}\pi\frac{1}{4}(6I_1 - I_3 - 2I_4 - 3I_5 + 4I_6 - 2I_7 - 3\alpha_{11}^2 I_2 - 19\alpha_{11}^2 I_3 + 7\alpha_{11}^2 I_5 + \alpha_{11}^4 I_2) \tag{F.23}$$

The integrals I_{03}^n, I_{22}^n and I_{23}^n are given in appendix D, and

$$I_{04}^{n}=\int_{0}^{\lambda_{11}a} uJ_1(u)\frac{dJ_1(u)}{du}\frac{d}{du}\left[J_0\left(\frac{\lambda_{0n}}{\lambda_{11}}u\right)\right]du \tag{F.24}$$

$$I_{24}^{n}=\int_{0}^{\lambda_{11}a} uJ_1(u)\frac{dJ_1(u)}{du}\frac{d}{du}\left[J_2\left(\frac{\lambda_{2n}}{\lambda_{11}}u\right)\right]du \tag{F.25}$$

$$I_1=\frac{1}{\lambda_{11}^2}\int_0^a J_1(\lambda_{11}r)\left(\frac{dJ_1(\lambda_{11}r)}{dr}\right)^2\left(\frac{d^2J_1(\lambda_{11}r)}{dr^2}\right)r\,dr \tag{F.26}$$

$$I_2=\lambda_{11}^2\int_0^a J_1^4(\lambda_{11}r)\,r\,dr \tag{F.27}$$

$$I_3=\int_0^a \frac{1}{r^2}J_1^4(\lambda_{11}r)\,r\,dr \tag{F.28}$$

$$I_4=\frac{1}{\lambda_{11}^2}\int_0^a \frac{1}{r^4}J_1^4(\lambda_{11}r)\,r\,dr \tag{F.29}$$

$$I_5=\int_0^a J_1^2(\lambda_{11}r)\left(\frac{dJ_1(\lambda_{11}r)}{dr}\right)^2 r\,dr \tag{F.30}$$

$$I_6=\frac{1}{\lambda_{11}^2}\int_0^a \frac{1}{r^2}J_1^2(\lambda_{11}r)\left(\frac{dJ_1(\lambda_{11}r)}{dr}\right)^2 r\,dr \tag{F.31}$$

$$I_7=\frac{1}{\lambda_{11}^2}\int_0^a \frac{1}{r^3}J_1^3(\lambda_{11}r)\frac{dJ_1(\lambda_{11}r)}{dr}r\,dr \tag{F.32}$$

Setting the cos(ωt) terms from the case when it is multiplied by $J_1\cos\theta r dr d\theta$ equal to zero gives

$$\frac{df_2}{d\tau}=F_1+\nu f_1+K_1f_1(f_1^2+f_2^2+f_3^2+f_4^2)+K_2f_4(f_2f_3-f_1f_4) \tag{F.33}$$

Here

$$F_1=\frac{2a}{(\lambda_{11}^2a^2-1)J_1(\lambda_{11}a)} \tag{F.34}$$

and

$$
\begin{aligned}
&K_1=K_{10}+\Delta K_1\\
&K_{10}=\frac{1}{16}K(-18I_1+3I_3+6I_4+9I_5-12I_6+6I_7+\alpha_{11}^2(9I_2-7I_3-21I_5)-3\alpha_{11}^4I_2)\\
&K=\frac{1}{(\lambda_{11}^2a^2-1)J_1^2(\lambda_{11}a)}\left(\frac{\lambda_{11}^3}{g\alpha_{11}}\right)\\
&\Delta K_1=-\frac{2\sigma_{11}}{\lambda_{11}^2}K\hat{G}_1
\end{aligned}
\qquad \text{(F.35)}
$$

$$
\begin{aligned}
&K_2=K_{20}+\Delta K_2\\
&K_{20}=K\frac{1}{8}(-6I_1+I_3+2I_4+3I_5-4I_6+2I_7+\alpha_{11}^2(3I_2+19I_3-7I_5)-\alpha_{11}^4I_2)\\
&\Delta K_2=-\frac{2\sigma_{11}}{\lambda_{11}^2}K\hat{G}_2
\end{aligned}
\qquad \text{(F.36)}
$$

Setting the sin(ωt) terms from the case where it is multiplied by $J_1\cos\theta r dr d\theta$ equal to zero gives

$$\frac{df_1}{d\tau}=-\nu f_2-K_1f_2(f_1^2+f_2^2+f_3^2+f_4^2)+K_2f_3(f_2f_3-f_1f_4) \qquad \text{(F.37)}$$

Setting the cos(ωt) terms from the case where it is multiplied by $J_1\sin\theta r dr d\theta$ equal to zero gives

$$\frac{df_4}{d\tau}=\nu f_3+K_1f_3(f_1^2+f_2^2+f_3^2+f_4^2)-K_2f_2(f_2f_3-f_1f_4) \qquad \text{(F.38)}$$

and finally setting the sin(ωt) terms from the case where it is multiplied by $J_1\sin\theta r dr d\theta$ equal to zero gives

$$\frac{df_3}{d\tau}=-\nu f_4-K_1f_4(f_1^2+f_2^2+f_3^2+f_4^2)-K_2f_1(f_2f_3-f_1f_4) \qquad \text{(F.39)}$$

Equations (F.33), (F.37), (F.38) and (F.39) are the four first order nonlinear differential equations which the generalized coordinates f_1, f_2, f_3 and f_4 must satisfy.

The integrals and Bessel function parameters independent of tank size are given in appendix H.

Appendix G Coefficients in the stability investigations of sloshing in a vertical circular cylindrical tank

The coefficients in the set of homogeneous algebraic equations which are used in the stability investigations are

$$
\begin{aligned}
d_{11} &= 2K_1 f_1^{(o)} f_2^{(o)} + K_2 f_3^{(o)} f_4^{(o)} \\
d_{12} &= \nu + K_1[f_1^{(o)2} + 3f_2^{(o)2} + f_3^{(o)2} + f_4^{(o)2}] - K_2 f_3^{(o)2} \\
d_{13} &= 2K_1 f_2^{(o)} f_3^{(o)} + K_2[f_1^{(o)} f_4^{(o)} - 2f_2^{(o)} f_3^{(o)}] \\
d_{14} &= 2K_1 f_2^{(o)} f_4^{(0)} + K_2 f_1^{(o)} f_3^{(o)}
\end{aligned}
\tag{G.1}
$$

$$
\begin{aligned}
d_{21} &= \nu + K_1[3f_1^{(o)2} + f_2^{(o)2} + f_3^{(o)2} + f_4^{(o)2}] - K_2 f_4^{(o)2} \\
d_{22} &= d_{11} \\
d_{23} &= 2K_1 f_1^{(o)} f_3^{(o)} + K_2 f_2^{(o)} f_4^{(o)} \\
d_{24} &= 2K_1 f_1^{(o)} f_4^{(o)} + K_2[f_2^{(o)} f_3^{(o)} - 2f_1^{(o)} f_4^{(o)}]
\end{aligned}
\tag{G.2}
$$

$$
\begin{aligned}
d_{31} &= d_{24} \\
d_{32} &= d_{14} \\
d_{33} &= 2K_1 f_3^{(o)} f_4^{(o)} + K_2 f_1^{(o)} f_2^{(o)} \\
d_{34} &= \nu + K_1[f_1^{(o)2} + f_2^{(o)2} + f_3^{(o)2} + 3f_4^{(o)2}] - K_2 f_1^{(o)2}
\end{aligned}
\tag{G.3}
$$

$$
\begin{aligned}
d_{41} &= d_{23} \\
d_{42} &= d_{13} \\
d_{43} &= \nu + K_1[f_1^{(o)2} + f_2^{(o)2} + 3f_3^{(o)2} + f_4^{(o)2}] - K_2 f_2^{(o)2} \\
d_{44} &= d_{33}
\end{aligned}
\tag{G.4}
$$

For the planar motion the coefficients are

$$
\begin{aligned}
d_{11} &= 0 \\
d_{12} &= \nu + K_1 \gamma^2 = -F_1 \frac{1}{\gamma} \\
d_{13} &= 0 \\
d_{14} &= 0
\end{aligned}
\tag{G.5}
$$

$$
\begin{aligned}
d_{21} &= \nu + K_1 3\gamma^2 = -F_1 \frac{1}{\gamma} + 2K_1 \gamma^2 \\
d_{22} &= 0 \\
d_{23} &= 0 \\
d_{24} &= 0
\end{aligned}
\tag{G.6}
$$

$$
\begin{aligned}
d_{31} &= 0 \\
d_{32} &= 0 \\
d_{33} &= 0 \\
d_{34} &= \nu + K_1\gamma^2 - K_2\gamma^2 = -F_1\frac{1}{\gamma} - K_2\gamma^2
\end{aligned}
\tag{G.7}
$$

$$
\begin{aligned}
d_{41} &= 0 \\
d_{42} &= 0 \\
d_{43} &= \nu + K_1\gamma^2 = -F_1\frac{1}{\gamma} \\
d_{44} &= 0
\end{aligned}
\tag{G.8}
$$

For the nonplanar motion the coefficients are

$$
\begin{aligned}
d_{11} &= 0 \\
d_{12} &= \nu + K_1\gamma^2 + K_1\zeta^2 \\
d_{13} &= K_2\gamma\zeta \\
d_{14} &= 0
\end{aligned}
\tag{G.9}
$$

$$
\begin{aligned}
d_{21} &= \nu + K_1 3\gamma^2 + K_1\zeta^2 - K_2\zeta^2 \\
d_{22} &= 0 \\
d_{23} &= 0 \\
d_{24} &= 2K_1\gamma\zeta - 2K_2\gamma\zeta
\end{aligned}
\tag{G.10}
$$

$$
\begin{aligned}
d_{31} &= d_{24} \\
d_{32} &= 0 \\
d_{33} &= 0 \\
d_{34} &= \nu + K_1\gamma^2 + 3K_1\zeta^2 - K_2\gamma^2
\end{aligned}
\tag{G.11}
$$

$$
\begin{aligned}
d_{41} &= 0 \\
d_{42} &= d_{13} \\
d_{43} &= d_{12} \\
d_{44} &= 0
\end{aligned}
\tag{G.12}
$$

The coefficients M_i, i=3,4,5,6 in the nonplanar sloshing equations are

$$
M_3 = \begin{vmatrix} d_{34} & d_{13} \\ d_{24} & d_{12} \end{vmatrix}, \quad M_4 = \begin{vmatrix} d_{12} & d_{13} \\ d_{24} & d_{21} \end{vmatrix}
\tag{G.13}
$$

$$
M_5 = \begin{vmatrix} d_{13} & d_{12} \\ d_{12} & d_{13} \end{vmatrix}, \quad M_6 = \begin{vmatrix} d_{24} & d_{21} \\ d_{34} & d_{24} \end{vmatrix}
$$

Appendix H Values of Bessel function parameters and integrals for nonlinear sloshing in a vertical circular cylindrical tank

In chapter H.1, the values of the Bessel function parameters and integrals which are independent of the tank dimensions are given. In chapter H.2, the values for the example in chapter 5.3.9, for a tank with diameter 1.0 meter and water depth 0.5 meter, are given. The values of the zeros and associated values of Bessel functions are taken from Abramowitz and Stegun "Handbook of Mathematical Functions".

H.1 Values independent of tank dimensions

λ_{11} is the first root of $J_1'(\lambda_{1n}a) = 0$, where $\lambda_{11}a = 1.841190$.

n	$\xi_{0n} = \lambda_{0n}a$	$\lambda_{0n} / \lambda_{11}$	$\xi_{2n} = \lambda_{2n}a$	$\lambda_{2n} / \lambda_{11}$
1	0.000000	0.000000	3.05424	1.65884
2	3.831706	2.081103	6.70613	3.64228
3	7.015587	3.810355	9.96947	5.41469
4	10.173468	5.525485	13.17037	7.15318
5	13.323692	7.236457	16.34752	8.87878
6	16.470630	8.945644	19.51291	10.59799
7	19.615859	10.653902	22.67158	12.31355
8	22.760084	12.361616	25.82604	14.02682

Table H.1 Values of Bessel function parameters.
λ_{0n} are the roots of $J_0'(\lambda_{0n}a) = 0$ and λ_{2n} are the roots of $J_2'(\lambda_{2n}a) = 0$.

i	I_i
1	-.012955
2	.112807
3	.060036
4	.049676
5	.017590
6	.025647
7	.033292

Table H.2 Values of integrals, independent of tank size, defined in appendix F.

n	I_{01}^n	I_{02}^n	I_{03}^n	I_{04}^n	I_{21}^n	I_{22}^n	I_{23}^n	I_{24}^n
1	.123801	.280781	.404584	.000000	.024717	.085142	.160763	.050906
2	.049218	.028625	-.066804	-.144663	.037645	.043731	.001088	-.080287
3	-.000374	-.004536	.000785	.005717	.017027	.015099	-.000155	-.032281
4	.000055	.001710	-.000123	-.001874	.009783	.010698	.000045	-.020437
5	-.000015	-.000852	.0000345	.000903	.006337	.005819	-.000007	-.012164
6	.0000056	.000498	-.0000129	-.000516	.004454	.004784	.000006	-.009231
7	-.0000025	-.000321	.0000058	.000328	.003297	.003071	-.000003	-.006371
8	.0000013	.000220	-.0000029	-.000224	.002542	.002704	.000002	-.005244

Table H.3 Values of integrals defined in appendix D and F. The integrals are independent of the circular cylindrical tank dimensions.

The values of I_{01}^4, I_{01}^5, I_{02}^4 and I_{04}^4 are slightly different from the ones given in Hutton (1963). The values of I_{03}^n and I_{22}^n given in Hutton, should be divided by λ_{11}^2 to obtain the values here. In Hutton (1963) only the values for n=1,2,3,4,5 are given.

n	$\xi_{0n} = \lambda_{0n}a$	$\xi_{2n} = \lambda_{2n}a$	$J_0(\lambda_{2n}a)$	$J_2(\lambda_{2n}a)$
1	0.000000	3.05424	1.000000	0.48650
2	3.831706	6.70613	-0.402759	-0.31353
3	7.015587	9.96947	0.300116	0.25474
4	10.173468	13.17037	-0.249705	-0.22088
5	13.323692	16.34752	0.218359	0.19794
6	16.470630	19.51291	-0.196465	-0.18101
7	19.615859	22.67158	0.180063	0.16784
8	22.760084	25.82604	-0.167185	-0.15720

Table H.4 Bessel function parameters, independent of tank size.

H.2 Values of constants in the example

Tank diameter [m]	1.0
Water depth in tank [m]	0.5
g [m/s^2]	9.81
$J_{11}(\lambda_{11}a)$	0.581865
$\lambda_{11}a$	1.841190
λ_{11}	3.682380
σ_{11} [rad./s]	5.860954
T_1 [s]	1.072041
α_{11}	0.950909
K_0	0.856343
F_1	0.719090
K	6.615132
$\hat{G}_1$	-0.039292
$\hat{G}_2$	-0.023219
K_1	0.509537
K_2	1.280300
K_3	0.286185
K_4	0.261226

Table H.5 Input data and some calculated constants for the example in chapter 5.3

In the evaluation of the coefficients K_1 and K_2 the infinite series terms are approximated by their first five terms. To indicate what errors this finite series approximation might cause, it is seen from table H.6, that the values of the last two terms in the calculation of $\hat{G}_1$ and $\hat{G}_2$, which contribute to K_1 and K_2, were less than a half percent of the values of the first two terms.

n	Terms in the series of $\hat{G}_1$	Terms in the series of $\hat{G}_2$
1	-1.0068056E-02	3.9997209E-02
2	8.4297676E-03	1.1992961E-02
3	-3.7613969E-02	-7.5145587E-02
4	-3.3114462E-05	-5.3455879E-05
5	-6.1854498E-06	-9.8765922E-06

Table H.6 Terms in the series of $\hat{G}_1$ and $\hat{G}_2$, equation (F.20) and (F.21).

n	λ_{0n}	λ_{2n}	σ_{0n}	σ_{2n}
1	.000000	6.10848	.000000	7.723875
2	7.663412	13.41226	8.666457	11.470566
3	14.031174	19.93894	11.732246	13.985743
4	20.346936	26.34074	14.128108	16.074908
5	26.647384	32.69504	16.168205	17.909169

Table H.7 Roots of $J_{mn}'(\lambda_{mn}) = 0$ and natural frequencies σ_{mn} of the mn't sloshing mode, for the circular cylindrical tank with diameter 1.0 meter and water depth 0.5 meter.

n	Ω_{0n}	Ω_{2n}
1	0.256288	0.344593
2	0.095622	-0.462650
3	8.765405	-0.023222
4	-0.020211	0.007129
5	0.006604	-0.003394

Table H.8 Ω_{mn}; constants defined in appendix D, for the circular cylindrical tank with diameter 1.0 meter and water depth 0.5 meter.

Appendix I The orthogonality condition of the eigenfunctions

Green's second identity states that

$$\iiint_{\Omega}(\psi_n \nabla^2\psi_m - \psi_m \nabla^2\psi_n)\,d\tau = \iint_{S}(\psi_m \frac{\partial\psi_n}{\partial n} - \psi_n \frac{\partial\psi_m}{\partial n})\,dS \tag{I.1}$$

where S is the surface enclosing the fluid volume Ω. ψ_m and ψ_n are the eigenfunctions, and it is necessary that they have continuous derivatives of the first and second order. The normal direction **n** is into the fluid. When $\nabla^2\psi_m=0$ and $\nabla^2\psi_n=0$ it follows from equation (I.1) that

$$\iint_{S}(\psi_m \frac{\partial\psi_n}{\partial n} - \psi_n \frac{\partial\psi_m}{\partial n})\,dS = 0 \tag{I.2}$$

Since

$$\frac{\partial\psi_m}{\partial n} = \frac{\partial\psi_n}{\partial n} = 0 \tag{I.3}$$

on the rigid walls, the integral in equation (I.2) is equal to

$$\iint_{S_F}(\psi_m \frac{\partial\psi_n}{\partial z} - \psi_n \frac{\partial\psi_m}{\partial z})\,dS = 0 \tag{I.4}$$

where S_F is the free surface z=0. By using the free surface conditions

$$\frac{\partial\psi_m}{\partial z} = -\lambda_m\psi_m \tag{I.5}$$

$$\frac{\partial\psi_n}{\partial z} = -\lambda_n\psi_n \tag{I.6}$$

on z=0, equation (I.4) becomes

$$\iint_{S_F}[\lambda_n - \lambda_m]\psi_n\psi_m\,dS = 0 \tag{I.7}$$

This means that for $\lambda_m \neq \lambda_n$

$$\iint_{S_F}\psi_n\psi_m\,dS = 0 \tag{I.8}$$

PREVIOUS DR.ING. THESES

Department of Marine Hydrodynamics

Løtveit, Magne	:	A Study of Pressure- and Velocity Relations in the Slip-Stream of Propellers of Single Screw Ships to clarify the Propeller Action behind the Hull. 1963. (in Norwegian)
Dahle, Emil Aall	:	A Study of the Coefficients in the Differential Equations for the Rolling Motion of a Vessel. 1971. (in Norwegian)
Langfeldt, Jan N.	:	A Theoretical and Experimental Study of the Feasibility of Two-Phase (Gas-Water) Jet Propulsion of Craft. 1972.
Berg, Tor Einar	:	Manoeuvring of Vessels. 1978. (in Norwegian)
Skjærdal, Svein O.	:	Wave Induced Oscillations of Ship Hulls. 1978.
Nielsen, Finn G.	:	Hydrodynamic Relations of Oil Booms. 1980.
Liapis, Nicolas	:	Hydrodynamic Analysis of the Ship-Buoy System. 1980.
Pettersen, Bjørnar	:	Calculation of Potential Flow about Ship Hulls in Shallow Water with Particular Application to Manoeuvring. 1980.
Rye, Henrik	:	Ocean Wave Groups. 1981.
Utnes, Torbjørn H.	:	Forward-Speed Effects on the Hydrodynamic Motion Coefficients of a Surface-Piercing Body. 1982
Børresen, Rolf	:	The unified theory of ship motions in water of finite depth. 1984.
Aarsnes, Jan Vidar	:	Current Forces on Ships. 1984.
Skomedal, Nere	:	Application of a Vortex Tracking Method to Three-Dimensional Flow Past Lifting Surfaces and Blunt Bodies. 1985.
Løken, Arne Edvin	:	Three-dimensionl second order hydrodynamic effects on ocean structures in waves. 1986.
Aanesland, Vidar	:	A Theoretical and Numerical Study of Ship Wave Resistance. 1986.
Sortland, Bjørn	:	Force Measurements in Oscillating Flow on Ship Sections and Circular Cylinders in a U-Tube Water Tank. 1986.
Falch, Sigurd	:	A numerical study of slamming of two-dimensional bodies. 1986.
Lian, Walter	:	A numerical study of two-dimensional separated flow past bluff bodies at moderate KC-numbers. 1986.
Braathen, Arne	:	Application of a vortex tracking method to the prediction of roll damping of a two-dimensional floating body. 1987.

Gang Miao	:	Hydrodynamic Forces and Dynamic Responses of Circular Cylinders in Wave Zones. 1989.
Greenhow, Martin	:	Linear and Non-Linear Studies of Waves and Floating Bodies. Part I and Part II. 1989.
Chang Li	:	Force Coefficients of Spheres and Cubes in Oscillatory Flow with and without Current. 1989.
Jæger, Arild	:	Seakeeping, Dynamic Stability and Performance of a Wedge Shaped Planing Hull. 1989.
Hoff, Jan Roger	:	Three-dimensional Green function of a vessel with forward speed in waves. 1990.
Rong Zhao	:	Slow-Drift of a Moored Two-Dimensional Body in Irregular Waves. 1990.
Løland, Geir	:	Current Forces and Flow through Fish Farms. 1991.
Krokstad, Jørgen R.	:	Second-order Loads in Multidirectional Seas. 1991.
Mørch, Hans J. B.	:	Aspects of Hydrofoil Design; with Emphasis on Hydrofoil Interaction in Calm Water. 1992.
Steen, Sverre	:	Cobblestone Effect on SES. 1993.
Kvålsvold, Jan	:	Hydroelastic Modelling of Wetdeck Slamming on Multihull Vessels. 1994.
Ulstein, Tore	:	Nonlinear Effects of a Flexible Stern Seal Bag on Cobblestone Oscillations of an SES. 1995